Cardiff University
School of Engineering

Design and Development of Lightning Waveform Generators

A Thesis submitted for the degree of Doctor of Philosophy

Philip Leichauer
March 2017

Abstract

Aircraft are struck by lightning approximately once every 10,000 hours each. It is essential that this does not cause them to malfunction or otherwise endanger the craft or passengers.

Cardiff University commissioned the Morgan-Botti Lightning Laboratory (MBLL) to perform lightning testing to aid aircraft safety development. The work described in this thesis was undertaken while acting as the engineer and project manager to design, develop and build the laboratory. Its focus was upon ensuring that the lightning test waveforms were delivered, as required by test standards, in the best possible way that was achievable within budget.

A lightning test frequently involves 3 waveforms; a high current initial pulse (A, Ah and D waveforms) followed by a trailing component consisting of an intermediate current B waveform and a long DC discharge (C or C* waveforms), as specified in the aeronautical lightning test standard ED84.

A thorough understanding of the high current lightning test waveforms was gained by analyzing their mathematical description; this lead to developing A, Ah, D and B waveform generators optimized to make the best use of available equipment and reliably deliver the required waveforms.

Many options were considered for generating the C and C* waveforms. Capacitors were chosen on space and safety grounds over other technologies. Two modes of operation were implemented; firstly, a CR discharge where the waveform current sagged over the duration of output and, secondly, a PWM controlled flat discharge using a 3 phase buck converter topology.

The decision, mathematical understanding and circuits behind the development of the waveform generators are presented in to facilitate and inform future design of similar waveform generators or test facilities.

The laboratory has been operating successfully since 2011 with the D waveform, delivering direct effects lightning testing accurately to international standards. The B and C waveforms were tested successfully in 2014. In the years following, the Ah and A waveforms were implemented as designed also.

Contents

List of Figures

List of Tables

1. Introduction

This work was undertaken while designing and building the D, B and C generators for the Morgan-Botti Lightning Laboratory (MBLL) for Cardiff University. The area of study covers understanding and generation of the lightning test waveforms that are core to the function of the laboratory.

The laboratory was built to enable academic research in the field of lightning protection for aeronautical components and systems. It was part funded by an A4B grant and by donations of equipment from an industrial partner. The name of the laboratory is formed from the surnames of Rhodri Morgan, the first minister for Wales at the time of the initial scoping of the project, and Jean Botti the CTO of Airbus.

The laboratory design and build, as described by this thesis, started with a brand new, empty industrial unit and ended as a functioning test facility capable of aeronautical testing.

A lot of equipment had to be designed to fit within this space. The major parts were the test chamber, waveform generators and control room. The safety barriers, interlock and control system as well as ventilation systems had to neatly fit around these also. A systems engineering approach was required, which involved an initial scheme design to understand how to layout and operate the laboratory and identify what was needed to accomplish this. The tasks were then divided and tackled in parallel. This thesis reports on the most important and unique aspects of the project – the waveform generators.

Lightning tests, when undertaken for aircraft parts or systems as part of airworthiness compliance or pure research are generally small. For sample, a piece of composite wing skin when tested would likely suffer damage where an arc attaches to it. From experience, the area of damage to paint and the top layer is approximately 150 mm in diameter. To accommodate this with ample room for attaching conductors around this, 600 mm square sections of wing skin are often tested. Further examples of items to test include fuel pipes, pumps and vents as well as prop blades and helicopter root hubs. These are all similarly sized and the test chamber and initial test rig was built to accommodate and test a majority of

them. Larger items could be tested by building custom return conductors and possibly extending out of the front of the test chamber if required.

The waveform used to test an individual sample is specified as a composite of 3 separately defined waveforms – the return stroke, intermediate and trailing components.

The return stroke has a choice of 3 different commonly used waveforms. Aircraft are generally struck on extremities (wing tips, tail, leading or trailing edges or antenna) with the initial return stroke of a lightning strike. For these tests the A waveform is generally used but can be replaced with the Ah waveform for high altitude certification only. For test purposes, after the initial return stroke, there is a variable delay before a secondary return stroke flows along the lightning arc channel. As the aircraft is moving forward during this time and the arc channel is effectively stationary, these secondary return strokes can attach to anything following a leading edge (the middle of the wing for instance). For these secondary attachments, referred to as swept strokes (as in swept backwards, and plural as there is often several), the D waveform is used. The peak current in these waveforms is 200, 150 and 100 kA for the A, Ah and D waveforms respectively. By far the most common waveform used is the D waveform as a great majority of the aircraft comprises surfaces where lightning could be swept to as opposed to the extremities which attract the A or Ah waveforms.

The intermediate component has only 1 option – the B waveform. It forms a bridge between the high current return stroke and the relatively low current trailing component. It has an average current of 2 kA over 5 ms, delivering 10 C of charge transfer through a sample. The charge transfer is comparable in order to that in the return strokes while the current is 2 orders of magnitude lower. It is however, nearly 1 order of magnitude higher than the trailing component (peak current of the reference B waveform is approximately 4 kA).

The trailing component when applied to the trailing edge of aircraft structures is applied as the C waveform. It is defined as waveform of 400 A average current over 500 ms delivering a charge transfer of 200 C. The C waveform is considered by the test standards to represent a high threat level test of the full charge transfer of a lightning strike. This can only happen at trailing edges as there is nowhere for arc to be swept back to. The trailing component is applied as the C* waveform

elsewhere on aircraft. This is simply a truncated version of the C waveform with the same average current but much shorter time scales. There are 2 mechanisms that limit the charge transfer at points forward of trailing edges. The arc attachment point is dragged along by the aircraft, the arc is stretched through the air above beside or below (depending on the location) the aircraft. The arc channel is separated from the surface by the boundary layer. A new attachment point forms when either the steady state voltage is sufficient to break down the air across the boundary layer (the longer the arc is stretched the higher the voltage) or when a secondary restrike occurs which would supply enough inductive voltage from its fast rise time to punch through the boundary layer. It also has to punch through the dielectric paint covering the surfaces which can lead to longer dwell times for thicker paints. Therefore the dwell time varies considerably based on aircraft speed and boundary layer thickness. The likely values used for speed are those associate with the minimum take off and landing speeds, which are the slowest speeds the aircraft is ever likely to fly and thus the speeds where the dwell time would be longest. Whereas the boundary layer thickness can vary quite dynamically over an aircraft and differ greatly between aircraft. Fortunately, it is not for a test house to inform a customer of the dwell time required but for the manufacturer and certifying body to agree one before carrying out any testing. While this description was long it serves to illustrate why the C* waveform is specified as being between 1 and 50 ms in duration with charge transfers ranging between 0.4 and 20 C. The standard suggests 20 ms would usually be sufficient with a charge transfer of 8 C.

To deliver the return strokes, the High Current Waveform Generator was designed and built. There are 2 commonly used topologies for delivering these. Firstly, using an LCR circuit where a relatively high voltage capacitor bank discharges through the circuit resistance and inductance to deliver the waveform. The inductance limits the rise time and efforts are usually made to minimise it as far as possible. Secondly a clamped circuit that uses a smaller capacitance but usually higher voltage to ring current into the inductance of the output section of the circuit. Once peak current is reached, a clamp fires to short out the capacitor bank and allow current to circulate through the inductance and resistance of the output section and load/sample to deliver the waveform. The topology chosen was the LCR method as it eliminated the complexities of the clamp circuit and a system of

sufficient performance could be built using as many freely available parts as possible.

The intermediate and trailing component waveform generators differ from the one for the return stroke in that a great deal of added inductance and resistance is necessary in their circuits to achieve the waveforms. This allowed a good deal of flexibility in the layout of the generators, which in turn lead to combining them into a single system (which still allowed both waveforms to be generated separately).

An LCR topology was chosen to deliver the B waveform as it allowed the possibility of following the reference waveform as closely as possible. It was also the simplest topology that could deliver the waveform, requiring only an on switch (thyristors were used) and completely emptying the charge stored within its capacitor bank during the discharge. This makes delivering a waveform with a known charge transfer trivial.

The C and C* waveform generator was conceived to deliver the waveform using 2 control strategies. Firstly a truncated CR discharge where the current delivered would decay over the duration of the waveform before being switched off once sufficient charge had been delivered. Secondly, a PWM controlled discharge that would allow a flatter waveform, more closely matching the square wave of the test standard. Both strategies required a switch that could be turned off, so IGBTs were chosen. To accomplish the PWM method, the outputs of the switches were configured as damped buck converters.

The B and C waveform generators were built together and their outputs combined in a custom filter that let the relatively fast B waveform through but heavily attenuated the oscillations of the PWM controlled C waveform.

1.1. Thesis objectives

The objectives of this PhD research project were to:

- Survey the present day laboratories that perform lightning testing for aeronautical systems
- Gain an analytical understanding the lightning waveforms required by the test standards
- Apply the analytical understanding to present schemes for waveform generators that deliver the standard waveforms exactly

- Explore how by relaxing the rise time (while remaining within specification) the D, Ah and A waveforms could be delivered using LCR circuits
- Apply the analytical understanding to design a practical solution for the high current generator, making as much use of available parts as possible
- Building and testing of the high current generator to the extent that it can produce a D waveform (with design work in place for extending it to deliver the Ah and A waveforms also
- Use the analytical understanding to design, build and test a waveform generator to exactly produce the B waveform as described in the standard
- Compare methods of storing energy to deliver the C waveform
- Design, build and test a waveform generator to produce the C waveform as described in the standard
- Design a custom filter to integrate the outputs of the B and C waveform generators, which also acts to protect them from all fault conditions when connected to the high current waveform generator

1.2. Contributions to new research

Approximately 95% of the design of the lightning test facility and all bespoke equipment within it were designed by myself. The exceptions to this was the latitude given to the technician who assisted assembling the facility regarding where and how to mount some items and the layout of relay logic in the control interface. The help, assistance and encouragement of the technician was excellent – he now runs the facility and was trained to do so while building it.

All except 3 equations presented in this thesis are my own work and started from those found in basic textbooks and undergraduate study before being taken further here. The 3 exceptions are standard inductance formulae.

The major contributions of this work include:

- A generic analytical solution to the double exponential waveform, revealing how to implement over, critically and underdamped waveforms exactly with LCR circuits. Examples proving this are given.
- Exploration of the solution space for implementing an LCR circuit that delivers the peak current and action integral as required by the test standards. This revealed a maximum capacitance that could deliver a given peak current, if inductance and action integral are fixed. Below the

maximum capacitance, 2 solutions of voltage and required respective resistance were revealed.

- The application of the 2 solution approach to design the high-current generator to deliver a fast and slow version of the A waveform, Ah waveform and D waveform, within the requirements of the test standards.
- Building and testing of the generator to the point where it can deliver the D waveform, including the development of a low inductance spark gap and variable resistor.
- The design of a high power variable resistor with a very large number of discrete resistances covering the range required to set up all required waveforms for the facility.
- The design of a low inductance spark gap.
- Application of the LCR solution to design the B waveform generator. This included designing a thyristor stack and driver to initiate the waveform. Testing of this waveform.
- Optimization of capacitance and charge voltage of CR and PWM solutions for the design of the C waveform. Implementation of a design that allowed both solutions to be used, including design of the IGBT switching arrangement (3 phase buck converter) and required snubber networks. Testing of this waveform generator in both CR and PWM modes.
- Design of a filter to merge the B waveform and C waveform, removing as much of the high-frequency switching components from the PWM implementation of the C waveform, but allowing the B waveform to pass without distortion. The filter also had to resist injection of high voltage from the high-current generator. Testing of this filter.

1.3. Thesis contents:

Chapter 2 – Literature Review: A literature review introducing lightning and the aeronautical test standards used to protect against it. This includes descriptions of other present test facilities and brief descriptions of their lightning test capabilities.

Chapter 3 – Description of the Laboratory: The decisions made while building the test facility and constraints it placed upon the waveform generators are presented. It shows that a holistic approach was taken in order to fit everything

into the space and integrate the waveform generators and their control, safety and measurement systems.

Chapter 4 – High Current Waveform Generator: The options to design the high current D, Ah and A waveform generator are presented. The reference waveforms are then explored analytically to understand how best to generate them. It was found that very high voltage, energy and cost would be required to produce them perfectly. Clamped and LCR circuits were explored to find a solution using as much of the available equipment as possible. It was found that 2 solutions, with different rise times, for each waveform could be produced with the waveform generator proposed. The generator was designed and built, including a novel variable resistor and inexpensive low inductance spark gap. The waveform generator was built and tested to the extent where it could deliver the D waveform.

Chapter 5 – Intermediate and Trailing Component Generator: The B and C waveform generators were combined into a single chassis, allowing their outputs to be combined before coupling to the High Current Waveform Generator and Test Rig. A design for the B waveform generator is designed by analysing the reference waveform to replicate it as accurately as possible with an LCR circuit. The C waveform generator energy storage options are explored, justifying the choice of capacitors. A novel design allowing both resistively stabilised and PWM controlled generation of the C waveform from the same equipment is presented. A filter network is designed to combine the B and C waveforms. The build of both generators is presented including discussion of switching options. The outputs of the generators are tested showing that both B and C waveforms (in both modes of operation) are deliverable within the specification of the standards.

Chapter 6 – Conclusion: Conclusions, describing the understanding gained, the implementation of the work, testing of the waveform generators and future work.

2. Literature review

In order to undertake the work, knowledge of the field in general was required. This chapter introduces natural lightning and considers its properties. Because the laboratory is to be used for aeronautical testing; the lightning threat to aircraft is presented in terms of the need for protection, followed by a summary of the international standards required for certifying functionality of the lightning protection. Lastly, an anonymized summary of how other laboratories have implemented waveform generators shows a range of possible approaches to delivering the required functionality of the laboratory.

Without natural lightning, there would be no need to develop test facilities to protect aircraft or structures from it. In order to fully understand what a lightning direct effects test facility must do to inform the designers of protection or qualification systems, natural lightning must be first studied.

2.1. Books for background information

Several authors have gathered a good deal of information regarding lightning and protecting structures from it:

- Martin A. Uman
    - The Art and Science of Lightning Protection [1]
    - The Lightning Discharge [2]
    - All About Lightning [3]
- Vladimir A Rakov and Martin A. Uman
    - Lightning Physics and Effects [4]
- R. H. Golde
    - Lightning Protection [5]
    - Lightning
        - Volume 1: Physics of Lightning [6]
        - Volume 2: Lightning Protection [7]
- Vernon Cooray
    - The Lightning Flash [8]
- Sir Basil Schonland
    - The Flight of Thunderbolts [9]

A historical record of lightning interacting with ships is presented by Hugh Cannell. It discusses in a colloquial way how they have been protected but does not give guidance for how to implement it on newer vessels. Nevertheless it is interesting and useful from the prospective of having a wider view of the subject.

- Hugh Cannell
    - Lightning Strikes – How Ships are Protected from Lightning [10]

While these authors present a good insight into the physics of lightning and how to protect ground based structures, they do not present information regarding information regarding protection of aircraft or the waveforms required to prove adequate protection levels are met; there do not appear to be any books on that matter. Section 2.3 presents the main test standards and a discussion of the test waveforms for aeronautical equipment.

Several books on pulsed power and high voltage engineering have proved useful as a background to the subject:

- H. Bluhm
    - Pulsed Power Systems [11]
- T. H. Martin, A. H. Guenther and M, Kristiansen
    - J. C. Martin On Pulsed Power [12]
- G. A. Mesyats
    - Pulsed Power [13]
- H. M. Ryan
    - High-Voltage Engineering and Testing [14]
- A. Haddad and D. Warne
    - Advances in High Voltage Engineering [15]

Pulsed power usually concerns itself with much faster waveforms than are used with lightning testing, and there again do not appear to be any books directly covering the subject.

A very good coverage of silicon switches if presented by Balgia that proved an excellent insight into how they work and they are discussed in terms of application by Erickson and Maksimovic:

- B. Jayant Baliga
    - Advanced High Voltage Power Device Concepts [16]
- Erickson and Maksimovic
    - Fundamentals of Power Electronics [17]

While attempting to gain insight into how LCR circuits behaved, aside from undergraduate physics texts, 2 more specific books were read:

- Irwin and Nelms
    - Engineering Circuit Analysis [18]
- Gang Lin Luo and Hong Ye
    - Synchronous and Resonant DC/DC Conversion Technology, Energy Factor and Mathematical Modelling [19]

These were insightful and useful to the extent that they showed mathematical solutions for many circuits. Many other lecture notes, presentations and papers were read also – but none had a fully explored stepped response for an LCR circuit that could be used to easily inform useful circuit parameters.

The wide range of books read show that a through literature search was indeed undertaken and demonstrates why the design approach was taken from the ground up. This thesis fills in the gaps by presenting a useful mathematical understanding of LCR circuits and illustrates the decisions behind and methods used to build the lightning waveform generators.

When building circuits, resistance and capacitance is reasonably easy to calculate or specify when ordering components. Inductance on the other hand is more of a geometry based problem. This is especially so for the Fast Waveform Generator, where inductance of the whole transmission lines, connections, switch, output resistor and test rig had to be minimised. For that, the very in-depth book by Grover was often referred to:

- F. W. Grover
    - Inductance Calculations [20]

All books in this section were read during the period of study.

2.2. Lightning Strike Mechanism

This section is a very brief summary of how a lightning strike occurs.

2.2.1. The electric field within thunderclouds

DC electrical breakdown of small (1 to ~50 mm) air gaps requires approximately 3 kV/mm for sphere-sphere gaps, reducing to approximately 1.9 kV/mm for point-plane gaps [21], at room temperature and pressure. While the breakdown voltage with distance is reasonably linear, it is reduced significantly at 1 m to 1 kV/mm and at 10 m to 0.35 kV/mm [22] for switching impulses of 80/2,500 μs for rod-plane gaps. The small air gap values are helpful for building the lightning test facility as it is of the correct order of voltage. The long gap values indicate that as the distance to be broken down increases, there is a slow decrease in the electric field required to do so.

The minimum electric field intensities required to produce a lightning discharge appear to be of the order of 0.4 kV/mm as this was the highest field strength detected in a thundercloud, found by firing instrumented rockets into them [23]. At the reduced atmospheric pressure found high in thunderclouds, it has been shown in laboratories that ice crystals (3 to 20 mm in diameter) start to corona between 0.35 and 0.45 kV/mm [24]. Whereas in similar conditions, a where water drops are present without ice crystals, the voltage required for the onset of corona is increased to 0.9 kV/mm [25]. This suggests the presence of ice greatly increases the chance of a lightning discharge.

2.2.2. The electrification of thunderclouds

Numerous electrification methods for thunderclouds have been presented and are discussed in excellent detail within the books on lightning mentioned in section 2.1. All agree that the electrification is powered by the enormous convective air currents within the clouds but differ in detail regarding how exactly charges are separated. A good review paper of the subject was written by C Saunders, discussing 12 different methods [27].

Whatever the charging effect is, charge does indeed separate and lead to a large dipole distribution, positive at the top and negative at the bottom [28]. There is also, as can be seen in Figure 1, a small region of positive charge at the base of the cloud, which Feynman summarises nicely [29]:

"The top of the thunderstorm has a positive charge, and the bottom a negative one – except for a small local region of positive charge in the bottom of the cloud, which has caused everybody a lot of worry. No one seems to know why it's there, how important it is – whether it is a secondary effect of the positive rain coming down, or whether it is an essential part of the machinery."

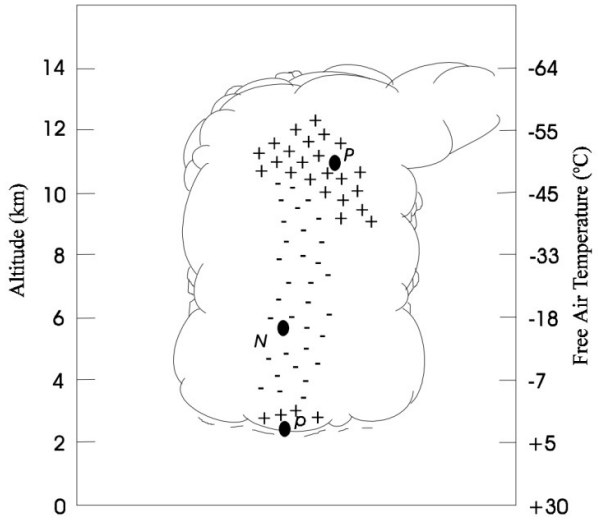

Figure 1 – Charge distribution in a thundercloud [28]

It is interesting to note that Earth's atmosphere has a nominal electric field of ~100 V/m, which extends to approximately 50 km where it is sufficiently conductive to form a uniform shell around the planet with a potential of approximately 400 kV. And that the much higher occurrence of negative lightning (as the large negative charger centre is closer to the ground than the positive) drains negative charge from the atmosphere, thus effectively pumping positive charge into it [29]. A large proportion of this charge is likely lofted from the top of thunderclouds by sprites. These are funnel shaped discharges, starting at a point in a cloud and terminating over a wide area at high altitude [30]. While sprites have been seen by aircraft [31] they do not spear to have posed a danger and are not mentioned in any aeronautical safety standards, whereas lightning is.

2.2.3. The lightning discharge

Here, a typical discharge from a negatively charged region of a cloud to ground is described. It is a summary derived from descriptions by Cooray [8], the lightning test standard ED84 [28] and Feynman [29].

A breakdown within the cloud initiates the discharge. This initiates the very topmost part of a stepped leader structure. This is not particularly bright, but can be seen as a luminous discharge moving 1/6 the speed of light and stepping ~50 m before pausing for ~50 μs. Then, after the pause, stepping another ~50 m in a slightly different direction and repeating. The direction of each hop is generally towards the ground as the strong negative charge in the cloud is attracted to it. On occasion, after one of the ~50 μs pauses, a stepped leader may branch the channel giving rise to forked lightning. When the stepped leaders approach the ground, corona discharges (sometimes several) can be induced from the surface towards them. Whichever stepped leader first connects to the ground initiates the return stroke. The structure created by the stepped leader is at approximately the potential of cloud's negative charge centre as it is electrically connected to it and not earth.

The return stroke is the draining of the stepped leader structure and occurs as a wave of ground potential racing up towards the cloud at the speed of light. If it reaches a fork, then that is drained also. This rapid draining of charge from the structure gives rise to the bright flash associated with lightning and the high currents that pose a hazard to aircraft and other structures.

A continuing current may continue for 10s to 100s of ms after the initial return stroke. During this period, if the sudden grounding of part of the cloud induces subsequent discharges which connect to it, then a dart like leader, swiftly moving down the open channel from cloud to ground will refill the channel with charge. Once this dart leader reaches the ground, a secondary return stroke will again drain the charge and return the channel to near ground potential.

Thus the first return stroke, continuing current and secondary or subsequent return strokes are shown to arise.

2.2.4. The occurrence of lightning

There are approximately 1.4 billion lightning flashes per year over the whole world. With a surface area of 510 million km^2, this gives an average flash density of about 2.7 lightning strikes per km^2. Figure 2 shows a map created by NASA [32], ilustrating that lightning strikes are far from uniformly distributed. The data was gathered over the period of May 1995 to December 2013 by 2 satellites and depicts the average number of flashes per sqkm per year.

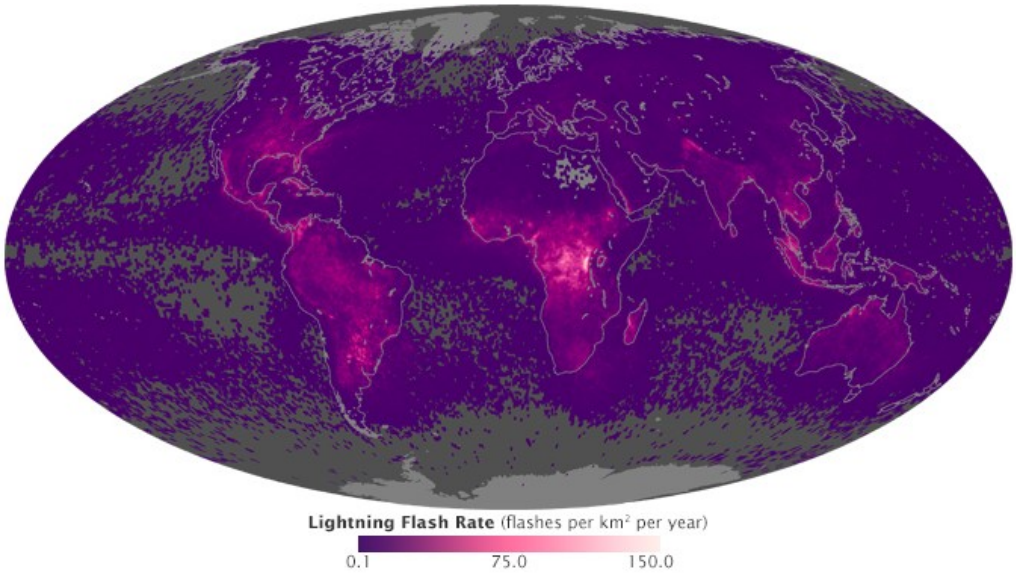

Figure 2 – One year global lightning data from [32]

The flashes can quite easily be seen to concentrate on land, to a lesser extent around the tropics and away from the poles. Further, they are less prevalent in arid regions such as the Sahara, where the lack of thunderclouds and rain give way to desert. At higher latitudes, there is generally a lower chance of lightning, but if present, it has a higher chance of cloud to ground rather than cloud to cloud discharges as clouds are closer to the ground [4].

2.2.5. Polarity

When considering cloud to cloud discharges, polarity is somewhat irrelevant. It is bi-directional and must be between an area that is more positive to one which is more negative or vice versa. However, where cloud to ground discharges are concerned, polarity very much does matter. A majority of the cloud to ground discharges are negative [4]. This is due to the base of the cloud generally being negatively charged and closer to the ground (where an aircraft would be taking off/landing) than the positive top (which aircraft can usually avoid when flying between airports).

The test standard ED-84 [28], presented in Figure 3, shows a model current waveform of a severe negative lightning discharge.

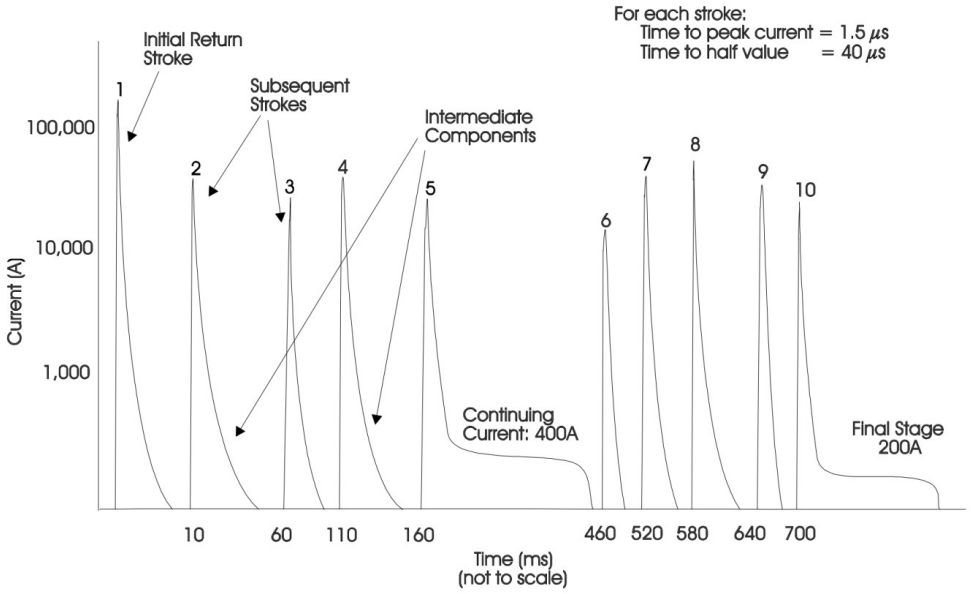

Figure 3 – Depiction of natural negative lightning current examples from ED84 [28]

Figure 3 shows fast rates of rise to high current levels, and quite short but varying decay times with some having a continuing current after the flash. As noted in section 2.2.3, an initial return stroke can be followed by several subsequent return strokes through the same arc channel.

The positive lightning waveform is depicted with a very different model as shown in Figure 4 where the standard shows a single slow waveform with none of the subsequent strokes of the negative discharge.

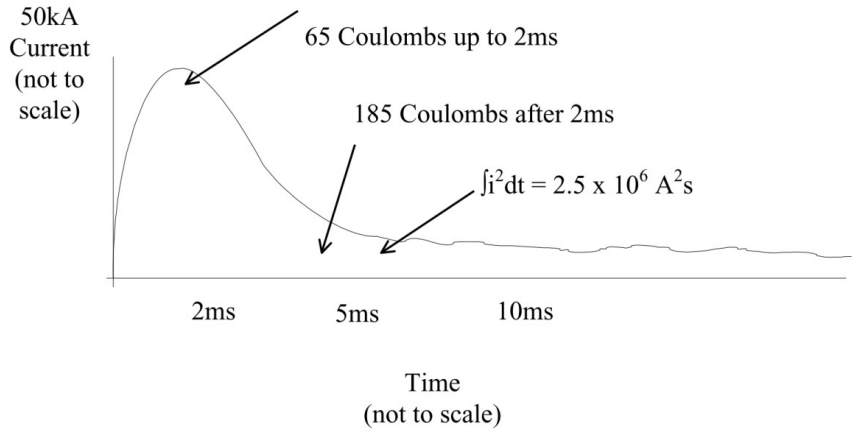

Figure 4 – Depiction of natural positive lightning current examples from ED84 [28]

While positive lightning strikes are less frequent than negative strikes, they pose a different and significant threat as they are often more powerful.

2.2.6. How powerful is lightning

Table 1 summarises data from ED84 [28] including, the peak current, charge and action integral parameters shown for natural negative lightning to ground strikes. The 95% column gives a level for which 95% of strikes have higher or harsher parameters than the figures listed (for the continuing current, 98% is used for the continuing current). Thus, the 5% values, representing a much smaller proportion of the total lightning strikes with a particularly high level; only 1 in 20 strikes expected to be above this. The statistical distribution of lightning parameters is not Gaussian – lightning current cannot approach infinity at the furthest extreme nor exist without a current magnitude of at least a few kA.

The term used to describe how powerful the current waveforms are is action integral. The energy delivered to a sample is the integral of the instantaneous product of the current and voltage across it, this is equivalent to the action integral multiplied by the resistance of the test object. Action integral has interchangeable units of A^2s or J/Ω.

Table 1 – Natural negative lightning parameters [28]

Negative Flashes	Units	95%	50%	5%
Number of strokes		1.5	3.5	12
Time intervals between strokes	ms	8	35	140
Charge in flash	C	1.3	7.5	40
First stroke peak current	**kA**	**14**	**30**	**80**
First stroke action integral	A^2s	6E+03	6E+04	6E+05
First stroke charge	C	1.1	5.2	24
Subsequent peak current	**kA**	**4.6**	**12**	**30**
Subsequent action integral	A^2s	6E+02	6E+03	5E+04
Negative subsequent charge	C	0.2	1.4	11
Continuing current in negative flashes		98%	50%	2%
Continuing current amplitude	A	33	140	520
Continuing current charge	C	7	26	110
Total charge in aggregate waveform	C	8.3	33.5	150
Total action integral of aggregate waveforms	A^2s	7E+03	8E+04	1E+06

Note the last rows of Table 1, where the parameters are summed into an effective aggregate waveform. The purpose of aggregating the waveform parameters is to ensure that where a single conductor may carry all current, it can be applied with the three waveforms and not require both first and second return strokes.

Table 2 shows the peak current, change and action integral for positive lighting strikes; the list of parameters is much shorter due to being a single impulse rather than a series of impulses.

Table 2 – Natural positive lightning parameters [28]

Positive Flashes	Units	95%	50%	5%
Peak current	kA	4.6	35	250
Charge	C	20	80	250
Action integral	A^2s	2.50E+04	6.50E+05	1.50E+07

Measurements of peak current from 60 transmission towers are summarized in Figure 5 [33]. Up to 120 lightning currents have been recorded for negative downward strikes. The highest current measured was 130.2 kA. The graph shows the peak current plotted against the cumulative probability (calculated for a given lightning strike as the proportion of strikes having equal or more current). While the x-axis is logarithmic, the y-axis appears to be an arbitrary scale fitted to make the distribution a straight line.

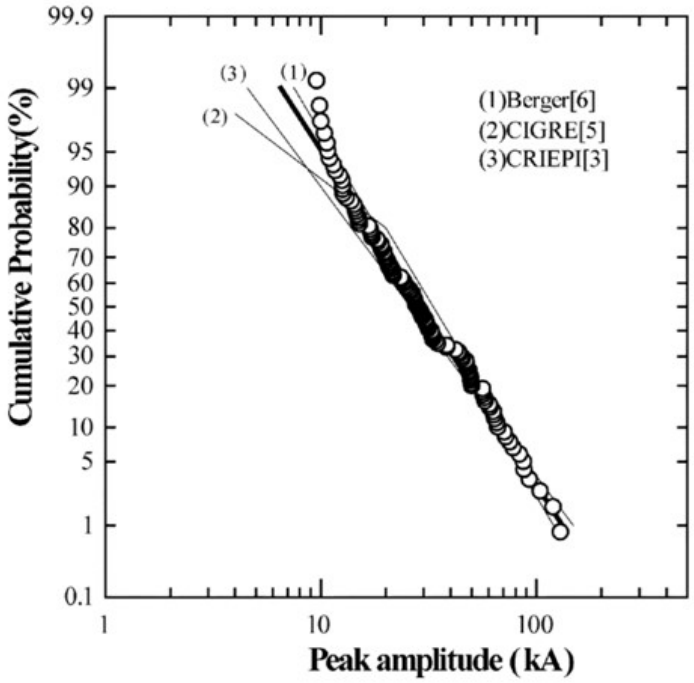

Figure 5 – Lightning current vs probability [33]

At no point in the standards is a voltage mentioned in association with a lightning strike. The voltage along the whole lightning path is irrelevant for protecting

aircraft or other objects from it, as an exceedingly large proportion of the voltage is dropped carrying current across the several km length of arc. This is likely 1 MV per km for lightning relevant currents between 7 and 100 kA [34]. While an object with even 0.1 Ω of resistance would have a voltage drop across it only of the order of 10 kV for a 100 kA current. This is perhaps 100^{th} or 1000^{th} of the voltage across the whole lightning arc, and so lightning can be viewed as a very high impedance current source compared to any expected load, aircraft, building or test sample.

2.3. Aircraft testing

2.3.1. Why lightning testing?

Aircraft are frequently struck by lightning – roughly once in every 10,000 hours of flight [35]. Large aircraft that have sufficient size to cause a perturbation to the electric field near stepped leaders have an increased chance of being struck, and often initiate the lightning strike themselves [36]. For example, a volume of air or cloud that has a field strength too low to initiate corona from present particles, whether ice or water, will not initiate a breakdown and lead to lightning. But when a large conductive aircraft flies into it, the whole structure will become polarised by the ambient field. If for example the aircraft is flying towards a negative charge centre, its nose will become strongly positive and the tail strongly negative. The field is thus enhanced in the air around the aircraft and corona is induced. Having induced the corona, it can rapidly extend through the air along the field lines of the ambient electric field, much like the initial leaders of a lightning strike. The corona extending from the aircraft effectively enlarges the conductive structure perturbing the ambient field and may trigger a lightning strike. This mechanism leads to aircraft being struck approximately 10 times more than would be expected for a given volume of air the same size as one and has a greater effect on larger aircraft than small as they perturb the field more.

Table 3 shows a record of significant lightning events where there was loss of life. While unlikely a complete list for the world's fleet of aircraft, it does show that aircraft can and have been disastrously affected by lightning. Gladly, the work undertaken in developing standards and studies using the state of the art facility such as the one constructed at Cardiff, ensure that lightning rarely has a disastrous effect on an aircraft.

Table 3 – List of aircraft lightning disasters

Date	Carrier/info	Location	Aircraft	Losses
26/06/1959	Trans World Airlines [37]	Milano (Italy)	Lockheed L-1649A Starliner	All (68)
12/08/1963	Air Inter [37]	Lyon (France)	Vickers 708 Viscount	All (20) + 1 ground
08/12/1963	Oan Amercian World Airways [37]	Elkton, MD (USA)	Boeing 707-121	All (81)
24/12/1971	LANSA [37]	Puerto Inca (Peru)	Lockheed L-188A Electra	91 with 1 survivor
09/05/1976	Islamic Republic of Iran Air Force [37]	Madrid (Spain)	Boeing 747-131F	All (17)
05/09/1980	Kuwait Air Force [37]	Montelimar (France)	Lockheed L-100-20 Hercules	All
08/02/1988	Nürnberger Flugdienst Flight 108 [37]	Mulheim (Germany)	Swearingen SA.227AC Metro	All (21)
17/04/1999	Tail no GPB, BGA 3705 [38]	Northall (UK)	Schleicher ASK 21	None, 2 survived
16/07/2002	G-BJVX [39]	Near the Leman 49/26 Foxtrot platform in the North Sea	Sikorsky S-76A+	All (11)
22/02/2008	G-REDM [40]	North Sea, approximately 165 nm north-east of Aberdeen	Eurocopter AS332L2 Super Puma	None, 17 survived
25/09/2001	G-RJXG [41]	Manchester (UK)	Embraer EMB-145EP	None, 21 survived
21/01/2005	G-TIGF [42]	Dutch Sector, North Sea	Aerospatiale AS332L Super Puma	None, 2 survived
03/03/2006	G-CHCG [43]	104 nm north-east of Aberdeen VOR/DME	Eurocopter AS332L2 Super Puma	None, 20 survived
19/01/1995	G-TIGK [44]	Near Brae 'A' oil production platform	Asrospatiale AS332L	None, 18 survived

Date	Carrier/info	Location	Aircraft	Losses
15/02/2000	G-TIGT [45]	Approximately 4 nm west of Brent B oil rig	Asrospatiale AS332L	None, 20 survived
17/11/1999	G-BHBF [46]	3 nm northeast of Coltishall, Norfolk	SIKORSKY S76A (MODIFIED)	None, 5 survived
22/02/1999	G-PUMM [47]	Peterhead, 20 nm north-east of Aberdeen, Scotland	AS332L	None, 19 survived
12/12/1997	G-BWZX [48]	10nm East South East of Sovereign Explorer Oil Rig	Eurocopter AS 332L	None, 11 survived

2.3.2. Lightning Test Standards

For building a lightning test facility, there are several standards that need to be adhered in order to comply with and provide a service for lightning safety certification. A laboratory that complies with the standards would be suitable for both academic research and commercial lightning testing.

- STANAG-4236 – Lightning Environment [49]
    - A description of the lightning environment that NATO aircraft are expected to withstand
- ED-113 – AIRCRAFT LIGHTNING DIRECT EFFECTS CERTIFICATION [50]
    - Describes how aircraft and aircraft components can be certified against lightning direct effects – guidance on how to use test facilities and lightning test standards
- ARP5577 – AIRCRAFT LIGHTNING DIRECT EFFECTS CERTIFICATION [51]
    - US version of ED-113
- ED-14G – Environmental Conditions and Test Procedures for Airborne Equipment [52]
    - Describes which waveforms should be used for particular aircraft systems, briefly the waveforms themselves and how to perform the tests
- DO-160 – Environmental Conditions and Test Procedures for Airborne Equipment [53]
    - US version of ED-14

- ED-84 – AIRCRAFT LIGHTNING ENVIRONMENT AND RELATED TEST WAVEFORMS [28]
    - A complete description of the test waveforms used to certify aircraft lightning safety
- ED105 – AIRCRAFT LIGHTNING TEST METHODS [54]
    - A description of the test methods that are expected to be applied to aircraft in order to certify they are sufficiently protected from lightning strikes

2.3.1. Types of tests

The direct effects lightning tests involve either conduction of current or the attachment of the lightning arc root. Both of these may be used to prove fuel systems are safe for flight.

Attachment tests are relevant for components or structures that are likely to be struck, such as wing tips, landing gear, propellers etc. These are points of high electric field located at the extremities of the aircraft or anything that protrudes. It is also relevant for any structures which may move into the lightning arc after it has been initiated at another part of the aircraft.

Attachment tests are performed by mounting a sample in a test rig and positioning an electrode approximately 100 mm above the sample's surface. This would require a large voltage (about 300 kV) to break down; much higher than most direct effects lightning test machines use. Further, it can be unpredictable where an arc may choose to attach if driven by breakdown. Therefore, a fine filament of wire is often used to direct it and reduce the voltage needed for the test.

Figure 6 shows the recommended arc diverter electrode [54] from ED105. This is required to prevent erosion products (molten and oxidised metal) of the electrode contaminating the arc attachment to the sample surface. The stream of ejected metal from the electrode is referred to by the standard as the arc jet.

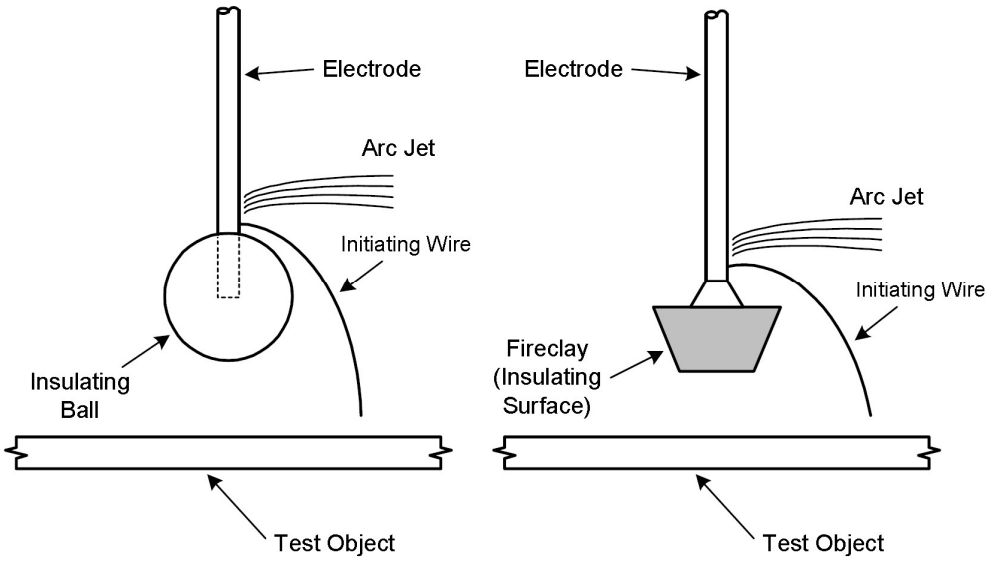

Figure 6 – Arc attachment test diverter electrode examples from ED105 [54]

Conduction tests are simpler than arc tests. The sample is bolted into a test rig and a sturdy conductor is used to target the lightning current waveform to the desired attachment point.

For structures, such as landing gear, wing tips, fuselage or engine housing etc., both attachment and conduction tests may show that a sample component can carry the current without breaking or otherwise being damaged. For example, it is important that hinges or bearings do not weld and that magnetic forces do not deform the structure.

For fuel system tests, sparking and ignition are looked for. This can involve photography to record light from sparks or flammable gas to show whether or not an ignition hazard was present. The photography and flammable gas tests are more sensitive to sparks than aeronautical fuel. This ensures a margin of safety can be proven by the tests.

The material types tested are any that can be used in an aircraft; generally light structures made from aluminium alloys or carbon composites. Aluminium has been the main skin material for aircraft since before the dawn of high volume passenger travel. More recent passenger aircraft are using an increasing amount of composite/man-made materials.

Aluminium being a conductive material, is excellent at carrying lightning currents without much heating or damage (resistivity of aluminium = 2.8 e^{-8} Ωm). Aluminium has the same resistivity in all directions as it is homogeneous.

Carbon fibre composite is not a homogeneous material. It is usually made from sheets of woven or unidirectional material, layered to the required thickness and bound with epoxy. The conductivity is highest along the length of the fibres and least through the layers. This is simply due there being no insulating epoxy resin along the length of the fibres [55].

2.4. The lightning test waveform(s)

The relevant waveforms for building a direct effects test facility are given in ED84. The most common waveforms used in lightning testing are summarized in Table 4.

Table 4 – Lightning test waveform parameters [28]

Waveform	Current	Charge (C ± 10%)	Action (x 10^6 A^2s)	Rise time max (us)	Duration nom (ms)
A	200 kA ± 10%	n/a	2	50	n/a
Ah	150 kA ± 10%	n/a	0.8	37.5	n/a
D	100 kA ± 10%	n/a	0.25	25	n/a
B	2 kA average	10	n/a	n/a	5
C	200 to 800 A	200	n/a	n/a	500
C*	Min. av. 400A	0.4 to 40	n/a	n/a	5 to 50

The A, Ah and D are high current waveforms, B is the intermediate current waveform and C and C* are the trailing currents waveforms. For the A, Ah and D waveforms, the maximum rise time is used to constrain the front of the waveform. For these waveforms no nominal duration or fall time is specified as that aspect is constrained by the action integral. The waveforms are described separately and in more detail in later sections.

Lightning is a complex waveform and the test standards simplify the application of it, by breaking it down into the application of 1 of 3 initial discharge (A waveform, Ah waveform and D waveform), an intermediate moderate current discharge (B waveform) and the trailing component (C waveform or its truncated from C* waveform).

The A waveform is for parts of the airframe that is hit by the initial return stroke of the lightning. The Ah waveform is similar in application as A waveform but for high

altitude cases only. The D waveform is for parts that are likely to be hit with a restrike (once the lightning arc has been swept back from the initial attachment point).

The initial discharges are described in the test standards as follows: A waveform, Ah waveform and D waveform are 200, 150 and 100 kA impulses, with action integrals of 2 x 10^6, 0.8 x 10^6 and 0.25 x 10^6 A^2s, respectively. In the standard, these are described using double exponential equations as well as maximum time to peak current and the action integral that must be delivered, and the tolerances for each.

The B waveform is an intermediary between the fast, high current waveforms and the trailing component. By using it, the laboratory test waveform shape more closely approaches that of natural lightning. It is described essentially as the delivery of 10 C of charge within 5 ms. However, it is also described as a double exponential waveform, similar to the fast impulses but much lower current (4 kA) and longer in duration.

The C waveform is the trailing component and described as a 400 A discharge for 500 ms, delivering 200 C. The truncated form is called the C* waveform and is simply a shorter version of the C waveform, often 20 to 50 ms in duration and delivering 8 to 20 C, respectively.

Tests following aeronautical standards generally require a composite waveform comprising 3 test waveforms depending on the location of the interest on the airframe. For the nose or forward facing attachment points, the waveforms are A, B then C*. For areas where the waveform can be swept back onto and then off again, the waveforms are D, B then C*. Finally, for the rearmost attachment points, the waveforms are A, B then C.

The high current waveforms are described consistently, with a peak current that must be attained within a given period of time and a total action integral to be delivered. Only a single high current waveform would be used in a test.

The intermediate and trailing currents are less consistently described. This appears to an attempt to allow a wide scope for delivering the waveforms rather than matching the shape of natural lightning. The B waveform represents an initial moderately (1/100th of waveform-A and 10 times that of waveform C) high current

and is then followed by either the C or C* waveforms. Thus, generally there are 2 waveforms used together to make up the trailing component.

All 3 high current waveforms as well as the B waveform can be described using a double exponential equation. These take the form of equation (1).

$$I = I_0\left(e^{-\alpha t} - e^{-\beta t}\right) \quad (1)$$

Where:

- I_0 is a scaling factor and has the units A
- α describes how fast the waveform decays and has units s^{-1}
- β describes the waveform rise time and has units s^{-1}

The α and β terms are somewhat interactive and, if complex numbers are used, can describe a ringing waveform. Perhaps thankfully, the parameters given in the standards are real rather than complex and all the described waveforms are unipolar and slightly over damped. Table 5 summarizes the parameters for the most important reference waveforms as described in ED84 [28].

Table 5 – Lightning test waveform double exponential parameters [28]

Waveform	I_0 (A)	α (s^{-1})	β (s^{-1})
A	218,810	11,354	647,265
Ah	164,903	16,065	858,888
D	109,405	22,708	1,294,530
B	11,300	700	2,000

It should be noted that the waveforms described in Table 5 are the reference waveforms and are presented by the standards as a possible solution, but they are not the only allowable solutions. For example, the peak current for the A, Ah and D waveforms has a tolerance of ±10% which if implemented would scale I_0 for the resultant waveform. The waveforms are also allowed significantly longer times to peak and do not have to be unipolar. A longer time to peak reduces β and a slower overall waveform would reduce both α and β. A critically damped waveform cannot be described by Equation (1) as in that instance, α and β are equal and the exponential terms cancel. For an underdamped waveform, α and β become

complex numbers and can again be used in the equation. In this latter case, the waveform becomes a damped sinusoid.

Section 3.5 explores the mathematical solutions for the waveforms in greater detail and the solutions for generating each potential waveform are presented also.

Figure 7 shows plots of waveforms A, Ah and D using the data from Table 5 with Equation (1). Each is a lower current version of the last. Interestingly the maximum di/dt of each waveform is the same. Because of this, the lower the current, the faster the peak is reached.

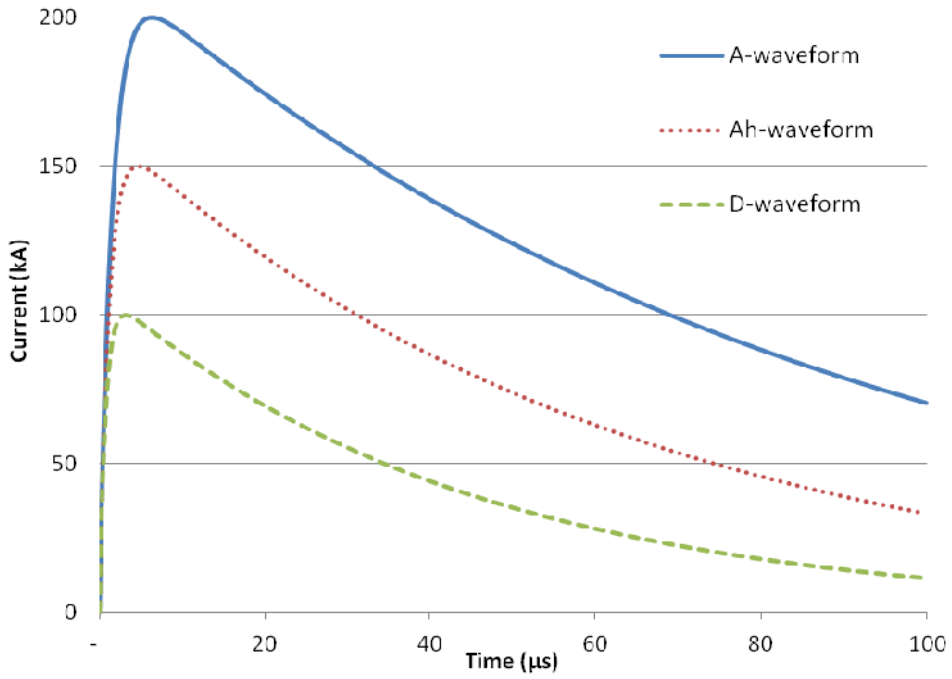

Figure 7 – Plots of high current test waveforms from Table 5, using Equation (1)

The trailing component waveforms are significantly lower in current than the A, Ah and D waveforms. Figure 8 shows the lowest part of the A waveform together with the double exponential B waveform and the square-wave C waveform. The B waveform, often described as the intermediate waveform can clearly be seen to act as a buttress between the A and the C waveforms.

While the reference B waveform is described with a double exponential, it is primarily required to deliver 10 C within 5 ms and is not expected to extend (or count as the B waveform) beyond that point. It can clearly be seen that the tail of the B waveform quite neatly lines up with the C waveform. As such, it is expected

that the very tail of the B waveform would contribute to the start of the C waveform.

The C waveform is presented as a 400 A square-wave, starting at 5 ms, immediately as the B waveform finishes. In both Figures 8 and 9, it is depicted as ending at 10 ms; where it would deliver a charge transfer of 2 C from its 5 ms duration. This is much shorter than would usually be used but was chosen for clarity of the figures. It is trivial to imagine the square-wave extending 50 times wider than the graph. Various alternate scales were experimented with to present the waveform shapes and non were found to be satisfactory due to distortion of the A and B waveforms.

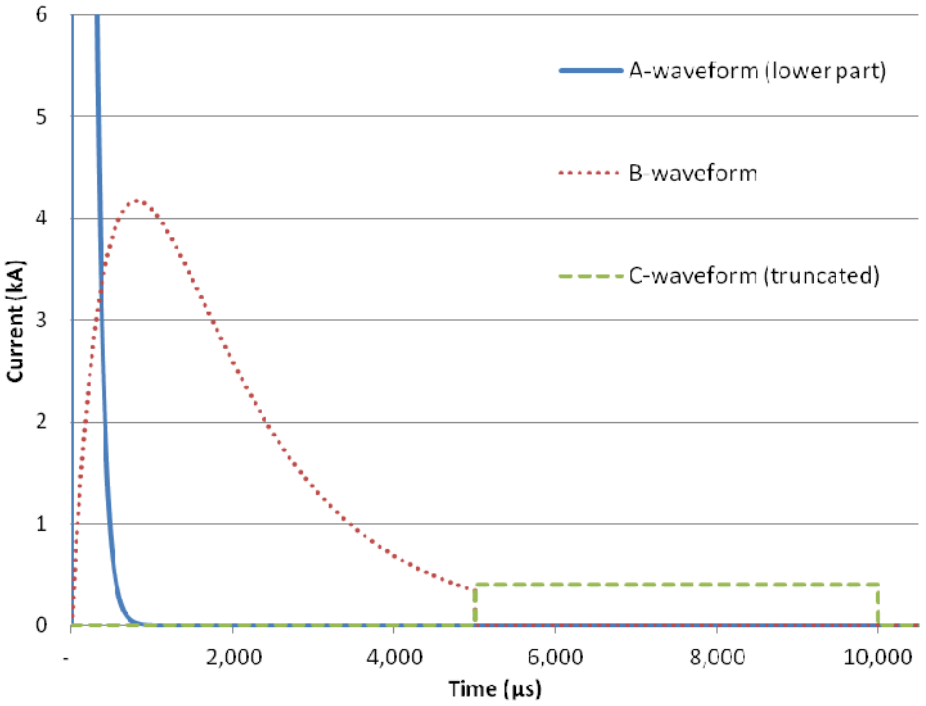

Figure 8 – Plots of trailing component waveforms

Figure 9 shows the combined current of the 3 waveforms presented in Figure 9. The A waveform can be seen to quite neatly tie in with the B waveform. The faster decaying Ah and D waveforms would have a small valley before the B waveform peak.

As there is wide latitude for how to implement the waveforms, these figures should only be considered examples of how it could be achieved and not a verbatim must. For example there is no requirement for the small step between the end of the B

waveform and the start of the C waveform. The transition could be seemless which for any implementation where they share an inductor between the generators and the load would likely be the case.

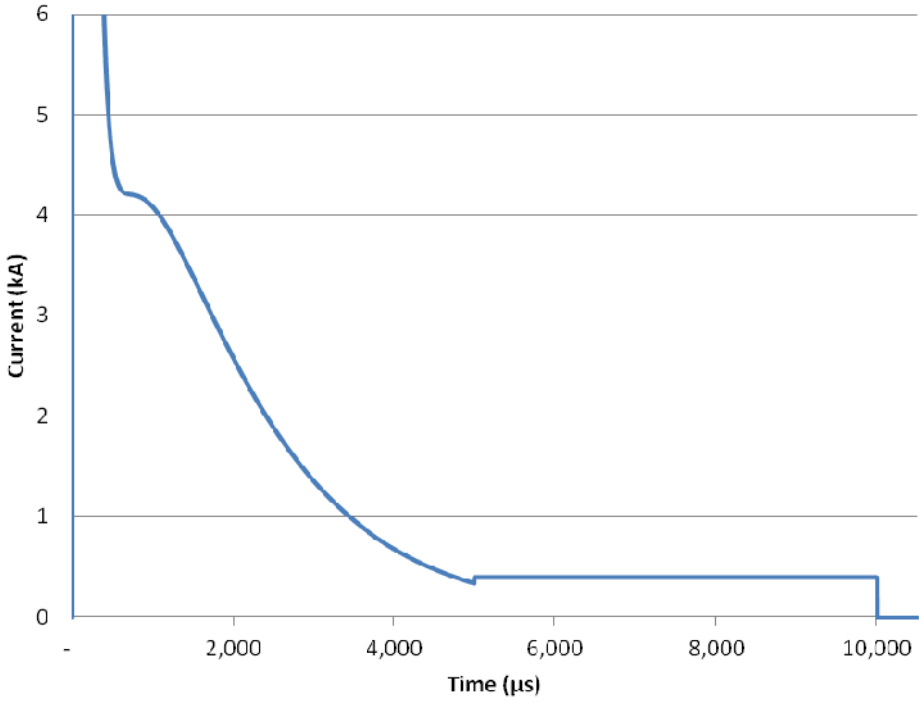

Figure 9 – Composite lightning test waveform

It is interesting that for a lightning strike that attaches to the nose and tail of an aircraft, the A waveform would be used for testing both attachment points. For the nose, the trailing component would consist of the B and C* waveforms whereas for the tail it would be the B and C waveforms. As the airframe moves between restrikes, these would attach to fuselage behind the initial strike, and so hop back across the airframe. At these attachment points, the test waveforms applied would be D, B and C*. As the rear attachment point cannot be swept backwards, all restrikes would be carried by that one point. This perhaps raises the question as to whether or not the rear attachment point should be tested with a combined waveform of A, B, C*, D, B, C* etcetera as opposed to a single set of A, B, C waveforms. The former would certainly have a higher action integral from the additional D waveforms even. However, this is not how aircraft are tested and the latter set of waveforms is used, ignoring any restrike currents. This may appear to under test the rear attachment points. Further consideration of this is beyond the scope of this thesis.

2.5. Other laboratories

Information regarding Sandia Lightning Simulator (SLS) is from published literature and it is described in section 1.5.1. Other laboratories are presented anonymously and discussed only in terms of their waveform generators and without complete circuit parameters to ensure no breach of confidence. This is due to the commercial nature of the systems. The information has been gathered over many years of working in the industry, discussing work with other laboratory technicians as well as visits to many of the facilities. The most illuminating discussions have been with those who have built the other laboratories. The waveform generators from these anonymized laboratories are described as Lightning Waveform Generator 1 through 8 and are presented in sections 1.5.2 to 1.5.9.

2.5.1. Sandia Lightning Simulator

The Sandia Lightning Simulator (SLS) [56], can produce both A and D like waveforms. It is unique in that it can first inject the A like waveform, start the continuing current of the C like waveform and then inject a D like waveform. The system is presented in Figure 10.

These waveforms are not quite the same as used in aircraft testing, because the generator was designed to qualify nuclear weapon safety components and systems. Since such systems could be in a harsh environment, the test parameters are somewhat tougher than for aircraft. The return stroke, or A-like waveform, has about 40 C of charge compared to the 16 C called for in aeronautical standards.

The SLS comprises Marx generators, insulated with oil and housed in steel tanks. These generate the 200 kA A-like and 100 kA D-like waveforms. The C-like waveform is generated by a motor generator set, which uses its own inertia to store energy and release 100s of A for 100s of ms.

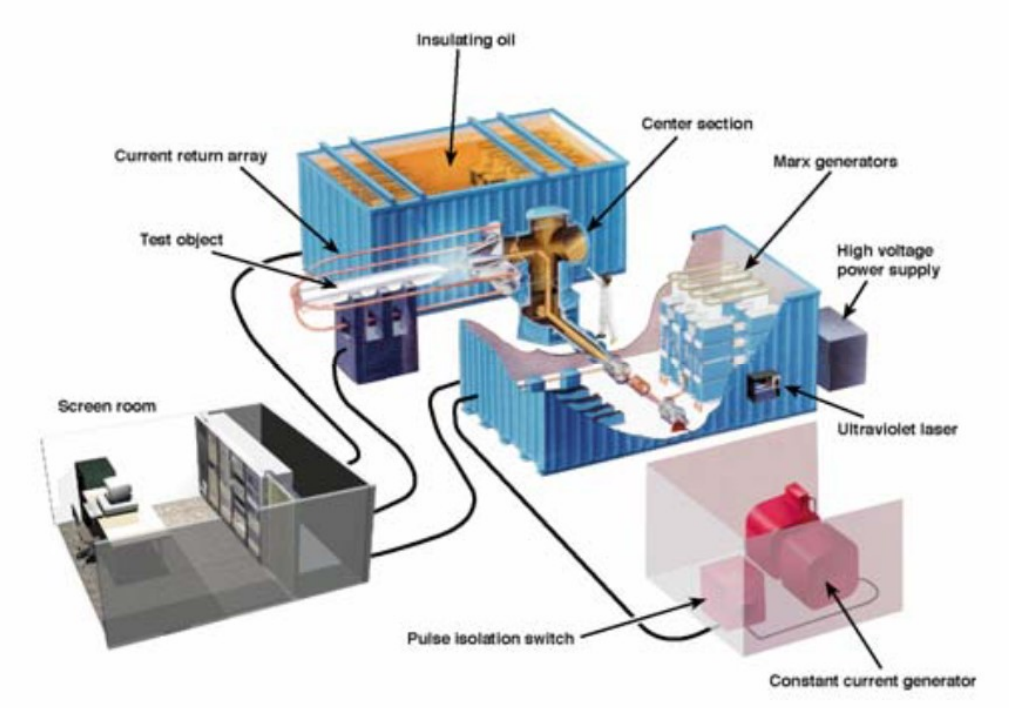

Figure 10 – Sandia Lightning Simulator

2.5.2. Lightning waveform generator 1

A plurality of Marx generators in parallel are used to produce the high current waveforms A, D etc. They are arranged in a horseshoe around the test sample, where their current paths meet and combine. By virtue of this, different numbers of Marx generators, charge voltage and added circuit resistance allow for a wide variety of current waveforms. Since there was no clamp circuit present, the charge delivered by the system is limited by what was initially stored in the capacitors in the Marx generators. Therefore, increasing the number of generators in parallel allows for a larger area under the curve for a given voltage or a longer tail for a given peak current. This can also be accomplished by higher initial charge voltage. The peak current is controlled by adding circuit resistance. Furthermore, combining the current paths at the sample allows each Marx generator to only have to overcome its own inductance and that of the sample. The horse shoe arrangement keeps the current paths the same for each Marx generator and spreads their effective current loops out as much as possible. This makes the generator predictable (by having the same inductance in each Marx generator) and keeps the overall inductance reasonably low (parallel paths).

C and C* waveforms are generated by discharging a capacitor bank through a high power rheostat in series with the load. Removing charge from the capacitor bank through a pulse would lower the driving voltage; this is overcome by lowering the circuit resistance with the rheostat, allowing a flatter current waveform.

The B waveform was not addressed with this system and despite being in the test standard, those that ran the laboratory considered it unnecessary.

2.5.3. Lightning waveform generator 2

A single capacitor bank was used to generate all the high current waveforms A, D etc. The flexibility of the machine comes from the diode crowbar circuit. It operates by the capacitor bank ringing current into the inductive output structure (including the sample holder) and allowing the diodes to naturally commute at the zero voltage crossing. By varying the initial voltage and the resistances of the output and crowbar resistors, a wide variety of waveforms can be produced.

The diode stack had many parallel paths which used resistors for current sharing. To keep inductance as low as possible, each series chain of diodes and resistors had semi-coaxial return paths around it (4 threaded rods which both carried the current and the clamping force). The fast waveform switch was a pneumatically operated open air moving spark gap.

The C and C* waveforms were generated using a large lead acid battery bank. This effectively acted as a constant voltage source. Its internal as well as an external resistance were used to control the current. The external resistance is mostly in the form of a resistive inductor that serves the purpose of preventing the high current waveforms from entering the battery bank as well as stabilising the output current. It was switched using a large relay contactor with internal arc horns to facilitate turning off the relatively high voltage DC current.

This machine did not produce the B waveform.

2.5.4. Lightning waveform generator 3

To generate the high current waveforms A, D etc. a large capacitance 2 stage circuit resembling a Marx generator (weighing approximately 15 tonnes) was used. The capacitance could be varied by disconnecting sets of capacitors or only using a single stage - by also varying the output resistance and charge voltage, a range of waveforms were achievable.

The variable output resistor comprised many series linked low inductance stainless steel elements. Resistance was varied by shorting out a number of the elements.

It was possible to vary the inductance by increasing the gap in part of its distributed stripline structure from approximately 4 mm to 1,500 mm over a width of approximately 2,500 mm.

The capacitors in one stage were charged positively, while those of the other stage were charged negatively. The positive bank frame was hard earthed while the negative was soft earthed through a large high voltage resistor. The main discharge switch was a single triggered spark gap that connected the positive of the first bank with the negative of the second, thus, elevating the frame connection of the negatively charged capacitor bank to double the charging voltage and initiating the waveform. For low voltage operation, a pneumatically operated conductor could be used to bridge the spark gap.

The inductance of the whole system was circa 3.5 μH with the load attached.

The B and C or C* waveforms were generated together by ringing current into an LC circuit, then sometime after the peak (which forms the B waveform), a crowbar was fired across the capacitor bank, shorting it out and allowing the current freewheel through the inductor to create C or C* waveforms. This part of the circuit was switched with ignitrons. It used a much smaller inductor for the C* waveform than when producing the C.

Anecdotally, a lesson was learned regarding flash over to concrete floors. It was suspected that a carbon fibre filament from an earlier test came to rest upon an insulator and bridged it to the concrete. This short circuited the high current part of the generator, bypassing its output resistor and discharging with an exceedingly high (estimated between 1 and 2 MA) current through the concrete to the reinforcement. This blew a crater in the concrete and shattered windows.

2.5.5. Lightning waveform generator 4

The high current waveforms are produced in much the same way as lightning waveform generator 3 (it was built to replace it), but with a higher designed output voltage to allow more margin for day to day use and the ability to increase output current and action integral on the occasion that a customer requested it (such requests for custom waveforms occurred occasionally).

The B and C waveforms were generated separately. The B waveform was produced using an LCR circuit and switched with an ignitron. The C and C* waveforms are produced using the partial discharge of a very large, low voltage capacitor bank (a recycled physics experiment PSU), controlled by an IGBT semiconductor switch. While low voltage in comparison with the other capacitor banks, it had sufficient excess voltage to allow a large series resistance to stabilise the output current.

2.5.6. Lightning waveform generator 5

This generator could produce reduced current A, Ah and D waveforms, but not the trailing components (B, C and C*). It was mainly used for offsite testing where the reduced current waveform was used to induce electrical transients in airframes. The topology was an LCR circuit, using an array of high voltage capacitors and was discharged using a pneumatic spark gap. The generator was mounted on several trolleys allowing for movement offsite.

In order to match the capacitance to individual airframe plus return conductor inductance, the output resistance could be varied. This was accomplished using a variable distance between copper plates in a liquid resistor. It was switched using a pneumatically operated open air spark gap. This comprised 3 electrodes – 2 stationary ones connected to the circuit and a 3rd electrically floating electrode that could be swung through the gap to trigger it.

Anecdotally, a lesson was learned regarding protection resistors. The charging resistor, which comprised a long chain of disk resistors, assembled around a single nylon threaded rod, exploded. This occurred after repeated rapid cycling of the generator over-heated the resistor, carbonising the outside of the nylon rod. This then tracked, causing an arc within the resistor, which blew it apart dramatically.

2.5.7. Lightning waveform generator 6

The system comprised a series/parallel array of capacitors arranged and charged as one larger capacitor. This was discharged through a triggered spark gap and resistance into the inductance of the load and circuit. For the D waveform, this was sufficient to generate the waveform. However, to generate the larger A waveform, the capacitance was too low to deliver the longer tail. So, a clamp circuit was used to allow the current to recirculate in the load circuit and a small additional resistance. To discharge the main capacitor bank, a 3 electrode gap was used

(Trigatron configuration). A much higher voltage was used to fire the clamp circuit than was present on the main capacitor bank. Rather than a compact trigger unit, this used a large, off the shelf Marx generator to generate this trigger pulse. The complex set of spark gaps was apparently quite challenging to set up for a given test.

The inductance of the whole system was approximately 2.5 μH with the load attached.

The C waveform was produced using a lead acid battery bank. There was no attempt to produce the B waveform.

2.5.8. Lightning waveform generator 7

This generator was predominantly designed for testing wind turbines rather than aircraft parts, but is included due to similarities. The waveform used for such tests has a very long tail and much higher action integral than that of the A or D waveforms.

The waveform used for testing wind turbines is commonly referred to as the 10/350, depicting the rise time of 10 μs and time to half peak of 350 μs. This has approximately 5 times the area under the curve and thus, 5 times the energy and charge delivered than in an aeronautical A waveform (10^7 J/Ω opposed to 2 x 10^6 J/Ω).

To deliver such a waveform, the only practical solution was to use a clamped circuit. This necessitated a fairly high voltage, partly to make the output reasonably stable but also due to the fact that a large test object has a large inductance due to large dimensions of wind turbine blades.

While exact circuit parameters were not disclosed for commercial reasons, it was a point of pride that their trailing current or C-like waveform, could be extended for 1000s of C; again, much more severe than required for aircraft testing.

2.5.9. Lightning waveform generator 8

The closest fit to the A waveform specification that a test facility can generate, is accomplished by lightning waveform generator 8. It is similar to a single unit of the oil insulated Marx generators described at Sandia. However, it was designed to operate into a 10 uH load, such a massive, hanger scale return structure designed to house whole aeroplanes. The circuit requires around 200 kJ and a voltage just

under of 600 kV. The clamp is a spark gap with electrodes separated by a tube filled SF_6 gas that ceases to be an insulator once a large laser is fired through it.

The mentioned return structure is best imagined with the waveform generator injecting current into the nose of the aircraft. It was a series of conductors that connected the ground connection of the generator to a rear attachment point of the aircraft. The spacing of the conductors from each other and from the aircraft was designed such that the current density distribution was close to that if it were in free space. If the current was returned using a single conductor draped along the floor under an aircraft, the current injected would tend to flow near the return conductor due to the inductance of the structure and it requiring the least amount of energy to do so.

While designed to deliver 200 kA waveforms, this waveform generator is usually only used at much lower currents to avoid stressing test airframes with the full current. This requires scaling up measured cable loom currents and voltages appropriately.

This generator was custom built by a 3rd party for the company that uses it and was quite expensive. When performing scaled down current waveform tests, it performance is exactly the same as "Lightning waveform generator 5", which was assembled with available components and as such was not at all expensive.

3. Description of the general laboratory and special consideration

3.1. Introduction

In order to perform lightning testing, many systems are required and they all needed to be housed in the relatively small facility. Firstly, somewhere was needed to put a sample and test it. Since the tests are both loud and messy (because samples can explode), a test chamber with adequate ventilation was required. To generate the waveforms, large, well-insulated waveform generators were required and these had to be housed within a safety interlocked HV area. Control and diagnostic systems as well as a place for staff, students and customers had to be made available. Many items had to be considered and scoped before any one of them could be committed to. The budget for the project was circa £1.75M with an additional contribution of equipment from a decommissioned laboratory of the industrial partner. This chapter outlines the considerations behind many of the decisions that led to the final layout of the test facility.

3.2. Main components to design and fit into the space

The standards call for a high current waveform, followed immediately by the trailing component, which is itself made from 2 different shaped waveforms. This calls for 3 waveform generators, which were required to be variously flexible. Each generator requires energy storage, a method of charging and discharging it safely, trigger systems and a pulse forming network. These had to be coupled together and fed using appropriate sized cables and bus bars into the test chamber.

The test chamber and waveform generators had to be in an interlocked HV area in order to keep staff safe from accidental exposure to HV. At the minimum, current diagnostics were required to record the test waveforms. Provision of space for voltage and optical (photographic) diagnostics also had to be made available.

A control room, in which operators may safely run the machine, take measurements and discuss the test with customers, was required. For maximum safety, this had to be a sound-proof and earthed structure, and all interfaces with the HV area were required to be either via fibre optic or pneumatic means. All control voltages were to be 24 VDC or less – both within the HV area and from the safety system into the control room.

Additionally, a small workshop for building the laboratory and later for test rigs was required, along with storage for spares and components given to the lab.

3.3. Size of generators vs. space available

All the other laboratories visited prior to setting up the MBLL had a good deal of space available. This enabled the space to fit the generators with a great deal of convenience – in some cases, this meant placing them somewhere in a vast hanger and in others, building HV barrier walls around the generators once they had been constructed. As an example, in lightning waveform generator 4 from chapter 1, the high current generators have about 300 m^2 if the test cell and a small loading area (which could also be used for oversized tests) were included. Even larger buildings house lightning waveform generators, 1, 7 and 8 (see section 2.5), which can accommodate large sections of or whole aircraft for the purpose of testing.

In Cardiff, the unit in which to build the generators had about 110 m^2 to accomplish the same, with the remainder of the unit to be used for a small workshop and control room. This presented the first challenge, as many other larger facilities were quite full and used stacking of devices vertically as well as a mezzanine levels to fit everything in. Designing for such a tight space was exceedingly challenging.

The small space limited the possibility of testing large structures and certainly eliminated whole aircraft. However, testing of whole aircraft was not thought to be necessary as there was no convenient way to get one to the laboratory. While samples are usually small, keeping the facility as flexible as possible by maintaining as much area for testing as could reasonably be achieved was an important aspect of early design decisions.

3.3.1. Layout considerations

Before any design work could be carried out, a scoping exercise was required to see how the space could be used. It involved estimating the size of various options for each generator and being as inventive as possible with stacking components vertically. This allowed front end decisions to be made that would facilitate each generator having enough space and allow the order of instillation to be planned. The resulting layout in Figure 11 shows the main components, spaces for staff to walk and trunking to power the generators. A person is shown for scale.

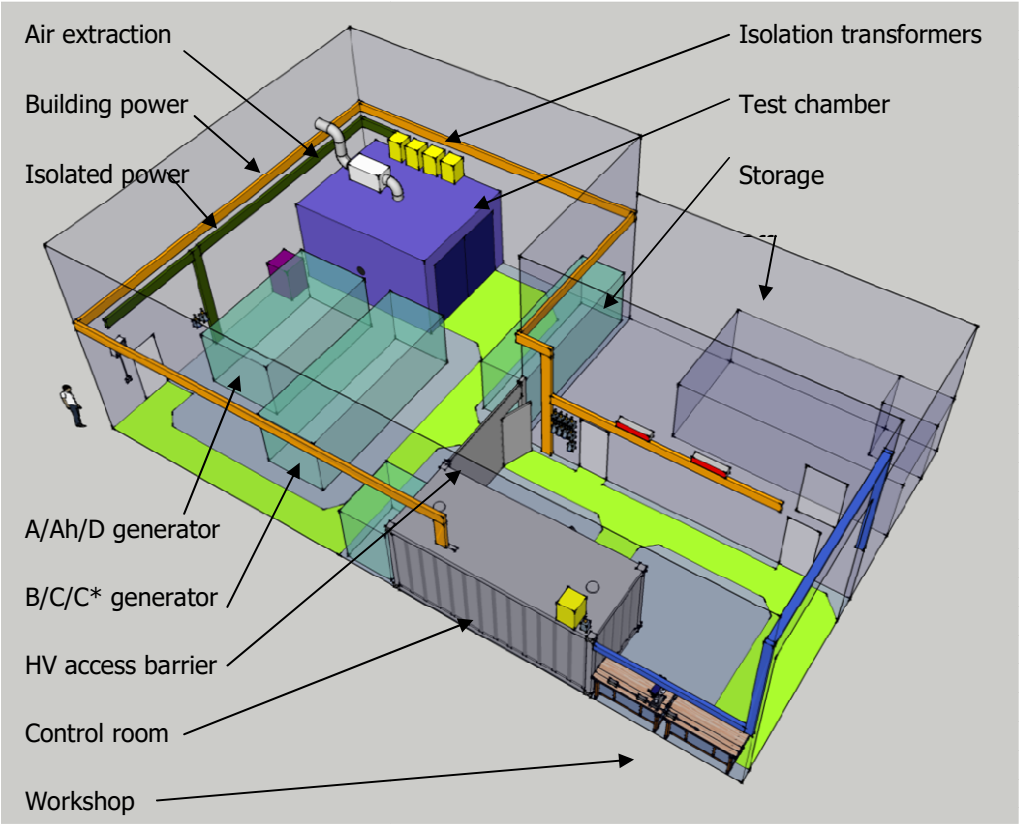

Figure 11 – Final layout of MBLL

Arriving at this took a considerable effort and over a month. It was preferred initially to have the test chamber facing the main doors so large items could be tested. However, that complicated walkways, access and connections. Perhaps ideally the generators and the test chamber would have been swapped, but that would have involved moving the fire escape.

The major early decisions are summarised below and/or described in the following sections.

- HV area
    - The whole back of the facility, allowing a short HV barrier
    - The HV barrier would be a gate large enough to move all major components through and would have a smaller gate for general use
    - Both the large and small gate would use a single captive key interlock system to keep that simple
    - The barrier would be solid to discourage running cables through it

    - Enough IO via fibre connections will be available to eliminate the need to run cables across the HV barrier
    - Everything will be solidly earthed, at least twice, to a solid ground plane that itself is earthed to both the building and 2 ground rods installed behind the building. The HV barrier door was solidly connected to the ground plane using flexible braids
    - All ground/earth bonds were tested to ensure they were well made using a microhmmeter. Each connection should be retested if remade or at least once per year
- Electrical (power)
    - A single interlocked power supply will energise the HV area
    - Additional power supplies would be installed for fans, lights and outlets – with isolation transformers where appropriate
    - The laboratory power shall use new and separate distribution boards from the office
    - All power cables entering the HV area shall be armoured and run in earthed cable tray. They shall also have individual rotary switches to control energisation and allow them to be locked off for maintenance
- Pneumatics
    - A compressed air system shall be installed for pneumatic operation of earth and dump switches, pneumatic logic position switches for safety related equipment (switches, earth sticks and fire escape) and actuation and purging of the spark gap for the fast waveform generator
- Control room
    - This would be an ISO container as it would fit and allow off site fabrication
    - It would not directly view the experiments to avoid issues with directly viewing arcs – cameras and monitors are much safer and movable cameras allow anything to be viewed whereas a window would have been fixed
- Fast waveform generator
    - A wheeled frame to facilitate moving it into position and making space for work to be carried out

    - Vertical capacitors with busbar connections on top and a vertical variable output resistor
- Trailing component generator frame
    - A wheeled frame with an end dedicated to chargers and control
    - Split into 2 levels and 2 sides with a large amount of HDPE shelf and wall space to easily facilitate mounting HV equipment (as it is an insulator)
    - The lower level on one side for capacitors (for both B and C/C* waveforms)
    - The other lower level for C/C* waveform switching
    - The shelf above the capacitors for charger connections and earth and dump switches
    - The shelf above the C/C* waveform switching was to be used for the output filter
- Test chamber
    - As big as much floor space and ceiling height as reasonably practical
    - No fixed shelving, work benches or test fixtures – to keep it reconfigurable
    - Flexible connections to test rigs from a solidly mounted low inductance high current bushing

For such a small space, that lacked a crane, anything large required planning to get into place. The order of assembly was:

- Ground plane – a 5mm thick steel floor throughout the HV area
- Test chamber
- Shelving to keep the area tidy
- B/C/C* generator frame
- A/Ah/D generator frame
- Control room
- HV Barrier

The ground plane was installed to prevent accidental breakdowns through the concrete to reinforcement – it also provided a low inductance return path for any such breakdown to return to whichever generator is feeding it. The earth star point

for the generators was located under the high current bushing into the test chamber. This was a large aluminium connection which was heavily bolted to a steel connection welded to the ground plane. The resistance from the ground plane to the earth connection of the high current bushing was measured using a new, factory calibrated, microhmmeter and found to be 60 μΩ.

With the larger pieces in place, work began to finalize the designs of and build the generators. To make the most of the space, the generator frames were on wheels, allowing one to be pushed aside while working on another.

The only lifting apparatus available was a 500kg hydraulic lift with enough height (3 m) to place items on top of the frames, test chamber and the highest storage shelves. This had to be considered while designing everything as I had to make sure it was possible to lift every item into place safely.

3.4. Test chamber and control room

The test chamber is the heart of the test facility – it is where the experiments that give reason for the facility take place. The control room is a safe place for people – usually including those requesting the test and those performing the tests (researchers, students and facility staff).

3.4.1. Acoustics

Lightning is loud; so loud it can be heard from many miles away. But that is the sound of a very long arc through air. A lightning test involves only a short arc – however, the energy delivered can blow structures apart, adding to the noise. Such explosions range from a small amount of erosion of conductive mesh on the surface of a carbon fibre sample, which ejects the nonconductive paint surface. To an arc forming inside a structure, expanding any gas present and likely evaporating material to add to the pressure rise, which very often shatter and burst a sample.

The energy stored in the A/Ah/D waveform generators is quite comparable to that in a stick of dynamite; while usually dissipated in resistors, it can be coupled into exploding specimens. It should be further considered that in high speed video clips of lightning tests, shockwaves are often seen as well as hypersonic debris (circa 3 times the speed of sound). From my own experience working with Lightning Waveform Generator 4 (see section 2.5), attempting to create high threat sound pressures in a lightning test facility (for safety verification), calculated sound

pressures circa 155 dB at 1 m has been generated. This was by running an A waveform through a 500 mm long fuse wire (0.1 mm copper) which was inside a 1" diameter Tufnol tube with 1/8" walls. This subjectively matched the loudest tests that all those working at that laboratory had experienced.

Anecdotally, this same method was used at that facility to prove that their first test chamber had been built in a substandard way. Acoustic plasterboard did not stand up well to the overpressure created, with the walls moving about 50 mm and the window snapping. That test chamber was replaced with one I designed and was heavily constructed with welded steel on the inside and for mass, 25 mm of marine ply on the outside. Its performance was much better. This is mentioned as that experience formed the basis of making sure the test chamber was designed very solidly and to handle the acoustic pressured from the very start.

When performing a test, resistance is used in the circuit to dampen it for the correct waveform; this consumes energy and thus reduces the risk of generated sound. However, if a test sample had an unexpected resistance that is much greater than the circuit resistance, it would likely explode, releasing much of the circuit's energy exceedingly quickly. This has occurred in my experience for several reasons including earth straps pulling off (due to high magnetic forces) or evaporation of conducting material, causing it to become open circuit or high resistance part way through a test. It has also occurred when a customer has given a sample to the test house and not realised all of the conducting surfaces have been anodised rather than alochrome plated. Thus, sound is the primary hazard that could not be eliminated and so had to be minimised.

In the case of Cardiff's test facility, with a maximum expected threat level of 155 dB at 1 m, this is, in theory, reduced to ~ 120 dB close to the HV boundary by being ~ 8 m away. While this would work in free space, the reverberant space of an industrial unit would add to the energy received, however,the solid door and convoluted path the sound would take to get to a listener there would lessen it. So 120 dB outside of the HV boundary was taken as a starting point for estimating what further protection would be required.

Whenever testing with the doors of the test chamber open, all those present had to wear 30 dB or better hearing protection. This would reduce the maximum sound pressure to 90 dB, which is reasonable considering it is a short impulse and likely to

occur very rarely. However, while tests are often quieter, a reason for having the doors open is to give distance to an expensive high speed camera from the test sample. The only reason to use the high speed camera would be to watch an arc or a sample explode. So some tests would be expected to approach 90 dB even with ear defenders.

Part of the reason for choosing 30 dB or better ear defenders was that it is at the better end of what is achievable with good quality off the shelf units – specifically the 3M Peltor Optime III units which are rated to give a reduction of 35 dB. The reason for specifying 30 dB and not 35 dB is to allow for tolerance and choice.

Subjectively the ear defenders were found to work very well while testing the facility. Sound pressure measurements were attempted but we did not have access to a system capable of measuring pulses accurately.

3.4.2. Test chamber and test rig

The tests carried out in the test chamber present a range of hazards that needed addressing. Furthermore, it required designing such that tests may be carried out in convenient manner. In order to accomplish this, the first task was to understand how much space would be required.

3.4.2.1. Room size

The size of the chamber was determined by what must go in it and how work would be carried out. Most samples are square in shape of with 0.6 m sides or less. A vertical semi-coaxial/square test rig about 1.2 m per side was envisaged for testing such samples. A minimum of 0.9 m space around this was deemed reasonable for working. This gives a 3 m square work area. To allow for space within the test cell for tools, test gear and a standalone ventilation system, the final test chamber had a floor area approximately 4x4 m and 2.9 m ceiling height.

3.4.2.2. Roof loading

With the test chamber being so large, and with acoustic attenuating walls approximately 0.25 m thick, this used up a good deal of the floor space in the laboratory. Thus, it was essential to use the roof space as a place to put light weight plant related equipment, freeing up and decluttering the rest of the facility a little. The nominal loading was 1 tonne plus 2 people. The equipment included isolation transformers and primary ventilation system for the test chamber, a rack

containing the control system and charger for the A, Ah and D waveform generator and its earth and dump system.

3.4.2.3. Acoustics

As mentioned above, the high sound pressure of the lightning tests presents a hazard to facility staff. Where possible avoiding reliance on PPE is essential in reducing risk. In order to eliminate the requirement to wear 30 dB or better ear defenders, the test chamber was designed to have an attenuation of at least that. This coincided with what was achievable within the space and budget by a specialist company.

The resultant room was constructed as 2 separate shells with a 50 mm air space between them. These shells were perforated on the inside, filled with rock wool and had an outer skin of sheet steel. The doors were heavily constructed in a similar manner but only a single layer thick.

3.4.2.4. Ventilation

Destructive testing naturally produces dust by disintegrating parts of the samples. Soot, smoke and vapour are also generated from partial combustion started by the high temperature lightning arc. Metallic samples produce very little soot, smoke and vapour while carbon fibre and similar materials produce quite a lot. The HSE presents literature on classifying fibres and their potential hazards [57] and the use of carbon nanomaterials in the workplace [58].

It is important to minimise staff exposure to the airborne hazard. This was accomplished with 2 separate fan systems:

- Permanent extract fan – drawing air out of the test chamber, through 3 filters in series – a pre filter, High Efficiency Particulate Air (HEPA) filter and carbon filter. The fan exhausted through the rear of the building. For particulate emissions, the filters were chosen to better what was required for industrial woodworking be sufficient for handling asbestos. For ozone and other odours, the carbon filter was chosen to have a higher residence time than generally used for spray painting or catering. Very little literature was available for lightning test facility exhausts, so the HSE was directly asked whether this seemed an appropriate level, which they confirmed. This high level of filtration was to ensure that any air leaving the building

was as free from contaminants as possible. It also generated a slight negative pressure in the test chamber, ensuring the flow of air was into and not out of it – thus keeping the rest of the laboratory as free from contamination as possible. This provided several air changes per hour. The fan was chosen to be quiet so as to not be a nuisance or disturb those in or outside of the laboratory.

- Hi-flow filter – a standalone filtration system that sat entirely within the test chamber, ensuring any leaks it could have, were contained in the test chamber. This had a pre-filter and a HEPA filter. Its primary use was to rapidly reduce the airborne contamination within the test chamber so that staff could renter it as quickly as possible without a requirement for wearing respirators. It achieved this by having a flow rate equivalent to 200 air changes per hour. Due to filtering and returning some air from the room every 18 seconds, the effective half-life of contamination could be considered to be approximately 18 seconds (this assumes good mixing of the exhaust with the remaining air in the room, which is plausible due to high fan power making air in the room turbulent). Running the fan system for 3 minutes (180 seconds or 10 half-lives) would, it was hypothesised, reduce the contamination by a factor of 1024. In this same 3 minutes, most of the heavy particles should have settled to the floor too.

The use of both of these systems, as well as staff using respirators when necessary, would ensure minimal risk from airborne contamination.

3.4.2.5. Blackout

While performing conduction tests of fuel system components (such as a vent, pump or pipe connection) or fuel tank skins (much of an aircraft wing), evidence of sparking from the sample would show a possible ignition source.

The only sparking if any would come from fasteners or brackets under test – there would be no lightning arc. In order to record where the sparks were coming from, a camera is often used, with the shutter open for the duration of the test. This required minimal reflections within the test chamber so as to eliminate confusion as to where the sparking was located. Therefore, the interior of the test chamber was painted matt black and, where possible, items in the chamber were also matt black.

Naturally, the black paint made it a very dark place to work, so bright lights were fitted to the ceiling for use when staff set up the tests.

3.4.2.6. Isolation for power

In the haste of setting up a test, it is quite possible for something such as an oscilloscope or vacuum cleaner to be left plugged into the mains power and also accidently across part of the output of the lightning test machine. To prevent injecting lightning test currents into the domestic mains supply, the power to the sockets was protected by isolation transformers and backed up with lightning surge arresters.

Where possible, it is best to use battery operated equipment in the test chamber, keep it tidy and use insulating (plastic or wood) tables.

3.4.2.7. Electrical noise and ground plane

The fundamental frequencies of the lightning test impulse are relatively low (several to 10's of kHz) and so the structures are too small to be efficient radiators. However, the front edge and of the waveform and the arc can generate wideband RF noise. In an attempt to contain this, the structure of the whole test chamber was made from steel and when specified requested that it was well bonded together. It was supplied as large panels and assembled on site with screws.

While the test chamber was a reasonably well bonded structure, it was not designed to be a safety barrier or extension of the ground plane. A wide aluminium grounded busbar was used to ground the isolation transformers, charger and earth/dump switches mounted on its roof.

The floor under the waveform generators and test chamber was covered in steel plate. This resulted in a ground plane that effectively surrounds the tests being carried out. This was not to aid tests, but to ensure that if part of the output of the lightning test generators is injected into the structure, it would return to the generator with the minimal of impedance and so have as benign effect as possible. This is important as the high currents of possible faults (induced by shorting the test rig to a wall for example) should ideally only give rise to low voltages with reference to ground so as to not flash over themselves to other equipment (such as the cables inside the power sockets mounted to the walls).

3.4.3. Control room

The control room is where staff and customers reside while tests are being performed. Various options for such a room were considered and a 20-foot International Organization for Standardization (ISO) container was settled on. It provided sufficient internal space while allowing enough left for a workshop. A great benefit of using an ISO container was that it could be constructed off site and be supplied finished.

ISO containers are frequently modified for uses other than shipping. The main modifications were sealing the double door at the end and installing a more office like door in the side. An obvious off the shelf solution was not available so I designed it with the following considerations and had it made by the same supplier as the waveform generator frames.

3.4.3.1. Control room interfaces

The control room contained a PC running LabView, used to both control the waveform generators and display/record data from a networked oscilloscope. It could also display video from cameras within the HV area and test chamber. These cameras were movable to allow any area of interest to be viewed. Additionally, software allowed remote control of diagnostic imaging ranging from thermal to high speed and still SLR cameras.

Cameras were used to view inside the test chamber as they completely avoid exposure and thus possible damage to staff eyesight from the lightning arcs, with the added benefit of being able record the footage.

The safety system was housed within the control room along with the firing controls; these are described in more detail below.

In order to ensure flexibility for future unforeseen tasks, several spare fibre LAN ports were made available, along with bare fibres for simple binary signalling to test apparatus.

3.4.3.2. Control room acoustics

While the test chamber attenuates the noise of the arc and any exploding samples reasonably well, it can only do so much. Furthermore, if one of the waveform generators was to suffer a breakdown, the sound emitted from that would not be contained within the test chamber, thus, there would be no attenuation.

To address both of these aspects, the ISO container had a good deal of sound deadening (to dampen self resonance of panels) and damping (to reduce internal reverberation). Specifically, the inside of its metal walls and ceiling were coated with a thick bituminous, fibrous layer. Then, 75 mm of high density acoustic foam was installed before being covered with punched steel sheets. There was not a particular dB goal, the design was more a best effort approach, guided by experience of building other such systems. The net effect was similar in attenuation to the test chamber and protected staff from external noise. However, it had noticeably subjectively less echo than the professionally designed test chamber.

3.4.3.3. Control room ventilation

Even though the test chamber had a good deal of attention to detail paid to the ventilation and contamination control, the air supplied to the control room was filtered. Leaving this running effectively slowly polished the air in the whole of the laboratory as air was drawn from the building, filtered as it was put into the control room and then exhausted back into the building. This had the beneficial effect of keeping the dust levels low in the control room and thus the IT equipment kept rather clean. Furthermore, the sound insulation acted as excellent thermal insulation, thus leaving the ventilation running constantly kept the temperature stable. Without it, the IT equipment and several staff would generate sufficient heat to make it unpleasant to work in.

3.4.3.4. Power filtering and electrical noise

Power entering into the control room was filtered by a screened room type mains filter. This was to assist in protecting the equipment present from any electrical noise generated during testing or a fault condition.

The fully welded structure of the ISO container also provided an excellent and inexpensive screened room to protect equipment within from induced currents arising from a possible fault in a high current pulse generator.

3.5. IT, power, safety and diagnostics

The IT system in the laboratory has 2 functions; firstly, for the general office use, and secondly, for control of and data recording for the lightning test equipment.

The office part was completely conventional, using a server for data storage along with a router for internet access. This was connected using a switch to computers using CAT6 cable.

The laboratory side differed as all major connections were made using fibre-optics. This ensured electrical isolation, preventing noise and fault currents passing through the IT system.

Electrical power was quite conventional for a small industrial unit, but it was a limiting factor for how fast capacitor banks could be charged.

The safety system was standalone and designed to be as fail safe as possible. It was designed in conjunction with the safety and operating documentation to ensure simplicity and ease of use. While setting up the laboratory, permission to operate the facility was limited to the technician and myself (the operating staff) and only if both of us were present and were following strict but simple procedures and risk assessments. Access for other persons was limited to them observing and only entering the HV area once its safe state had been verified by the operating staff.

3.6. Diagnostics

The most important aspect to measure of a lightning test is the shape of the current waveform. This allows the test to be crosschecked with requisite standards to confirm whether or not the current discharge was within specification.

Optical measurements to see if sparking has occurred are also important. As if sparking does occur in a fuel system it could present a hazard. Ignition hazards can also be checked for with sensitive flammable gas mixtures.

Structural weakening can be checked for by thermal means – it is important that structures do no anneal if metallic or degrade chemically if composite.

3.6.1. Current

The composite waveform is challenging to measure; with the A waveform having a maximum current of 200 kA and the C waveform decaying to 200 A. There are 3 orders of magnitude over which accurate measurements must be made.

While it would have been quite possible to measure the currents of the waveforms with resistive shunts, it would have involved coupling measurement equipment directly to the high power circuits. In general operation that would have likely been

easily achievable. However, it could not be assured that fault currents could not induce or directly inject damagingly high signals into attached oscilloscopes and their associated equipment. Therefore isolated non-contact measurement methods were mandated.

The solution was to measure the waveform components separately. Using a bespoke Rogowski coil and integrator, designed specifically for the A/Ah/D waveforms and a hall-effect device for the lower amplitude B/C*/C waveforms. These were the most economical device types to use. A Rogowski coil is best suited to higher frequency transient pulses and the hall-effect devices are best for the DC like square wave of the C waveform.

The outputs from these sensors were captured on an oscilloscope, which could be controlled remotely over the network.

Cross-calibration of devices with others from the HV laboratory at Cardiff University and several current transformers from the industrial partner gave confidence that the current diagnostics could be believed and were sufficiently accurate.

The hall-effect sensor was one of the largest standard models by LEM. Using a commercially available device proved cost effective and meant spares did not have to be purchased. The device had to be protected from over current when in general operation as that would saturate the device and cause erroneous measurements. It had also to be protected from very high fault currents which could cause permanent damage. Fortunately, the large resistances in the trailing component generator output filter greatly limited fault currents and allowed mounting of the device close to the high current bushing into the test chamber.

The Rogowski coils and their integrators were bespoke. A primary high current coil was to be used for the main high current measurement and a suite of smaller coils and associated integrators was made available for future tests. For example, a section of wing could be coupled to a set of return conductors such that currents could be measured coming out of each side and perhaps a spar connection beneath it also.

Unfortunately, the Rogowski coils tended to ring at a very high frequency (several MHz) which commenced at initiation of the high current waveforms. While this settled down and allowed the tail to be clearly seen, it was not ideal. A low pass

filter applied to the data could be used to resolve clean lightning waveform as the ringing frequency was much, much higher than the waveform.

Upon inspection of the integrators, they initially appeared to be suitable, but further reading and simulating the circuits in SiMetrix revealed that the inputs were not equal impedance. They did have balanced input circuits, but these became nonlinear when the slue rate of the op-amps was approached.

It would, in hindsight, have been better to purchase a suite of Rogowski coils from a company that specialises in pulsed power measurements and not lower frequency power distribution systems.

A low pass filter when applied to the data worked as an intermediate solution and where possible (including for the results in this thesis), a current transformer was used rather than the Rogowski coils.

A solution to the noise problem was proposed and designed, but implementing it was outside the scope and timescale of the initial project. It involved replacing all the integrators with an in house solution. This would have critically damped inputs which acted as a 2^{nd} order low pass filter for the input to a fast instrumentation amplifier before a standard active integrator circuit. This would properly match the Rogowski coil cables at the integrator end, cancel a very large proportion of the common mode signal and roll off a good amount of anything that was left.

A further improvement could be gained by remaking the Rogowski coils in a more symmetrical way and implementing matching at the coil end as well as the terminating end of the cables. Though by that point, since everything would have been replaced, simply ordering a solution from another supplier would likely prove successful also.

The eventual solution for measuring the high current waveforms implemented at the laboratory was to have a bespoke current transformer made to fit around the return conductors. This was implemented after the work carried out for this thesis was completed. A suite of Rogowski coils from a different supplier was also purchased with successful results for measuring the distribution of currents in test samples.

The information in this section demonstrates the challenges associated with the measurement system. It shows that while the initial system did work, its performance was not as good as hoped but that it was solved to good effect later.

3.6.2. Light

As mentioned in the section regarding the test chamber, it was painted matt black for the purposes of taking photos during tests. Cameras can be triggered using a variety of means from USB remote control to fibre-optic shutter releases. Generally, such use of cameras is to look for sparking from joints or fixings.

It is essential to know that the shutter was open for the duration of the application. Before the test waveform was triggered and immediately after, separate LEDs were strobed into optical fibres which terminated in the camera's field of view. If an image captured both strobed tell-tales, then the shutter was open when the waveform was applied.

High-speed cameras were used during arc attachment tests to see how the surface of a sample behaved as it was eroded by the arc. These required very bright lighting due to their inherently short shutter speeds (750,000 frames per second has a maximum shutter speed of 1.33 µs).

3.6.3. Thermal

Lightning testing can deliver a very high power density to a sample. This can heat it or parts of it up rapidly. The heating can present an ignition hazard or reduce the structural integrity of parts. Predominantly, thermal cameras were used for observing hot-spots and their temperature profile over time. For hard to reach places, thermal labels were used to detect maximum temperatures reached.

3.6.4. Flammable gas

While the laboratory was not conceived to initially use flammable gas as a diagnostic, its use in detecting ignition hazards in fuel systems laid out in test standards necessitated the test chamber to be made structurally sound.

Flammable gas tests involve filling or surrounding a sample with a gas mixture that has an ignition threshold of or slightly lower than 200 µJ; this being more sensitive than aviation fuel even in worst case scenarios. Thus, if no ignition occurs with the sensitive gas, then ignition of aviation fuel/air would not occur either. However, when ignition does occur, the flammable gas rapidly expands. The overpressure due to this could damage a poorly built chamber.

3.7. Power

The mains incomer into the building was 80 A, 3 phase. With perfect power factor, this would allow 57.6 kW of power to be delivered to loads. Specifically, it was necessary to calculate how much power could be delivered by 3 phase chargers into the capacitor banks in the waveform generators. However, due to simplicity, with the office on 1 phase, drawing 4 kW, the remaining headroom across the 3 phases was 45.6 kW. With an expected power factor of chargers around 0.75 and expected charger efficiency of 0.95, the upper limit of power available for charging waveform generators was 32.5 kW. While this might appear quite low, it is sufficient to charge the capacitor banks within a minute. This aligned well with available capacitor charging units. The cost of capacitor chargers also increases with their power throughput, so charging faster would have used more of the budget.

3.8. Interlocks and access control

The interlocks for the laboratory were essential. They keep people present safe from the hazards involved with high-voltage equipment. To ensure that the interlocks were as reliable and as immune to interference as possible, the decision was made to keep them standalone.

By keeping the logic simple and the input/output count low, relay logic could be used. Further, by using logic high as the safe condition, verifying functionality was simple as all conditions could be checked by a combination of testing the inputs and pulling relays to simulate them failing.

To perform a test:

- The HV area must be searched to ensure no persons are present, the equipment is in apparent working condition and not cluttered and the earth sticks have been removed and are on their designated holders (which are monitored by the safety system)
- The HV area must be closed to remove the key before inserting it into the interlocked switch allowing power to the charging/high-voltage systems. When the key is turned allowing power to be energised, a siren sounds for a short time indicating imminent test and indicator lights illuminate until the HV area is safe to enter again

- Checks only allowing operation of the charging systems once the earth or dump switches were open and the safety earth sticks were returned to their hangers

To re-enter the HV area:

- Checks that the dump switches are closed followed by a time delay before starting closure of the earth switches
- Checks that the earth switches are closed followed by a time delay before releasing the key to re-enter the HV area

The status and release of the interlock key were monitored and controlled electrically. All other interlocks were monitored pneumatically.

In the event of the control system loosing power, the pneumatic valves controlling the earth and dump switches return to the close switch state. To avoid the earth switches closing before the dump switches, restrictors were used to dampen the closing speeds. This allows gravity to return the earth and dump switches to the closed position.

In the event of power failing in the laboratory, if the door to the HV area was locked, power to release the interlock key would also be lost and so access to the HV area would not be granted. The interlock system would then grant access to the HV area once power is re-established and the relay logic detects safe conditions are met.

3.9. Distributed control system – LabVIEW

The control system was designed from the ground up to use LabVIEW. This enabled a PC in the control room to control the separate parts of the laboratory via fibre-optic, thus, keeping them electrically separated. Furthermore, it allowed robust and configurable input/output cards to be placed where required and the ability to adapt quickly as specifications evolved. Making this decision allowed purchasing a majority of the control system well in advance of finishing the design of all the other components. It was aided by Cardiff University's links with National Instruments.

The main components of the system were:

- A control PC running LabView which sets parameters for triggers and records results from the rest of the system
- An interface (CompactRIO chassis configured as a real-time controller and housed in the interlock control panel in the control room) with the interlock system that informed the control PC of its state (summarised as a binary ready to operate signal) and allowed the pneumatic control for earth and dump switches as well as the fast waveform generators pneumatically operated moving spark gap switch. It did not control and could not override the interlock system which would hold all earth and dump switches closed if the HV area was open, earth sticks were not in place or an emergency stop button had been pressed
- Control for the A/Ah/D waveform generator's charger (CompactRIO chassis configured as a real-time controller and housed in the A/Ah/D waveform generator's charger rack on the roof of the test chamber)
- Control for the B/C*/C waveform generator's charger (CompactRIO chassis configured as a real-time controller and housed in the B/C*/C waveform generator's charger rack which in turn was in its frame)
- An FPGA based trigger system for firing the B/C*/C waveforms (CompactRIO chassis configured as FPGA target and housed in the B/C*/C waveform generator's charger rack which in turn was in its frame)
- Fast (1 GHz sample rate) and slow (1 MHz sample rate) oscilloscope modules housed in a PXI chassis in the diagnostic rack next to the test chamber. These were to record current from the fast and trailing component waveforms respectively

3.10. Conclusion – laboratory build

A great deal of systems engineering was required to ensure all the features that would be required for a fully function laboratory would fit into the space and work effectively and safely.

After scoping the possible designs for each element of the laboratory, from the test chamber to the waveform generators, control room and storage, a plan was formed for how to integrate the solution. This essentially involved ordering all long lead

time items as soon as possible, then commencing the build from the back wall forward. It meant a lot of decisions had to be made very early in the project and anything that could not be decided on immediately had to have interfaces understood and space left for it.

The use of wheeled frames for the waveform generators assisted by limiting the amount of space lost around them for assembly. This allowed enough room to be freed up on whichever side was being worked upon. While this aspect might seem trivial, the assembly of the waveform generators was planned while designing the frames to ensure the lifting equipment would have access.

By using a robust relay logic system for safety, the requirement for reliability was relaxed for the rest of the control system (from critical to essential). This allowed a distributed computer controlled system for charging, triggering and data collection. It also meant that the safety system could not be broken by updating the LabView control system.

4. Optimized Design of the Fast, High Current Waveform Generator

4.1. Introduction - A/Ah/D waveform generator

Optimising the design of the fast, high current waveform generator was the first goal of the PhD project. It was distinct from a design and build approach, which could be guided by experience, a little circuit analysis (using PSpice or similar software) and iterative changes until a system is correct. Specifically it required time to explore the mathematical understanding of the waveform generators and approach their design from a theory prospective in a way that would be appropriate as part of the PhD research. The goals included, finding the best solutions that could be reasonably achieved, proving them, and informing future users how to set up the waveform generators, thus avoiding future trial and error and simplifying operation.

The research assisted greatly in the build of the MBLL, giving certainty to decisions and saving time by eliminating the need to tune the circuit after it was built.

Due to the complex interaction of all sub components, the design was somewhat iterative as changing one part or basis for decision would have cascading effects on other parts – as such, it was essential that development was undertaken in a progressive manner. This resulted in a number of similar solutions being explored before the presented ones being honed in upon.

Firstly, a top level design brief/specification was devised – from the test standards and to make best use of available equipment and funds. Then all possible methods of delivering the specification were considered and analysed. Finally, the build and then testing of the generator confirmed its functionality was within specification.

Laboratory equipment from an old lightning test facility of the industrial partner was donated to Cardiff University, including parts from an old high current lightning waveform generator. This was analyzed and found to have several missing parts and lower than desired performance. However, the some of the individual parts were useful.

In order to design a new generator from scratch, the lightning test waveforms were analyzed mathematically. This analysis and exploration of double exponential

waveforms revealed that an LCR circuit could be used to perfectly match the test standards reference waveforms; though this would require a rather high voltage.

A spreadsheet tool was then produced to assist with the design of a lower voltage circuit that could be made largely with available parts. This allowed the circuit parameters to be chosen to ensure the waveform generator would robustly produce the required waveforms.

4.2. Design brief and constraints

The main goal was to deliver a high current waveform generator and test rig that can fit within the available space, which was both achievable and within the budget. The waveforms to deliver were A, Ah and D. It must be capable of both arc attachment and conduction tests to both aluminium and composite samples (which each have slightly different resistances and arc voltage drops).

A secondary aspect was that much of the effective budget was contribution in kind rather than cash. This was in the form of much of the equipment donated by the industrial partner. The most useful parts included:

- 10 of 20kV, 197µF capacitors
- 6 of 20kV, 32.8µF capacitors
- 60 of 30kV, 5µF capacitors
- 24 of 20kV, 15µF capacitors
- 1 of 200kV Marx generator
- 1 of multi gap clamp circuit
- 1 of 60kV, 10kW capacitor charger

The latter 4 items were part of the high current generator from the decommissioned laboratory. The 24 capacitors were used in an array arranged as 2 series rows of, 12 parallel capacitors – with the output fed into an inductive coaxial load. The current waveform could then be clamped by firing a multi-gap clamp circuit and allowed to freewheel through the load. However, the decommissioned generator was in poor condition and would have required a great deal of work to bring it back to life. Also, due to relatively low voltage and energy, the ratio of eternal resistance to the load resistance (sample resistance plus arc

voltage drop) was low, making it quite sensitive to changes in sample. This is explored in section 3.4.

4.2.1. Short specification of the waveform generator

- The space available for the high current waveform generator was approximately 6 m by 2.5 m. Auxiliary items could be located on the roof of the test chamber
- Funds available were limited, necessitating that available parts must be used where possible
- It had to produce the A, Ah and D waveforms within the specification laid out in ED84, starting with D, adding the others later
- It had to be as easy to set up and use as possible – if there was a complexity that could be eliminated, it should be eliminated
- It had to be as stable as possible (remain within waveform specification even if the sample resistance is a little higher or low than expected)

4.3. The original waveform generator

This section explains how the waveform generator that was donated by the industrial partner worked in its original laboratory and how it could have worked in Cardiff had it been complete.

The waveform generator donated by the industrial partner used a reconfigurable capacitor bank. Many combinations (each capacitor was 15 μF, 20 kV) of capacitances were possible, such as:

- 375 μF, 20 kV (All 25 in parallel)
- 90 μF, 40 kV (2 x 12, series parallel)
- 40 μF, 60 kV (3 x 8, series parallel)

The maximum charging voltage (from the supplied charger) was 60 kV, which equated to 3 capacitors in series. The maximum energy stored was 75 kJ and 72 kJ for 25 and 24 capacitor configurations, respectively. However, as it would generally be unwise to charge the capacitors to their full rated voltage (taking into account they've been used for ~20 years and the expected series configurations), the energies for a 90 % charge would be 60 kJ and 58 kJ respectively.

Figure 12 shows a diagram of one possible configuration for generating a D waveform (see Table 4) using the generator. Essentially, it would involve connecting the capacitors into a 2 x 12 series/parallel array, charging them to 36 kV and releasing the current through a spark gap, 240 mΩ of series resistance (of which up to 50 mΩ would be within the sample) and 2.4 μH of inductance shared between the capacitor bank, switch and test rig (including sample).

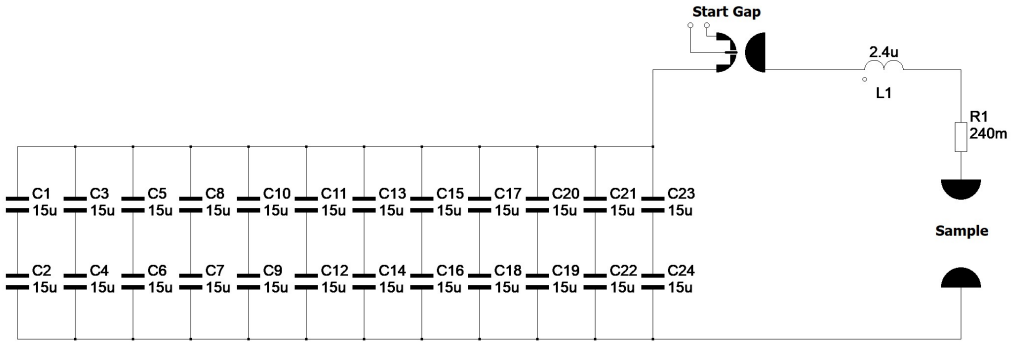

Figure 12 – Possible configuration for generating the D waveform

The inductance was an inherent part of the generator circuit and its connection to the sample and is depicted as the lumped element L1 for Spice simulation runs. It could be varied slightly by changing the shape of the sample return conductors. A 240 mΩ resistance is relatively large compared with a usual test panel and, as such, was quite advantageous to be able to use. The 36kV was chosen as it is 90% of the rated voltage of the energy storage capacitors.

As can be seen from Figure 13, the output waveform is unipolar, has peak amplitude of 100kA and the correct action integral of 0.25 x $10^6 A^2 s$. The rise time is 16.3 μs. The ideal waveform (Ref. Waveform -> D) from ED 84, calculated from the alpha and beta values is also shown. The peak current box shows the tolerance for both current (± 10%) and time to peak (up to 25 μs), and is shown on a majority of subsequent graphs. The tolerance given here is for the D waveform. For the Ah and A waveforms, the maximum time to peak is increased to 32.5 and 50 μs respectively while the tolerance for the current remains the same.

The waveform is slightly underdamped, which is not representative of natural lightning which is always unipolar. Whether or not this would effect a test is outside the scope of this thesis and is allowed by the test standards. However, an

overdamped waveform would eliminate this question and thus be preferable. Furthermore, customers subjectively prefer a unipolar pulse for exactly this reason.

Arriving at the topology shown in Figures 12 and 14 was a complex and iterative task as only about half the spark gap components were supplied and without a frame to orient them. This made piecing what existed of the donated generator together complex jigsaw with several parts missing.

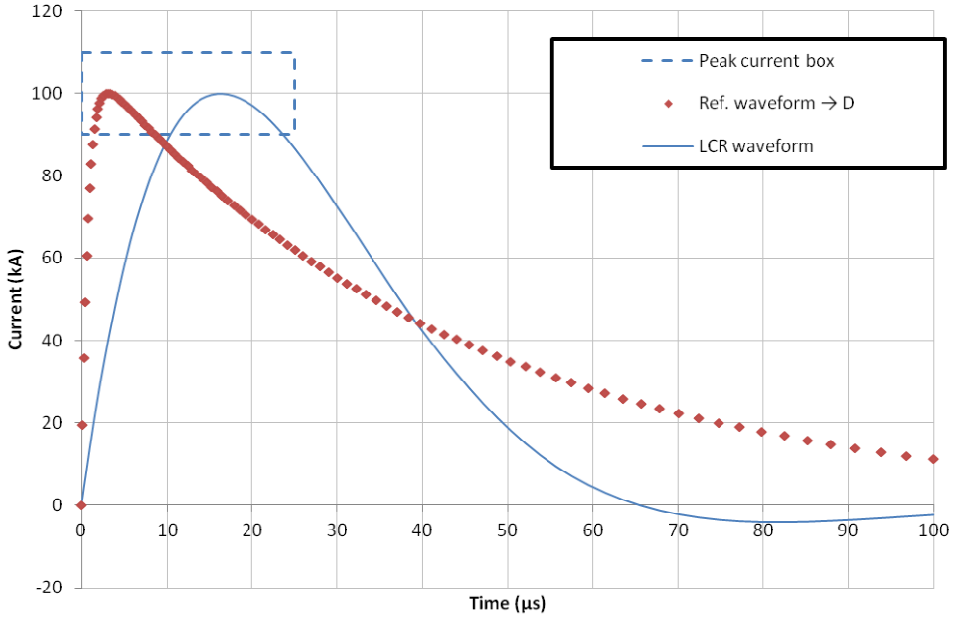

Figure 13 – Output of lightning simulator in the original D waveform configuration

Figure 12 shows the derived topology for delivering a D waveform. It was modelled using SPICE software to generate the current waveform shown in Figure 13. Figure 14 shows the circuit configuration for producing an A waveform. It is based upon discussions with the industrial partner who donated the equipment and an incomplete drawing from them. This circuit used a clamp sub circuit which adds 3 additional spark gaps (not counting the 4 in the external Marx generator used to trigger it).

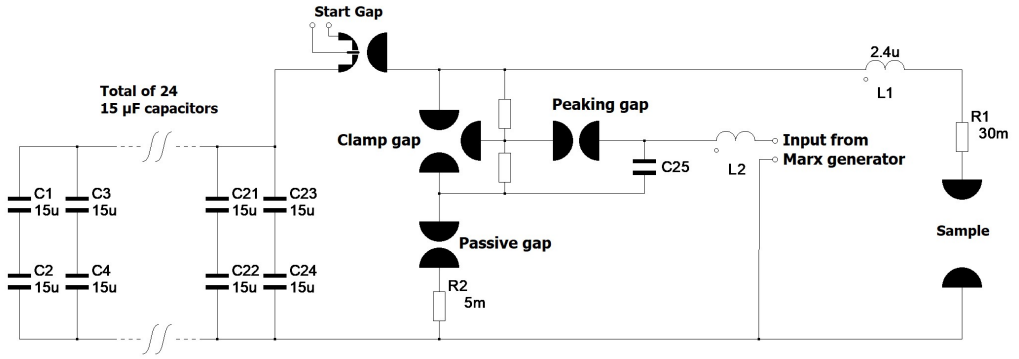

Figure 14 – Possible configuration for generating the A waveform

The clamp sub circuit comprises the clamp, the passive and the peaking gaps, together with an inductor and a peaking capacitor. The purpose of this sub-circuit is to hold off the full bank voltage (potentially 60kV) and then to be able to fire when there are close to 0V across it; this occurs when the capacitors have rung all or most of their energy into the circuit inductance. From that point on, the capacitors are not required to form part of the circuit, so the clamp switch is fired and the resulting LR circuit dissipates the inductively stored energy in the sample.

A 0.030 Ω (R1 in Figure 14) resistance is relatively small compared with a usual test panel and as such would cause the waveform to be highly dependent on the sample resistance. The initial charge voltage of 37 kV was chosen as it is close to 90% of the rated voltage of the energy storage capacitors.

As can be seen from Figure 15, the output waveform is uni-polar (referred to as the clamped current), has a peak amplitude of 200 kA and has the correct action integral of 2 x 10^6 A^2s. The rise time is 21 µs. The ideal waveform from ED 84, calculated from the alpha and beta values is also shown. The black waveform represents the strong oscillations that would occur if the clamp failed to fire.

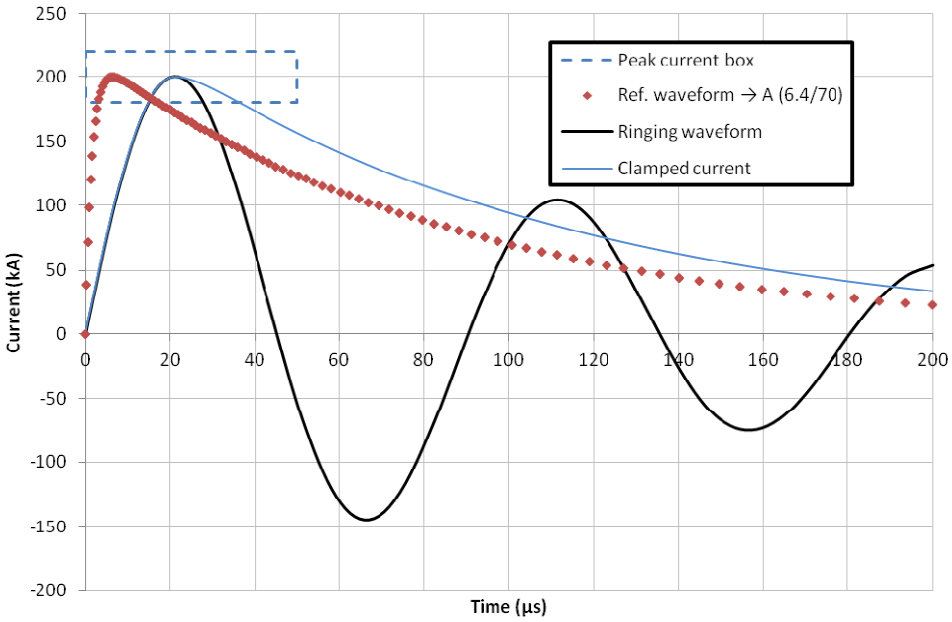

Figure 15 – Output of lightning simulator in the original A waveform configuration

4.3.1. The original waveform generator – parts needed

Many components of the original waveform generator were supplied. The values of the capacitors were all checked and found to be within tolerance. Successful high voltage withstand tests were also conducted. This involved taking each capacitor to its faceplate rating voltage rating then discharging before checking the capacitance had not changed. A higher voltage was not used as the capacitors appeared to be quite old and had uncertain usage histories and remaining life.

The following is a list and description of the parts that would need sourcing for the original waveform generator to function:

- Capacitor links
    - These link the capacitors together, thus forming a major part of the discharge circuit
    - These could be made inexpensively from 5mm aluminium sheet
- Start gap trigger
    - The start gap was a 3 electrode type, with a spark plug forming the trigger pin of the hot electrode
    - A HV pulse generator would be required to trigger it, though this is complicated as it is floating at the full capacitor bank voltage
    - This could be made in house or purchased from a third party

- Start gap
    - This was effectively the on switch
    - The electrodes were somewhat eroded, replacement and spares would be required
- Sample series resistance and frame
    - This was required as a fundamental part of the pulse forming circuit
    - The components used should be low inductance and able to withstand a high peak current and associated energy
    - Potentially available from HVR international
- Clamp series resistance and frame
    - This was required as a fundamental part of the pulse forming circuit
    - The components used should be low inductance and able to withstand a high peak current and associated energy
    - Potentially available from HVR international
- Switches, Resistors and Charger connection
    - The resistors were open circuit and heavily charred, indicating they were of insufficient heat capacity and need replacing
    - The switches did not close automatically or by gravity. Furthermore, they were not monitored by an interlock system. As such, they were completely unsuitable for use in a safety oriented system as they could leave the system live and without warning
    - Suitably sized resistors and auto closing switches would have to be purchased. Additional switches were required to short the capacitor bank at the HV and mid point after dumping the energy
- New insulators
    - The existing ones did not provide support for the capacitors (the insulators Tufnol sheets mounted on the generator frame with an additional layer of polythene – effectively an insulating table on which the capacitors were placed but not actually attached), it was important that they could not fall off the machine because they are expensive and have a long lead time and, most importantly, they must not fall on people
    - Further, the old insulators were of unknown condition
- Sound attenuation around the switching system

- The spark gaps were in free air, as such they would be extremely loud when operated
- Encasing or replacing them with pressurised gaps would solve this

4.3.2. The original waveform generator – conclusion

This section demonstrates that although a good deal of equipment was supplied by the industrial partner, it did not constitute a functioning lightning waveform generator. It could not produce a particularly stable A waveform (as the resistance in the clamp circuit was low compared to possible sample resistances). Furthermore, considerable effort would be required to make the machine functional as it lacked many essential parts, such as the load series resistance, the clamp switch and the trigger start gap.

It was estimated that the time required to make the waveform generator functional again would consume the available budget and the duration of work would be approximately 25 weeks of CU staff time as well as that of external contractors. About 1/3 of this time would be spent designing the new components while the remainder would be for constructing and fitting them to the machine.

4.4. Options for a new waveform generator

The topologies generally used for high current lightning waveform generators are LCR or Clamped LCR circuits. An LCR circuit operates by discharging a capacitor through inductance and resistance. A Clamped LCR circuit differs in that the driving capacitor is shorted out after delivering all of its energy into the circuit inductance. These are further explained below.

An LCR circuit can be used to deliver unipolar waveforms if sufficiently damped. The initial charge voltage of the capacitors will act upon the circuit inductance and give maximum di/dt at switch on. This will quickly increase the current to the point where the voltage drop across the circuit resistance becomes equal to the remaining charge voltage on the capacitors. At this point, with the voltage across the circuit inductance now zero, maximum current is reached. For very damped circuits, the tail of the waveform is essentially the capacitor draining though the circuit resistance. This is a reasonable description for a circuit that would simulate the reference lightning test waveforms which have a short time to peak and much longer time to half height.

Each waveform, whether or not it is specified in the standards, has a charge that will be delivered through a sample by it. With an LCR circuit, this charge must be entirely stored within the circuit's capacitance before the discharge commences. Therefore, for a given waveform, the product of the capacitance and voltage is constant. The implications of this are that for a larger inductance, more voltage is required and thus more energy must be initially stored. This can lead to large energy storage requirements for short rise times and larger inductances.

A clamped waveform generator has the advantage that it can have a high initial voltage which is useful for overcoming circuit inductance and quickly increasing the current to peak value, while not having to store all of the charge that will pass through the sample in the circuit capacitance. This is facilitated by current circulating through the circuit's inductance, sample, clamp switch and a small resistance, which bypasses the capacitance.

For clamping, a self-commutating diode option seemed an ideal choice, but, unfortunately, it would be rather expensive. A 100 kV diode stack capable of carrying 200 kA for a brief period would typically involve 16 chains of 30 series diodes, all resistively balanced. That is 480 diodes, plus resistors and frame. It would likely cost £100k – which was considered to be an expensive solution.

A triggered spark gap (TSG), if fired at maximum current, coincides with roughly zero volts driving the circuit from the capacitor bank. This means the spark gap must be capable of withstanding the full capacitor bank voltage but be able to be triggered when there is very little potential across it. This seems paradoxical but is quite possible with a sufficiently large impulse. The Marx generator that was used to drive the clamp switch of the inherited generator was very large for a trigger – using approximately a 10 kJ, 200 kV pulse to activate the crowbar on a 58 kJ, 40 kV waveform generator itself. While the voltage would be useful for breaking down the air gap, usually energy would be minimised for cost reasons. So this trigger was possibly over specified for the purpose.

The inherited TSG was also known to be rather difficult to set up to reliably fire every time. Some other lightning generators have used sulphur hexafluoride (SF_6) as an insulating gas, allowing the electrodes to be closer together. This makes it easier to withstand the voltage and to sustain conduction once triggered. These

SF_6 clamp arrangements were triggered with an intense laser pulse which is costly and complex. SF_6 is also a very powerful greenhouse gas.

A clamped LCR circuit also involved the complexity of timing the clamp accurately after initialisation of the waveform and then triggering the clamp circuit with minimal jitter.

An LCR circuit, without the complexities of an additional clamping device was therefore very attractive from the prospective of being inexpensive and simple. It only required an on switch. If a mechanically closed switch was used, it would be initially far too wide to spontaneously fire. Once activated, it would close from the wide open setting down to the self-discharge distance for the gap at the capacitor bank charge voltage. With lower voltages, the delay from starting to move the gap to triggering would increase. However, as the high current waveform was to be the first of the waveforms in the composite lightning discharge, timing for the start did not matter. Timing for all other waveforms would be triggered by the onset of current in this first waveform.

Because of the simplicity and ease of use afforded by eliminating the clamping system, associated timers, and avoiding expensive purchases, the LCR topology was chosen.

4.5. Exploring the double exponential waveform – the specification

In order to fully understand how to generate the lightning test waveforms, described in test standards by double exponential equations, an understanding of the equations is required. If a circuit could be designed to match and reliably deliver the waveforms exactly, it could be considered ideal.

ED84 [28] describes the over damped test current waveforms with Equation (1).

$$I(t) = I_0\left(\mathrm{e}^{-\alpha t} - \mathrm{e}^{-\beta t}\right) \qquad \text{(Equation 1 repeated from Section 2.4)}$$

The parameters are:

- I_0 Constant describing the amplitude (higher than I_{max} of the waveform)
- α Term defining the fall of the waveform (larger value = faster fall)
- β Term defining the rise of the waveform (larger value = faster rise)

It is perhaps counter-intuitive that α would define the fall and β the rise. However, it can clearly be seen that in all cases where a lightning waveform is specified, β is larger than α, and a larger exponent decays faster than a smaller (due to minus term), which must mean it describes a later part of the waveform than α.

Figure 16 shows an example of a double exponential waveform representing the current in the B waveform from ED84. Also shown are the α and β terms expressed separately. It is clear that the area under the double exponential is equal to the area between the 2 single exponential curves.

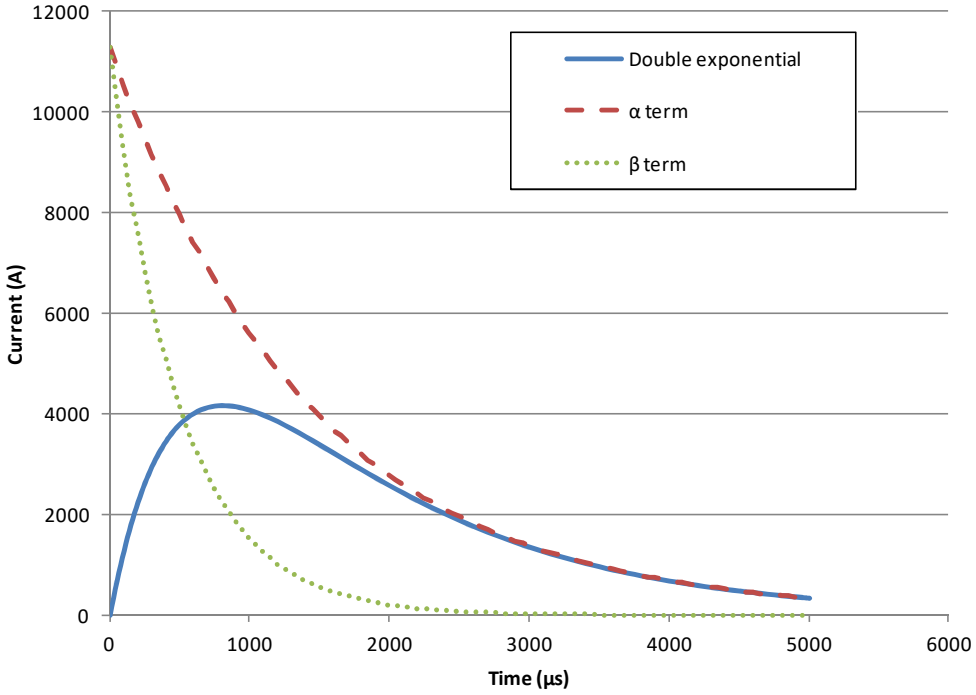

Figure 16 - Example of double exponential current waveform:

B waveform; I_0 = 11,300; α = 700; β = 2,000

Underdamped waveforms can be described using the same formula, but α and β terms become complex numbers; whereas for the critically damped case, α equals β and the equation stops working. This is explored further in section 3.5.6.

The double exponential waveform is often used as an approximation of the voltage output by a Marx generator, through a resistor, into a capacitor in parallel with a resistor [59]. In that approximation, the inductance of the capacitor bank and other conductors are not taken into account. The use in that context is not to be confused with the use of double exponential equations here. In the context of a

lightning waveform, the double exponential waveform is used, by the test standard, to describe the current that should be used to test a sample or whole airframe.

It was not expected that commencing investigation of the double exponential current waveforms from the lightning test standard would reveal solutions for an LCR circuit to deliver them. However, as will be shown below, it indeed did.

The double exponential waveform when used to describe the voltage on the output of a Marx generator in the above case, becomes an increasingly accurate approximation, as the resistance of the circuit dominates any parasitic effect of circuit inductance.

In the case of an LCR lightning current waveform generator, it becomes increasingly accurate as any effect of stray capacitance is dominated by the bulk L, C and R elements.

Several parameters are of interest. The peak current, the energy and charge deliverable by the waveform as well as the maximum rate of change of current. The peak current is simply the highest point on the curve. The energy deliverable is described in terms of the action integral. The charge is simply the area under the waveform in Coulombs. Lastly, the maximum rate of change is the slope immediately as it starts. These parameters can be found by analysing the reference waveform without applying any prior knowledge of electronics.

It was considered that exploring these parameters could assist specification for a circuit as a check to compare with a SIPCE simulation. However, it was found, while exploring the equations as presented below, that the parameters for an LCR circuit could be directly derived, leaving the SPICE simulation as the check.

In order to make the analysis relevant for developing a lightning waveform generator, these definitions apply:

- R is the resistance of the whole circuit (generator, test rig and sample)
- L is the inductance of the whole circuit (generator, connections, capacitors internal structure, test rig and sample)
- C is the is the capacitance of an envisaged capacitor bank which is initially charged – small parasitic capacitances are not considered
- V_0 is the initial charge voltage of the capacitor bank

4.5.1. Charge

The charge, being the area under the waveform is found by integrating the equation from t = 0 to t = ∞. The following shows the integration of (1):

$$Q = I_0 \int_0^{\infty} \left(\mathrm{e}^{-\alpha \mathrm{t}} - \mathrm{e}^{-\beta \mathrm{t}}\right) dt \tag{2}$$

$$Q = I_0 \left(\frac{e^{-\beta \times \infty}}{\beta} - \frac{e^{-\alpha \times \infty}}{\alpha}\right) - I_0 \left(\frac{e^{-\beta \times 0}}{\beta} - \frac{e^{-\alpha \times 0}}{\alpha}\right) \tag{3}$$

$$Q = I_0 \left(\frac{0}{\beta} - \frac{0}{\alpha}\right) - I_0 \left(\frac{1}{\beta} - \frac{1}{\alpha}\right) = -I_0 \left(\frac{1}{\beta} - \frac{1}{\alpha}\right) = I_0 \left(\frac{1}{\alpha} - \frac{1}{\beta}\right) \tag{4}$$

The solution neatly falls out of the integral as all the t = 0 terms become 1 and the t = ∞ terms, 0.

Knowing that all the charge within the waveform comes from what was initially stored within the capacitor, and that the capacitor is completely discharged without recycling of the charge (as with a clamped circuit), the product of the capacitance and voltage is known (following on from Equation (4)):

$$Q = CV_0 = -I_0 \left(\frac{1}{\beta} - \frac{1}{\alpha}\right) \tag{5}$$

Figure 17 shows the integral of the example waveform. Note that the numerical solution converges towards the analytical (10.5 C).

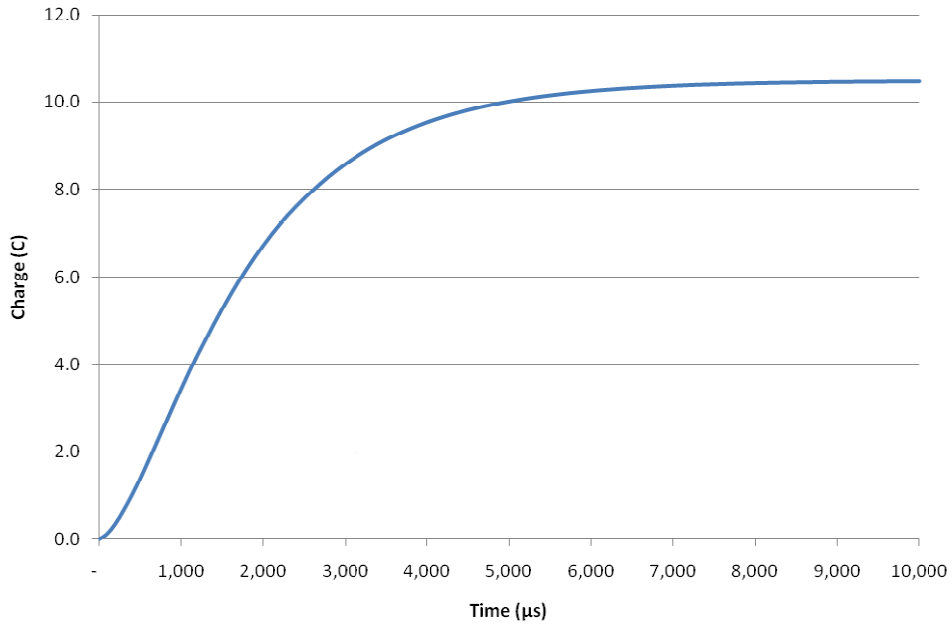

Figure 17 – Integral of current waveform in Figure 16

Equation (5) usefully informs that to maintain a given waveform profile and peak current, an increase in circuit voltage would require a proportional decrease in capacitance.

4.5.2. Energy

Assuming constant resistance (which is likely to be the case when testing a metallic sample with a direct connection rather than an arc), the power absorbed by the whole circuit resistance at any given instant is:

$$P = I^2 R \tag{6}$$

Where I is the instantaneous current and R is the circuit resistance. Both of these are known. The integral of the power with respect to time is the energy delivered to the resistance of the circuit (which includes any load such as a test sample). It has the form:

$$E = R \int_0^\infty I^2 dt \tag{7}$$

$$E = R{I_0}^2 \int_0^\infty \left(e^{-\alpha} - e^{-\beta t}\right)^2 dt \tag{8}$$

As the current is initially zero, the circuit has no initial magnetic energy. Thus, the energy can only come from what has been stored in the capacitor before the discharge begins:

$$E = \frac{C{V_0}^2}{2} = R{I_0}^2 \int_0^\infty \left(e^{-\alpha} - e^{-\beta t}\right)^2 dt \tag{9}$$

The remaining terms after cancellation:

$$\frac{C{V_0}^2}{2} = R{I_0}^2 \left(\frac{2}{-\beta-\alpha} + \frac{1}{2\beta} + \frac{1}{2\alpha}\right) \tag{10}$$

Clearly from Equation (10), the units can be seen to be $\Omega A^2 s$ or Joules.

Dividing both sides by R, normalises the energy per unit resistance. This value is described as the action integral. The units are $A^2 s$, or, typically more usefully put, J/Ω. It is often used to describe waveforms and is useful for understanding the threat level posed by one as multiplying it by the resistance of a load gives the energy delivered:

$$\frac{CV_0{}^2}{2R} = I_0{}^2\left(\frac{2}{-\beta-\alpha}+\frac{1}{2\beta}+\frac{1}{2\alpha}\right) \quad (11)$$

Action integral is essential when choosing semiconductor switching devices for high current waveforms, by comparing with the maximum device action integral from a datasheet. Figure 18 shows the integral of the square of the example waveform (Figure 14). It can be seen that the numerical solution converges towards the analytical solution of 28,544 J/Ω as t goes to ∞.

While it is conventional for action integral to be a fixed value for a complete waveform, Figure 18 shows it time passes. Such graphs can be useful for seeing where in a waveform a structure would melt and change from being a solid conductor to an arc.

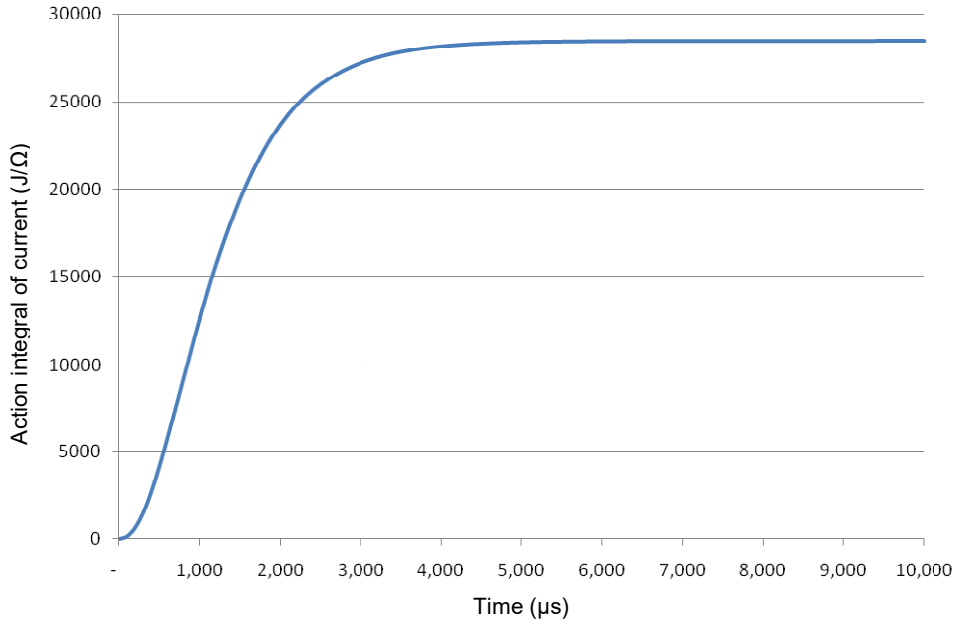

Figure 18 – Integral of current^2 of waveform from Figure 16

Equation (11) usefully informs – that to maintain a given waveform profile and peak current, an increase in stored energy requires an equal increase in system resistance to consume it.

4.5.3. Max di/dt

The maximum di/dt occurs at t = 0, when the full voltage of the capacitor bank is across the circuit inductance. Clearly, this is the instance when the capacitor has

its maximum voltage and without current flowing, there is no drop across the resistor. The following is the derivative of (2):

$$\frac{dI(t)}{dt} = I_0\left(\beta e^{-\beta t} - \alpha e^{-\alpha t}\right) \tag{12}$$

Which has the solution a t = 0 of:

$$\frac{dI(0)}{dt} = I_0(\beta - \alpha) \tag{13}$$

Knowing that di/dt in an inductor is the driving EMF over the inductance, for t = 0:

$$\frac{V_0}{L} = I_0(\beta - \alpha) \tag{14}$$

The analytical solution for the example waveform is (14,690,000 A/s).

Equation (14) usefully informs that to maintain a given waveform profile and peak current, an increase in inductance would require a proportional increase in capacitor voltage.

4.5.4. Time to peak

In a unipolar pulse, the only time when di/dt = 0 is at peak current. Arguably, it is also 0 at t = ∞, but for any real system of interest, that root can be ignored. Following on from (12):

$$0 = I_0\left(\beta e^{-\beta t_{Imax}} - \alpha e^{-\alpha t_{Imax}}\right) \tag{15}$$

Dropping the constant and rearranging:

$$\alpha e^{-\alpha t_{Imax}} = \beta e^{-\beta t_{Imax}} \tag{16}$$

Taking the natural log of each side:

$$ln(\alpha) - \alpha t_{Imax} = ln(\beta) - \beta t_{Imax} \tag{17}$$

Then, rearranging for the time of peak current:

$$t_{I_{max}} = \frac{ln(\alpha) - ln(\beta)}{\alpha - \beta} \tag{18}$$

The analytical solution for the example waveform is $t_{I_{max}} = 0.0008\text{s}$, which is in agreement with Figure 16. The time to peak is scale invariant and thus the same for any initial charge voltage.

4.5.5. Maximum current

Equation (1) gives the current as a function of time. Equation (18) gives the time to peak. Therefore, the maximum current is:

$$I_{max} = I_0 \left(\mathrm{e}^{-\alpha \frac{ln(\alpha)-ln(\beta)}{\alpha-\beta}} - \mathrm{e}^{-\beta \frac{ln(\alpha)-ln(\beta)}{\alpha-\beta}} \right) \tag{19}$$

4.5.6. Calculating circuit parameters

Equation (5) can be rearranged to show V_0 is a function of C:

$$V_0 = \frac{-I_0\left(\frac{1}{\beta}-\frac{1}{\alpha}\right)}{C} \tag{20}$$

From equation (11), R can also be found to be a function of C and V_0:

$$R = \frac{C{V_0}^2}{2{I_0}^2\left(\frac{2}{-\beta-\alpha}+\frac{1}{2\beta}+\frac{1}{2\alpha}\right)} \tag{21}$$

Equation (20) can be substituted into (21), giving R as a function of C and eliminating V_0:

$$R = \frac{\left(\frac{1}{\beta}-\frac{1}{\alpha}\right)^2}{2C\left(\frac{2}{-\beta-\alpha}+\frac{1}{2\beta}+\frac{1}{2\alpha}\right)} \tag{22}$$

Equation (14) can be rearranged to show that L is a function of V_0, L can be found in terms of C by substituting in Equation (20):

$$L = \frac{V_0}{I_0(\beta-\alpha)} = \frac{\left(\frac{1}{\alpha}-\frac{1}{\beta}\right)}{C(\beta-\alpha)} = \frac{1}{C\alpha\beta} \tag{23}$$

Having generated equations relating R, C and L to α and β, it was thought that by rearranging the equations, α and β could be found in terms of R, C and L. This was indeed the case (which took a lot of paper to arrive at):

$$\alpha = \frac{R}{2L} - \sqrt{\frac{R^2}{4L^2} - \frac{1}{LC}} \tag{24}$$

$$\beta = \frac{R}{2L} + \sqrt{\frac{R^2}{4L^2} - \frac{1}{LC}} \tag{25}$$

Rearrangement of Equation (20) for I_0:

$$I_0 = \frac{-CV_0}{\left(\frac{1}{\beta} - \frac{1}{\alpha}\right)} = \frac{CV_0}{\left(\frac{1}{\alpha} + \frac{1}{\beta}\right)} \tag{26}$$

These look like the general solutions for a second order differential equation, which was checked and found to be true. However, doing so was not as illuminating as the approach taken in this chapter.

This shows that the α and β terms in the original double exponential equation can be described in terms of capacitance, inductance and resistance. This makes sense as it is these terms that determine the frequency of oscillation and the dampening of waveform.

For real, positive values of R, L and C, both α and β will be positive and β always larger than α (even for complex solutions, as long as +j is considered positive).

As can be seen by inspecting Equation (14), for real values of V_0 and L, either I_0, α and β are all real or all complex. The waveform solutions have the following properties:

- Overdamped (I_0, α and β are real) $\frac{R^2}{4L^2} > \frac{1}{LC}$
- Critically damped (α and β are equal) $\frac{R^2}{4L^2} = \frac{1}{LC}$
- Underdamped (I_0, α and β are complex) $\frac{R^2}{4L^2} < \frac{1}{LC}$

While the double exponential equation works and provides an exact solution for both overdamped and underdamped cases, it does not work for the critically damped case. Fortunately, only an infinitesimally small change in L, C or R from the critically damped case is required for the double exponential equation to describe the waveform.

For completeness, effort was made to derive an equation for the critically damped case. After attempts to modify the double exponential equation failed, it was started from scratch, using logic similar to that used above.

As a critically damped waveform does not oscillate, the current will always be positive; therefore, complex terms would not be required to describe it. That ruled out sine terms. A single exponential would not work as the current would have to start from 0 A. However, a normal exponential starts at 1 and decays, which does look like the tail.

Attention was turned to the initial conditions. The initial rate of change of current is given by V_0/L. Multiplying this by t satisfies the initial conditions of zero current with the correct initial gradient. As a normal exponential starts at 1 before decaying to zero as t increases, it seemed a sensible guess to multiply it by the initial conditions and use it to deliver the decaying tail of the waveform.

To test this, an exponent was required. Equation (24) and Equation (25) become equal when $\frac{R^2}{4L^2} = \frac{1}{LC}$ and that the square root term cancels and is zero. This is shown for clarity in Equation (27):

$$\alpha = \beta = \frac{R}{2L} \tag{27}$$

It seemed sensible to try this as the exponent (as the $\sqrt{\frac{R^2}{4L^2} - \frac{1}{LC}}$ term is zero when critically damped) and was found to work, giving critically damped current exactly. Equation (28) shows the equation found and illustrates that there are 2 equal solutions:

$$I(t) = \frac{V_0}{L} te^{-\alpha t} = \frac{V_0}{L} te^{-\beta t} \tag{28}$$

In the critically damped case, I_0 is not useful as it is infinite. This can be seen by inspecting Equation (14) and decreasing β until it is equal to α.

As an example to show Equation (24) and Equation (25) do reveal α and β from values of L, C and R, SIMetrix was used to calculate the current waveform for 3 different sets of component values and starting voltages. Table 6 shows the circuit parameters used. These were randomly chosen and inspected to ensure they are not simply scaled versions of each other. Set 1 and Set 2 are overdamped and underdamped respectively and used Equation (1) for the current. Set 3 is critically damped and used Equation (28) for the current.

Table 6 – Circuit parameters for D waveform

Parameter set	Inductance (H)	Capacitance (F)	Resistance (Ω)	Cap charge (V)
Set 1 (Over d.)	1.1	1	2.5	3
Set 2 (Under d.)	0.4	3	0.5	1.5
Set 3 (Critically d.)	0.5	2	1	3

Equation (20) was rearranged to find I_0 as a function of the initial capacitor voltage and the found values of α and β for the underdamped and overdamped cases. As mentioned above, I_0 becomes infinite when α equals β.

Figure 19 shows the simple test circuit used in SIMetrix to numerically solve for the current waveforms (in this case Set 1). C1 has a value of 1.1 F and an initial charge (IC) of 2.5 V. L1 has a value of 1 H and an initial current (also referred to as IC in the software) of 0 A. The resistance was set to 2.5 Ω. The time step was set to 0.1 s, which created 101 data points.

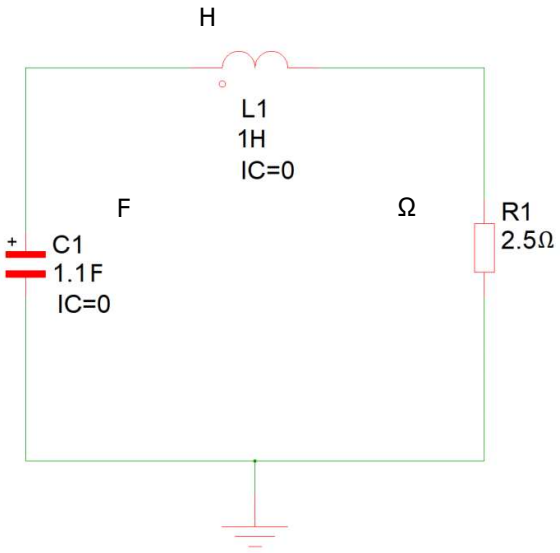

Figure 19 – Test circuit used in SIMetrix to evaluate Set 3

The values in Table 7 were created using the values from Table 6 and Equation (24) for α, Equation (25) for β and Equation (26) for I_0. By setting the inductor initial current to 0 A, the circuit effectively self initiates as soon as the numerical solver starts, thus, eliminating the need for a switch or timer in this circuit.

Table 7 – Circuit parameters for D waveform

Parameter set	I_0	α	β
Set 1 (Over d.)	2.206	0.518	1.755
Set 2 (Under d.)	0.000-2.818i	0.625-0.665i	0.625+0.665i
Set 3 (Critically d.)	∞	1	1

The calculated values for Set 1 are real numbers, while those for Set 2 are complex. To compute complex numbers required installing the Data Analysis pack that comes with Microsoft Excel but was otherwise trivial. These were calculated using Equation (1) at the same 101 time points as those calculated numerically. The same was done for Set 3 but using Equation (28)

Figure 20 shows the numerical and analytical waveforms overlaid upon each other for Set 1. It can clearly be seen that the curves match perfectly.

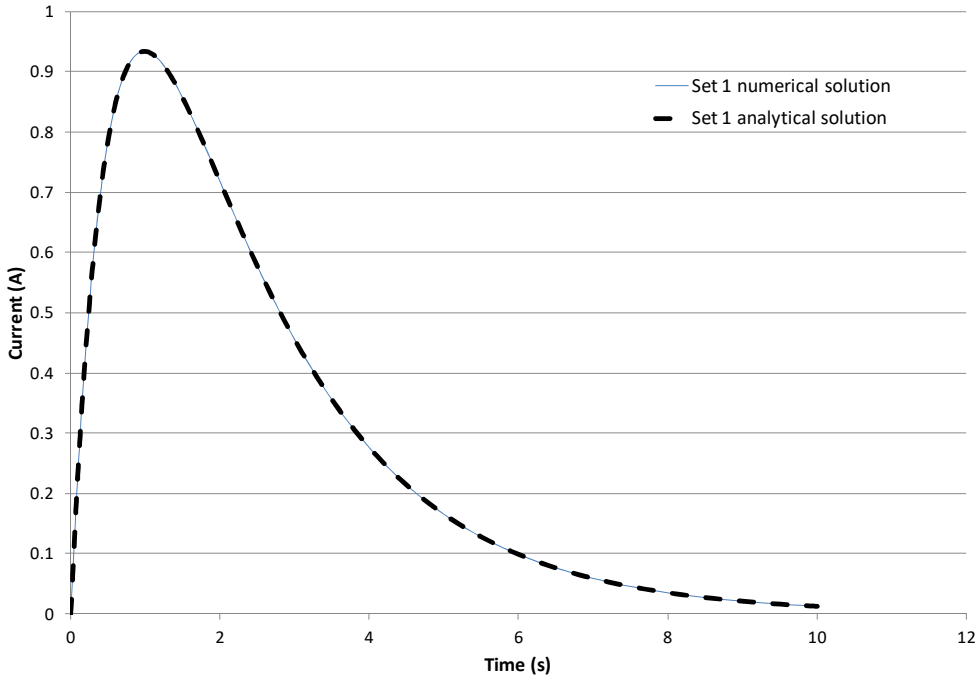

Figure 20 – Numerical and analytical current waveforms for Set 1

If the analysis time window is widened such that the tail of the waveform has very strongly decayed (many times the time to half current), the numerical and analytical results do differ when solved using SIMetrix. This is because the solver has a resolution and not because there is a real mismatch. To check this, Microsoft

Excel was used to perform a numerical calculation with 10,000 time steps. A closer tolerance was then seen between the numerical and analytical solutions. However, this is of little interest other than the check, as the difference only occurs once the current has decayed to approximately 1 millionth of the peak current.

Figure 21 shows the numerical and analytical waveforms overlaid upon each other for Set 2. These can also be seen to match perfectly. With both Set 1 and Set 2 showing agreement between analytical and numerical solutions, it is demonstrated that Equation (24) and Equation (25) are correct. A very large number of other comparisons were made, including solutions for the I_0, α and β values from the standards. In every case they agreed.

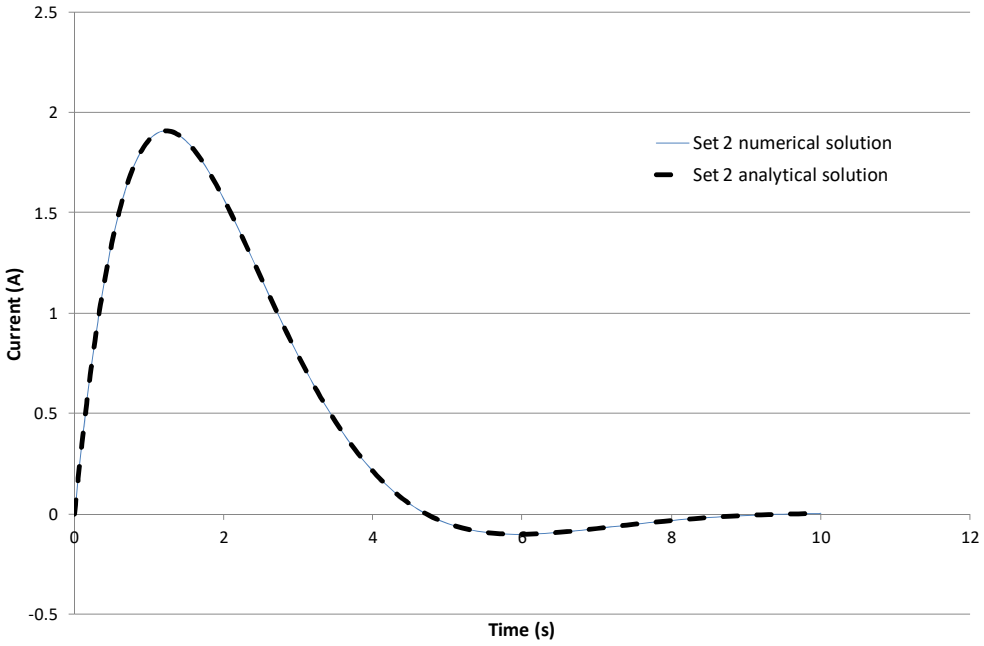

Figure 21 – Numerical and analytical current waveforms for Set 2

Figure 22 shows the numerical and analytical waveforms overlaid upon each other for Set 3. It can clearly be seen that the curves match perfectly and confirms the double exponential equation, when used with complex values, can describe a damped oscillating waveform.

It is interesting to note that Equation (18) always gives the time to the first current peak even if the system is under-damped and has many positive and negative peaks and thus roots.

Using Equation (18) to find the time to peak for the waveform shown in Figure 19, which does have more than one peak, even if it is heavily attenuated, gives 1.227 seconds, which is correct.

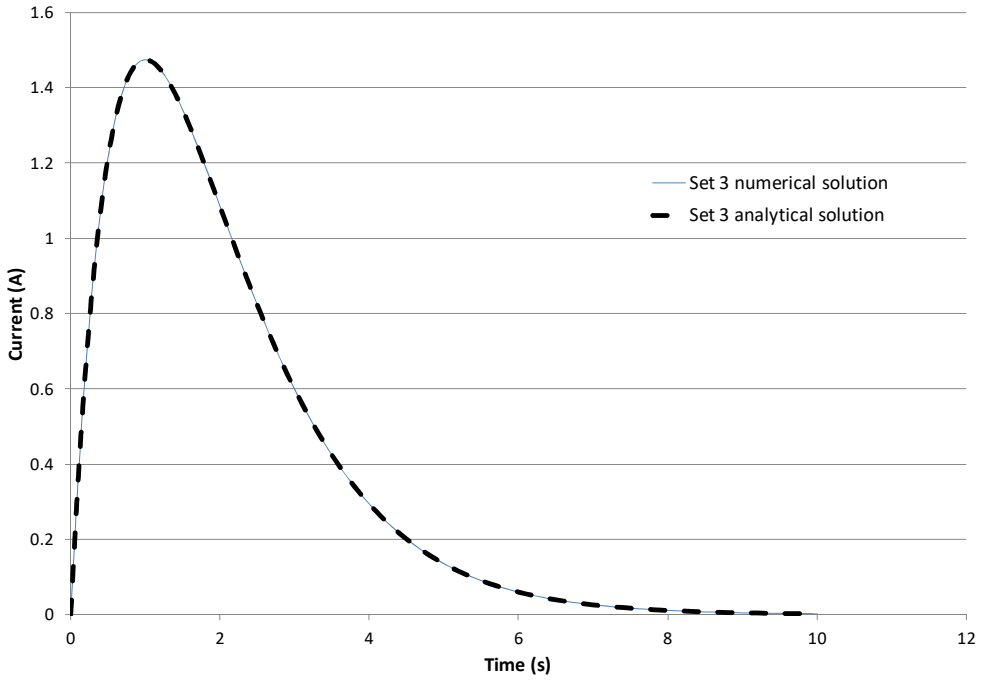

Figure 22 – Numerical and analytical current waveforms for Set 3

The perfect match between the numerical and analytical solutions when using complex numbers to represent an oscillating waveform has, thus, been shown. The extension of using Equation (24) and Equation (25) in the complex domain has been shown also.

With these equations, it was to possibly describe a double exponential waveform in terms of L, C, R and V_0:

$$I(t) = \frac{CV_0}{\left(\frac{1}{\frac{R}{2L} - \sqrt{\frac{R^2}{4L^2} - \frac{1}{LC}}} - \frac{1}{\frac{R}{2L} + \sqrt{\frac{R^2}{4L^2} - \frac{1}{LC}}}\right)} \left(e^{\left(-\frac{R}{2L} + \sqrt{\frac{R^2}{4L^2} - \frac{1}{LC}}\right)t} - e^{\left(-\frac{R}{2L} - \sqrt{\frac{R^2}{4L^2} - \frac{1}{LC}}\right)t} \right) \quad (29)$$

While Equation (29) is rather cumbersome it was easy enough to handle with a spreadsheet. It is worth pointing out that if complex numbers are used for α and β, then the equation can be used to understand under-damped circuits that oscillate.

4.5.7. Approach to determine waveform generator circuit parameters

To complete the exploration of the equations, the solution of circuit parameters for a given α, β and I_0 were derived.

It transpires that there are a continuous set of unique circuit parameters (L, C, R and V_0) for any given waveform shape. Therefore, at least 1 parameter has to be decided upon before the remainder can be solved for.

These equations are presented here as a record of those used in numerous spreadsheets to calculate the circuits for the waveform generators. Further, they are not obviously found in any text books or other publications.

A. If the inductance is known, the following calculations can be used

Rearranging Equation (23) to give capacitance:

$$C = \frac{1}{L\alpha\beta} \tag{30}$$

From Equation (22) and (30) the resistance can be derived:

$$R = L(\alpha + \beta) \tag{31}$$

From Equation (20) and (30) the initial voltage can be derived:

$$V_0 = -I_0 L\alpha\beta \left(\frac{1}{\beta} - \frac{1}{\alpha}\right) \tag{32}$$

B. If the resistance is known, the following calculations can be used

Simplifying and rearranging Equation (22) for capacitance:

$$C = \frac{(\alpha+\beta)}{R\alpha\beta} \tag{33}$$

From Equations (23) and (33), the inductance can be derived:

$$L = \frac{R}{(\alpha+\beta)} \tag{34}$$

Substituting Equation (34) into Equation (32), the initial voltage can be found:

$$V_0 = -\frac{I_0 R\alpha\beta}{(\alpha+\beta)}\left(\frac{1}{\beta}-\frac{1}{\alpha}\right) \tag{35}$$

C. If the capacitance is known, the following calculations can be used

Rearranging Equation (33) for resistance:

$$R = \frac{(\alpha+\beta)}{C\alpha\beta} \tag{36}$$

Rearranging Equation (23) to give inductance:

$$L = \frac{1}{C\alpha\beta} \tag{37}$$

Finding voltage if C was known was shown in Equation (20):

$$V_0 = -I_0\frac{1}{C}\left(\frac{1}{\beta}-\frac{1}{\alpha}\right) \quad \text{(Equation 20 repeated)}$$

D. If the initial voltage is known, the following calculations can be used

Rearranging Equation (32) for L:

$$L = \frac{-V_0}{I_0\alpha\beta\left(\frac{1}{\beta}-\frac{1}{\alpha}\right)} \tag{38}$$

Rearranging Equation (20) for C:

$$C = -I_0\frac{1}{V_0}\left(\frac{1}{\beta}-\frac{1}{\alpha}\right) \tag{39}$$

Rearranging Equation (35) for R:

$$R = \frac{-V_0(\alpha+\beta)}{I_0\alpha\beta\left(\frac{1}{\beta}-\frac{1}{\alpha}\right)} \quad (40)$$

4.6. Testing the mathematical derivation

Waveform B was used for deriving and understanding the circuit parameters from α, β and I_0. In order to test the analytical equations, waveforms A and D from ED84 were inspected. They have the following parameters:

- Waveform A
  - I_0 218,810
  - α 11,354
  - β 647,265
- Waveform D
  - I_0 109,405
  - α 22,708
  - β 1,294,530

As shown above, at least one circuit parameter is required in order to derive the others. The inductance was chosen as it is related to the physical size of the circuit, including the sample. A reasonable inductance of 5 μH was chosen; because the spread of inductances from visited laboratories was from 2.5 μH to 10 μH and 5 μH is in between. The lowest value was not used as it is expected the high voltage would require reasonable distance between conductors, which increases inductance. However, the chosen value was towards the lower end of the range to avoid requiring an unnecessarily high initial charge voltage.

To produce the A waveform using an over damped LCR circuit, where L is set as mentioned above, the following parameters are required:

- Resistance = 3.29 Ω
- Capacitance = 27.2 μF
- Inductance = 5.00 μH
- Voltage = 696 kV

Figure 23 shows a comparison of the I_0, α and β values for the A waveform with a circuit that uses the above mentioned parameters. It can be seen to fit precisely.

Note the peak current box, it is the reference area where the peak current must be in order to count as a successful test according to ED84. The size of the box allows for unexpected resistances in a sample to alter the peak current and a more inductive/lower voltage machine to deliver the peak current later.

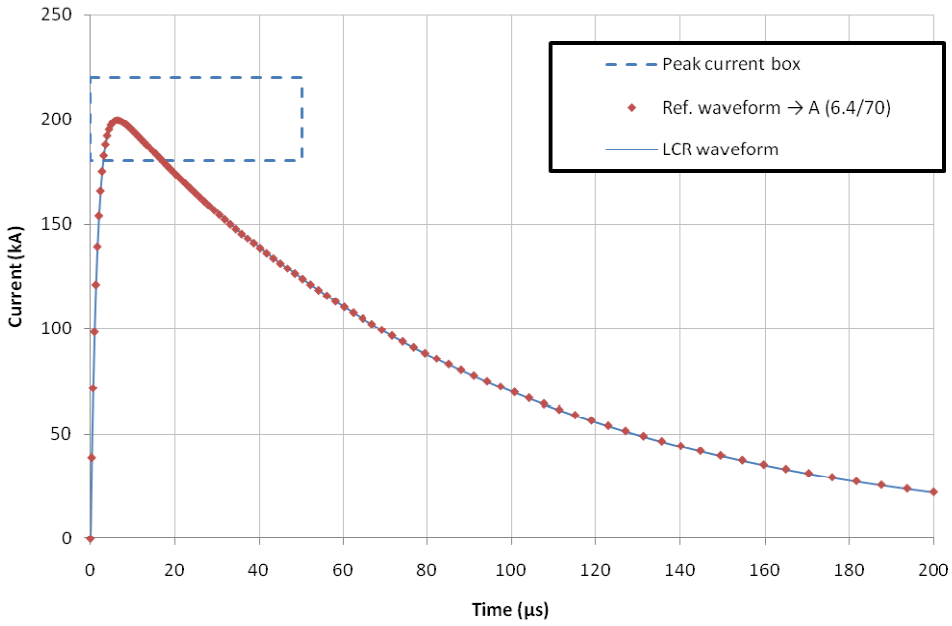

Figure 23 – Comparison waveform an LCR circuit waveform and the standard waveform

Figure 23 presents an example of using I_0, α and β with a single known parameter; in this case inductance, which is used to calculate the capacitance, resistance and initial charge voltage of an LCR circuit. The precise fit of the reference waveform (analytically solved) with the LCR waveform (numerically solved), further confirms the equations used are correct. The previous examples (Figure 18, Figure 19 and Figure 22) performed the check in the reverse order, starting with inductance, capacitance, resistance and initial charge voltage, and delivering I_0, α and β. Therefore, the equations are shown to work in both directions, from circuit parameters to a double exponential equation (or Equation (28) for critically damped case) and vice versa.

Due to the high voltage (696 kV), the machine would almost certainly have a Marx configuration, thus lowering the voltage per stage and simplifying insulation and charging considerations. Because capacitors would unlikely be used at the maximum rated voltage as this would lower the reliability of the machine – a fully

erected maximum voltage of 800kV would give adequate margin. Thus, the maximum stored energy would be 8.86MJ. The estimated price for the capacitors is very high. Insulating the system under oil, high voltage triggering and safety systems would further add to this high price. This is feasible and would produce an impressive machine, all be it an expensive one.

For reference, the circuit parameters to produce a D waveform into 5μH:

- Resistance = 6.57 Ω
- Capacitance = 6.80 μF
- Inductance = 5.00 μH
- Voltage = 696 kV

Figure 24 shows a comparison of the I_0, α and β values for waveform D with a circuit that uses the above mentioned parameters. It can also be seen to fit precisely.

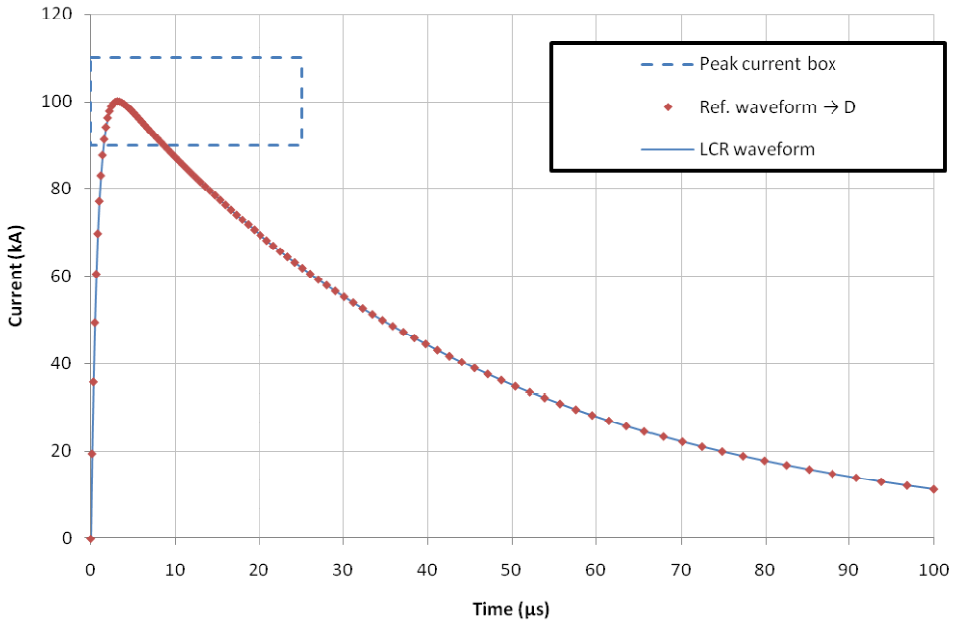

Figure 24 – Comparison of waveform D from LCR circuit and the standard waveform

The voltage requirement for the D waveform is exactly the same, but the energy is lower than for the A waveform (¼ of the energy). Because the voltage is the same, it would be just as challenging to design as a machine to produce an A waveform. Furthermore, if the capacitance within the A waveform generator could

be split into 4 parallel chains, then it would also be able to produce D waveform by using a single one as the capacitance is ¼ of what is required for A waveform.

The above circuit parameters were tested using SIMetrix software and the waveforms were found to correlate exactly with those described in the standard. This was repeated using Microsoft Excel software for generation of the graphs.

4.7. Possible compromise – a clamped circuit

With such high voltages required to deliver the waveforms with a perfectly matched shape, a reduction in energy can be achieved if a clamped circuit is used. This immediately causes the waveform to deviate from a true double exponential. Such a solution is how the lightning generator 8 works (see Chapter 1). Clamped circuits, especially ones that are required to provide a range of waveforms, can be very complex to design, setup, and run compared with the simple LCR solution. However,since the capacitance is only required to ring current into the inductance of the circuit, it can be greatly reduced.

The circuit operates by ringing the energy stored in a capacitor bank into an inductor. Then, once the current peaks and the voltage across the capacitor bank (and its internal resistance) is zero, the capacitor is shorted with a small resistance. The circuit is then freed of the capacitance and so no longer an LCR circuit but, effectively, a more simple LR circuit. The current then decreases exponentially as it flows through the clamp resistance.

Using the same 5 μH as with the above examples, an LR discharge, starting with 200 kA and reasonably matching the tail of waveform A requires approximately 50 mΩ of resistance in the clamp.

The capacitance and the series resistance was adjusted until the peak current (200 kA) and rise time, was identical to the standard A waveform (6.36 us, though often rounded up to 6.4 when describing the waveform). The resistance in series with the capacitors that initiate the waveform has to be selected to prevent too much voltage reversal should the clamp fail. Attempt was made to limit this to about 75%. The capacitance and series resistance were found to be 6.75 uF and 250 mΩ, respectively.

A perfect theoretical diode was chosen for the clamp in the SPICE software, as that eliminated any timing requirement. The full circuit parameters are shown below and the circuit shown in Figure 25:

- Cap resistance = 0.250 Ω
- Clamp resistance = 0.0565 Ω
- Capacitance = 3.75 μF
- Inductance = 5.00 μH
- Voltage = 271 kV

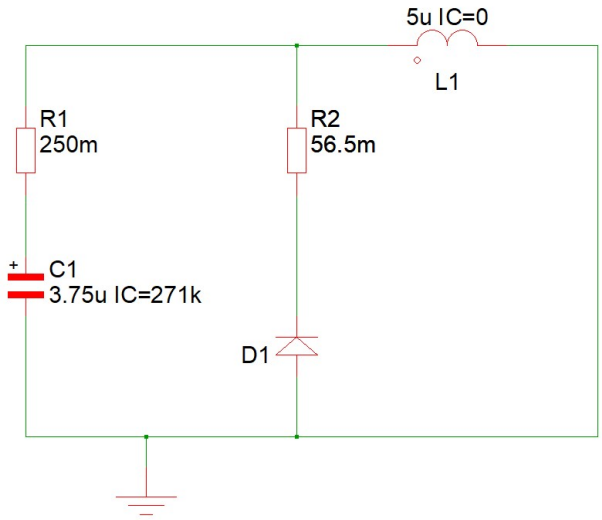

Figure 25 – Clamped waveform generator circuit

Figure 26 shows the ringing waveform to illustrate how rapidly it oscillates in its undamped state. The figure further shows the clamped and reference waveforms for comparison. The clamped current waveform reaches peak current at the same time as the reference waveform and follows the tail very well, though the leading edge does lag the reference waveform a little.

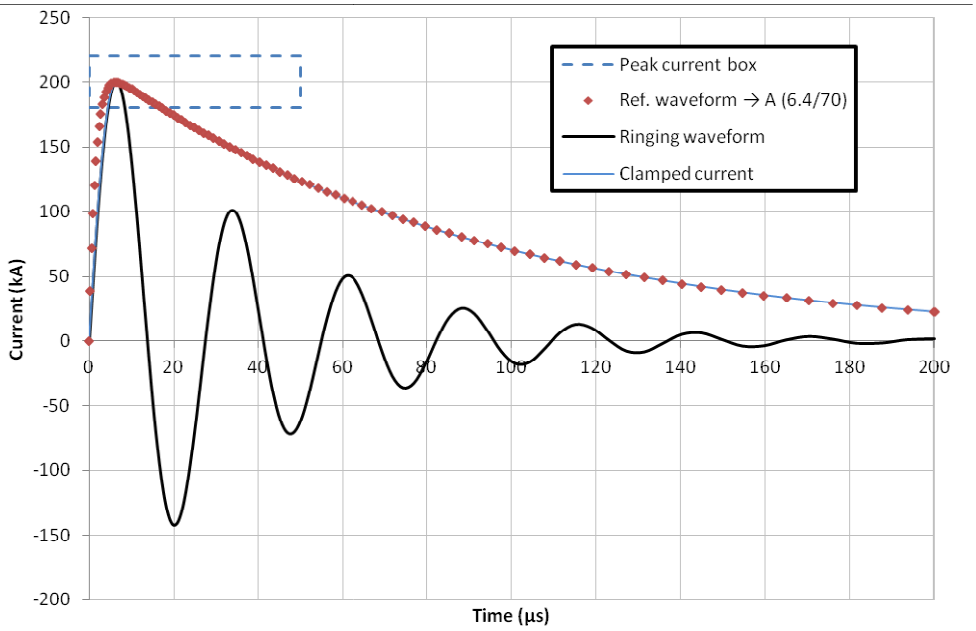

Figure 26 – Comparison of waveform A with output from clamped circuit

For clarity, Figure 27 shows an enlarged proportion of the early stages of the waveform to illustrate this lag.

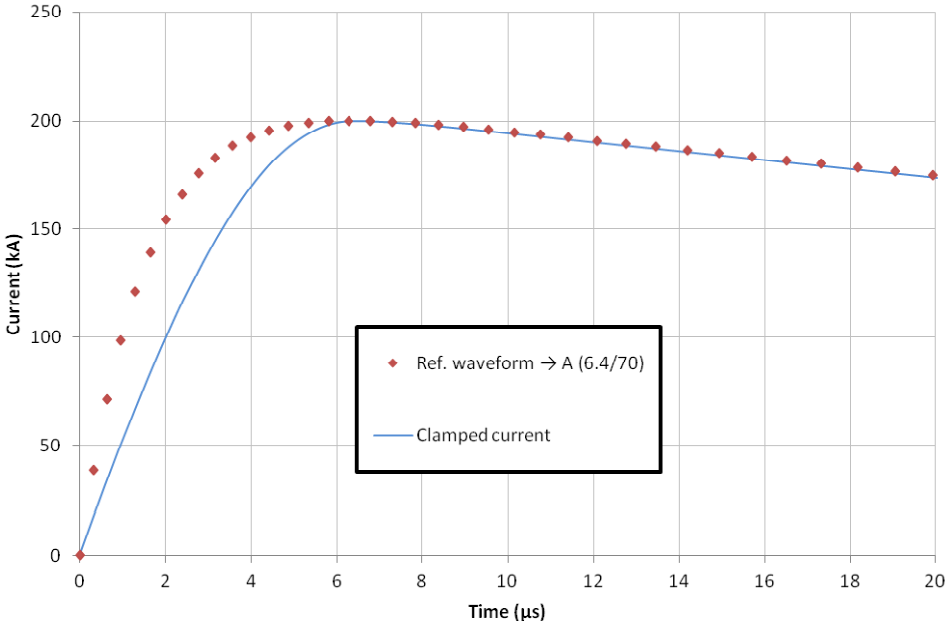

Figure 27 – Enlarged view of Figure 26

The stored energy in the clamp circuit would be 140 kJ. This is a huge reduction from the many MJ required to deliver the reference waveform using the LCR

method with the same inductance. While a reduction in energy very likely equates to a lower cost for capacitors, the chance of the clamp circuit not firing and the capacitor bank oscillating as shown in Figure 26 would have to be taken into account during fault analysis. This would very likely require robust foil type capacitors with fairly low energy density as metalized film capacitors usually do not cope well with high voltage reversal.

4.8. Greatly reduced voltage LCR circuit

Compromising on rise time, but still remaining within the specification, allows for a vast decrease in both voltage and stored energy. Since the rise time may be extended from 6.4 μs to 50 μs, it can be seen that for a given inductance the voltage could be reduced nearly by a factor of 8 simply due to the lower di/dt requirement (50/6.4 = 7.8125). Reducing voltage allows for a more compact circuit as there is less chance of flashover. So, a slightly reduced inductance can be allowed for. This then allows a further reduction in voltage.

Rapidly, a relatively inexpensive LCR circuit that could produce the desired waveforms emerged. This provided a much simpler solution (than if matching the reference waveform), that would be unlikely to require oil insulation or a Marx arrangement. Also, by not using a clamp circuit, it would only have one spark gap to trigger and a single resistance to set. Such a system would be relatively simple to design, setup, and operate, if the voltage and energy levels could be kept relatively low.

For an LCR circuit, with a given inductance, there is a maximum capacitance beyond which it is impossible to attain both the required peak current and action integral. At that critical capacitance, there is a single solution of initial charge voltage which will deliver the required peak current and action integral.

More generically, it was found to hold that for a given inductance, capacitance, and fixed action integral, there was a distribution of peak currents with a single maximum. Figure 28 shows an example of this.

By extension, as soon as the capacitance is less than the maximum that can attain a particular peak current, for the given inductance and action integral, there are then 2 circuit solutions for producing the desired peak current. This is explored and

made use of in section 3.11 to provide 2 different voltage solutions for each of the waveforms the high current waveform generator is designed to make.

Figure 28 shows the range of peak currents attainable with 3 uH of inductance and the largest capacitance (300 uF) that can deliver a peak current of 200 kA while also delivering a 2 x 10^6 J/Ω action integral. The peak is the single solution for producing 200 kA with 300 uF, and occurs at 38.1 kV with 0.109 Ω of circuit resistance. This would require 220 kJ of stored energy, which – from the engineering and especially the budgetary standpoint would have been possible to use as a circuit solution – however, as can be seen in Figure 29, the waveform is slightly underdamped and thus not unipolar. Having a significant -25 kA peak a short time after the initial 200 kA peak certainly does not replicate nature.

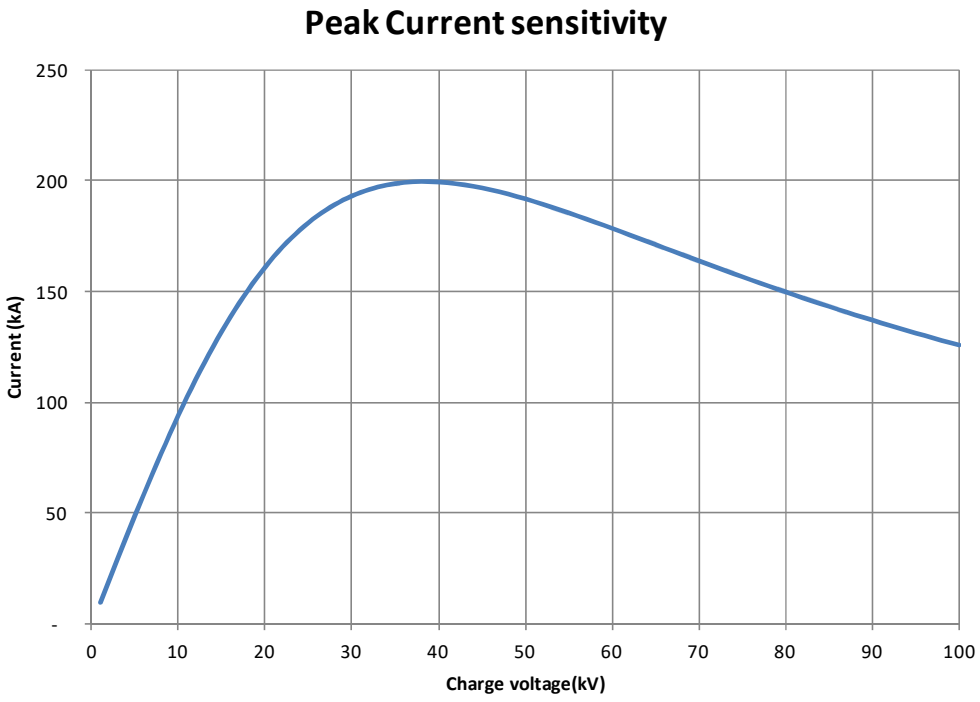

Figure 28 – Peak current vs charging voltage delivering 2 x 10 ^{6} J/Ω with 3 µH inductance and 300 µF capacitance

The rise time of the waveform is 35.6 µs and so within the 50 µs of the standard.

Keeping the inductance the same and decreasing the capacitance to 200 µF gives 2 solutions for the voltage required to deliver a 200 kA peak. This is shown in Figure 30.

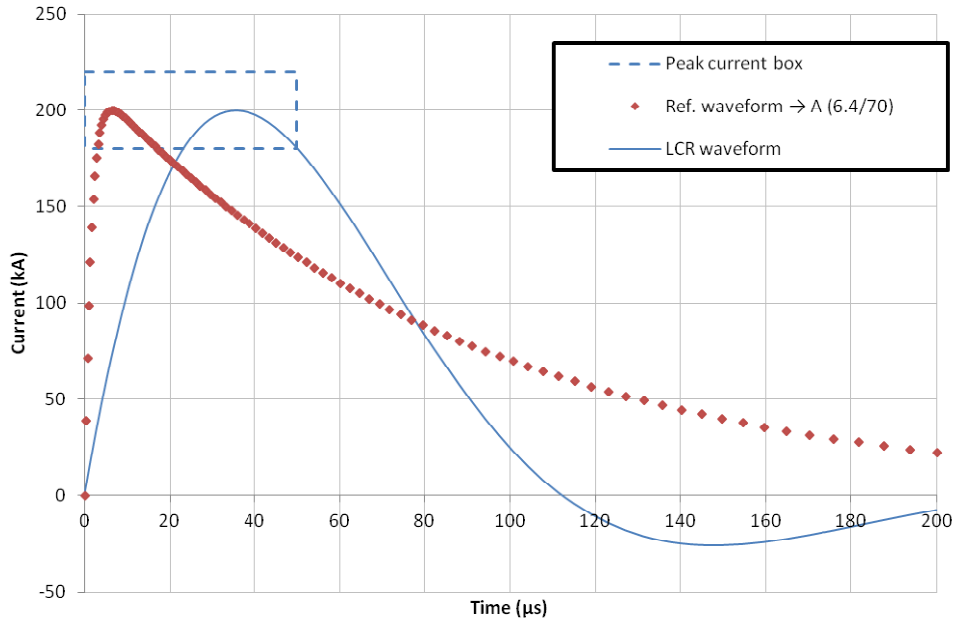

Figure 29 – Highest current waveform attainable delivering 2 x 10 ^{6} J/Ω with 3 µH inductance and 300 µF capacitance

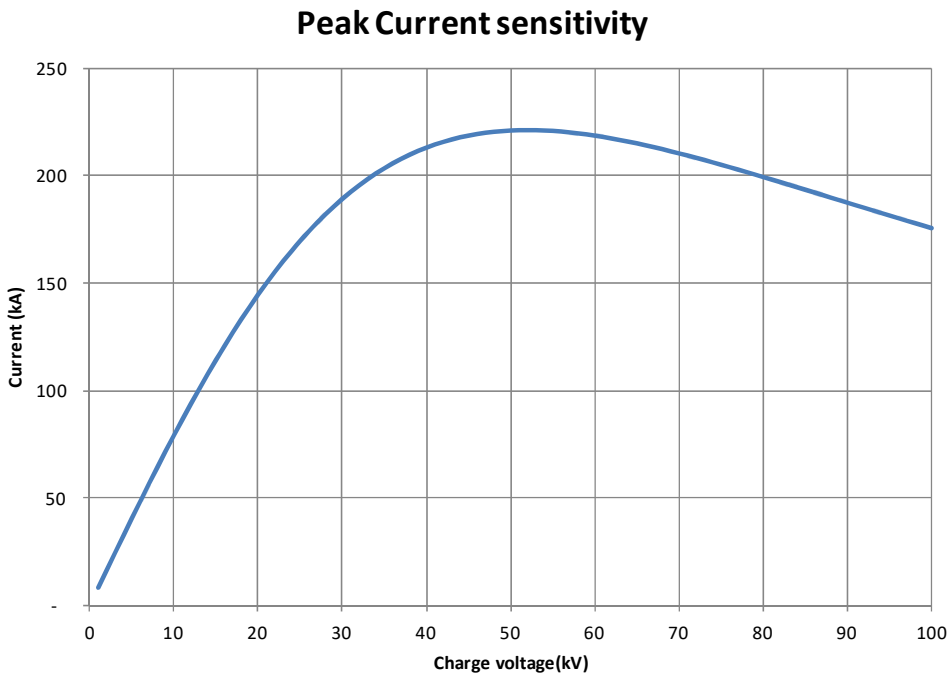

Figure 30 – Peak current vs charging voltage delivering 2 x 10 ^{6} J/Ω with 3 µH inductance and 200 µF capacitance

The lowest voltage solution giving 200 kA under these circumstances is shown in Figure 31, where peak current is reached at 33.7 µs and requires, by coincidence,

33.7 kV, thus 110 kJ of stored energy and a circuit resistance of 57 mΩ. It is rather underdamped, and this low resistance may be a little too low for practical purposes (it would be quite sensitive to changes in sample resistance). Furthermore, an underdamped waveform is not unipolar and so differs from natural lightning which is. Also, having a second peak after passing through zero current would perhaps act like 2 successive lightning pulses rather than 1. However, the test standard does allow ringing waveforms.

For the example shown in Figure 30, the voltage where the waveform is critically damped is 70.0 kV.

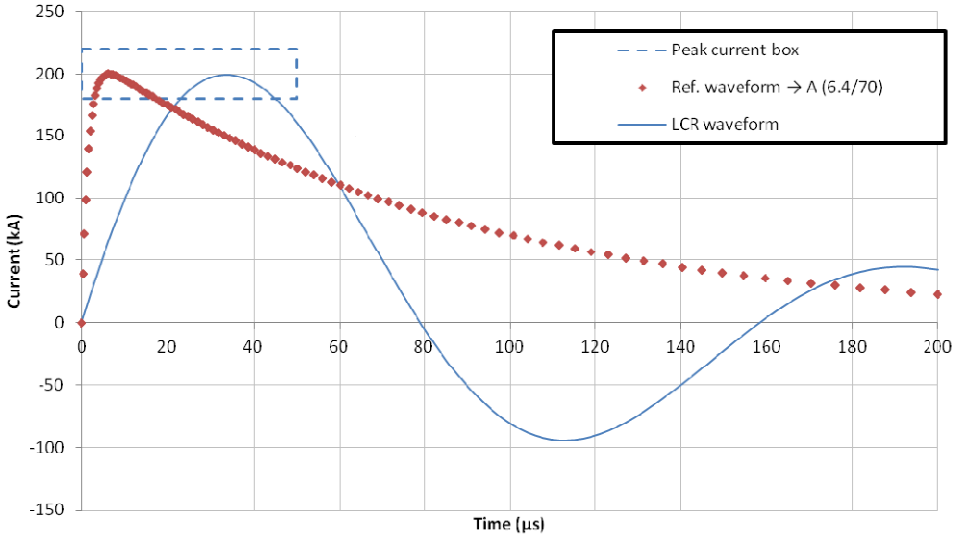

Figure 31 – Lowest voltage solution delivering 2 x 10 ^{6} J/Ω with 3 µH inductance and 200 µF capacitance

Figure 32 shows the higher voltage solution where peak current is reached in 22.4 µs. This requires 79.3 kV, thus 629 kJ. In order to keep the action integral the same, this increase in energy requires a proportional increase in circuit resistance to 315 mΩ.

Both from inspecting the waveform in Figure 32 and checking that the charge voltage of 79.3 kV is above the critically damped threshold of 70.0 kV, it can be seen to be overdamped and thus unipolar.

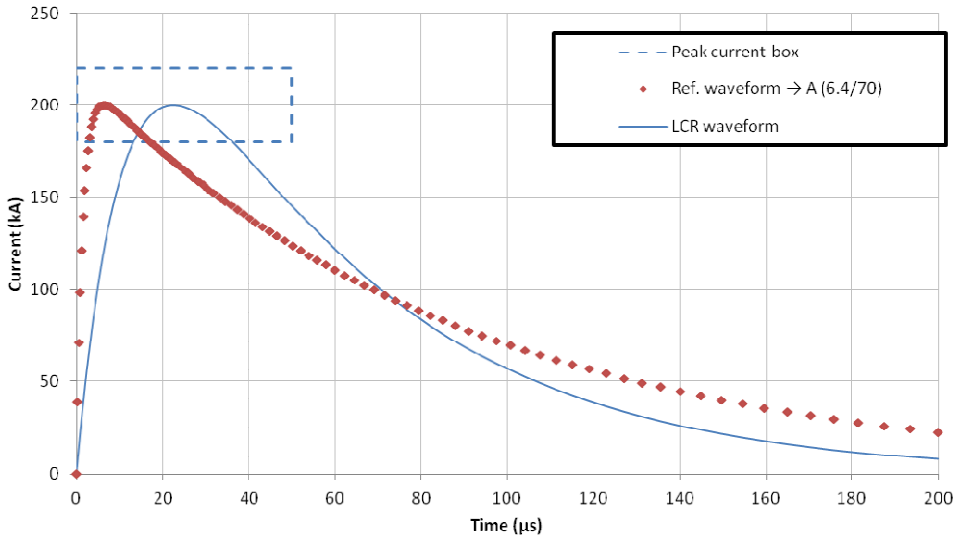

Figure 32 – Highest voltage solution delivering 2 x 10 ^{6} J/Ω with 3 µH inductance and 200 µF capacitance

The 2 solutions for a desired peak current, allow an interesting flexibility for designed generator to produce both solutions, simply by changing the voltage and the resistance.

The higher voltage solution will always be more stable than the lower with regard to variance in sample resistance as the overall resistance is higher.

The initial charge voltage where the resultant waveform transitions from overdamped to underdamped can be arrived at by solving the critically damped condition $\frac{R^2}{4L^2} = \frac{1}{LC}$ for constant L, C and A_{Int} (action integral). The solution starts logically with the energy stored in a capacitor being equal to the action integral times the circuit resistance:

$$\frac{CV^2}{2} = A_{Int}R \tag{41}$$

Equation (41) can be rearranged for R:

$$R = \frac{CV^2}{2A_{Int}} \tag{42}$$

Equation (42) can then be put into the critically damped condition to eliminate R:

$$\frac{R^2}{4L^2} = \left(\frac{CV^2}{2A_{Int}}\right)^2 \frac{1}{4L^2} = \frac{C^2V^4}{16{A_{Int}}^2L^2} = \frac{1}{LC} \tag{43}$$

Equation (43) can be rearranged for V and solved as all other terms are constants:

$$V = \sqrt[4]{\frac{16\ Int^2 L}{C^3}} \tag{44}$$

Equation (44) was tested and found to be correct by comparing it to when α and β are equal for various waveforms. Where the voltage is greater than the threshold given by this equation, the waveform is overdamped and underdamped if below the threshold.

4.9. The load – sample and test rig

Having established a thorough understanding of how in theory a lightning waveform generator could be made, using circuit analysis, simulation and from first principles, it is now possible to optimise the design and construction of the generator.

The purpose of a waveform generator is to deliver a specific current profile through a test sample. The test sample requires mounting in a test rig that had to be flexible enough to cater for a variety of test sample types and sizes.

A coaxial system was envisaged. This had a centre electrode that allowed either conduction or an arc to be attached to a sample (consider this the core of a coaxial line). The current was to be returned via 4 conductors from a conductive plate to which the sample was attached.

Figure 6 shows the typical type of electrode that is required for an arc type test. The jet diverting electrode is to prevent metal that is evaporated and ejected during the arc from being directed as a jet towards the sample, and possibly changing how the arc interacts with the sample. The electrode has to be at least 50 mm away from the sample, and there is no specification for the size of the ball. The initiating wire must be equal to or less than 0.1 mm in diameter to ensure it is consumed early on in the discharge and interferes with it as little as possible. This wire removes the necessity to have enough voltage to jump the gap to the sample and facilitates precise referencing of the initiation of the arc to a position on the test sample (such as a particular bolt). If the wire were too large, it would remain a solid conductor well into the discharge, which would cause the test to transform from a conduction test to an arc attachment test well after the waveform has started.

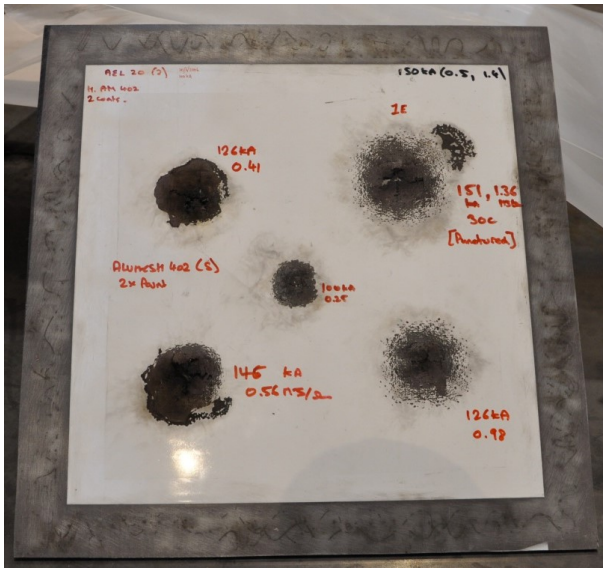

Figure 33 – Example of a test sample

Experience and discussion with industry indicated that samples are frequently 600 x 600 mm square in shape, which is a convenient size that is several times larger than the area damaged with a lightning impulse. Figure 33 shows a typical lightning test sample taken, with permission, at Cobham's facility. As can be seen, there have been tests to several parts of the surface. This requires either the centre electrode to be movable or a movable tip to place the arc where required.

M8 stainless steel threaded rod and standard phenolic resin balls (usually used on machine control levers) were chosen for the electrode as they are inexpensive, readily available and expected to be reasonably long lasting. The choice of stainless steel was influenced by having seen brass used elsewhere and discussions with technicians. Brass has been frequently used as it is easy to machine. Eliminating machining steps except for cutting it to length removed this constraint. This allowed the use of stainless steel which is less expensive than brass and has a higher melting point (Stainless steel ~1450 °C vs. brass ~920 °C), potentially extending its useful life. Galvanised steel was not chosen as the arc would release zinc fumes which are potentially hazardous if inhaled.

The test rig was designed for convenience to fit around the sample and people operating the laboratory. This leads to the following considerations:

- The sample should be mounted horizontally and at a convenient height to facilitate bolting it down to a strong, conductive mount.
- Enough height above the sample should be available to facilitate easy access for bolting operations and moving/connecting arc electrodes or conduction paths.
- Samples may not always be a flat wing skin. More space in the central volume of the test rig would allow greater future flexibility.
- The inductance should be as low as possible, as higher inductance requires higher voltage, energy and expense.
- The structure should be substantial and strong to endure magnetic forces and debris from exploding samples.

Figure 34 shows the coaxial test rig when it had just been built. It was designed to have a stripline connection to the waveform generator, which merged with the desired coaxial structure of the rig itself.

Figure 34 – Designed and constructed coaxial test rig

The current paths are shown in Figure 35 – an early sketch of the test rig with insulators removed and plat separation exaggerated. The top plate usually connects to the generator output, making it positive with respect to ground.

Convention current flow is indicated showing it flowing onto a very wide, square plate, down conductive rods to the lower plate before making its way to the sample. From the sample, either an arc or a physical connection would carry it to the centre electrode before flowing to the centre plate which is ground referenced. For clarity, yellow indicated to positive connection of the generator output to the sample and red represents the ground connection to the electrode.

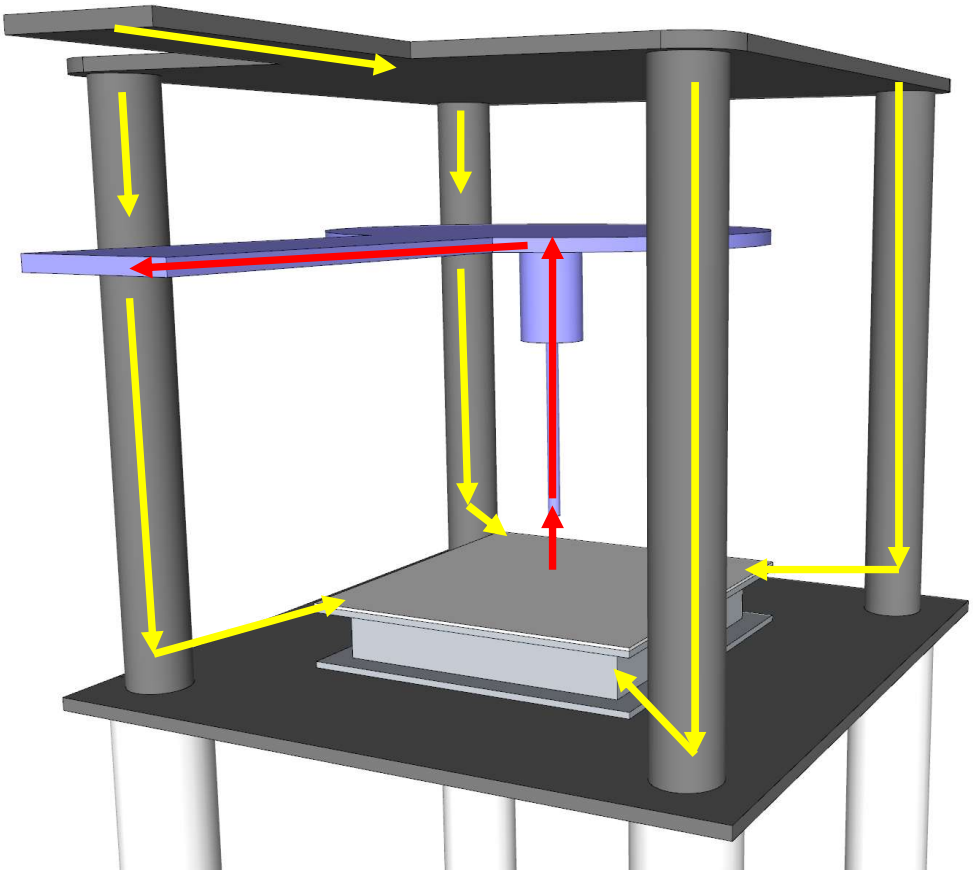

Figure 35 – Current paths within test rig

If the connection polarity requires reversing, flexible cables from the bushing into the test chamber can be swapped over.

4.9.1. Test rig circuit parameters

The design of the test rig was not a key objective of this work, but understanding its characteristics was required to design a waveform generator. Specifically, the inductance, resistance (mostly arising from the sample) and any voltage drop across the arc need to be quantified and determined accurately.

The inductance was estimated to be between that of a 1 m long 1.2 m diameter coaxial structure with a 0.05 m diameter central conductor (inductance approximately 1 μH given by Equation (45)) and that of a 1.2 m diameter circular hoop of 0.025 m diameter conductor (inductance approximately 2.5 μH given by Equation (46)). This was because the structure would not be perfectly coaxial, having only 4 conductors returning the current from the sample mounting plate to the generator connection; these were 0.025 m in diameter. The overall size of the coaxial structure was about 1.2 m square (rather than diameter) and 1 m tall. It was estimated that inductance would be approximately 1.5 μH. Once built this was found to be very close to the actual value as measured with a Wheatstone bridge and by observation of behaviour in a simple oscillating circuit with known capacitance. The exact value and frequency were lost in the haste of progress. However, that the eventual circuit performance was very close to what was predicted, confirms the low inductance of the test rig.

Inductance of coaxial conductors with major diameter D and minor d and negligible skin depth (skin depth at 1 kHz in aluminium is ~2.5 mm and all frequencies of interest are much greater than this, meaning the skin depth will be shallower):

$$L = 2\ln\left(\frac{8D}{d}\right)10^{7} \quad (45)[20]$$

Inductance of circular turn with circular section conductors with major diameter D and minor d and negligible skin depth:

$$L = 2\pi D\left(\ln\left(\frac{8D}{d}\right) - 2\right)10^{7} \quad (46)[20]$$

The resistance of an aluminium sample is vanishingly small (several μΩ) and measurements on the supplied test samples indicated that a carbon fibre test sample could have a resistance up to 50 mΩ but more often closer to 25 mΩ.

The voltage drop across an arc of relevant current levels for lightning testing, through air, has been found to be almost 3 V per mm of arc length (based on previous experience at another laboratory). This previous personal experience measuring this voltage over a very wide range of parameters (current and arc length) is useful for understanding this voltage drop, it is not possible to reference that work given its commercial confidentiality. However, knowing it to be the case was exceedingly helpful in designing the lightning test facility. With an arc length

of 220 mm (100 mm gap, plus 20 mm to get round the diverter and a further 100 mm with a wandering arc, possibly eroding the surface further and further away from the electrode), the voltage drop would be approximately 665 V.

A voltage drop of 665 V at the peak current for the A waveform (200 kA) would be equivalent to a 3.3 mΩ resistance. However, it cannot be readily converted to a resistance as the voltage does not vary much with current. It thus behaves like a Zener diode rather than a resistor.

To summarise the design criteria for the test object and test rig:

- Inductance 1.5 μH
- Resistance 0 to 50 mΩ
- Arc volt drop 0 if conduction, 665 V for arc of 100 mm length

4.10. Proposed new waveform generator

The analytical modelling for the generator and its parameters showed how the test standard could be implemented perfectly. However, the voltages required were excessive and not achievable with the donated components or budget available.

The spreadsheet used to generate the plots for the previous sections, was implemented by adapting the equations to solve for the initial capacitor voltage and resistance if capacitance, inductance and action integral were given. This involved a macro to run a solver function (see Appendix 1). While not as elegant as mathematical solutions, it allowed rapid homing in upon circuit parameters for testing ideas. Incidentally, this solver function was how 2 separate voltage solutions for a given capacitance were discovered as the solver found the first solution it came to when starting from either excessively high or low voltages.

The maximum output voltage of the donated charger was 60 kV. As a new charger would use a large proportion of the budget, putting it to use was desirable. Thus the maximum voltage available was limited to this.

The use of 60 kV would allow the waveform generators components to be relatively close together as the maximum breakdown distance is of this voltage is approximately 20 mm in air. Keeping feed and return transmission lines and conductors close together would allow a low inductance to be attained relatively simply.

As the load had a predicted inductance of 1.5 μH, it was decided that this would be the upper limit for the waveform generator and that while undertaking the design the goal should be to make it 1.5 μH or less. Therefore, the first 2 parameters for designing a system were predicted/known: a maximum of 60 kV and total circuit inductance of 3 μH. Also, with a carbon composite sample having a resistance up to 50 mΩ, the total circuit resistance would ideally be several times higher than that to make the circuit less sensitive to changes in sample resistance.

4.10.1. Proposed new A and D waveform generator

The industrial partner supplied a selection of capacitors to project; some of these were still in their factory wrapping. The general specifications of the capacitors were:

- 10 of 197.5 μF, 20 kV, 400 kA low reversal discharge capacitors (39.5 kJ)
- 6 of 32.8 μF, 20 kV, 150 kA high reversal discharge capacitors (6.56 kJ)

It is interesting to point out that each of the 197.5 μF capacitors can hold more than half the energy of the whole of the original capacitor bank. The use of several of them would allow greater circuit resistance and, thus, greater stability against load impedance variation.

These capacitors had been obtained by the laboratory in Paris in order to refurbish the original waveform generator and increase its performance. No information as to how this would be accomplished was supplied. Furthermore, as will be outlined below, additional components had to be purchased. This is not to the detriment of whatever topology was planned for that laboratory. It does however,strongly suggest that the solutions proposed in this thesis were not the same as ones planned by the industrial partner – as they are impossible to implement wholly with the donated equipment.

The proposed new waveform generator would be built using the 197.5 μF capacitors. With their high current capability, a single string could have been used to deliver the required current, although it would not have enough energy or charge for the A waveform alone. This allowed enormous flexibility over the layout and circuit topology as there were many ways to arrange 10 capacitors with associated support components. Both clamped and unclamped circuits were studied, ranging from a single string to 10 capacitors in series to what is presented below.

Figure 36 shows a 3 by 4 series-parallel array (which required purchasing 2 additional capacitors). It was conceived to have links allowing it to operate as a single string of 3 capacitors, with the charger connected to the topmost layer and the intermediate layers allowed to float. As long as the capacitance of the capacitors were sufficiently equal, the voltage would share sufficiently equally across them. However, this could not be relied upon to return the intermediate layers to ground. Thus each layer would have to be shorted out resistively to drain residual charge and then robustly grounded to ensure safety before the capacitor bank could be approached.

A further safety feature, designed from the outset was the R002 resistor, which was 100 Ω. This ensured that if the capacitor bank were fired without a load, the charge would have somewhere to dissipate. It also ensures that all parts of the test rig are held at the same potential until a test waveform is triggered.

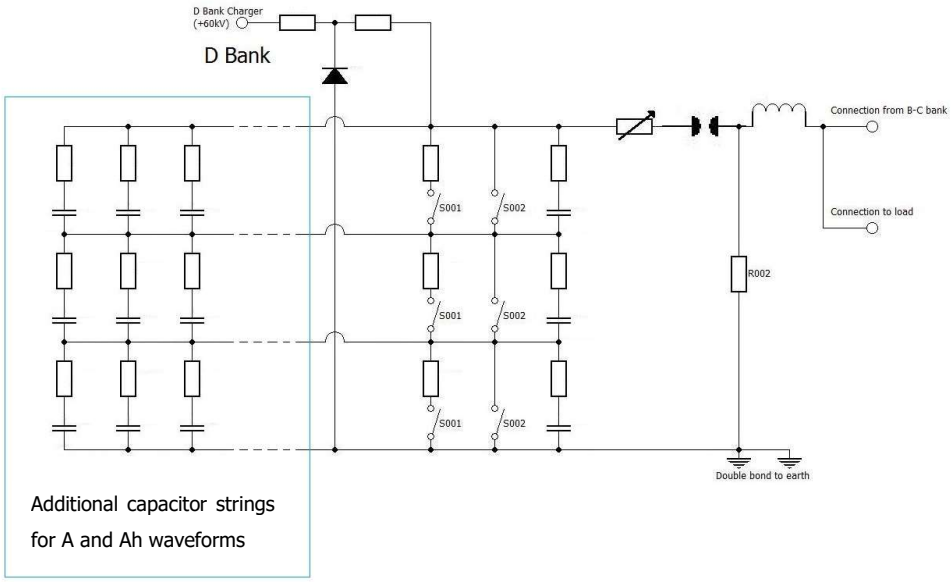

Figure 36 - Proposed new waveform generator

The use of a single string to form the D waveform naturally fell out of the equations to form an unclamped uni-polar pulse. Having only 3 capacitors in series allows the bank to be charged using the charger supplied to MBLL. The D waveform is the most important from the respect that it is used for about 95 % of aeronautical direct effects lightning tests. Being made of only 3 capacitors, it would allow this part of the circuit to be finished in advance of adding on more capacitance for other

waveforms. This was useful for achieving goal of firing the capacitor bank as early as possible in order to reach a milestone for the work.

Increasing the capacitance later, allowed for an A waveform also to be generated with an unclamped uni-polar pulse. However, it would require the purchase of 2 more capacitors identical to the first 10. This choice avoids the complexity of having a clamped generator. For the university environment, this is beneficial as it is vastly simpler to operate. An unclamped topology allows for a good level of repeatability and stability with regard to sample impedance. This is because all the energy within the capacitors is dissipated either in the sample or the series resistance. No energy is lost in a part of the circuit not in series with the sample, such as the continued oscillations of the capacitors after the clamp fires in a clamped topology. Furthermore, eliminating a clamp removes any requirement for accurately timing its firing which would be sensitive to changes in waveform shape.

Comparing the proposed circuit in Figure 36, with the circuit of the donated generator in Figure 12, it is obvious that the new circuit is far simpler. Firstly, the clamp circuit has been eliminated and secondly, only half as many capacitors are required for making the A waveform. It is even simpler to begin with, as only 3 of the capacitors are required so as to get the generator going with a D waveform.

4.10.2. Proposed new waveform generator – 3D sketch

The proposed generator, using 3 of the 197.5 μF capacitors initially, and later a further 9 of them, required very few components to put together. The shape of the transmission line, repeatedly folding back on itself, is dictated by the requirement of low inductance by keeping the conducting surfaces facing each other and wide to keep flux density and thus inductance low.

Figure 37 shows an early conceptional 3D sketch of what the proposed new generator would look like for the D waveform part only. The 3 capacitors can be seen with a semi coaxial arrangement of ceramic resistors on their outputs. Each capacitor had 8 parallel stacks of 6 resistors (the concept shows 4 parallel stacks but the built version had 8). The individual ceramic resistors in the stacks were 125 mΩ for a total resistance of 93.8 mΩ per capacitor and 281 mΩ per chain of 3 capacitors. This resistance is required to dampen high current oscillations and avoid high voltage reversal in a short circuit condition and usefully provide a distributed resistance to dampen out parasitic oscillations (that could occur in the

distributed capacitance and inductance of the transmission lines) and take a share of the overall circuit resistance.

The yellow item represents the place of the spark gap (triggered by moving one electrode closer to the other). The decision to use a moving spark gap was made very early on as it would eliminate the setting of gaps and trigger voltages associated the donated generator, which was known to be time consuming. Aside from being simpler to use, it could be triggered pneumatically, eliminating any electrical interfaces. By doing so, it was expected to be simple to ensure safety and thought likely to be cost effective.

The stack of resistors on the right represents the output variable resistor. It would comprise several sections each of different resistance, so affording, by various combinations, a wide range of output resistances. In the concept, all sections are drawn the same as at that time, exactly how to build the resistor assembly had not be finalised.

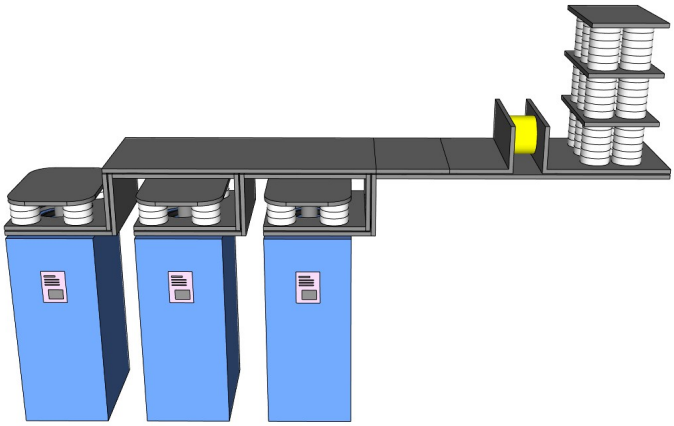

Figure 37 - D waveform part

The whole assembly as pictured was approximately 2.5 m long and 0.5 m wide. The transmission line on the right hand side was conceived to continue right through the wall of the test chamber, simply held in place with a large plastic, insulating clamp.

The operating voltage of 60 kV is relatively low, facilitating relatively simple insulation. It was initially conceived that 4 layers of 1 mm thick PTFE sheet would be used between the transmission lines. The use of multiple layers allowed

generous margins when overlapping sections of insulation and mitigates the effects of punctures through a single layer. The insulation around the output resistor, spark gap and connection to the load would be stressed at the full 60 kV whereas the branches to the capacitors would have a reduced stress of 20 kV each. The aggregate 4 mm thickness of PTFE is quite excessive for the voltage withstand – even a single 1 mm sheet would be. It was chosen due to being quite tough but still easy to bend at that thickness and also readily available.

If the PTFE sheet did not extend beyond the edge of the transmission lines, the 4 mm gap would not hold off the 20 kV let alone the 60 kV. Therefore the PTFE had to protrude a distance. A low current, high voltage power supply was used to explore surface discharge voltage across the PTFE. A gap of 240 mm was found to withstand 60 kV even if quite dirty, so a protrusion of 120 mm was chosen as any tracking would have to go over both the upper and lower surfaces of it to traverse between transmission lines. In theory less could have been used on the capacitor branches, but in order to keep things simple, 120 mm was used everywhere.

The folding of the transmission lines was an important aspect of keeping the inductance low as it keeps the surfaces carrying current facing each other. Arriving at the concept was not trivial. Figure 38 shows the terminal of one of the capacitors. It was obvious that a coaxial connection to the capacitors would be suitable. The concept started with a plate bolted to the capacitor and a 50mm diameter brass rod screwed into the centre connection.

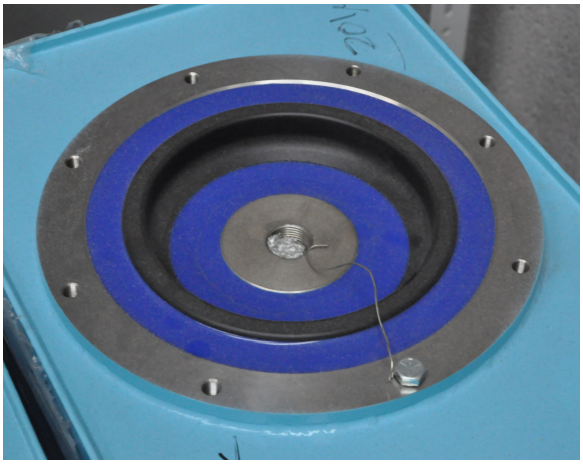

Figure 38 – Capacitor output bushing - high current waveform generator

It seemed logical to connect the capacitor mounted plate to the transmission lines. A second plate was envisaged, insulated from the capacitor connection by sheets of PTFT, on top of the first. This second plate would require some means of connection to the brass rod. As can be seen in Figures 37 and 39, a spreader plate was used to allow connection to several stacks of resistors to make the connection.

Figure 39 is an extension of the conceptual sketch of what would be required to upgrade the generator to be able to generate an A waveform (circuit shown in Figure 36). It was essentially an extension of the capacitor section to one side of the D waveform part. The brown links allow the capacitors to be separated and, thus, the system configurable for either a D or an A waveform. Almost all the components were identical to ones used in the D only part, so few new parts would have to be designed, making the upgrade simple to plan and implement. The sketch indicated that a likely size for the waveform generator was 2.5 m long and 2.5 m wide.

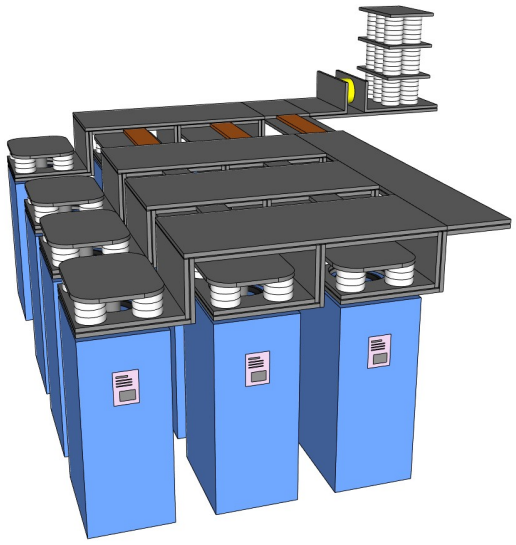

Figure 39 – A waveform upgrade

The final version would include a frame, insulators, the charger connection as well as earth and dump switches. Most of this was stacked on top of the waveform generator, not taking up any further floor space.

Furthermore, it also included an additional link in the capacitor bank such that 2 strings of 3 capacitors could be used for generating the Ah waveform. The reason for it not being included in the above drawing was an initial perceived necessity for

the D and A waveforms only – with the Ah waveform considered a nice to have but largely unnecessary. The D waveform is generally the one used in lightning testing with A waveform a close second in importance, but making up only ~5% of actual tests. The Ah waveform is hardly ever used; though since it was found to be trivial to include, it was pulled back into the specification.

4.10.3. Proposed new waveform generator – Waveform D

The following describes the reference D waveform shown in Figure 40:

- I_0 = 109,405 A
- α = 22,708 s^{-1}
- β = 1294530 s^{-1}

Figure 40 also shows the potential D waveforms – both the low and high voltage solutions which meet the peak current and action integral requirements for the capacitance and inductance. The low and high voltage solution rise times were 18.3 µs 14.6 µs respectively. The rectangle around the waveform peaks represents the allowable window for a peak to occur and both usefully fall within this. The limits are 90 to 110 kA and 0 to 25 µs for current and time respectively (described in ED 84).

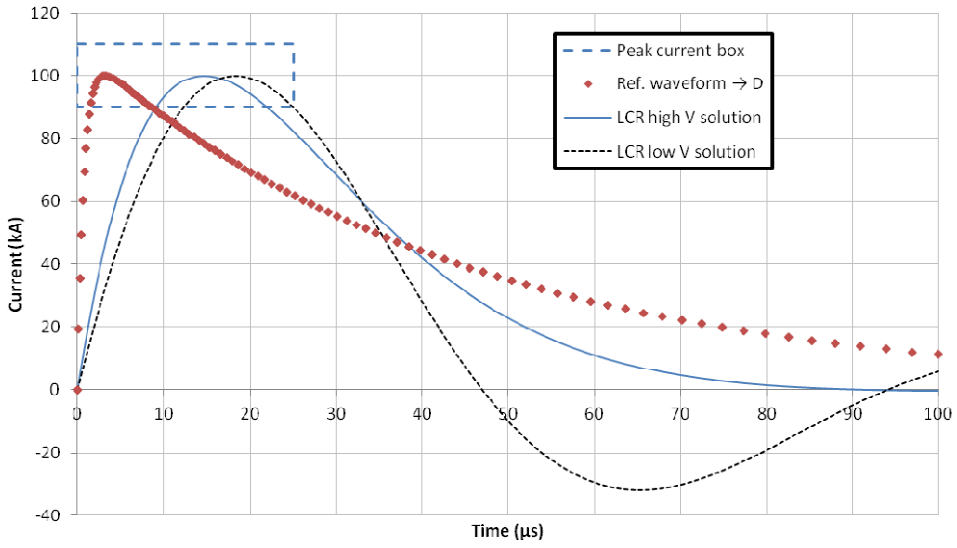

Figure 40 – New D waveform

The circuit parameters to produce this are shown in Table 8.

Table 8 – Circuit parameters for D waveform

		Low voltage solution	High voltage solution
Voltage	(kV)	33.3	53.5
Resistance	(mΩ)	146	337
Capacitance	(μF)	65.8	65.8
Inductance	(μH)	3.00	3.00
Peak current time	(μs)	18.3	14.6

This is the most commonly used waveform. As such, it was the proposed first step. It would use 3 capacitors in series as shown in Figure 41 which depicts the high voltage solution.

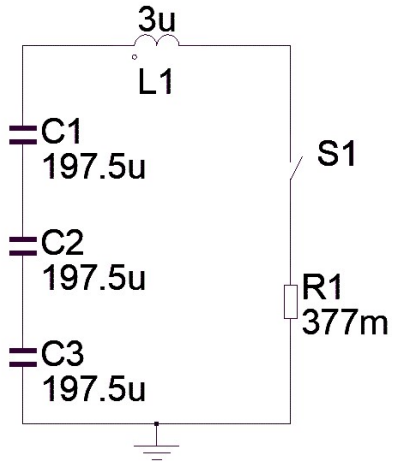

Figure 41 – Circuit for generating the D waveform

4.10.4. Proposed new waveform generator – Waveform Ah

As mentioned above, if it is possible to produce the Ah waveform simply, then by making it available, it would add to the flexibility and capability of the waveform generator.

The following describes the reference Ah waveform shown in Figure 42:

- I_0 = 164,903 A
- α = 16,065 s^{-1}
- β = 858,888 s^{-1}

Figure 42 also shows the potential new Ah waveforms; with rise times of 25.9 and 20.6 μs. The rectangle around the waveform peaks represents the allowable

window for a peak to occur. The limits are 135 kA to 165 kA and 0 to 37.5 μs for current and time respectively.

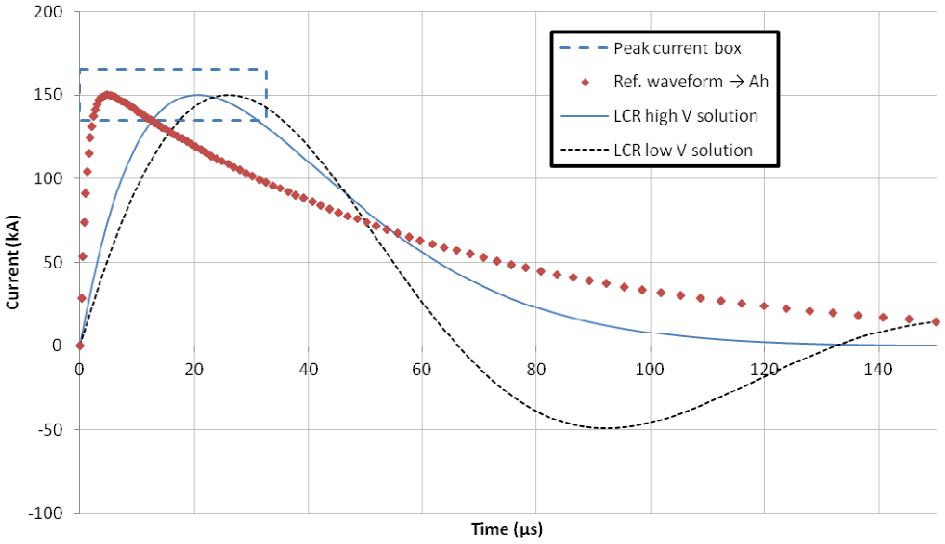

Figure 42 – New Ah waveform

To produce the waveforms in Figure 42, the parameters given in Table 9 are required.

Table 9 – Circuit parameters for Ah waveform

		Low voltage solution	High voltage solution
Voltage	(kV)	35.0	57.5
Resistance	(mΩ)	101	272
Capacitance	(μF)	132	132
Inductance	(μH)	3.00	3.00
Peak current time	(μs)	25.9	20.6

The circuit to produce this waveform would use 2 parallel strings of 3 series capacitors and is shown in Figure 43.

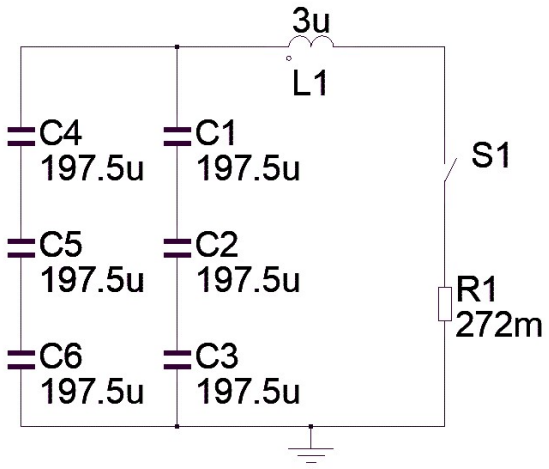

Figure 43 – Circuit for generating the Ah waveform

4.10.5. Proposed new waveform generator – Waveform A

The following describes the reference A waveform shown in Figure 44:

- I_0 = 218,810 A
- α = 11,354 s^{-1}
- β = 647,265 s^{-1}

Figure 40 also shows the potential new A waveforms; with rise times of 36.5 and 29.3 μs. The rectangle around the waveform peaks represents the allowable window for a peak to occur. The limits are 180 kA to 220 kA and 0 to 50 μs for current and time respectively.

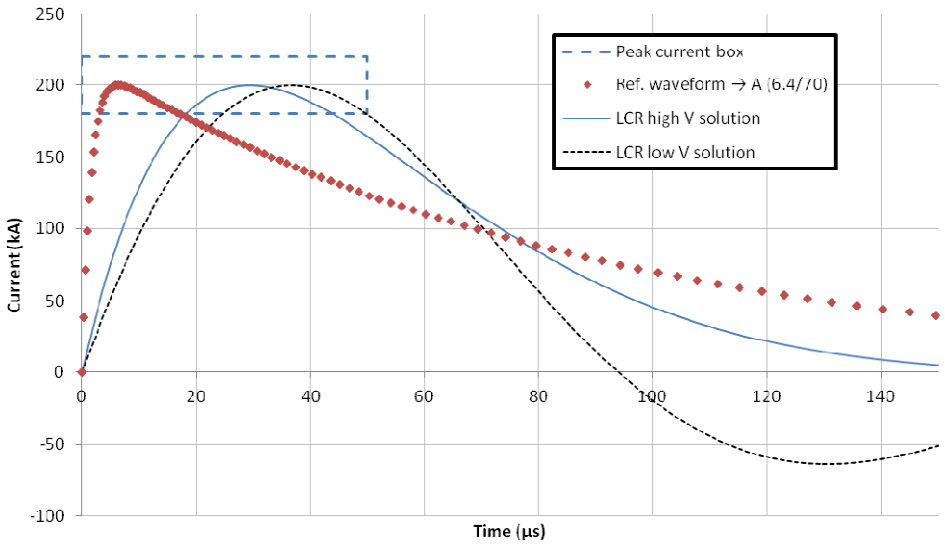

Figure 44 – New A waveform

To produce the waveforms in Figure 44, the parameters given in Table 10 are required.

Table 10 – Ccircuit parameters for A waveform

		Low voltage solution	High voltage solution
Voltage	(kV)	33.3	53.5
Resistance	(mΩ)	73	188
Capacitance	(µF)	263	263
Inductance	(µH)	3.00	3.00
Peak current time	(µs)	36.5	29.3

The circuit to produce this waveform would use 4 parallel strings of 3 series capacitors, as shown in Figure 45.

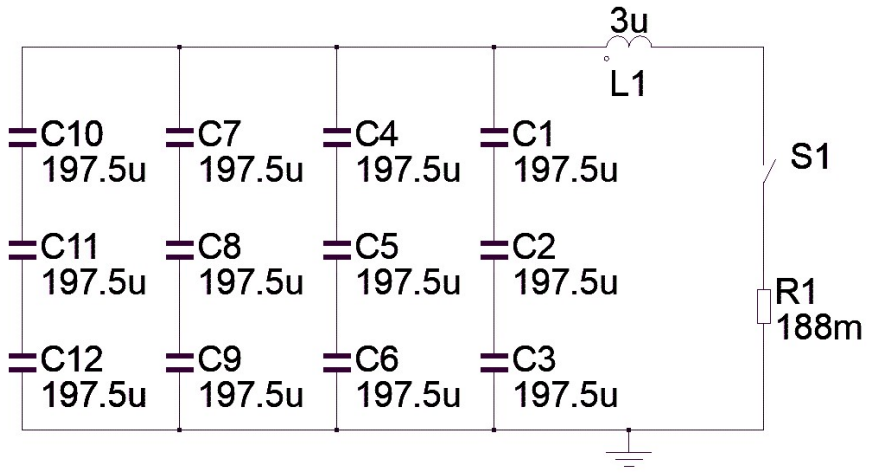

Figure 45 – Circuit for generating the A waveform

4.10.6. Proposed new waveform generator – Decision

Many other waveforms (from lesser used test standards or custom specifications for a specific task) are called for while performing lightning tests. Initially, only a D waveform would be possible, but later on, when it has been upgraded, the Ah and A would be available also. The system would not be limited to producing only these waveforms as it can be charged to any voltage up to 60 kV and have a wide variety of resistances, and inductances. With the upgraded assembly, including all of the capacitors, many combinations of series and parallel configurations are possible (some of these would involve robustly shorting out series connections). Almost any waveform with parameters less than the A waveform and not requiring more than 10% voltage reversal of the capacitors would be feasible.

4.10.7. Proposed new waveform generator – estimate of work and cost

The proposal was to build the generator to the state where it can produce a reliable D waveform, then add a second capacitor chain for the Ah waveform. Later, once more funds were available, upgrade to be able to produce a very reliable A waveform also.

Quite a lot of the work required was simple machining of aluminium plate. Most of the insulation could be achieved with PTFE sheet that was simple to cut. The most complex part of the construction were the safety switches, their connections and the resistor layouts.

The items needed for the first stage – to produce a D waveform include:

- 25 m PTFE sheet (1 mm thick, 1200 mm wide)
- Approximately 200 carbon ceramic resistors (125 m Ω)
- Approximately 8 m of aluminium sheet (15 mm thick, 500 mm wide), machined to suit
- A frame on which the assembly will stand (including support for the earth and dump switches)
- Insulators to stand the capacitors on, and clamp the transmission line together
- A new spark gap (pneumatically triggered)
- Pneumatic earth and dump switches (6 contactors were required)

Aside from the more detailed design, most of the work was done by local engineering companies as there was no spare capacity in the University's workshop. To finalise the design of the machine, from this outline circuit and 3D sketch, it took approximately 500 hours that were squeezed into 6 working weeks. Such a time had to be fitted into the project without causing the final deadline to slide significantly to the right. To assemble the machine, 4 weeks of 2 people sufficed. The switches and resistors had a 2 month lead time. Again, this did not move the final deadline to the right significantly.

In order to upgrade the system to use all 10 capacitors plus 2 new ones and so be able to produce the A waveform:

- 75m PTFE sheet (1mm thick, 1200mm wide)
- Approximately 180 carbon ceramic resistors
- Approximately 24m of aluminium sheet (15mm thick, 500mm wide), machined to suit
- Insulators to stand the capacitors on, and clamp the transmission line together
- 2 additional + 1 spare capacitors

Upgrading to produce the A waveform would require little additional design as it would mostly be an exercise of repeating previous orders. This eliminated potential risks and uncertainties. To assemble the extension, 5 weeks of 2 should suffice.

4.11. Comparison, old and new

In order to critically compare the old generator waveform with the proposed new one, the following criteria are put forward and scored for the old and new systems.

Table 11 – Comparison of old with proposed new generator

Criteria	Suresnes system	Proposed new system
Must produce reliable D waveform	Good	Best
Allowable output inductance (higher is better)	2.3 μH	3 μH
D waveform time to peak (faster is better)	16.3 μs	14.4 μs
Must produce reliable A waveform	Not feasible for carbon	Good
A waveform time to peak (faster is better)	21.0 μs	28.8 μs
Man hours required to produce a reliable D waveform into carbon samples (lower is better)	25 weeks	13 weeks
Further expense required to produce a reliable A waveform into carbon samples (lower is better)	Not feasible for carbon	True
Further man hours required to produce a reliable D waveform into carbon samples (lower is better)	Not feasible for carbon	4 weeks
Maximum usable voltage (higher is better)	36 kV	54 kV
Available energy for D waveform (higher is better)	58 kJ	95 kJ
Available energy for A waveform (higher is better)	58 kJ	380 kJ
Maximum sample resistance for D waveform (higher is better)	0.23 Ω	0.38 Ω
Maximum sample resistance for A waveform (higher is better)	0.035 Ω	0.19 Ω

As can be seen in Table 11, the proposed new system wins on all points, from giving a more robust waveform to being less expensive and time consuming to put

together. It was not biased towards the new system; it simply made use of much newer and higher energy density capacitors to increase system energy while reducing parts count. It was also quite clear that the old generator was not ideal if an A waveform was ever desired from the test facility. This was due to the very low energy that could be stored in the array of 24, 15 uF capacitors not allowing much circuit resistance to stabilise the arc. The output resistance of the generator would be low compared to a sample which degrades stability and makes it behave more like a voltage source than a current source.

4.12. Proposed new waveform generator – decision

Section 4.10 presents the proposal for using the equipment donated to MBLL to develop a cost and time effective solution for producing the D waveform. It used the mathematical understanding presented earlier in section 3.5 to develop a scheme design for a waveform generator that would be robust and simple to use.

Section 4.11 compares the proposed waveform generator with the option of refurbishing the one donated by the industrial partner where the proposed system is shown to be a better system overall.

The decision to use the new design seemed clear and was agreed with by the industrial partner. While it did not use their original system they were quite happy that as many parts of it would be put to use along with the components purchased for its upgrade.

The waveform generator would be designed to produce the D, Ah and A waveforms but the build process would be limited to the D waveform only. At a later date, funding allowed for extending the capacitor bank to produce the Ah and A waveforms also.

4.13. Building the waveform generator

The process of building the waveform generator began with arranging the capacitors on the frame in their insulating mounts as shown in Figure 42. The insulators were high-pot tests to ensure that they could hold off much more than the 60 kV working voltage. Figure 46 also shows the beginnings of the coaxial connections that topped each capacitor.

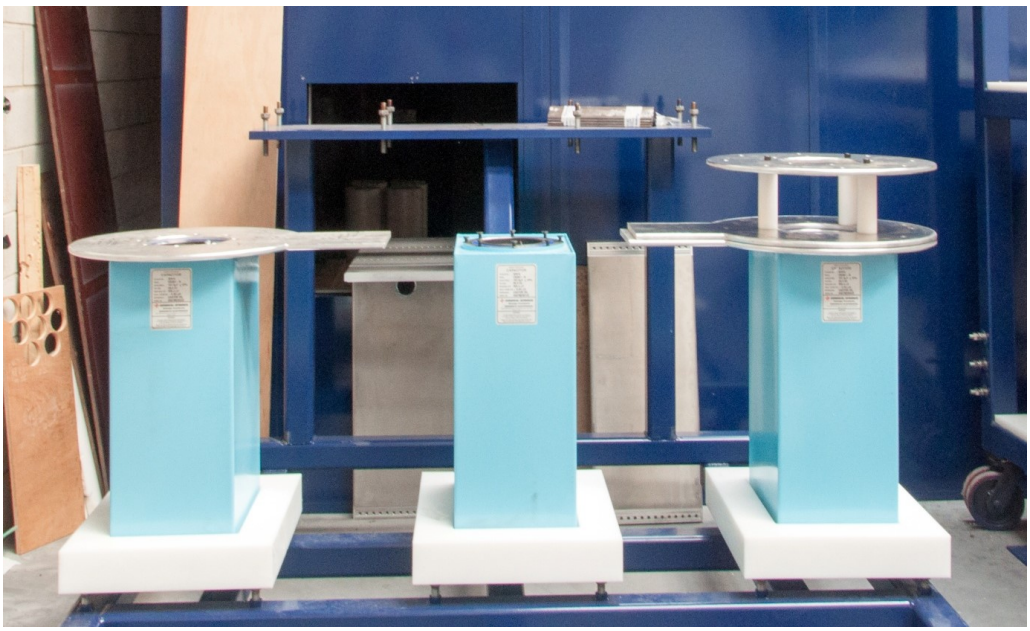

Figure 46 – The part built D waveform section of the capacitor bank

Behind the capacitor bank, the aperture into the test chamber is visible. Through this, a rather robust stripline carried the current to the test rig; it was also the location of the current measurement Rogowski coil. This is shown in Figure 47 with spacing between top and bottom plates exaggerated and without PTFE insulation. Once leg was outside the test chamber and the other inside. This was partly for stability and partly doubling up on the electrical connection to the ground plane. Connection to the ground plane was made by welding steel angle to and bolting the legs to the angle.

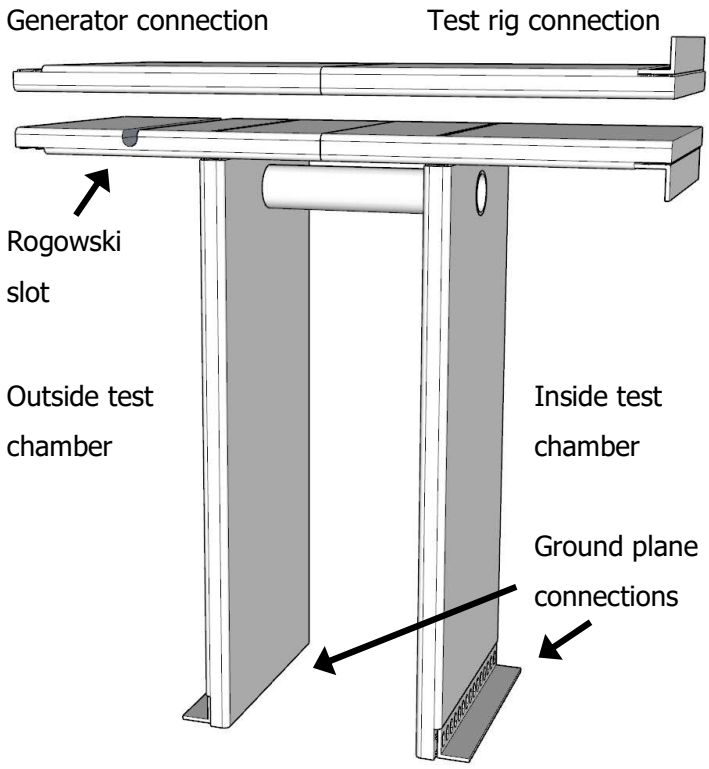

Figure 47 – Earth star point and high current bushing

To prevent light, sound, dust and smoke escaping from the test chamber, a plastic baffle was installed that fitted tightly against the high current bushing. A tube was installed to allow cables for Rogowski coils to pass into the test chamber. For the main high current measurement, a slot was made through the lower plate into which a large Rogowski was installed for measuring the high current waveforms.

Figure 48 shows the complete waveform generator capable of the D waveform. On top of the test chamber, there are 6 switches; these are dump and shorting switches for each section of the capacitor bank. In the foreground, earth sticks can be seen proving that the sections are grounded before working in close proximity to the generator.

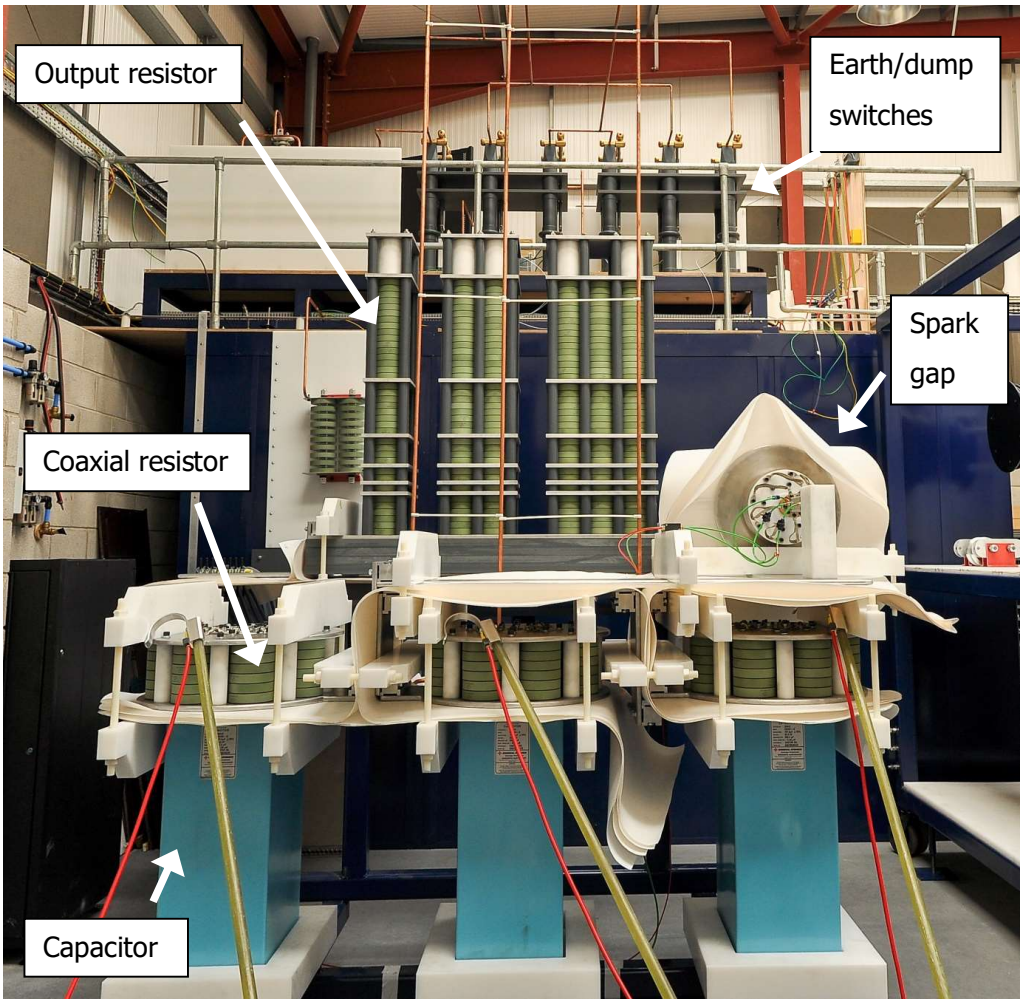

Figure 48 – Fully assembled D waveform section of capacitor bank

Above the right most capacitor, the pneumatically operated spark gap bridges the capacitor bank section to the output resistor section of the strip line conductor. To its left, sits a large resistor stack. This was designed to be as configurable as possible, allowing a great many graduations of resistance between its minimum and maximum value.

As described in section 3.11.2, a coaxial resistor assembly was used atop each capacitor to limit fault currents (that could occur should there be a short across part of the circuit). The inductance was for the coaxial connection was calculated as a coaxial assembly using Equation (47) 0.15 m long with centre and outer conductor diameters of 0.05 (d) and 0.4 (D) m respectively.

$$L = Length\ x\ ln\left(\frac{D}{d}\right) x10^{-7} H \qquad (47)[20]$$

The inductance calculated for each capacitor connection was 32 nH which is quite comparable with the capacitors internal inductance.

The stripline transmission lines were 250 mm wide and designed to be spaced apart with 4 layers of 1 mm thick PTFE. However, since the edges of the strip line were rounded over and the PTFE was tricky to flatten perfectly, the dimensions for calculation are 240 mm width with a spacing of 5 mm and length of approximately 6 m including the high current bushing into the test chamber.

$$L = Length\ x\ 4\pi\ x\ \frac{Spacing}{Width}\ x\ 10^{-7} H \quad (48)[20]$$

The inductance of the stripline transmission lines is estimated to be 157 nH. Combined with the 3 capacitor connections (32 nH each) and internal inductances of (30 nH each), the inductance of these combined parts is estimated as 343 nH. This left 1.1 mH for the spark gap switch, output resistor and connection between the high current bushing and the test rig.

4.13.1. Output resistor

A variable output resistor was required to as each waveform called for a different resistance. In order to deliver this, the required resistances needed to be understood. The distributed coaxial resistors within the capacitor bank would account for part of the resistance, leaving an additional that would be made up of the output resistor and the sample. Table 12 shows the additional resistances that would be required to deliver these waveforms. It should be immediately obvious that for the low voltage solutions for the D and Ah waveform, the resistance required was negative. This meant that there was too much resistance distributed within the capacitor bank.

Table 12 – Additional resistance for waveforms with initial configuration (8 parallel strings of 6 resistor elements in each coaxial assembly)

Waveform configuration	Capacitor bank distributed resistance (mΩ)	Additional resistance for low voltage solution (mΩ)	Additional resistance for high voltage solution (mΩ)
D	281	-135	55.7
Ah	141	-39.6	131
A	70.3	2.68	118

Having too much distributed resistance occurred because design work had to fit around all the other aspects of the project. The reason for using 6 resistive elements in series in each coaxial assembly was the pulsed voltage rating of 10 kV each. With a total charge voltage of 60 kV, it seemed sensible to use 6 in series to mitigate any combinations of fault condition that could present 60 kV to a single unit. The coaxial assemblies were also scheme designed before the low voltage solutions for the waveforms were conceived. Having as much of the resistance distributed as possible in the low inductance coaxial resistors seemed a sensible way of avoiding the problem of designing a large, low inductance, variable output resistor assembly – by reducing its size and ideally complexity also.

In order to deliver both the high voltage and the low voltage solutions, the number of series elements within the distributed coaxial resistor assemblies on the outputs of each capacitor would have to be reduced from 6 to 2. With 8 parallel strings of 2 series connected resistors, and each element having a resistance of 125 mΩ, this would lower the resistance of each assembly from 93.75 to 31.25 mΩ. Table 13 shows the additional resistances required to deliver the waveforms (output resistor plus load resistance). With the updated configuration, the resistances are all positive. While the D waveform section was initially built with the 6 element high resistor strings, it was later reduced when the Ah and A waveform sections of the capacitor bank were added.

Table 13 – Additional resistance for waveforms with updated configuration (8 parallel strings of 2 resistor elements in each coaxial assembly)

Waveform configuration	Capacitor bank distributed resistance (mΩ)	Additional resistance for low voltage solution (mΩ)	Additional resistance for high voltage solution (mΩ)
D	93.8	52.3	243
Ah	46.9	54.1	225
A	23.4	49.6	165

The use of 2 resistive elements in series in each coaxial assembly would no longer allow them to withstand a brief instantaneous voltage of 60 kV. However,as each coaxial resistor assemblies were in series with individual 20 kV (maximum operating voltage) capacitors, and there were 3 capacitor-resistor assemblies sharing the 60 kV maximum charge voltage of the capacitor bank. This would still provide

protection for the capacitors should there be a short circuit around the spark gap, output resistor or high current bushing (through wall of test chamber). It would keep the resistor elements at or within their pulsed voltage rating in the event of a capacitor suffering an internal short circuit. It would also provide adequate rating in the case of a short circuit occurring between a part of the 60 kV transmission line or a ground connected object and another part at either 20 kV or 40 kV (the intermediate nodes).

The full analysis of fault conditions showed that the initial approach was over cautious and a lower distributed resistance would allow generation of all low and high voltage solution waveforms, with achievable additional resistance.

Table 13 shows a single resistance for each waveform and that in all likelihood a single 50 mΩ resistor would have delivered all 3 low voltage solution waveforms within specification as long as the test sample resistance was negligible. If the circuit behaved exactly as designed and the test samples were always the same, then perhaps 4 values for the output resistor would have sufficed.

However, the circuit had yet to be built and variances in the aggregate inductance and the resistance of connections, as well as the tolerance of the ceramic resistor elements themselves gave uncertainty to the exact final values that would be required. And coupled with the wide variance in sample resistances (from the effective short circuit of a conduction test of a well bolted joint, to an arc test of a large and much more resistive carbon structure) the exact values for a resistor were not certain.

A variable resistor was required to enable a selection of resistances. The minimum and maximum resistances from Table 13 are 49.6 and 243 mΩ respectively. The variable resistor would have to cover this range and ideally be able to deliver a range of resistance around the values specified to enable a degree of tuning for the circuit. A wider range of resistances would likely be beneficial for creating custom waveforms later.

Various topologies were explored before deciding upon a quite unique solution. The resistor stack was effectively 3 binary configurable resistors in parallel. The minimum resistance was 34.7 mΩ and the maximum 385.4 mΩ. There are more than 65,000 possible combinations in total. This might seem excessive and perhaps

complex to set up. However, the same spreadsheet that was used to design the variable resistor could be used to instruct the user of the settings required for a given resistance. This spreadsheet was incorporated into the capacitor bank setup spreadsheet for seamless use.

All the resistor elements were 100 mm diameter, 25 mm thick ceramic disk type with a resistance of 125 mΩ. These were identical to those used in the capacitor output resistors. By working with the supplier to find the most cost effective single type of resistor element that could be used in both fast waveform generator applications (capacitor connection and output resistors), the individual item cost was minimized.

Table 14 shows the distribution of resistances in the variable output resistor. Each binary chain had a base layer made of 6 resistors. This could not be bypassed and functioned to ensure that there were at least 6 layers of disk resistors in series in each subset to ensure it would be able to withstand 60 kV pulsed discharges and not over volt the individual elements. Stages 1 to 5 could be individually shorted out and so provide 2^5 combinations from each chain. The total number of combinations available from the 3 combinations binary chains in parallel is 32^3 or 32,768.

Table 14 – Resistances of each stage of each binary chain of the output resistor

	Binary chain 1 (2 parallel chains)	Binary chain 2 (4 parallel chains)	Binary chain 3 (6 parallel chains)
Resistance per layer (mΩ)	62.5	31.3	20.8
Base stage – 6 layers (mΩ)	375.0	187.5	125.0
Stage 1 – 1 layers (mΩ)	62.5	31.3	20.8
Stage 2 – 2 layers (mΩ)	125.0	62.5	41.7
Stage 3 – 4 layers (mΩ)	250.0	125.0	83.3
Stage 4 – 8 layers (mΩ)	500.0	250.0	166.7
Stage 5 – 16 layers (mΩ)	1,000.0	500.0	333.3
Max set resistance (mΩ)	2,312.5	1,156.3	770.8
No. combinations	32	32	32

Table 15 shows the range of resistances available from the output resistor. Those in the normal mode column are for the resistor as described thus far. It can be

seen that the range does not extend quite low enough for the 50 mΩ required by the low voltage solutions (see Table 13). The Low R (resistance) mode of operation was implemented to resolve this and extend the range of achievable resistances lower. This was accomplished by building a separate resistor that could be bolted in parallel with the output resistor. It comprised 8 parallel chains of 5 disk resistors and had a non-adjustable value of 78.1 mΩ. This was carefully chosen to ensure that the low range of values would overlap the normal mode and double the number of achievable resistances.

Table 15 – Range of resistances from output resistor

	Normal mode	Low R mode
Max resistance (mΩ)	385.4	65.0
Min resistance (mΩ)	62.5	34.7

While fewer chains could have been used and perhaps fewer stages (miss out the single resistor layer), to give a resulting reduction in combinations, approximately the same number of resistor elements would have been required to build them. For example, if binary chains 1 and 2 were combined they would be identical to binary chain 3, and the number of combinations would be reduced to 1,000 in normal mode. Very likely enough, but the small amount of engineering effort to have 3 chains rather than 2 allows for the very smooth and continuous range of resistances over the required range.

Figure 49 shows a sketch of the transmission lines, capacitor connections and what was an initially for the output resistor. Rather than being split into parallel chains, only a single binary resistor was drawn. It would have used the same number of resistors elements (12 elements in parallel to withstand the current which necessitated 37 layers to achieve the resistance of 385 mΩ). However,it would only have had 32 combinations, 3 orders of magnitude less than the implemented solution. Furthermore, as the plates to short out each layer would have to be the full width of the resistor assembly, they may have been heavy and would have required a similar number of bolts as the final solution.

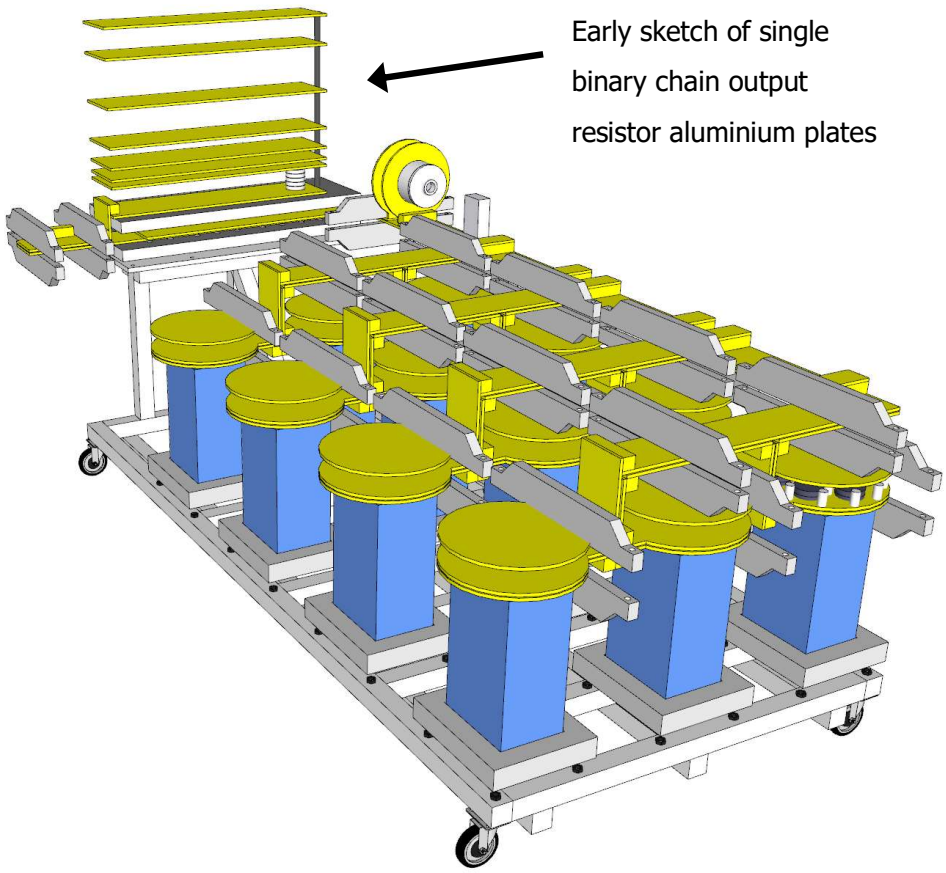

Figure 49 – Fully assembled D waveform section of capacitor bank

Figure 49 was drawn while designing the busbars and links between sets of capacitors. It was non-trivial to designing it to be easily maintained let alone to be built without the help of lifting equipment. Each section and layer had to go atop the last and not be heavier than 25 kg (weight limit for staff). Only the capacitors were heavier than this and were lifted into place very carefully with a long reach pallet lift.

4.13.1. The spark gap

Figure 50 shows a close up of the spark gap. The pneumatic actuator can be seen braced against an insulating plastic block. It pushes a rather heavy (8 kg) brass conductor through a plastic bushing, thus avoiding welding that might occur if a sliding contact were allowed. The weight of the conductor dampens movement in response to the pressure generated inside the spark gap when it fires. The movable conductor has a set of 8 braids carrying current to it, to keep inductance low and reduce the magnetic force acting on any individual one. A tungsten-copper faced hemisphere is mounted on the movable conductor. Initially the spark gap is

held open at approximately 100 mm. When the spark gap is pneumatically triggered, the moving hemisphere approaches a stationary hemisphere which is connected to the output of the switch. When it reaches the self-discharge distance for the charge voltage of the capacitor bank, the waveform is initiated. The minimum distance is approximately 0.5 mm which ensures a wade operating range but also, by not touching, the hemispheres can't weld together.

Figure 50 – Pneumatically operated high current spark gap switch

A significant amount of heat, ozone and nitrogen-oxygen species are produced. This is flushed by purging the internal volume with air for 10 s. The purge air exhausts through a pair of pneumatic silencers which also limit the internal pressure when the it is triggered and the air inside rapidly expands as it is heated by the arc.

Figure 51 shows a 3D sketch of the interior of the spark gap. Considerable efforts were made to make it as coaxial as possible and thus keep inductance to a minimum. How to minimise distances between conductors, while maintaining adequate spacing, to withstand both air and surface breakdown had to be considered also.

The inductance of the switch was predicted to be similar to a purely coaxial assembly the same size as the switch – 400 mm long, with outer and inner diameters of 350 and 50 mm respectively – which is approximately 150 nH.

The low inductance spark gap switch was not easy to design, but exceedingly inexpensive – circa £1k – for a ~100 kV, 200 kA switch. This is about 1/50th of the commercial cost. This facilitated purchasing spares of the major components.

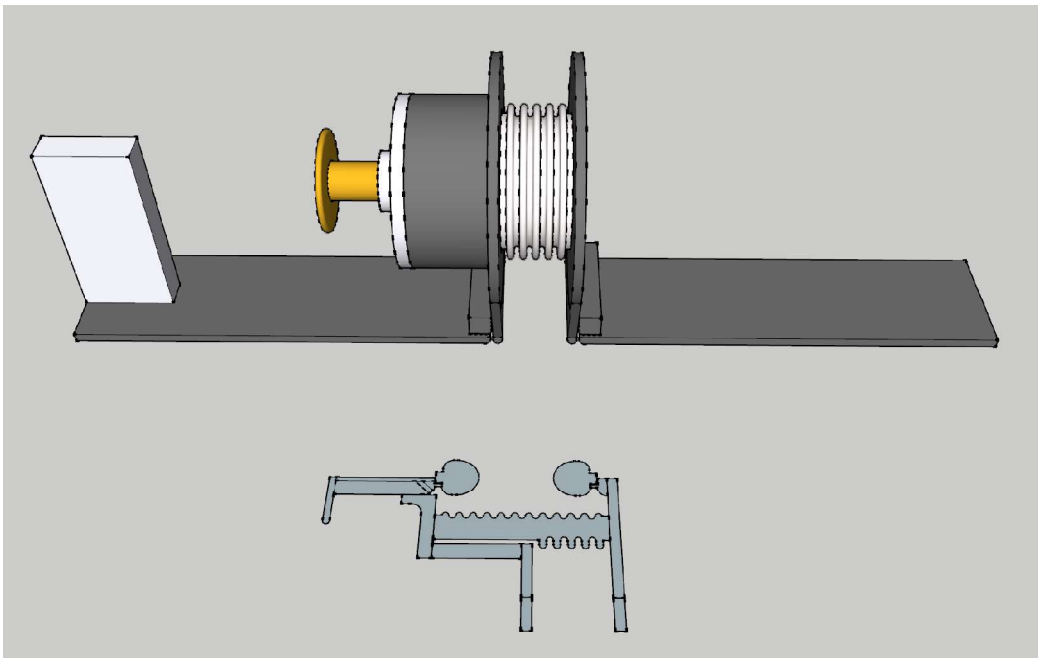

Figure 51 – 3D sketch of pneumatically operated spark gap

4.14. Current measurements

After initial commissioning of the waveform generator, building up the charge voltage one step at a time, a test pulse carrying 100 kA was performed. The waveform is shown in Figure 52. The time to peak was 16.5 μs and the action integral is 0.26 x 10^6 A^2s.

The measurement was taken by passing a conductor carrying all the current through a current transformer, which was connected to an oscilloscope through an attenuator. This was done to protect the oscilloscope from possible electrical spikes. Perhaps an over cautious approach but it was one of the very first tests and so caution seemed sensible. The result was a small signal which has uniform noise from the least significant bit of the oscilloscopes quantisation error. No filtering was applied.

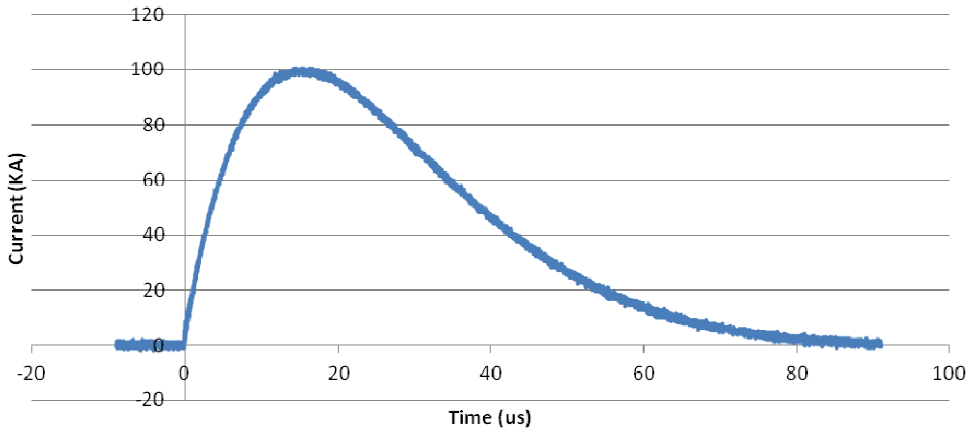

Figure 52 – An as recorded D waveform

Using a spreadsheet to analyse and fit an LCR circuit to these parameters, with a known capacitance of 66 µF and a charge voltage of 55 kV, the remaining parameters were found to be 381 mΩ and 3.5 µH.

This is quite acceptable regarding the test standard that requires the rise time to be within 25µs and the action integral 0.25 x $10^6 A^2 s$ ±20%. It is within 4%.

Upon inspection, it would appear that the waveform generator, including the output resistor, spark gap, high current bushing and connection to the test rig had an inductance of 2 µH together as opposed to the designed for 1.5 µH when in the D waveform configuration. When using it in the A waveform configuration, more capacitor chains will be in parallel and so would their inductances. Thus, it would approach the designed for inductance of 3 µH once fully complete.

Designing a waveform generator and keeping the inductance low was challenging, being 2 µH was sufficiently close to the 1.5 µH and a success. Even with the additional 0.5 µH of inductance, the waveform was within specification.

Figure 53 shows the waveform as designed plotted against the recorded waveform. This shows a very close correlation. The test was a conduction waveform to aluminium (without an arc and its small voltage drop). Where an arc is present, the shape is almost exactly the same, with a slight steepening of the very last part of the tail towards zero volts. This is due to the arc voltage drop being less than 1% of the capacitor charge voltage and, thus, having little effect.

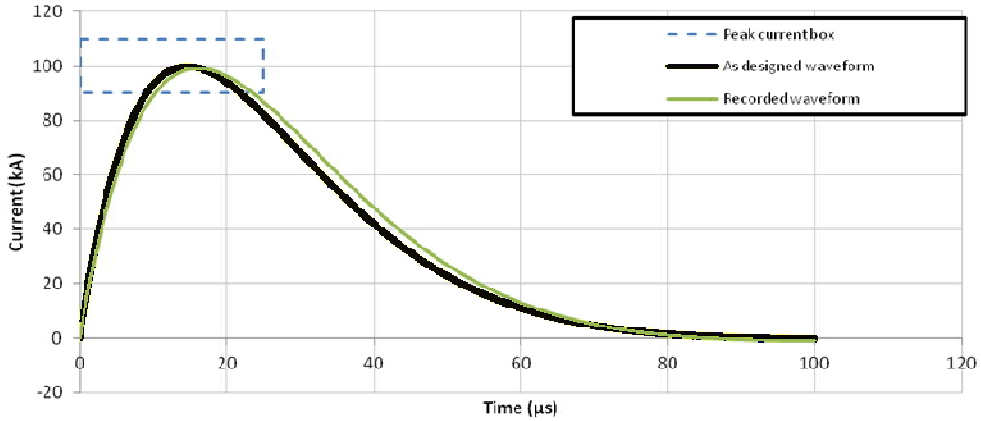

Figure 53 – Comparison of recorded and predicted D waveforms

Where different materials are used, such as carbon, where the resistance of the sample is higher, the resistance in the circuit should be reduced accordingly. A spreadsheet (see Appendix 1) was devised that could recall known setups of the bank and use them as a starting point for planning work. It would also inform the user of the settings for the variable output resistor.

If the waveform generator were set up for a test to an aluminium sample and a carbon sample were placed within the test rig, with a resistance of 30 mΩ, the peak current and action integral would reduce slightly. Figure 54 shows the recorded waveform against a predicted change should this occur. The peak current has been reduced to 95 kA and the action integral to 0.24 x 10^6 A^2s. This is 5% low for the current and 4% low for the action integral. Both are within specification of ED84. This shows a good robustness of the design.

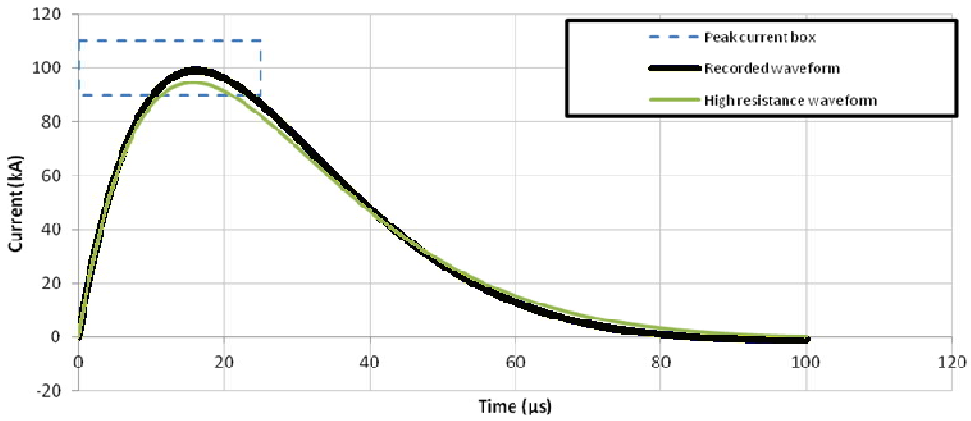

Figure 54 – Calculated change in waveform shape with high resistance sample

4.15. Conclusion - A/Ah/D waveform generator

The goals of the research were to optimize the design of a high current lightning waveform generator so that it could reliably produce waveforms A, Ah and D as specified in the test standard ED84. In addition to this, it had to fit within the space available, be largely made from available parts and require little in terms of man hours and budget to build. This was all achieved.

In order to optimize a waveform generator, firstly the waveform had to be analysed. The lightning test standards describe the waveforms with parameters for a double exponential equation. It was found when exploring this analytically that this same equation can be used to describe an LCR circuit. This was fully explored and revealed that if the α, β and I_0 parameters are known, along with a single circuit component value, then the remaining circuit component values can be derived.

Analysis tools were built based upon the derived circuit equations. These tools revealed that, in order to generate the waveforms as described in the standard, very high voltages and energies would be required. This was not achievable with the given components or budget. The tools were further developed to optimise circuit voltage and resistance given capacitance, inductance, peak current and action integral. This revealed that a circuit could be built that should be robust and easy to operate with available parts and still deliver waveforms that were within specification.

Building the laboratory involved taking the concept ideas and converting them into a working circuit while attempting to keep costs and effort requirements as low as possible. The circuit was designed to be built in 3 stages. Firstly, to generate a D waveform using a single series chain of 3 capacitors rated at 20 kV. Secondly, to include a second series chain to enable the Ah waveform. Finally, after the purchase of 2 further capacitors, 2 more series chains could be added to enable the A waveform.

The waveform generator was tested in the D configuration and produced waveforms very much as expected. When configured to generate a 100 kA D waveform, the action integral was 4% high and so well within the 20% allowable by the specification. The waveform generator was robust against unexpectedly high resistance samples. Putting a carbon fibre sample in and leaving it set up for aluminium could lower the output peak current by 5% and leave the action integral 4% low. These are both within the 10% and 20% tolerances allowed.

The robustness of the waveform along with a spreadsheet tool (see Appendix 1) that was developed to guide setting up of the generator makes for a very easy to use machine. This was an essential goal of developing the equipment. It is meant to facilitate others to perform research, and it is believed that it has accomplished that.

The slightly high action integral that is attained when a 100 kA D waveform is produced was due to the circuit inductance being slightly higher than planned for at 3.5 μH rather than 3 μH. While the performance was satisfactory, it is possible to lower the inductance. There are several ways to achieve this on the test rig.

- Larger diameter return conductors could be used. Presently, they are ~25 mm threaded rod. Increasing this to 100 mm would certainly have an effect, though not enough to gain the whole 0.5 μH
- Raising the height of the sample holder by 300 mm would effectively make the magnetic volume smaller
- A much thicker central conductor that attaches the arc to the sample could be used
- Adding additional conductors to the test rig/bus bar link
- Shortening the conductors to the test rig/bus bar link

Lastly, bypassing the circuit resistance with a capacitor has shown promise as an intriguing way of improving the rise time of a lightning waveform generator. Due to space constraints, this would likely not be a large capacitor, but it could still help reduce the effect of the slightly higher than desired inductance. Such a capacitor allows more volts early in the waveform to drive current into the circuit inductance, by bypassing some of the resistors impedance, therefore lowering rise time.

Future work, extending the circuit equation analysis to include an understanding of clamped waveform generators would be interesting, as this is a widely used alternative to the straightforward LCR circuit.

5. Optimisation and Design of the Trailing Component Generator

5.1. Introduction – Trailing component generator

Optimisation and design of the trailing component generator was the another goal of this work. It required the synergistic design of waveform generators that could deliver the B and C waveforms immediately after each other (without any period of zero current) and the filter that both combined their output and protected them.

The lightning test waveform usually comprises either the A, B and C waveforms or the D, B and C* waveforms as detailed in ED84. Other waveform combinations are occasionally requested by customers of lightning test facilities also.

The high current A/Ah/D waveform generator has been detailed in the previous chapter. It was optimised and designed before commencement of the work on the trailing component generator – that would generate the B/C/C* waveforms. This was possible as the high current generator always produces the initial waveform and the generator discussed in this chapter follows.

The trailing component generator had similar requirements to the high current generator. It had to be affordable, reliable and fit within the confines of the test facility.

There were many options for energy sources, and these were analysed and reduced in number until a solution was found.

The switching for the B and C waveforms, along with an abridged version of the information here was presented in an ICOLSE paper – Silicon switching in trailing component generators – see Appendix 2.

5.2. Design brief

The trailing component generator must connect to the output of the high impulse current generator and be able to feed current into the test rig following that delivered by the A/Ah or D waveforms. The generator must be protected from the output of the high current generator should a fault occur. Such faults include firing the high current generator into an open circuit. The full output of the high current generator would be presented, and potentially a doubling of the charge voltage

within the high current generators capacitors due to ringing into the output. The maximum charge voltage is 60 kV, thus up to 120 kV is in theory possible. Such voltage transients must not negatively affect the trailing component generator.

The waveforms have to be delivered within specification of ED84, which gives both ideal waveforms and very wide allowances compared to the fast waveforms for how this may be achieved. Preferably though, the ideal waveforms would be closely followed.

The generator must be safe to work on and around. All stored energy must be removed before people access the HV area.

The B and C waveforms are always the same, whereas the C* waveform is a truncated version of the C and frequently requested in a variety of durations and charge transfers.

5.3. Short specification

The B waveform is described by a double exponential and was used in the previous chapter to explore the properties of the equation and derive component values from it. The parameters are:

- I_0 11,300
- α 700
- β 2,000

However, the leeway is great, allowing any unipolar shaped pulse with an average current of 2 kA ±20% for 5 ms ±10% which can deliver a charger transfer of 10 C ±10%.

While a 2 kA square wave would be used to generate the B waveform, a damped LCR derived waveform could usefully have a current at 5 ms that made blending it into the 400 A C waveform a smooth transition.

The C waveform would ideally approach a square wave, delivering a constant current of 400 A for 0.5 s. However, the current can range between 800 A and 200A with durations between 0.25 s and 1.0 s so long as 200 C ±20% is transferred.

The C* waveform is a truncated version of the C waveform with an average current not less than 400 A and a duration between 1 ms and 50 ms, thus transferring up to 20 C of charge.

The load through which the waveform generator must deliver the waveforms is the same as with the high current generator:

- Resistance 0 to 50 mΩ
- Arc voltage 0 to 665 V

The trigger signal for setting firing the waveforms should be initiated by the high current generators waveform to avoid any timing jitter caused by the mechanical nature of its switch. As the B waveform always follows the D, Ah or A waveforms, triggering it by sensing the onset of current of the fast waveform would be ideal. The time window for a successful trigger if an arc test is being carried out requires an arc still present for the B waveform to discharge through. The D waveform is the shortest and would give a window at least 100 μs long to fire the B waveform.

The C waveform would ideally be triggered at the same time and adjusted to take into account the charge delivered by the B waveform. Doing so relaxes the triggering window significantly as the B waveform is quite slow – allowing at least 5 ms for the C waveform to start delivering current through the arc.

For conduction tests timing is relaxed further as there is no need to keep an arc channel open and merge the waveforms into each other. However, it would be ideal to keep them close together, so the same timing method should be used for both arc and conduction tests.

5.4. How the process progressed

The B waveform was explored in order to find a suitable circuit that could deliver the waveform as exactly as possible. This revealed that a good deal of inductance and resistance was allowable. Knowing this, much of the inductance and resistance for the B waveform was used within a filter designed to keep the high current waveform generators output from damaging the trailing component generator.

Options for the C/C* generator were then considered and optimised for stability and functionality with the trailing component generator's output filter.

Once a proposed circuit had been developed, a tender for the components progressed. Once that was complete, the component dimensions were known. The physical design of the system then began with great efforts to keep the circuit neat and accessible.

With the completed circuit, testing commenced to ensure the waveform generator could deliver the waveforms as required and withstand the high current generator firing into an open circuit.

5.5. B waveform generator

The B waveform was investigated as an attempt to match the double exponential waveform mentioned in the test standard was desired.

The B waveform was used in Figure 16 to describe the double exponential waveform. It is repeated here without the other explanatory traces for clarity as Figure 55, where a line has been drawn at 5 ms showing clearly that a great majority of the charge is delivered before this. The current at 5 ms is 340 A, which is very close to the ideal 400 A of the C waveform that follows it, potentially making blending the two quite seamless.

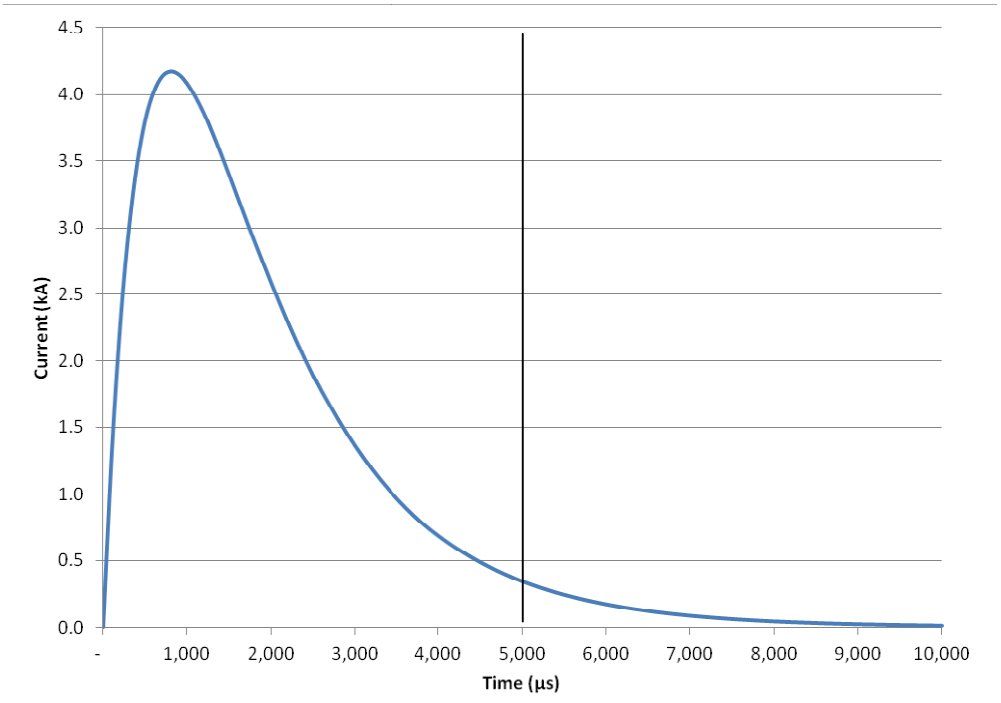

Figure 55 – The reference double exponential B waveform:

I_0 = 11,300; α = 700; β = 2,000

Using Equation (4), the total charge delivered by the waveform is calculated:

$$Q_{total} = 10.49C = -I_0\left(\frac{1}{\beta} - \frac{1}{\alpha}\right) \quad (49)$$

The charge delivered within 5 ms is calculated by stopping the integral then:

$$Q_{<5ms} = 10.00C = -I_0\left(\left(\frac{1}{\beta} - \frac{1}{\alpha}\right) - \left(\frac{e^{-0.005\beta}}{\beta} - \frac{e^{-0.005\alpha}}{\alpha}\right)\right) \quad (50)$$

The time to peak is calculated using Equation (18):

$$t_{peak} = 808\mu s = \frac{ln\left(\frac{\alpha}{\beta}\right)}{\alpha - \beta} \quad (51)$$

The peak current of the reference B waveform is calculated by using the time of the peak from Equation (51) with Equation (1):

$$I(peak) = 4173\text{A} = I_0\left(\text{e}^{-\alpha t_{peak}} - \text{e}^{-\beta t_{peak}}\right) \quad (52)$$

The action integral is calculated using Equation (11):

$$Action\ int. = 28.55kA^2s = -{I_0}^2\left(-\frac{2}{-\beta-\alpha} - \frac{1}{2\beta} - \frac{1}{2\alpha}\right) \quad (53)$$

The maximum rate of change of current is calculated using Equation (14):

$$Max\frac{di}{dt} = 14.69MAs^{-1} = I_0(\beta - \alpha) \quad (54)$$

A spreadsheet (see Appendix 1) was used to explore circuit parameters with the equations found in the last chapter for the case where capacitance is known:

$$R = \frac{(\alpha+\beta)}{C\alpha\beta} \quad \text{(Equation (36) repeated)}$$

Rearranging Equation (23) to give inductance:

$$L = \frac{1}{C\alpha\beta} \quad \text{(Equation (37) repeated)}$$

Finding voltage if C was known was shown in Equation (20):

$$V = -I_0\frac{1}{C}\left(\frac{1}{\beta} - \frac{1}{\alpha}\right) \quad \text{(Equation (20) repeated)}$$

It was spotted quickly that the action integral was quite low. This would afford a reasonable amount of circuit resistance without pushing energy stored in a capacitor or the voltage to unrealistic levels. Because of this, the decision was made very early on to use an LCR circuit to match the test standard's described waveform as closely as possible.

Table 16 presents a range of derived circuit parameters, calculated using the spreadsheet tool and starting with a range of capacitances, 1000 µF, 750 µF and 500 µF (presented in ascending order as smaller capacitances require higher voltages and thus more stored energy for a given charge).

Table 16 – Derived circuit parameters for generating B waveform

	Case 1	Case 2	Case 3
Capacitance	1000 µF	750 µF	500 µF
Resistance	1.93 Ω	2.57 Ω	3.86 Ω
Voltage	10.5 kV	14.0 kV	21.0 kV
Inductance	714 µH	952 µH	1,429 µH
Stored energy	55 kJ	73 kJ	110 kJ

It should be borne in mind that capacitors are usually the costliest part of a high voltage LCR circuit providing the rest of the circuit can be kept reasonably simple. The basis of this decision was made to use the 750 µF option detailed in Case 2. The 2.57 Ω of resistance would dwarf a test sample's resistance of 0 to 50 mΩ. The charge voltage of 14 kV would also dwarf the arc voltage drop of ~0.665 kV. Together, these factors should in theory enable the B waveform to be a set and forget feature of the lightning test facility. Always producing the same waveform, no matter what test sample is used.

The capacitors that were chosen and purchased as a result of a tender were 20 kV 250 µF units. A total of 4 were purchased with 1 kept as a spare and 3 put into circuit. Operating 20 kV capacitors at 14 kV should give them a very long life as it is well below the voltage rating. However, the charger chosen was rated to 20 kV also. This allowed the full voltage of the capacitors to be used should a customer/user of the laboratory wish to increase the charge transferred to 14 C.

5.5.1. Thyristor and gate drive

To generate the B waveform, the switch was required only to turn on and unleash the waveform in a single shot, completely draining the energy stored. It also had to be able to be timed accurately so as to start at the appropriate time.

The devices explored included ignitrons, spark gaps and thyristors.

While ignitrons are available and some very capable of holding off 20kV, accurately timed switching and conducting 15 C and 4 kA, they do contain mercury. Though this did not rule them out with proper handling, it did count against their use. The trigger units for ignitrons while simple require a relatively high voltage and current pulse to turn them on.

Spark gaps are largely as capable as ignitrons, but designing them to withstand high charge transfer can be challenging. Without adjustment of the gap distance or pressure, they often have a limited range over which they are triggerable and require relatively complex high voltage triggers. Furthermore, they are not readily available and usually quite expensive. The delay and jitter of a spark gap would likely be several μs which is much less than the 100 μs allowable window to initiate the waveform.

A single thyristor which could handle both the voltage and the current was not found. This presented the need to use a series chain to obtain the voltage withstand. The short pulse of the B waveform affords operation well beyond the steady state rating of the units. The delay and jitter of a thyristor, while longer in duration than a spark gap, would likely be less than 10 μs which is much less than the 100 μs allowable window to initiate the waveform.

Helpfully, the B waveform profile is rather similar to the single cycle over current ratings of thyristors and so assisted greatly in choosing one. This enabled them to be easily explored with the notion of using a series chain to attain adequate voltage withstand.

With series connection, triggering is complicated by the need to float all gate triggers to the local cathode potential. However, this is trivial to overcome with multiple isolating pulse transformers.

The choice was a thyristor string of 7 units, each with the boiler plate rating of 4500V and 800A.

Table 17 shows that though operating above the maximum average current; it is within specification of the surge ratings.

Table 17 – Comparison of requirements vs. B bank thyristor specification

Parameter	Requirement	Rating
Peak voltage	2850V	4500V
Peak current	4kA < 5ms	9000A for 8.3ms
Action Integral	$59kA^2s$	$330kA^2s$
Max di/dt	$15MAs^{-1}$	$150MAs^{-1}$

If approaching the maximum rated values and requiring a large number of devices, it would be wise to experiment. However, the approach taken was to find units with around twice or preferably higher rating in all areas.

With 7 units in series, the voltage rating would be 31.5 kV. This is sufficiently in excess of the maximum charge voltage of the capacitors and would thus afford a good deal of safety margin.

In order to trigger the gates of the thyristors, each had its own trigger board which consisted of a toroidal inductor, a current limiting resistor and a diode to prevent negative gate voltages. The trigger signal was a current impulse fed along a wire that threaded through all the inductors, effectively making them into a series chain of isolating transformers. The wire used had insulation rated to 30 kV and for good measure was run through a nylon tube for added insulation and rigidity. This insured excellent isolation from the trigger wire. Figure 56 shows this and how the pulse was formed by discharging a small capacitor through the wire that threads through the inductors. This circuit was designed as part of the PhD work and built in house quite inexpensively.

Since it was the same trigger signal fed to all thyristors at the same time, they should all trigger at the same time. Any slight imbalance should cause the voltage to rise very rapidly on a thyristor that was slow to trigger, which may at first seem detrimental. However, rapid dv/dt is a reliable trigger method for thyristors, so it, along with the already present trigger impulse, would encourage the slower thyristors to speed up.

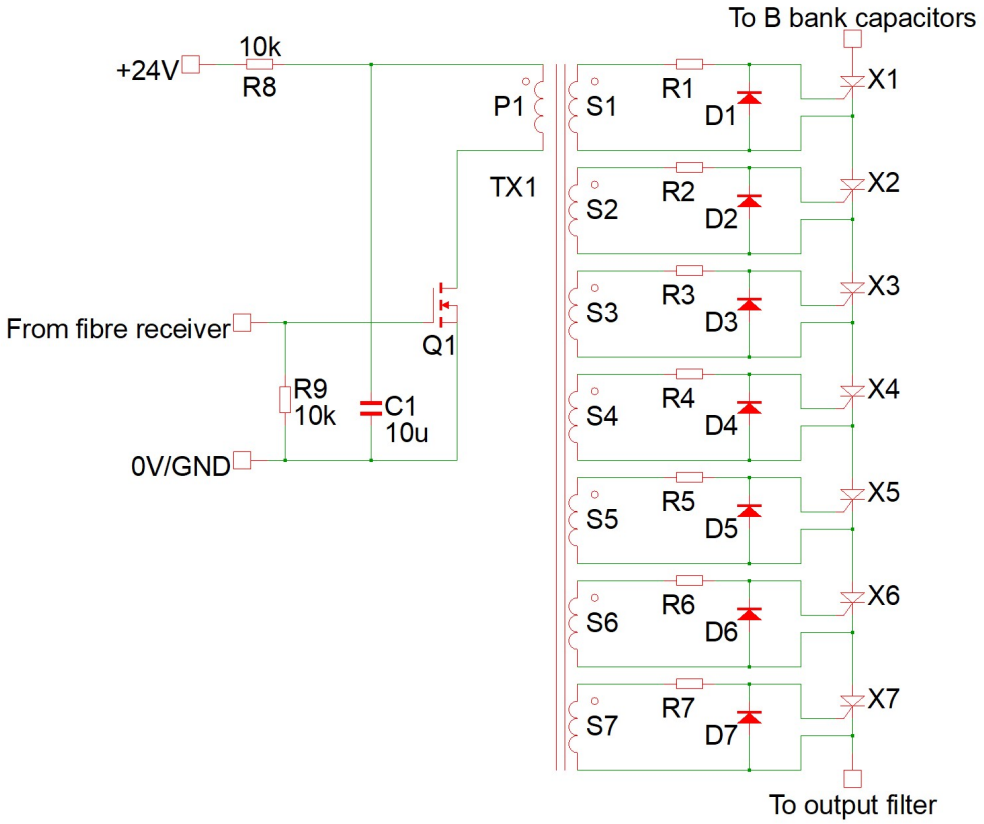

Figure 56 – Thyristor trigger circuit for B bank

The trigger for the circuit was very simple – using a magnetic pickup near the output bus bars of the fast waveform generator to drive a fibre optic transmitter passively. An isolated power supply powered the receiver and the driver proportion of the circuit to avoid ground loop interference and as a safety measure against in case a fault occurred and coupled the B waveform into the trigger circuit.

As the fibre sender was passive and triggered by the increasing magnetic field at the start of the fast waveform generators current discharge, accurate timing of the B waveform discharge was ensured.

5.5.2. The B waveform circuit

The essential parts of the B waveform circuit are the capacitors, resistor and inductor. The chosen values were:

- Capacitance 750 μF
- Resistance 2.57 Ω
- Charge voltage 14.0 kV
- Inductance 952 μH

The resistance can usefully be split and put to use in other parts of the circuit, providing it adds up to 2.57 Ω in whichever series parallel configuration proves useful. Part of the resistance was moved to the output of the capacitors – each of these resistors was 3 Ω. This limited the fault current in the case of accidental short circuit of the capacitors, to 6.6 kA maximum which was necessary as they cannot handle a complete short without damage. These 3 resistors, since they were in parallel had an aggregate resistance of 1 Ω. The remaining resistance was spread throughout the circuit between the capacitors and the load. This is further discussed in the filter section.

Figure 57 shows the basic form of the circuit. To the left of the capacitors, the charging and dump circuit can be seen. The diode is used to protect the output of the charger from a voltage reversal should the voltage across the capacitors becomes negative.

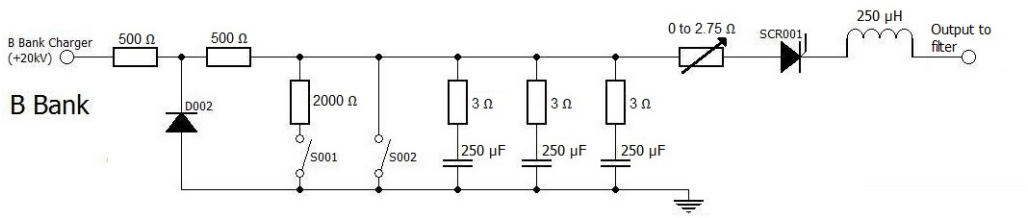

Figure 57 – Sketch of the B waveform generation circuit

5.6. Methods of producing the C and C* waveforms

The C and C* waveforms, not being of double exponential type, do not lend themselves naturally to a perfect circuit solution. Quite the opposite, a square wave cannot be produced by a passive circuit. Ideally, a controlled current source would be used. This section explores the options for creating these waveforms.

5.6.1. Waveform Specifications

The ED84 specification of the two pulses is:

- C (long C)
  - Current between 200 A and 800 A
  - Charge delivered 200 C
  - Duration of pulse 0.25 s to 1 s
- C* (short C)
  - Current between Average not less than 400 A
  - Charge delivered Usually between 8 C and 20 C
  - Duration of pulse Usually between 20 ms and 50 ms

The Stanag 4236 Annex C-specification is for the full C component only:

- C (long C)
  - Current 600 A
  - Charge delivered 300 C
  - Duration of pulse 0.5 s

Note, that Stanag 4236 [49] requirements have been included for comparative reasons and were not of primary interest for the laboratory whereas the waveform specification within ED84 specification are.

The pulse shape is flexible, in that anything that delivers the above will be considered satisfactory. However, it is preferable that it loosely approximates a square-wave, and that it does not continue at a lower level after the desired cut off time.

5.6.2. Sample Impedance and Stability

The information within the specification is not enough to design a C bank. However, several other parameters need establishing first. Estimates have been included to give a starting point from which to work.

The sample impedance is the load in which to deliver the current waveform. Unlike the other waveform generators, which have good reason to use a voltage much higher than the arc voltage, for the C waveform it does not, and ideally any driving voltage would be minimized.

The sample impedance must be considered and sufficient margin given. Under a short circuit condition, the sample impedance is largely its resistance (usually between 0 mΩ and 50 mΩ). When an arc is present, the voltage across the arc, while averaging 665 V can vary and is in addition to the resistance.

Often, as a sample is eroded by the arc, the arc becomes somewhat stretched and less stable. The instabilities themselves increase the length of the arc by twisting it and forming loops. This can be seen in slow motion footage of these trailing components.

Upper and lower bounds for arc voltage required defining. The lowest voltage a 100 mm arc would likely have is 300 V, which sets the lower bound. Allowing for the arc to wander, knot (tightly twist – so much so that occasionally it can break off a loop that can be seen in high-speed photography) and otherwise extend, an

upper limit of 1,500 V was chosen. This is of little concern for the B, D, Ah or A waveforms which have initial capacitor bank voltages well in excess of the highest likely arc voltage. But it is a concern if the driving voltage is of comparative magnitude to that of the arc.

The facility should be able to produce an arc into high impedance with a high degree of immunity to any instability. Ideally, the terminal voltage should be greater than 1500 V, and preferably nearer 3000 V. This allows the use of larger resistive and inductive components in the control/filter network, which both increase performance and decrease the complexity and cost of it. The cost reduction was facilitated by the inexpensiveness of increasing the resistances and winding the inductors by hand.

5.6.3. Other Criteria

The duty cycle of the apparatus is important as it helps define thermal loading of components such as resistors. Since lightning testing is destructive, a new sample requires installing in the test rig – which in turn requires unlocking, entering and re-locking the HV area. Together with time to raise and lower earth and dump switches and charge the capacitor bank, one shot every 5 minutes was expected to be the maximum repetition rate. Though realistically, it is optimistic to expect to run the facility this fast as samples are expensive and, scientific discussions regarding setup will greatly lengthen the time between lightning discharge tests.

The desired lifetime of components and the aggregate system was estimated. While designing for 10 years would likely be sufficient, designing for 30 would ensure the equipment would remain reliable over any reasonable expected life time of the laboratory. With 20 discharges per working day, a total of 120,000 operations of the equipment were designed for.

5.7. Energy storage option

Upon initial inspection, the method of energy storage seemed to be the central decision to make before designing the C waveform generator. The slow waveform opened options other than capacitors as used in the other waveform generators. There are several methods that could be used to store energy and discharged to produce the waveform:

- Batteries used as a DC source with resistive stabilisation
- Inductive energy storage with resistive stabilisation
- Capacitive energy storage with resistive stabilisation
- Flywheel energy storage as used in Sandia National Laboratories lightning simulation facility with a combination of resistive, phase angle or exciter current stabilisation
- Using grid power (directly rectified output of isolating transformer) with a combination of resistive and phase angle stabilisation

The next sections consider at each system in detail to explore what would be required to make a functioning waveform generator.

5.7.1. Batteries

Banks of batteries have long been used as a DC source, from days of Edison (supplying backup for the mains network) to modern day usage in UPS systems. They are also used in telephone exchanges, fork lift trucks and submarines. So, it seems that the technology is well established. Because of this, it has been considered and then used as an energy source for the C component by several laboratories.

While many different battery types are available, the obvious choice based largely on cost grounds was lead acid. Both automotive and large UPS batteries would be suitable. Supply and disposal/recycling chains are well established, further adding to their suitability.

Assuming the battery is in new condition and of sufficient capacity, it should easily be able to deliver the required currents. The greater the capacity (or more the larger the plate area), the lower the internal resistance will be and so there would be less voltage sag under load.

The expected waveforms call for anything up to 800 A, and a pulse for up to 1s, but only for a maximum of ~350 C total charge transfer. As such, the following specification was formed:

- Open terminal voltage of ~1,800 V
- Terminal voltage under the load of a 1,000 A pulse to be at least 1,500 V
- Duty cycle of 0.1% maximum (useful for considerations of cooling and charging)

The specifications in the form of a request for a budgetary estimate were sent to the several suppliers. The most favourable solutions were very similar to UPS configurations, supplied as a package with frames, chargers and isolators.

It is understood that other laboratories used a series string of 96 batteries (12V each, delivering 1152 V), however, it was proposed to increase the count to 150 (12V x 150 = 1800 V). This was to ensure that there were enough volts to overcome the diode drop in the solid state switch (~10 V) and resistive drop (~250 V) plus diode drop (~60 V) in the protection circuits as well as cope with high resistance encountered during tests to carbon based components. It should have a greater level of functionality when compared to the other facilities. The high resistance of the protection circuit greatly simplifies its design, makes it smaller and cheaper at the expense of a high battery bank voltage.

Given their varied and wide spread use, batteries offer the following advantages:

- Commercially available and used worldwide for many purposes, thus, having numerous suppliers and quick replacements available. The most comparable commercial use is battery backed uninterruptable power supplies.
- Somewhat proven technology in the lightning testing field.
- Perceived to be the cheapest option.

However, batteries have the following known disadvantages:

- High maintenance required – topping up water level and replacing resistive cells.
- Limited life ~ 7 to 10 years depending on quality of cells and use (7 years is average for UPS batteries).
- Permanently hot (in the electrical sense) being that there is always DC present. Several engineers have reported being frightened of working with them, while the suppliers have all expressed that while it is indeed dangerous, if one is careful, it is usually safe to work with battery banks. This does not give confidence, and so a remote method of breaking the battery bank down into sections of 60V maximum is recommended. This can be accomplished by a multiple ganged knife switch, but does add to the cost.

- The battery bank would need keeping in its own room to ventilate the out gassing hydrogen and ensure safety regarding the permanently live bursars, adding considerable cost as well as well as bulk.
- Several battery banks have caught fire. For this reason, they are banned from UKAEA sites. A bank of batteries, if shorted, would deliver a tremendous amount of power for a long duration. In order to protect against this, a system of fusing would be needed.

The following are estimates for the required parts to build a battery bank based on 2010 prices:

- Budgetary estimates for the batteries and racks have come in around £30k from both UPS Power and Chloride Power
- Replacements every 7 years would effectively cost £4k per year
- Battery charger ~£5k
- As the batteries require a room / cage for themselves, as well as added safety equipment, this is estimated to cost ~£15k
- IGBT output stage ~£15k
- Voltage monitor ~£2k
- Resistive ballast (wave-shaping resistor) ~£10k
- Protection circuit ~£15k (more like ~£25k if required to have a low resistance)
- Misc equipment ~£10k
- TOTAL (Including 2 years effective running costs) ~£110k

5.7.2. Inductive Energy Storage

The inductive energy storage method is well established - often referred to as a clamped circuit. Essentially, a capacitor is used to ring energy into an inductor (which is in series with the load). Once the voltage on the capacitor has reduced to zero and the peak current in the inductor is reached, the capacitor is shorted out. This allows the inductor to free-wheel through the load. There is usually some added resistance to enable the tail of the current to be controlled. Sometimes, a short can be applied across the load to cut the end off of the tail of the waveform. If used for the laboratory in Cardiff, this would be required as it is desirable to end the current at a predetermined time.

Clamped circuit inductive energy storage is used in several lightning test facilities (see introduction for more information):

- Lightning waveform generator 3 used this method to produce the BC* and BC waveforms. The BC* and BC waveforms were composite and cannot be separated, but could be altered with some degree of difficulty. It was considered that the BC* waveform was close enough to the standard but sometimes questioned as to whether the BC waveform was (which used a much larger value of inductance than when delivering the BC* waveforms). That was because the B component was over a much longer time scale than the desired 5ms (in the BC waveform case), and the tail of the C component was difficult to control and had a large proportion of its amplitude below 200A, as well as often starting above 800A.
- Lightning waveform generator 7 is a portable facility used for the testing of wind turbine components with a 10/350 waveform. It uses a small capacitor bank to ring current into the inductance of the wind turbine blade and its return conductor to produce a waveform with a 350 μs to half current tail with 100 C of charge transfer. While this waveform is much shorter and higher current than the trailing components, it is indicative that such high charge transfers are being achieved with clamped circuits.
- Lightning waveform generator 8 is capable of generating the A waveform with the desirable parameters of 6.4 μs rise and 70 μs time to half. Again this is not a trailing component waveform, but its use of a triggered crowbar shows further successful implementation of high coulomb spark gaps. It is the closest fit to the standard double exponential waveform from any laboratory, but uses very high voltage. This is considered, very expensive.

Inductive energy storage can lend itself to tests with long arcs. This is due to a very large inductance having ability to store a lot of energy and act as a reasonably stiff current source. Even so, the inductance needed for undertaking such a test would be approximately 1.5 H for the C waveform. An inductor of this value, capable of carrying the required current would likely weigh several tonnes.

The advantages of inductive energy storage include:

- A very large inductance can help produce a stable arc current as an inductor strives to keep its current constant over short timescales.

Inductive energy storage has several disadvantages including:

- Large inductors are bulky and expensive – the inductor used by Lightning waveform generator 3 to generate a combined B and C waveform was over 3500kg of very pure aluminium and used 20 square meters of floor space alone.
- A reasonably high voltage (estimated in the order of 20 kV) capacitor bank is required to ring the energy into the inductor.
- Switching is difficult, unless ignitrons are used, in which case there is a mercury hazard. Thyristors could be used but would need protecting from inductively driven voltage spikes.
- This is likely the most bulky and one of the most expensive methods of producing the C component waveform.

The following are estimates for the required parts to build an inductive energy generator based on 2010 prices:

- Estimate for capacitor bank to ring current into the inductor ~£50k
- Capacitor charger ~£10k
- Estimate for a 0.01 to 0.6H inductor ~60k
- Ignitron switching ~£15k
- Voltage monitor ~£2k
- Resistive ballast (wave-shaping resistor) ~£10k
- Protection circuit ~£10k
- Misc equipment ~£10k
- TOTAL (Including 2 years effective running costs) ~£167k

5.7.3. Capacitive Energy Storage

While batteries allow a reasonably stiff DC bus voltage from which to deliver a square wave discharge, a capacitor bank, unless exceedingly oversized would suffer significant voltage drop as charge is removed. This potentially makes shaping the waveform more complex (compared with constant current from a battery bank), but it is allowed for in the specification.

Capacitors can have terminal voltage well in excess of that required to deliver the C waveform (taken from the battery bank analysis above). This can eliminate series connections and balancing of individual devices. Furthermore, capacitors unlike batteries can be drained completely of energy and this made save and inert between tests. This is helpful for both maintenance as well as access to the space in which they reside, eliminating a permanent barrier around them – so long as they are within the HV area and it is appropriately locked when they are charged.

- Lightning waveform generator 1 generated the C and C* waveforms by discharging a capacitor bank through a high power rheostat in series with the load. Removing charge from the capacitor bank through a pulse would lower the driving voltage; this was overcome by lowering the circuit resistance with the rheostat, allowing a flatter current waveform.
- Lightning waveform generator 4 generated the C and C* waveforms by using the partial discharge of a very large, low voltage capacitor bank (a recycled physics experiment PSU), controlled by an IGBT semiconductor switch. While low voltage in comparison with the other capacitor banks, it had sufficient excess voltage to allow a large constant series resistance to stabilise the output current. The moderate voltage drop over the C waveform left a large voltage remaining on the capacitor banks which would have to be dumped. This excess energy was likely only possible as the capacitor bank was donated at zero cost and would not be as large if it had to be sourced new. It held approximately 1,000 C when fully charged. After a 200 C discharge, 80% of the initial voltage would remain.

Capacitive energy storage has not been used by many other test laboratories for the purpose of creating the C or C* waveforms. This has presumably been due to the very high cost of capacitors. However, with recent increases in energy density, increasing the amount of energy that can be stored in a single capacitor by a factor of 2 or 3 orders of magnitude, costs have come down.

Switching a capacitor bank discharge can be accomplished with a variety of components. These include IGBT and IGCT silicon switches as well as mechanical relays. Thyristors and ignitrons are harder to turn off at the end of a waveform bout could be used too.

The potential for high terminal voltage allows a large source resistance, greatly nullifying the effect of sample resistance. This could make setting it up for an experiment simple. There could be one voltage to charge to if performing conduction tests, and another increased to take into account the arc voltage drop for arc tests.

Capacitive energy storage would have the following advantages:

- Low internal resistance
- Once discharged and a short is applied, safe to handle
- High energy density leads to reduced footprint and low parts count
- Proven technology in the lightning testing field
- Several companies have extensive experience of producing this type of capacitor
- Not much more expensive than batteries
- Much more compact than batteries
- No maintenance required
- Long expected lifetime
- Potentially the lowest level of stored energy

There is one major disadvantage with a capacitive energy storage generator:

- Capacitors are a long lead time item (point mitigated if action is taken early – expect 14 weeks minimum wait)

The following are estimates for the required parts to build a capacitive energy storage generator based on 2010 prices:

- Estimate for capacitor bank ~£50k
- Capacitor charger ~£10k
- IGBT output stage ~£15k
- Voltage monitor ~£2k
- Resistive ballast (wave-shaping resistor) ~£10k
- Protection circuit ~£15k
- Misc equipment ~£10k
- TOTAL ~£112k

5.7.4. Flywheel Energy Storage

The Sandia Lightning Simulator [56] uses a flywheel to store energy for its C like waveform. Essentially it operates by using a motor to spin up a flywheel and, then, during the shot, uses the rotational energy to provide energy for the waveform. It is a complex system, and like the batteries, it requires its own room or large, robust enclosure to keep it in, due to the dangers of having a rapidly rotating multi tonne assembly.

Only the top fraction (~60% to) of the rotational energy would be available for use in the waveform. This is only possible with automatic voltage regulation which adds cost and mass to the exciter as it must have a wider operating range than one that generates a static field. The conversion efficiency is also likely to be limited, for example, the generator windings will have resistance and there will be several diode drops in the rectifier. Finally, the power factor of the load will likely be very low. The flywheel would likely weigh 1,000 to 2,000 kg, be 1 m in diameter and have to rotate at 1,500 RPM to store a total of 1.5 to 3 MJ. When doing so, the rim velocity would be ~180 mph.

Flywheel energy storage has its place in pulse power, but that is for slightly longer pulses (~seconds) and much higher levels of energy (>10 MJ). It is considered too complex a method to use to produce the waveform.

UKAEA uses 2 flywheels to supply power for the fusion reactor JET [60]. These are very large, each weighing 776 tonnes and are 9.8 m in diameter. They are housed sunken into enormous pits in the ground in a rather large hanger. In the 1970s when they were designed, it was the most sensible way of storing the vast amount of energy required, with each one able to store 1 MWh.

Anecdotally, after finishing working on the MBLL, but before completing this thesis, experience was gained at the United Kingdom Atomic Energy Authority, on JET, maintaining a circuit fed by one of the 776 tonne flywheels. The experience gained showed that they are indeed very high maintenance devices. They were quite lossy, with a peak theoretical efficiency of 47%. The actual efficiency was lower once windage losses from keeping them spinning for long periods of time between pulses was taken into account. They are expensive to run too, consuming £2.5M of electricity per year on top of a £1.1M service contract.

The advantages of using flywheel energy storage include:

- Capable of storing a vast amount of energy which could open the opportunity of a vastly extended C like waveform for experimental purposes

The disadvantages of using flywheel energy storage include:

- Complicated infrastructure and control systems
- Bulky and requires a room/building of its own
- Expensive

The following are estimates for the required parts to build a generator with flywheel energy storage based on 2010 prices:

- Having spoken with a supplier of UPS systems that include flywheels and previous experience scoping such systems, it is assumed that, due to power levels required, the cost would be around £750k for the flywheels alone.

5.7.5. Using Grid Power

Grid power was an interesting option if there is enough available. To form the waveform, a transformer rectifier arrangement could be formed with 3 or 6 phases (delta + star for 6) and thus 6 or 12 pulses per 20 ms cycle. A small amount of capacitance would be required for smoothing. Control of the current could be either via thyristors at the rectification stage or after rectification is completed. It was considered that if there was not already a sufficient supply to the building (roughly 2 MVA, taking into account the low expected power factor), then cost would be prohibitive. However, if the supply existed, then the costs would have been affordable.

The grid connection does not lead itself to use in long arc tests, as there is a ceiling on the available power and thus voltage across the arc. As such, with a high terminal voltage, the current would be limited. However, it could be used to ring current into an inductor; though such a method incurs the cost of the rather expensive inductor.

The advantages of using grid power include:

- If power was immediately available, the cheapest option
- A DC source and thus no limit to charge transfer

The disadvantages of using grid power include:

- Unlikely to have required power available and therefore expensive
- Likely to be bulky
- Electric costs will be increased by the supplier due to the intermittent use of power

The following are estimates for the required parts to build a generator supplied directly with grid power based on 2010 prices:

- About £50k with available power and prohibitive if not

5.7.6. The choice - Capacitors

The choice seemed was between batteries and capacitors. If going by cost alone, then batteries probably are marginally cheaper (depending upon how the future cost of replacement cells was taken into account). However, once space and safety was taken into consideration, then capacitors are preferable. It is suggested that these last 2 points are of major importance bearing in mind that available space is limited and safety is always of paramount importance.

Using an inductively stored energy system effectively delivers an LR decaying exponential shape and not a square wave – it was felt that improving the waveform was desirable. Furthermore, this system requires all the energy that would be delivered to the sample to be initially stored in capacitors – so use capacitors appears alone a more attractive option.

However, if the energy were stored in a superconducting coil, its inductance could be huge, allowing a relatively flat output waveform providing only a small proportion of the stored energy was consumed. Inductive energy storage devices are exceedingly expensive, so this was ruled out.

Flywheels were quickly written off as a means of energy storage because commercial systems were extremely expensive and, from experience, required costly maintenance while a home built system was considered too complicated and bulky. It would have been more interesting if a lower current (or power) for a longer duration was required.

Battery banks have been used for creating the C and C* waveforms in other laboratories. However, they are rather large; typically taking a good sized room to enclose them, which is essential for safety reasons. They have high terminal voltages and cannot be drained of energy before safe access is granted to an area.

This immediately eliminated them as an option. Space in the laboratory was at a premium, and there was nowhere to put an additional room.

Batteries have a design life circa 7 to 10 years which is not ideal as, at a future date, they would require replacing.

Grid power is a good option if there is enough available. To form the waveform, a transformer rectifier arrangement can be formed with 3 or 6 phases (delta + star for 6) and thus 6 or 12 pulses per 20 ms cycle. A small amount of capacitance is required for smoothing. Control of the current can be either via thyristors at the rectification stage or after rectification has completed. It is considered that if there is not already a sufficient supply to the building (roughly 2 MVA, taking into account the low expected power factor), then cost would be prohibitive. If the supply exists, then the costs were expected to affordable. However, the installed power to the building was 80 A per phase, eliminating this approach.

Finally, capacitors were chosen - mainly because they can be turned off after a pulse and be made safe where batteries can't. Also, if using high energy density metallised film, the system might need only a few capacitors, thus, keeping the parts count and size low. Further to this, a capacitor system was seen to have the following merits over a battery system: higher terminal voltage, lower internal resistance, and greater life, as well as the discussed safety advantage. The goal is to provide a system that is flexible, robust, a good level of ease of use, a high level of safety and cost effective.

5.8. Optimising the C/C* circuit

In the B waveform circuit, all the stored energy is consumed. This is not the case with the C waveform, a considerable amount of the energy and charge within the capacitors for the C waveform will remain after the discharge. This is due to the minimum voltage required to drive current through the circuits and load resistance/arc voltage drop. A minimum current here would be 200 A as specified in the standard which requires considerable voltage to drive through several ohms of resistance and a several hundred volt arc.

Having chosen capacitors as an energy storage means, the voltage will decay as charge is removed from them. This would produce an exponentially decaying waveform, which would be acceptable by the test standard. However, it would be

desirable to have a square wave and be able to choose its amplitude, duration and charge transfer by setting a dial or from the control system. If the system could be relied upon to constantly deliver the current into loads of varying voltage drop and resistance, that would be useful also, eliminating setting changes for different tests.

In order achieve closed loop control to deliver a square wave, the concept of using a large buck converter was developed. While looking for suitable switches, those attainable were found to be rather slower than desired. The notion of using several smaller switches in parallel arose as the input to a buck converter. And while attempting to current share equally between the switches, it seemed sensible to use a separate inductor and diode for each switch (the output section of a buck converter). It was a small step from that to the idea of a multiphase buck converter. This will be referred to from here hence as the PWM method as it would use pulse width modulation of the switches for controlling the output current.

Compared with a single phase buck converter, using several phases would enable the output current swings to be reduced by the number of phases and the frequency of such swings to be increased by the same factor. With smaller swings in output current and at a higher frequency, filtering them to further reduce the amplitude of ripple was simplified and allowed a low pass filter to be built using available parts.

However, initial scheme designs of a multi phase buck converter showed it would be somewhat more complex than a capacitor-resistor (CR) discharge. While the hardware to implement it would be similar, the control system would ideally be closed loop for the buck converter solution. The project overheads of setting up the measurement system and programming it seemed unlikely to fit within the time that could be allocated to it. Therefore the notion of building a CR discharge based waveform generator that could be upgraded to operate as a multiphase buck converter later seemed a sensible approach.

A capacitor bank would have to be sized to deliver 200 C into the load using both the CR and PWM methods. The capacitor bank size requirements are investigated for each method intern below.

5.8.1. Capacitor bank sizing for CR controlled C waveform

There is a requirement to maintain a current within the limits of 200 to 800 A. Therefore, only the top part of the voltage in a capacitor bank (voltage wise) can

be used to produce the waveform. This is because there must be enough remaining voltage to drive at least 200 A through any circuit resistance and across any arc voltage drop. The rest must be dumped and is of no use.

As an example, Figure 58 shows the initial stored energy vs the initial charge voltage, considering only that there must be 200 C available in the capacitor between the initial charge voltage and the load voltage drop of 665 V. The purpose was to explore the theoretical minimum energy that a capacitor bank may have and still deliver the charge to the load. Obviously, additional voltage would be required to overcome circuit resistance, so this is just a minimum and not a solution.

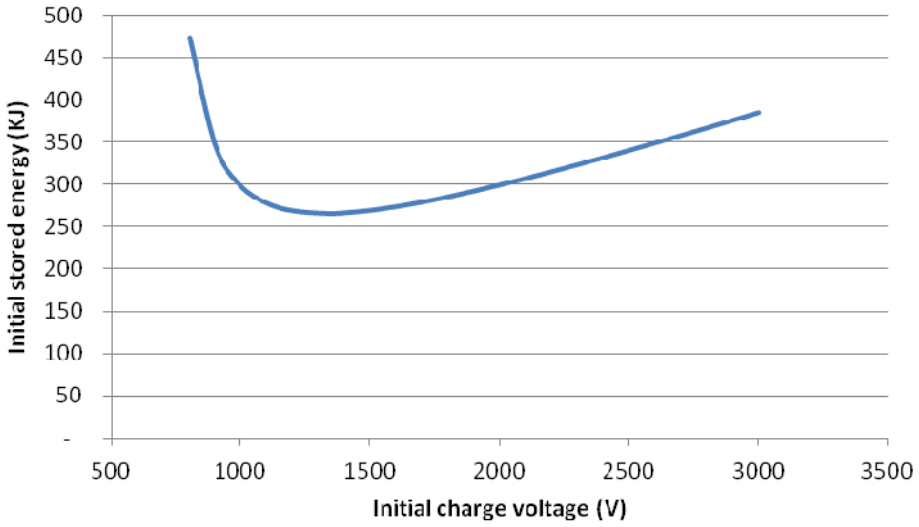

Figure 58 – Energy vs initial charge voltage to deliver 200 C

In this example, the load voltage drop is 665 V. As can be seen, there is a minimum energy storage requirement at 2 times the final voltage (thus, initial capacitor bank charging voltage of 1,330 V). Equation (55) was used to derive this graph where V_{Init} and V_{Arc} are the initial charge and arc voltages respectively and where $C_{Transfer}$ is 200:

$$E = \frac{C_{Transfer} {V_{Init}}^2}{2(V_{Init} - V_{Arc})} \tag{55}$$

However, as mentioned above, this did not account for any circuit resistance and considered charge only. Figure 59 shows the resistance as calculated to limit the maximum current to 800 A for a given initial charge voltage. It also shows the initial stored energy resulting from a capacitor bank of sufficient size to have enough voltage left to drive 200 A through the given resistance and 665 V arc drop,

after delivering a 200 C waveform. This should also be seen as a minimum energy to store for a given voltage. Excess initial energy storage energy would allow higher resistance and thus a flatter current profile.

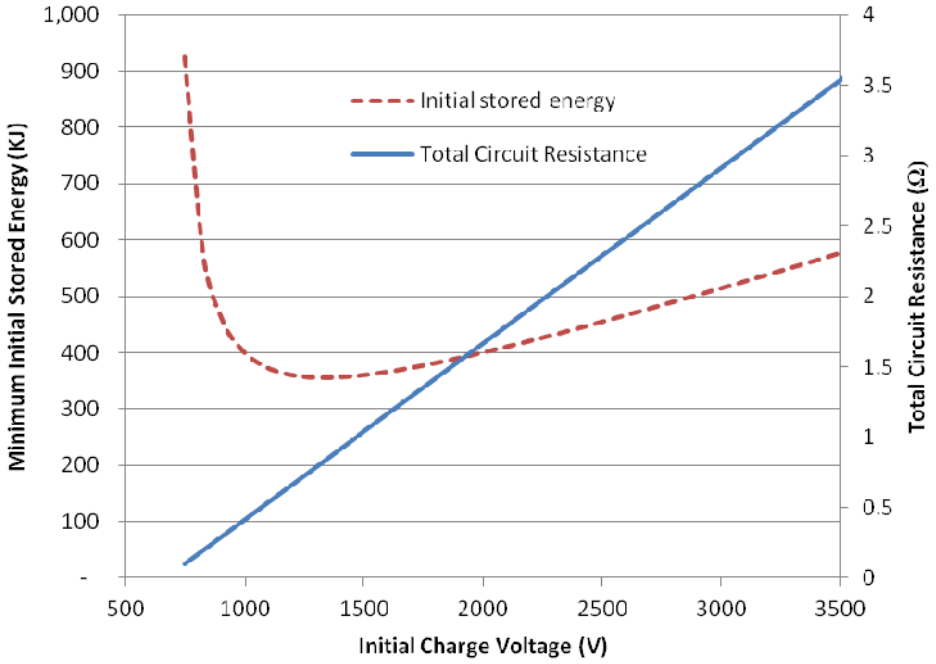

Figure 59 – Minimum initial stored energy and total circuit resistance vs initial charge voltage for CR discharge mode

The resistance is not dependant on the charge delivered by the waveform, only the initial charge voltage, the maximum allowable current (I_{Max}), which is 800 A and the arc voltage drop as shown in Equation (56):

$$R = \frac{V_{Init} - V_{Arc}}{I_{Max}} \tag{56}$$

The minimum initial energy to store in the capacitor bank is calculated using Equation (57) which uses the maximum allowable current (I_{Max}) along with R as calculated in Equation (56):

$$E_{Min} = \frac{C_{Transfer} V_{Init}}{2R(I_{Max} - I_{Min})} \tag{57}$$

The minimum initial stored energy as shown in Figure 59 is approximately 355 kJ at 1,300 V. Stability can be increased by increasing this further as the current limiting resistance can be increased also, leading to a more stable arc and greater likelihood

of achieving the desired current (sample impedances are similar, but often unknown and somewhat variable). The minimum energy is reasonably insensitive to small increases in initial voltage, but the resistance is directly proportional.

By increasing the initial voltage to 3,000 V, the initial stored energy increases to 520 kJ (an increase of 47%). This allows the total circuit resistance to be increased from 0.8 to 3 Ω (an increase of 275%). This seems a good trade off.

For completeness, Figure 60 shows the minimum capacitance required to deliver the C waveform through a 665 V arc against the initial charge voltage of the capacitor bank.

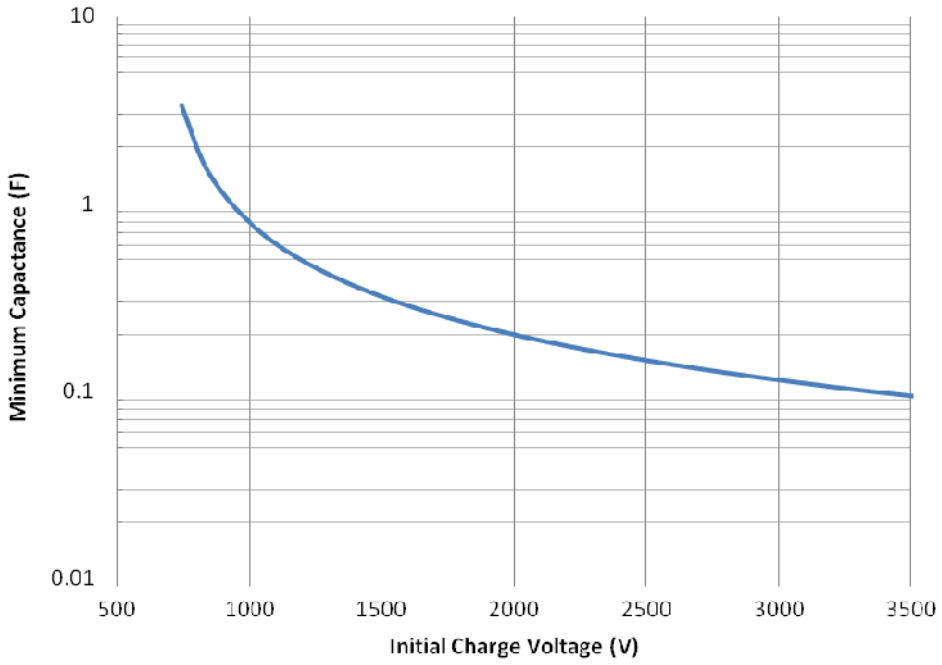

Figure 60 – Minimum capacitance vs initial charge voltage for CR discharge mode

The minimum capacitance is calculated using Equation (58):

$$C = \frac{C_{Transfer}}{R(I_{Max} - I_{Min})} \tag{58}$$

The minimum capacitance at the minimum energy point would be 0.42 F which is reduced to 0.11 F with an initial capacitor bank voltage of 3 kV.

5.8.2. Capacitor bank sizing for PWM controlled C waveform

While there is an accepted exponential decay in current when using the CR discharge method, using PWM in closed loop, a flat current profile can, in theory, be achieved. The reference current profile for delivering the C waveform is a 400 A square wave for 500 ms for a total of 200 C of charge transfer.

An ideal buck converter takes a high voltage low current input and outputs a low voltage high current with 100% efficiency. This would allow a constant output voltage to be delivered so long as the voltage within the capacitor bank is greater than it.

As with the CR method, firstly the hypothetical minimum energy storage requirement was investigated. The CR method had to store 200 C of charge above the arc voltage in the capacitor bank. Conversely, the PWM method has to store enough energy above the arc voltage to drive 200 C through the 665 V arc. Equation (59) shows how this is calculated.

$$E_{Arc} = C_{Transfer} V_{Arc} = 133\ kJ = \frac{1}{2}\ C\left({V_{Init}}^2 - {V_{Arc}}^2\right) \tag{59}$$

Rearranging this for the capacitance is shown in Equation (60):

$$C = \frac{2E_{Arc}}{\left({V_{Init}}^2 - {V_{Arc}}^2\right)} \tag{60}$$

Using this, the minimum initial stored energy is given Equation (61):

$$E_{Min} = \frac{E_{Arc}{V_{Init}}^2}{\left({V_{Init}}^2 - {V_{Arc}}^2\right)} \tag{61}$$

If it is assumed that all of the circuit resistance is in the output section of the buck converters (thus their input is directly connected to the capacitor bank), it is trivial to adapt the above equations for inclusion of the added loss across the resistor. It is after all simply IR. For example, adding 1 of resistance through which 400 A passes would effectively increase the output voltage drop to 1,065 V.

Equation (59) can be adapted to give the energy consumption of the whole output system including both the arc and circuit resistance (E_{Output}) and is shown in Equation (62):

$$E_{Output} = C_{Transfer}(V_{Arc} + IR) \tag{62}$$

The minimum initial stored energy is then calculated by Equation 63:

$$E_{Min} = \frac{C_{Transfer} {V_{Init}}^2 (V_{Arc} + IR)}{({V_{Init}}^2 - (V_{Arc} + I\ )^2)} \tag{63}$$

Figure 61 shows the minimum initial energy curves generated for 5 different circuit resistances. Naturally, as resistance was increased, the total system voltage drop increased also which limits the lowest initial charging voltages.

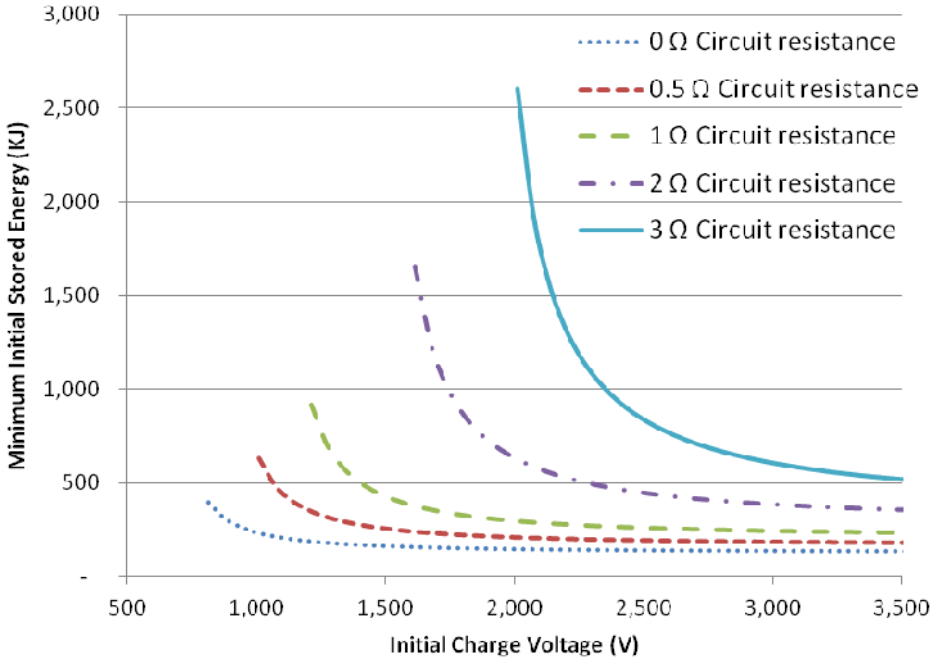

Figure 61 – Minimum initial stored energy vs initial charge voltage for PWM discharge mode for 5 circuit resistances

The minimum energy curves can be seen to drop very rapidly and then continue to do so indefinitely. So in theory, the lowest initial stored energy for any given resistance would be reached as the initial charge voltage reached infinity!

Fortunately, after the initial drop off, there is little to be gained by pushing the initial charge voltage more than about 1.5 times the voltage drop across the arc and system resistance. For example, with 3 Ω of circuit resistance, the total voltage drop is 1,865 V. At 1.5 times this, the initial charge voltage would be 2,780 V and the minimum energy initial energy would be 671 kJ. Only 80% of this would be left after the 200 C discharge. Increasing the initial charge voltage to 3,000 V

decreases the energy remaining in the capacitor bank remaining energy to 63% of the initial stored energy.

The minimum stored energy for each of the 5 resistances is shown in Figure 62:

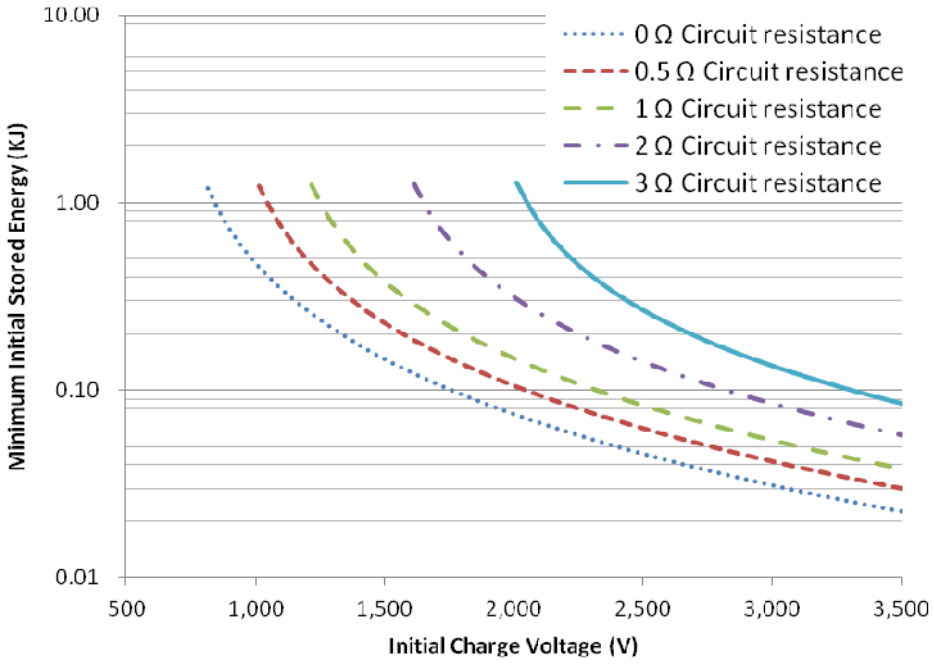

Figure 62 – Minimum stored energy vs initial charge voltage for PWM discharge mode for 5 circuit resistances

The capacitance can be calculated using Equation (64):

$$C = \frac{2C_{Transfer}(V_{Arc}+IR)}{\left(V_{Init}{}^{2}-(V_{Arc}+IR)^{2}\right)} \tag{64}$$

Unlike the CR mode, there is not a minimum energy to calculate a minimum capacitance for. For the 3 Ω example with an initial charge voltage of 3 kV, the minimum capacitance required to deliver the C waveform with a 665 V arc drop is 0.14 F.

5.8.3. Capacitor bank sizing discussion

A CR discharge can only deliver the amount of charge that is held in a capacitor bank, whereas a buck configuration moves energy from the capacitors into an inductor and then from the inductor into the load. Therefore, a buck converter consumes energy rather than charge; it effectively multiplies the charge within the

capacitor bank by the voltage input/output ratio. So, there is no charge requirement for the capacitor bank, only an energy requirement in buck operation.

Both Figures 59 and 61 showed the minimum energy that would be required to deliver the C waveform. The test standard (ED84) suggests a square wave of 400 A for 500 ms as the reference waveform, a larger capacitance would help facilitate this. For the CR method, the CR time constant would increase and so it would suffer less voltage drop. For the PWM method, it would allow longer arcs with higher voltage drops.

A 0.2 F capacitor bank was settled upon as it exceeds the 0.11 and 0.14 F requirements of the CR and PWM methods by 82% and 43% respectively which seemed reasonable.

If the 0.2 F capacitor was charged to 3 kV, it would hold 600 C of charge. Therefore the terminal voltage after removing 200 C would be 2 kV. Allowing a 600 V drop across the 3 Ω circuit resistance with the minimum current of 200 A flowing, this would allow for an arc voltage drop of 1,400 V. This is quite in excess of the expected voltage drop and would give a considerable margin of confidence for the design. For the PWM method, the 43% excess energy would allow the waveform to be extended to 296 C. In both cases, the circuit resistance can be lowered to further increase the amount of charge that can be delivered while maintaining the waveform current above 200 A.

Table 18 shows the parameters selected for the capacitor bank:

Table 18 – C bank waveform capacitor parameters

C bank waveform capacitor selection criteria		
Capacitance	0.2	F
Initial voltage	3,000	V
Initial energy	0.9	MJ

To meet the goal of lasting 120,000 operations, when ordering the capacitors, they were specified to have a working life of at least this number of cycles and 10,000 hours at maximum charge voltage. This allowed 5 minutes of waiting at full charge for each lightning test. The same was done for the B waveform capacitors as they were part of the same tender.

5.8.4. Predicted C waveform performance

There are 2 test types and 2 methods of controlling the C waveform generator's output. These are tests with an arc and to effective short circuits, which are termed conduction tests (where the load is effectively the sample resistance of 50 m Ω or less). The methods are the PWM and CR controlled discharges. The following graphs illustrate that the C waveform can be delivered in all cases and show examples of other waveforms that are within or extend the requirements of the test standard (ED84).

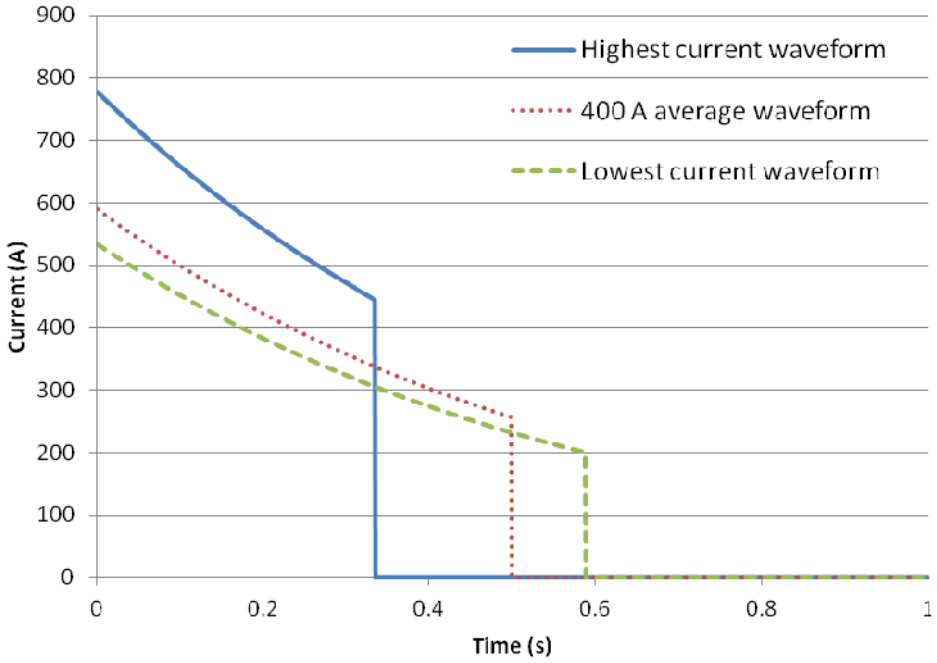

Figure 63 – CR controlled discharge for an arc test

Figure 63 predicts that the CR controlled discharge can deliver a 400 A average current, delivering 200 C within 0.5 s as required. The minimum and maximum currents are 256 A and 589 A respectively which are within the limits of 200 and 800 A. This requires an initial charge voltage of 2432 V.

Also shown in Figure 63 are the highest and lowest current waveforms into a 665 A arc that could be delivered by the capacitor bank. In the case of the highest current waveform, it is limited by the maximum charge voltage of the capacitors and has a peak current of 778 A. The lowest current waveform is limited by not being allowed to have less than 200 A and in this case has an initial charge voltage of 2264 V.

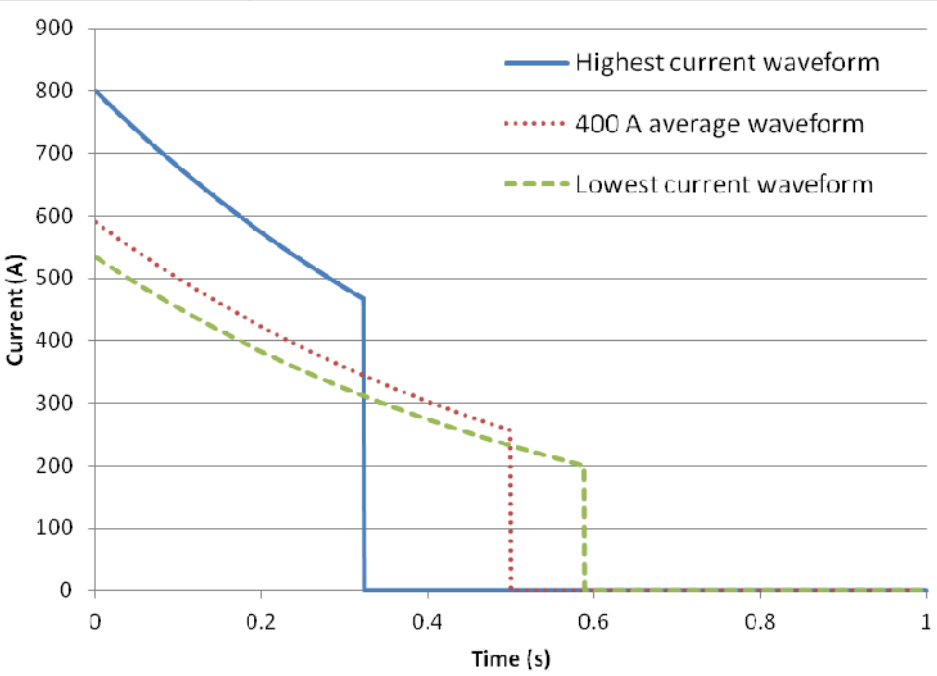

Figure 64 – CR controlled discharge for a conduction test

Figure 64 looks remarkably like Figure 63. This illustrates that the waveform shapes do not depend on the arc voltage (if it remains constant) but on the characteristic exponential curve of the CR discharge. This can be considered helpful as there would be consistency between arc and conduction tests.

The only difference between Figure 64 and Figure 63 is the highest current waveform extends to 800 A peak. This increase is facilitated by the lack of the arc voltage drop giving more voltage headroom to deliver the waveform. The charge voltages for the highest current and lowest current waveforms are 2,400 and 1,600 V respectively. The most compliant waveform is identical in scale and shape to the CR controlled arc test but the initial charge voltage is reduced to 1,768. This shows that the difference in initial charge voltage between the arc and conduction tests is the arc voltage drop alone and not a complex function. This potentially opens an interesting method of analysing the results of arc tests to calculate the voltage across the arc without having to directly measure it.

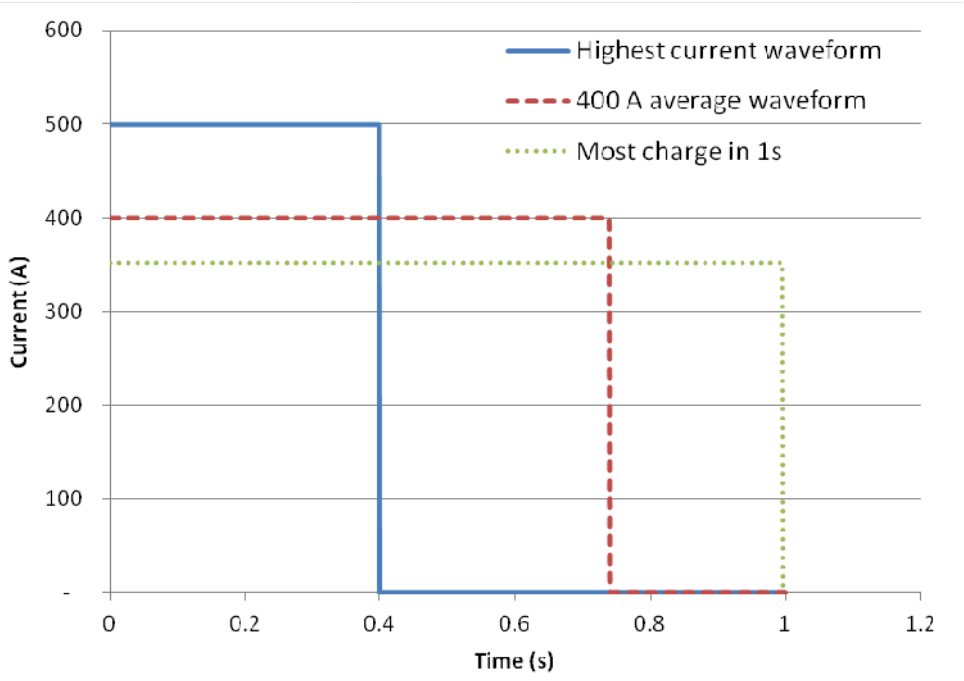

Figure 65 – CR controlled discharge for a conduction test

Figure 65 shows the maximum performance attainable for the PWM controlled discharge through an arc of 665 V with 3 Ω of circuit resistance. In all cases the initial charge voltage was the full 3 kV. The different currents would be generated by varying the PWM appropriately. The highest current waveform that could deliver 200 C would have an average current of 500 A. After delivering that, there would not be enough voltage left on the capacitor bank to maintain a flat current profile.

When delivering 400 A, less energy is consumed in the circuit resistance and the capacitor bank be run down to a lower voltage which increases the maximum deliverable charge to 296 C. This shows there is a good deal of margin to deliver excess charge if required for a test.

The standard allows a maximum time window for the waveform of 1 s. While maintaining a flat current profile, the maximum charge that could possibly be delivered in this time window is 351 C with an average current of 352 A.

For an arc test, the PWM method clearly demonstrates potential ability to deliver the waveform as required by the test standard. The control system that maintains the correct current can integrate it and automatically shut off once 200 C has been transferred.

When used to deliver a current waveform for a conduction test, the PWM control method potentially allows much greater charge transfers. A graph is not presented as the waveforms are very out of specification (and square waves are sufficiently simple to explain).

The highest flat profile current waveform possible delivering 200 C would have a current of 721 A and take 277 ms to deliver the waveform. If delivering a 400 A waveform, a maximum of 630 C could be delivered in 1.575 s. If the lowest allowable current of 200 A was used, a total charge transfer of 1,440 C could be transferred through the sample.

Figures 63 through 65 show that with both modes of operation there is potential to deliver the required C waveform for both arc and conduction tests. There is also margin for experimentation by changing the initial charge voltage. Furthermore, it would be possible to reduce the circuit resistance (possibly at the expense of system stability or safety if it is from a protection element) and extend the performance further. Importantly it is shown that it is feasible to implement both methods using the same hardware with the only difference being control signals.

5.8.5. C waveform switch

To generate the C waveform, at the very minimum, a switch was required to turn on and off at the beginning and end of the discharge. To implement a PWM controlled buck converter, the switch would have to turn on and off much more frequently.

The devised system has current feedback and can automatically raise and lower the output voltage to counter variations in load resistance and arc voltage when used in Pulse Width Modulation (PWM) mode. Therefore, using it is a simple matter of setting a dial rather than requiring the effort of understanding the load and changing resistors and initial charge voltage to suit. Further, when used in CR mode and the current is controlled only by the initial voltage and the circuit impedance, the waveform may still be ended once the desired charge transfer has been accomplished, making that mode of operation simple too.

The devices explored included relays, GTO thyristors, IGCTs and IGBTs. While devices such as ignitrons and thyristors can be used, the circuitry required to turn them off is cumbersome, essentially, requiring a reverse pulse to force a zero voltage commutation. Mechanical relays have been used. With their inertia,

careful timing may be required to operate them in synchronisation with the other waveforms.

IGBTs were the fastest and least expensive of the 3 types of switch, mainly due to the simple triggering requirements keeping the gate drive circuit costs low. While the IGBTs could in theory switch at 10k Hz, a significant amount of heat would build up within the device as each switching event has associated energy losses. For short bursts of up to 1 second, the IGBTs appeared to be capable of running at ~2 kHz without overheating. For robustness and a degree of cooling between lightning tests (every 3 minutes max), they were firmly bolted to thick aluminium sheets for thermal capacity and then in turn to air cooled heat sinks. The thermal capacity of the aluminium was such that it would only heat up a few degrees during a 1 s waveform duration. Since the generator was designed to operate only once every few minutes, this would allow plenty of time for convection to cool it back down. The very high thermal conductivity into the thermal inertia of the aluminium plate mitigated the low thermal conductivity of the heat sink into the air. Even so, a large heat sink was used to avoid requirement for a fan and associated power supply.

In order to smooth the output waveform, the use of multiple phases running with an even angular spread would help. The number chosen was 3, based on component cost, complexity and space required. This effectively reduces the current handling required by each device by a factor of 3.

The chosen IGBT modules were capable of holding off the full system voltage and so avoided series connections. The boiler plate rating was 6,500 V and 600 A. Table 19 compares the requirements of the circuit with the rating of the switch. As can be seen, there is at least a safety of 2 for all parameters.

Table 19 – Comparison of C bank IGBT requirements and specification

Parameter	Requirement	Rating
Peak voltage	3000V	6500V
Average Voltage	2500V	6500V
Peak current	250A	1200A for 1ms
Average current	133A	600A

Keeping well below the rated voltage and current allows for relatively low switching losses. It is estimated that each off-on-off switching cycle would deposit around 1 to 2 J into the switches junction. This necessitates a control algorithm which avoids excessive switching in order to reduce stress and excessive heating of the junctions. As mentioned, simply running at a reasonably low frequency is sufficient.

5.8.6. Switch protection methods

Protecting silicon switches from transients is important. A spark gap or ignitron can handle very large occasional discharges and survive self triggering by overvoltage, but a thyristor or IGBT usually cannot. Protecting them from excessive dI/dt, dV/dt, voltage and current was imperative.

For normal switching, dI/dt is simply controlled by circuit inductance. This will limit the rate of rise when the device is turned on. However, when it turns off, the inductance feeding current into the IGBT would cause the voltage to rise. To avoid local inductance on the input side overvolting the device, it needed to be minimised using wide bus bars and stripline connections. A passive snubber network was then implemented to smooth the remaining voltage spike.

By simply placing a capacitor across the IGBT, energy present in the local inductances would flow into it as the device switches off. This is a fairly standard approach but it can be improved upon.

If a capacitor is placed across the device to absorb an incoming spike, it will be charged to the supply voltage. When the IGBT turns back on, it shorts out the capacitor, and any energy within it is dissipated rapidly in the IGBT's gate.

For the design of the protection circuit, the full device rated current and the maximum charge voltage of the capacitor bank was used. The datasheet states

that local inductance should be limited to 200 nH or less (quite achievable using wide flat bus bars with small gaps between them). This gave 6.25 mJ of stored energy (E_s) for 250 A. With a starting voltage of 3 kV (V_1) and an upper limit of 6.5 kV (V_2), the smallest capacitor usable for a snubber is 376 pF, calculated using Equation 65.

$$C = \frac{2E_S}{{V_2}^2 - {V_1}^2} \tag{65}$$

However, it was only possible to keep the inductance below 200 nH close to the IGBT. The feeds from the capacitor banks were long and narrow. Their inductance has been estimated at 2 μH (calculated as a stripline of as built dimensions, see Equation (66)). This would have 62.5 mJ of energy at 250 A and require a 3.76 nF capacitor to prevent overvolting the IGBT.

Equation (66) gives the inductance of a transmission line near DC, where D is the distance between plates, T is the thickness of the plates, W is the width of the plates and S the length of the transmission line.

$$L = S\frac{4\pi\left(D+\frac{T}{2}\right)}{W}10^{-7} \tag{66}[20]$$

This was overcome by placing a 15 μF capacitor across the supply for each IGBT. Starting at 3000 V, the addition of 62.5 mJ would increase the voltage by only 1.4 V, calculated using Equation (67):

$$V_2 = \sqrt{\frac{2E_S}{C} + {V_1}^2} \tag{67}$$

With such a small voltage rise, the problem of snubbing the local inductance around the IGBT was all that remained.

As can mentioned previously, a simple capacitive snubber circuit can effectively absorb the incoming energy. However, it presents a problem at switch on, where the IGBT shorts out this charged capacitor leading briefly to an over current of the device.

The addition of a diode and resistor can allow the inrush current to the capacitor to be high, while eliminating the over current at switch on as it is reduced by the resistor. A schematic is shown in Figure 66:

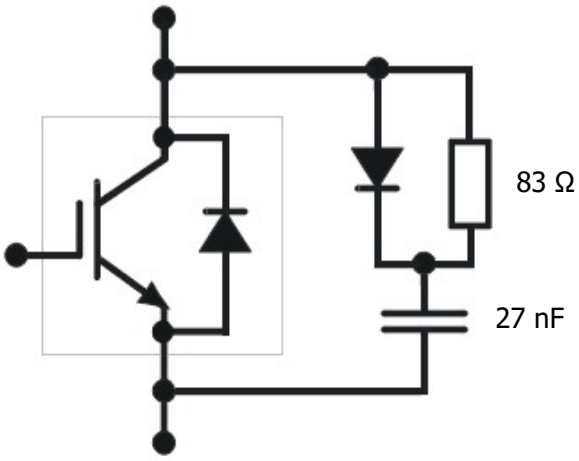

Figure 66 – Capacitor/diode/resistor snubber

The resistor must be able to absorb all the energy delivered to the capacitor without overheating. For example, at 3 kHz for ½ second and using the 62.5 mJ, the energy delivered is 93.8 J. This necessitated a resistor with a reasonably high thermal capacity to ensure it would not burn out. This snubber network was chosen for use in this work. Due to availability of parts, 3 snubbers were used per IGBT to reduce inductance through parallel paths, each with a 250 Ω and 9 nF, resulting in an effective snubber with 83 Ω and 27 nF. The resistance would limit the current to 36 A when operating at maximum capacitor bank charge voltage. This is much lower than the device limit of 650 A average.

The IGBT and snubber arrangement used a distributed strip line arrangement to minimise inductance. The stripline consists of a very wide aluminium plate (at the capacitor bank ground potential) and 2 wide strips above it (for the input and output of the IGBT respectively), insulated with 1 mm of PTFE. This is shown in Figure 67.

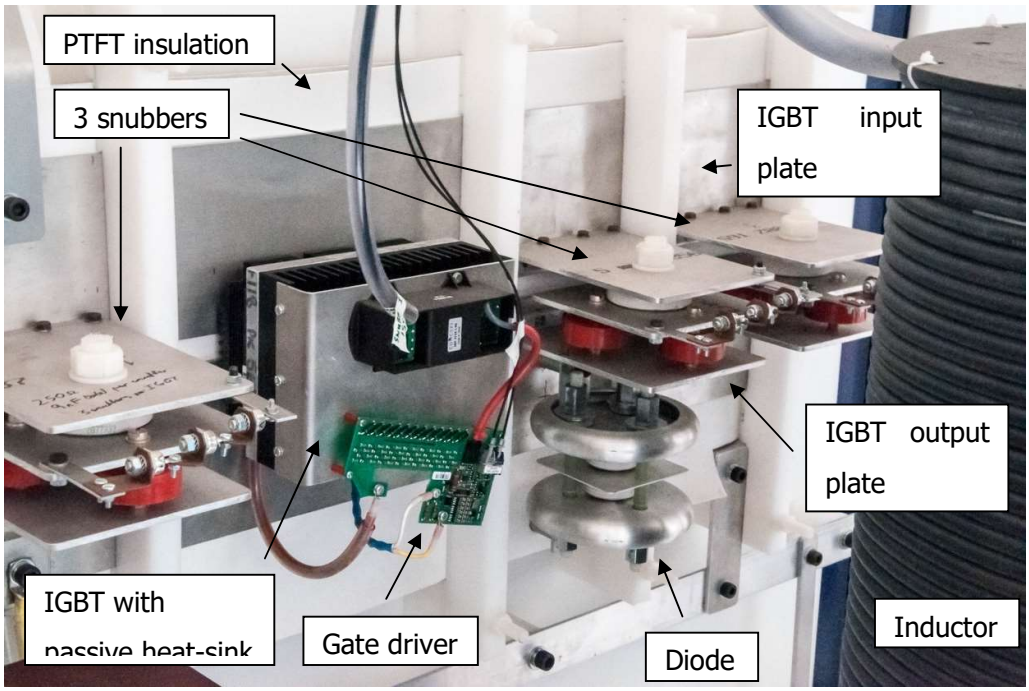

Figure 67 – Photo of snubber arrangement as built

Figure 68 shows the close coupling of the 15 µF capacitor to the IGBT power bus, the output inductor and a current sharing 10 Ω resistor.

The wide grounded plate can't be readily seen in the images as it is behind the PTFT and covers the whole area behind all other parts of stripline like structure. It facilitated a low inductance connection to the diode which allowed current to flow from the ground connected plate to the plate that collected the output of the IGBT. It also allowed a low inductance connection to one terminal of the 15 µF capacitor and the plate that fed in input of the IGBT.

As the input and output plates for the IGBT were wide, the 3 snubbers could be spread conveniently beside the IGBT but still act as a very low inductance bypass for spikes at turn off.

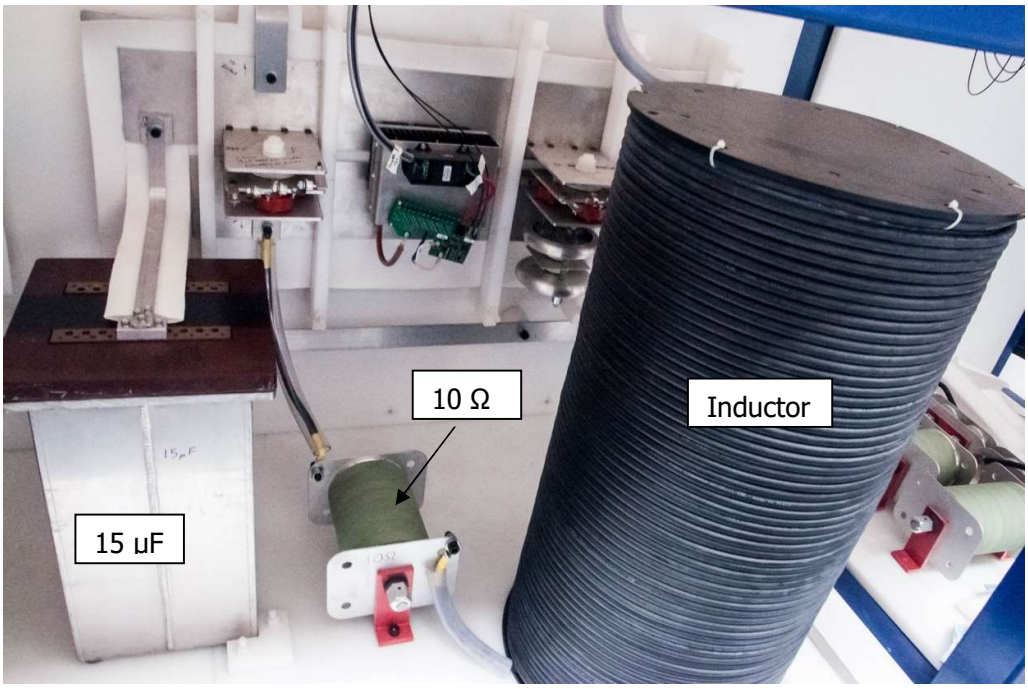

Figure 68 – Photo of single buck converter stage

The inductors were constructed in-house by winding 50 sqmm welding wire around large plastic bobbins, which were themselves made from large industrial pipe with machined end caps. Several layers were used, insulated with polyethylene sheet.

Designing and building the switching system was very interesting as it had to work, be robust and perhaps most importantly of all, be inexpensive. The parts purchased off the shelf were the IGBT and its diver circuit, the large diode (although that was a custom assembly) and the large resistor (also custom). The rest largely had to be made from spare components.

Figure 69 shows the general arrangement for the C bank. To the left, the bulk capacitance can be seen, and to the right, the 3 separate buck converters used. Each of the converters has a resistor on the output. The purpose of this resistor is to raise the output voltage at a converter in proportion to the current delivered so that currents share equally between them. A converter that draws more current than another will have a higher output voltage, and thus, if all else is equal, gradually lower its current. While this makes the system less efficient, it makes it more stable.

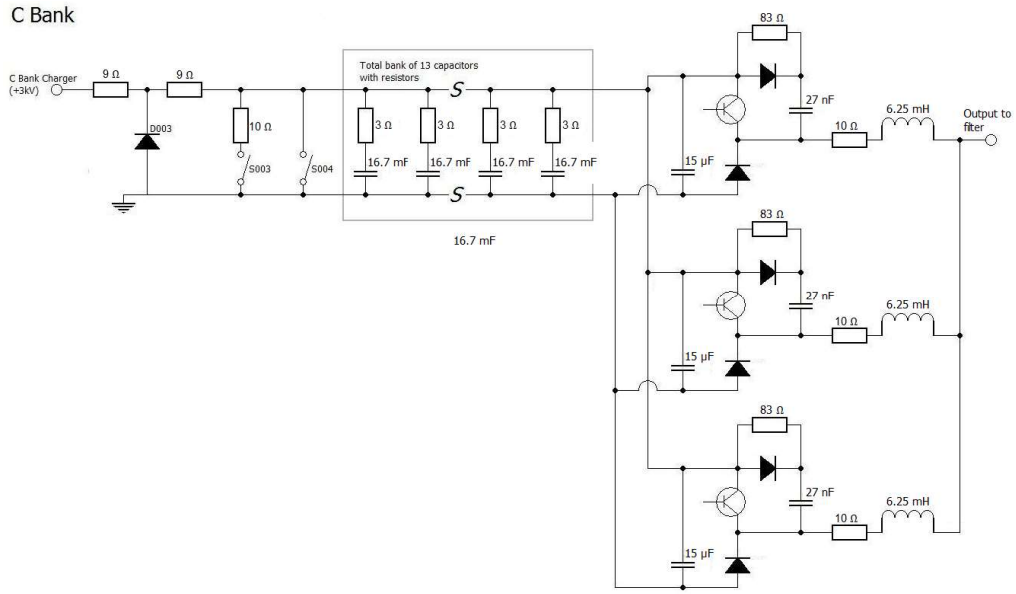

Figure 69 – C waveform generation part of trailing component generator

The frequency of operation of an individual buck converter is approximately 1.7 kHz. If all were in phase the output waveform would have current swings at that frequency. Figure 70 shows how this could manifest.

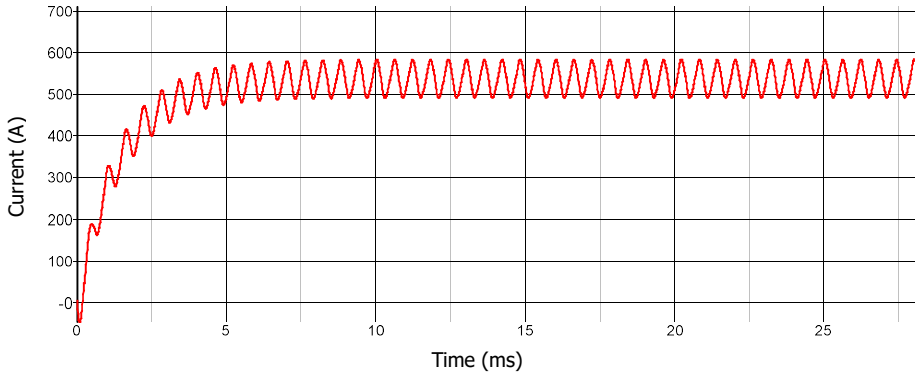

Figure 70 – C waveform using PWM mode with buck converters in phase

The effective frequency if running buck converters out of phase is 3 times higher at 5 kHz. Furthermore, the amplitude is reduced by a factor of 3 over the in-phase option as rather than delivering current from all 3 buck converters, it is delivering only one at a time. Figure 71 shows a much smoother waveform resulting from this multi-phase approach.

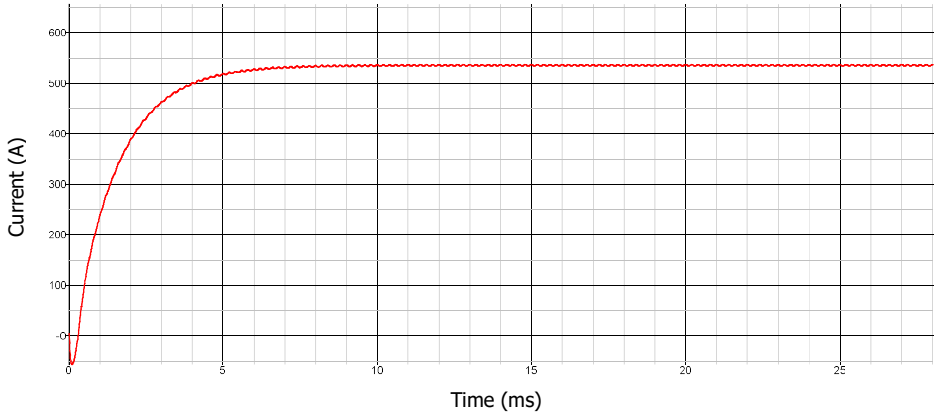

Figure 71 – C waveform using PWM mode with buck converters out of phase

The smoothness of the potential C waveform when using the PWM method to produce a flat current profile would likely be welcome by those commissioning tests at the laboratory. While natural lightning is almost certainly not a perfect square wave, the reference C waveform from the standard is. From personal experience, customers asking for a particular test waveform often expect it to look like a perfect implementation of the reference waveform.

5.8.7. Filter

A rather complex aspect of the trailing component generator was the filter that protects it from an open circuit fault condition of the high current generator. Designing it to serve multiple purposes at once involved a fine balancing act and a lot of iterative trial and error with SPICE software (SIMetrix).

It had to perform the following functions:

- Prevent current entering the trailing component generator from the high current generator
    - Design to withstand 120 kV (highest conceivable voltage oscillation)
    - Required a diode with a rating of 180 kV to give 50% headroom
    - The diode was not rated to handle the high dV/dt of a open circuit fault on the high current generator, so a filter was required to decrease the dV/dt
    - Adequately rated capacitors were not available, so lower voltage ones had to be used which in turn required protecting with spark gaps

- Allow the B and C/C* waveforms to merge seamlessly
    - Since the B waveform is higher in amplitude than the C/C* waveforms, an inductor could be used to allow the tail of the B waveform to pull up the current from the C waveform generator
    - Diodes were required to prevent the B and C/C* parts of the waveform generator firing into each other
- Filter out as much of the high frequency component from the C/C* switching if it is used in buck converter mode as possible
    - This required ideally as high an order low pass filter as possible
    - This low pass filter had to allow the B waveform to pass through unattenuated

Figure 72 shows the schematic of the resultant designer filter. It comprises 2 cascaded damped LC filters with an additional output inductor and damped spark gap protection for the capacitors.

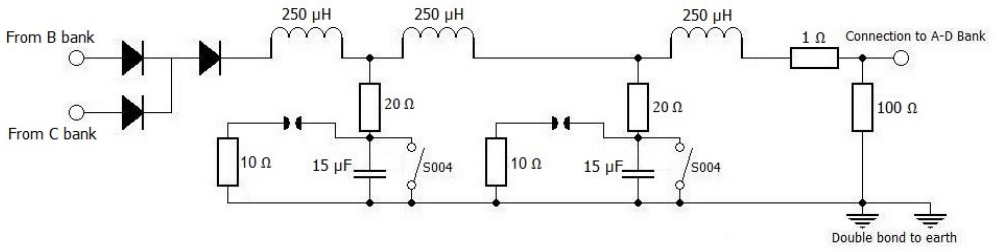

Figure 72 – Trailing component generator output filter

The resistors connecting the capacitors to the upper rail reduce the Q of the circuit considerably, to approximately 0.4. This was could ideally have been higher, perhaps closer to critically damped, but the components available did not allow for that. Figure 73 shows the transfer function of the filter.

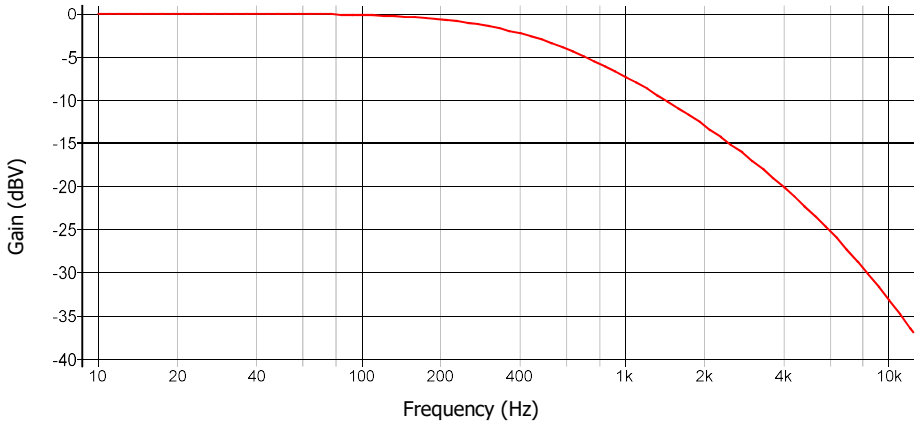

Figure 73 – Frequency response of trailing component output filter

Despite the low Q, the attenuation at high frequencies was quite considerable. This was important to prevent ringing and limit the maximum voltage delivered to the diodes, in the case of a fault where the A/D waveform generator is fired into an open circuit. Should such a fault occur, if the Q of the filter were high (more than critically damped), the voltage within it could exceed the initial charge voltage of the A/D bank. This was to be avoided.

Figure 74 shows a simulation indicating that, should the high current generator be fired into the trailing component generator, the voltage as seen by the diode would increase to a maximum of 60 kV, which is the maximum charge voltage. This is well below the 180kV rating of the diode stack and very little ringing appears present.

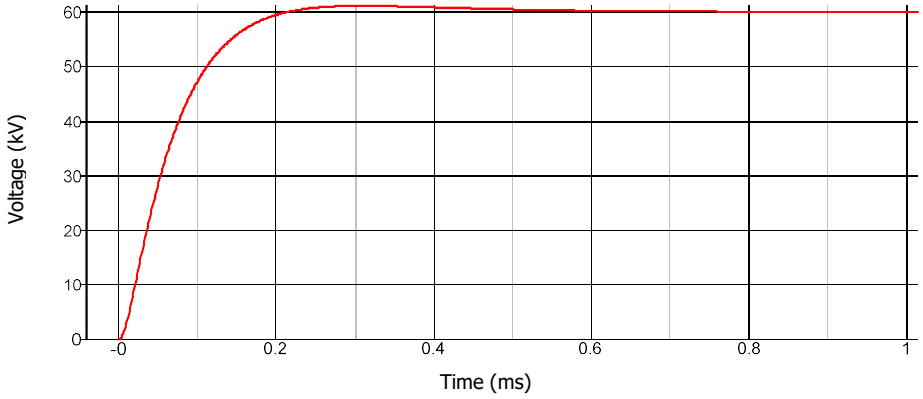

Figure 74 – Predicted worst case voltage transient on filter diode

The efforts to design snubbers and filters have all been taken well past what could have been considered sufficient. This represented the most that could reasonably be achieved to protect the waveform generators from each other and their switching transients. If sufficient had been aimed for and just missed, then the whole project could have been put at risk. So by implementing as robust a system as possible, if it didn't perform quite as well as expected, it would likely still be more than sufficient.

5.9. Testing of the trailing component generator

With the main elements of the trailing component generator in place, testing could proceed. Since it was a complex system and a fault in part of it could be detrimental to other parts, isolated sections were tested.

The first part to prove functionally of was the filter, to ensure that the high current generator could not cause damage if fired into the trailing component generator. The inputs to the filter from the B and C waveform generators were disconnected and grounded and the high current generator was fully charged then fired into an open circuit. The protection spark gaps both fired and the circuit survived. This was repeated several more times for confirmation.

Having gained confidence that the high current generator would not cause damage to the trailing component generator, the testing moved on to proving that the B waveform could be generated reliably. The Buck converter output of the C component part remained disconnected and earthed while the B component part was reconnected to the output filter.

The B waveform generator's capacitor bank was charged to 14.5 kV and triggered. It passed an excellently shaped waveform through a dummy test sample with a total charge transferred of 10.3 C. The test standard ED84 requires the waveform to pass 10C ±10% to be delivered within 5 ms. The charge delivered during this period was 9.25 C, which was 7.5% lower, while within specification (± 10%), this can be improved simply by increasing the charge voltage by 8% to 15.1 kV. The remaining part of the tail would merge with the C waveform, and so excess charge delivered is not of concern.

Figure 75 shows the shape of the B waveform has a desired double exponential shape as originally designed.

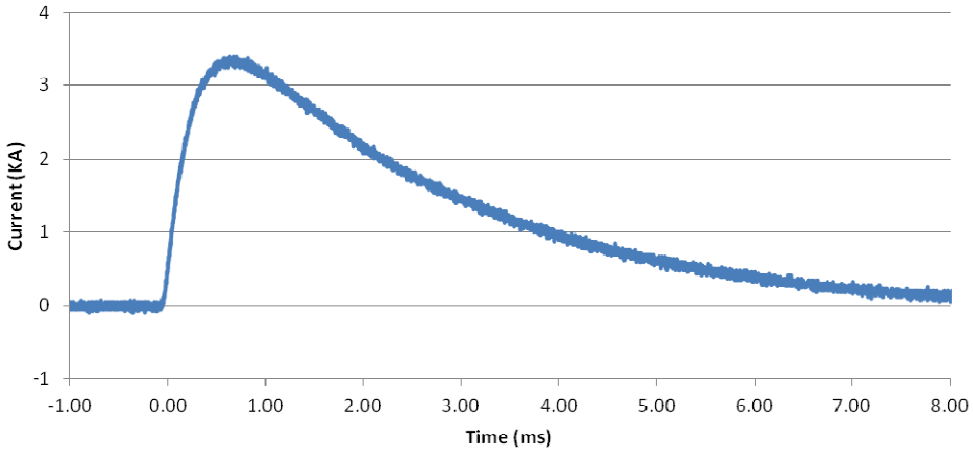

Figure 75 – Recorded B waveform current

Figure 76 compares the reference double exponential waveform from the standard with the recorded waveform.

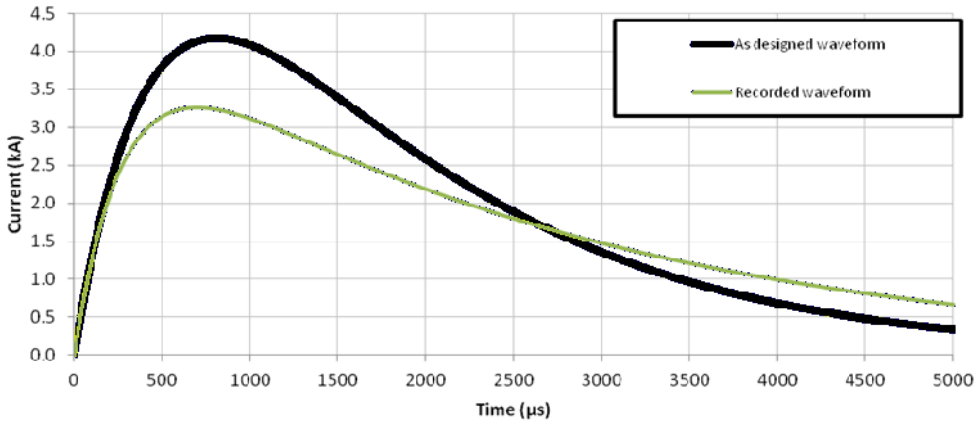

Figure 76 – Comparison of recorded and predicted B waveform current

The lower peak and longer tail were due to an additional 1 Ω of resistance in the trailing component generator's output filter than the initial design called for. This extra resistance was placed there are a precaution to increase the output impedance of the generator and desensitise it to sample impedance variation – especially where an arc could be involved. While another 2 Ω resistor was on order to put in parallel with the output resistance of the filter and eliminate the additional 1 Ω, the delivery date was outside of the project timescale. This resistor is in series with the output of both the B and C waveform generators and so reducing it would increase the capabilities of both.

The C waveform was tested in its both of its configurations. The CR discharge method was tested. This did not require writing any complex control software for the FPGA trigger controller.

The C waveform is trivial to implement to a shorted load, so an arc test was used to demonstrate the waveform generators ability. The test rig was set up with a 100 mm gap between a steel electrode (with arc diverter) and an aluminium plate with a fuse wire to initiate the arc.

The capacitors were charged to 3 kV and the pulse duration set to 1 s. It was expected to deliver more charge than the standard required – effectively a test of the envelope of the waveform generator's capability. In the case of the C waveform, exceeding the required specification clearly indicates that the specification can be achieved with margin.

Figure 77 shows a jagged current curve, this is due to fluctuation in the arc impedance. This varying current and presumably wildly twisting arc, made a very loud sound.

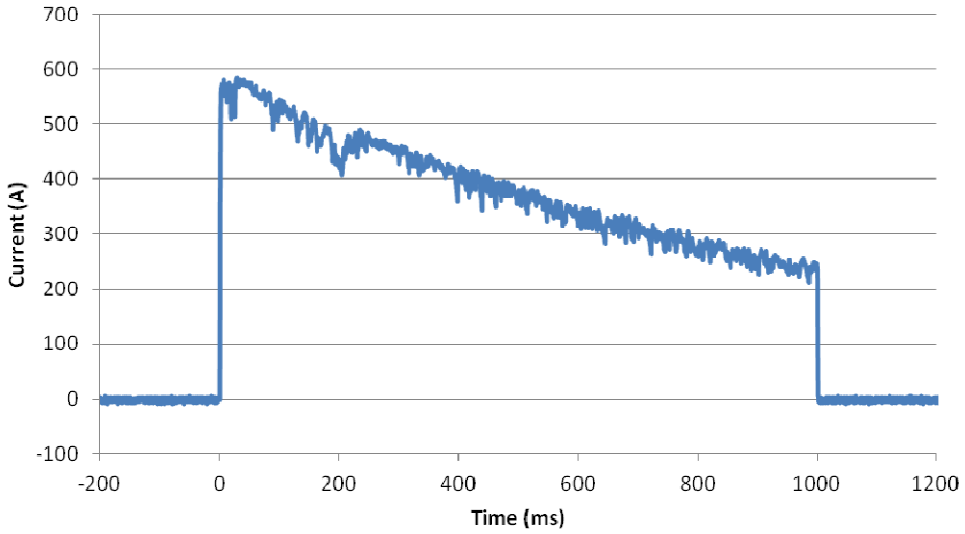

Figure 77 – Recorded C waveform current in CR discharge mode (V_{ch} = 3 kV)

The total charge delivered was 379 C, beating the stretch goal of 350 C from Stanag by 29 C. The charge delivered within 0.5 s was 231 C, this is within the ±20% tolerance of 200 C required by ED84. The time allowable for delivery of 200 C to a test sample is 0.25 to 1s, which was accomplished in 0.386 s, again within specification.

With experimentation, a correctly chosen voltage and pulse length could be found to more closely centre the waveform output within the test standard's specifications. No time was available for these tests though and shortly after performing the above work, the charger developed problems and could only charge to 1 kV without tripping out. This hampered testing of the PWM mode of operation.

The second test for the C waveform generator was to show how the PWM control method. Figure 78 shows the result of a test that was attainable with the capacitors charged to 1 kV, which due to the low voltage had to be done through a shorted output; a conduction test rather than an arc attachment test.

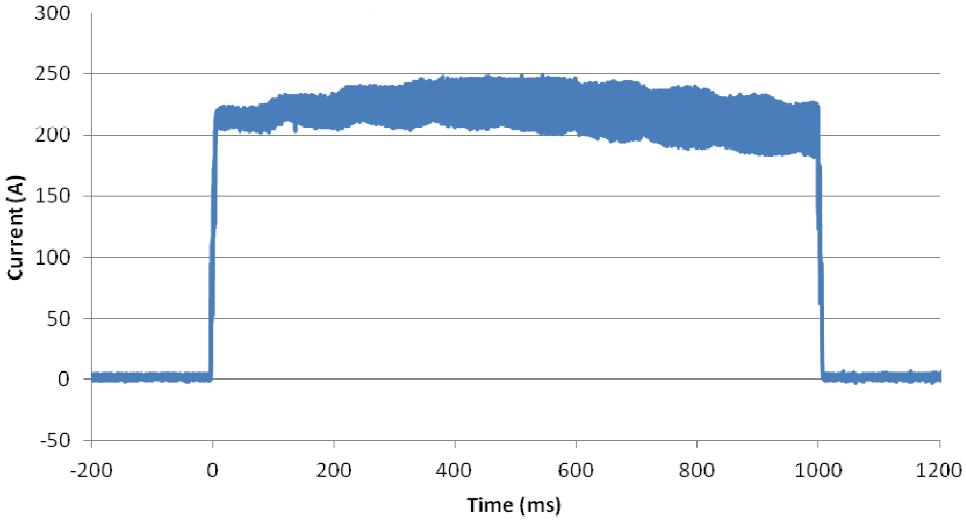

Figure 78 – Recorded C waveform current in PWM discharge mode (V_{ch} = 1 kV)

This did show that, within 1 s, the full 200 C could be delivered as required by the test standard and with a reasonably flat current profile. A total of 222 C was delivered which is 11% more than required by quite within the standard.

Because of the unfortunate situation with the charger, effort towards a closed loop 3 phase buck converter had slowed. The result above was generated with an open loop control signal that did not take current as an input. If current were used as part of the control, it would be trivial to end the waveform after 200 C had passed through the sample.

Naturally the voltage within the capacitor bank decayed during the pulse. To flatten out the waveform, the pulse width driving the buck converters was increased linearly throughout the pulse. This aspect was very successful.

The buck converter was used in its 3 phase mode and maintained the output current within ±25 A of the 220 A set point, but with a little bow throughout the waveform. It was expected to be a little flatter than this. Inspection of the waveform later indicated that 2 of the phases were firing together, to make a sort of 1.5 phase buck converter. This was caused by a bug in the FPGA programming. By design a rhythmic firing of the buck converters with one each at 0°, 120° and 240° was supposed to be implemented. However,2 buck converters were firing at 0°, none at 120° and a single one at 240°. Unfortunately, this analysis occurred after testing was concluded.

5.10. Future work

While the trailing component generator could deliver waveforms to the test standard's specifications, it could be improved also. Time ran out to finish implementing the closed loop control system which should be a major focus.

The main areas to focus effort are:

- Repairing or replacing the C bank charger to attain the full 3 kV charge voltage
- Install a second 2 Ω resistor in parallel with the one present in the final stage of the trailing component output filter, reducing the resistance from 2 to 1 Ω
    - This should push up the current of the B waveform and shorten the tail to more closely match that described in ED84
    - The lower resistance will be beneficial for operation of the buck converter by consuming less energy for a given current and so allowing either a lower capacitor bank charge voltage or a higher driving voltage
- Finish the LabVIEW software allowing the C waveform generator to operate in closed loop mode in both buck and LR configurations
    - This will allow the pulse to end after a specified charge transfer and make running the facility a little easier
- Fix the phase issue with the buck converter
    - This is probably a glitch in the hurriedly assembled LabVIEW code
    - It should flatten out the waveform a good deal

5.11. Conclusion – Trailing Component Generator

Both the C and C/C* waveforms were analysed to understand best how they may be delivered to a test sample. This involved comparing the waveforms with the load impedances, then adding sufficient margin to ensure stability.

The B waveform lent itself to being generated using an LCR circuit as it was described in the test standard with a double exponential equation. The main component choice was the capacitors, the resistance and inductance followed. By choosing the capacitors to have a voltage much higher than the arc drop, it was expected to be stable and deliver a consistent waveform.

Switch options were considered for the B waveform, and a thyristor was settled upon as it was the easiest to operate and quite inexpensive.

The C waveform (and its truncated version C*) are largely described as square waves by the test standard. Many options present themselves for making a moderate current square wave: flywheels, batteries, rectified transformer isolated utility supply and capacitors. Flywheels and utility supply were quickly ruled out on complexity and cost respectively. The remaining options were batteries and capacitors. Due to capacitors being more easily made safe (by complete discharge) than batteries, and are thus approachable and so not requiring a separate room, they were chosen based upon taking up the least room and being safer.

Having chosen capacitors for the C waveform, a choice of switch had to be made. It obviously needed a switch capable of turning off, so thyristors were not an option. Since the voltage and current fell within the ratings of large IGBT modules, these were chosen.

These IGBTs could operate much faster than required for simply turning on at the beginning of a pulse and off at the end. This allowed the development of a scheme that would allow the circuit to be upgraded (via software) to operate as a buck converter and flatten the current output by varying the duty cycle.

The trailing component generator that consists of both the B and C waveform generators required a filter to ensure that the high current generator (A/Ah/D waveforms) could not damage the relatively low voltage components. This was designed as a large diode rated at 180 kV with a snubber to limit the rate of dV/dt that the diode would see should the high current generator output be injected directly onto it.

Testing of the filter proved successful with no detrimental effect seen applying 60 kV to the output of the trailing component generator.

The B waveform was tested and proved that the waveform generator could deliver it within specification, though the wave-shape was a little more damped than the test specifications description due to a higher circuit resistance than ideal. This can be remedied later by installing a single 2 Ω resistor. However, since the waveform was within specification and robustly generated such that it would not be sensitive to the sample impedance, this is considered a success.

The C waveform when operated in the LR mode with decaying current was equally successful and capable delivering more charge than required than the 350 C called for in Stanag 4236. This meant that it would be very robust and capable of delivering the current profile required to meet the specification of ED84.

The voltage available for testing the C waveform using the 3 phase buck converter mode of operation was low at 1 kV due to a charger fault. However, the circuit was tested and found capable of flattening out the current profile as well as delivering a current transfer within specification. This was also a success but it would have been better to test it at a higher voltage that would have allowed higher current and an arc.

6. Summary and Conclusion

This work was undertaken while designing and building the D, B and C generators at the Morgan-Botti Lightning Laboratory for Cardiff University. The area of study covers understanding and generation of the lightning test waveforms that are core to the function of the laboratory.

Aircraft are often struck by lightning (circa once every 10,000 hours, each) and must survive this threat. Test standards have been developed to describe the threat and how to perform the tests in a way that will ensure aircraft safety.

Once initiated, a lightning arc channel is stationary in the air, through which an aircraft is moving rapidly. This leads to different parts of the airframe being susceptible to different parts of the lightning strike waveform.

Natural negative lightning usually consists of a high current initial discharge (the return stroke – A waveform) followed by an intermediate current (B waveform) and continuing current (C waveforms), which may be interspersed with a series of restrikes (subsequent strokes – D waveform); that is why lightning appears to linger and flicker to the naked eye. There are on average 2.6 restrikes after the initial discharge. As the aircraft travels forward during this process, different areas may be struck with these varying lightning waveforms.

The main goal was to build waveform generators to deliver all these combinations of waveforms accurately, reliably and in an affordable and timely manner. This required understanding the requirements, techniques and waveforms and translating this understanding to design. It is not novel to deliver the waveforms. The novelty is in the individual design of each waveform generator and their integration.

Optimising the design of the fast, high current waveform generator was the first objective to be achieved. It was distinct from the design and build, which could be guided with experience, Spice analysis and iterative changes until a system could be made to function appropriately and within specification.

The double exponential waveforms, described in the test standards, were explored to derive the charge, time to peak and maximum dI/dt. While analysing these equations, it was found that an LCR circuit solution could be found for any,

overdamped, critically damped or underdamped current waveform described using Equation (1).

A system to generate the reference waveform was evaluated. In order to generate the waveform as described in the standard and deliver these to a test sample, a reference solution was developed. The voltage and energy stored by a waveform generator, should the reference solution be followed, would have to be considerable (almost 700 kV and 9 MJ, respectively) to generate the A waveform. This was much too high for the small test facility and would require a huge expenditure on capacitors that could not be afforded.

More achievable solutions were explored by keeping the peak current and action integral the same, but increasing the rise time as permitted by the standards, which allowed for a reduction of the initial voltage from the reference design. The use of the mathematical understanding of the waveform equations and a numerical solver was used to explore the solution space for the lower voltage options.

It was found that, below a critical capacitance, there are 2 solutions for operation of an LCR circuit to deliver a waveform with a specific current and action integral with a fixed capacitance and inductance. These are essentially higher and lower voltage solutions with higher and lower resistances, respectively. This means that a waveform generator designed to generate the higher voltage solution can easily be modified to operate at the lower voltage solution simply by reducing the circuit resistance appropriately. This usefully gives access to 2 waveforms that deliver equal energy and peak current to a sample/load but with different rise times (the lower voltage solution being slower).

The high current generator was designed to be able to produce 2 distinct solutions for each of the D, Ah and A waveforms, hence maximising its ability without additional cost. In each case the higher voltage solutions are slightly overdamped and unipolar and the lower voltage solutions are slightly underdamped and oscillatory. While both are allowed within the scope of the test standard, natural lightning is unipolar. Therefore, it would generally be preferable to use the high voltage solutions. However, by being able to deliver both unipolar and oscillatory waveforms, the opportunity for future comparison of the 2 modes has been made available.

In order to assist with the test facility, many parts from a decommissioned laboratory were donated by an external partner. This included much of an old high current waveform generator as well as unused parts purchased to upgrade it. Since the old generator was neither complete nor a particularly capable machine (low energy and slow rise times), rather than fix it and accept the performance limitations, the design implemented for the laboratory started from a blank sheet.

The high current waveform generator was designed to make best use of the available parts and optimised using the detailed mathematical understanding of LCR circuits. It used strings of 3 capacitors, each 20 kV, 197 μF, in series, with a net 60 kV, 65.7 μF per string; a single string to generate the D waveform, 2 in parallel for the Ah waveform and 4 in parallel for the A waveform (for increased net capacitances of 131.4 and 16.8 μF respectively). It was designed in conjunction with a test rig, as that would determine the inductance of the system which plays a large factor in the waveform shape. The inductance of the test rig was expected to be approximately 1.5 μH, and it was chosen to match this to the inductance of the generator circuit for a total of 3 μH.

The waveform generator was tested in the D configuration and produced waveforms close to those expected. When the voltage and current were adjusted to deliver 100 kA, the action integral was 4% high, and so well within the 20% allowable by the specification. The waveform generator was robust against unexpectedly high resistance samples; for example, putting a carbon fibre sample in and leaving it set up for aluminium would lower the output peak current by 5% and leave the action integral 4% low. These are both within the 10% and 20% tolerances allowed, respectively.

Designing the waveform generator and test rig for a given inductance goal was challenging. After completing the build generator and testing of the generator, the inductance was found to be 3.5 μH and thus 16.7% higher than the designed 3 μH. This explained the 4% deviation in the D waveform. A plan was put in place to reduce the inductance by 0.5 μH and correct this small error. This involved increasing the effective diameter of the central conductor in the test rig.

The setup process for the high current waveform generator was aided by a spreadsheet tool. The inputs were the desired waveform and sample type. The outputs were the required resistance, number of chains of capacitors to use and the

initial charge voltage for the capacitor bank. The spreadsheet was able to suggest configurations and voltages for both standard and more custom waveforms by simply choosing the action integral and peak current.

The output resistor was designed to maximise flexibility of the waveform generator. The range of values required to cover the standard waveforms was 49.6 to 243 mΩ. While this could have been achieved with a few appropriately chosen discrete values, a novel resistor was designed to allow as continuous a range as practicable. It is a unique system comprising 3 low inductance binary chains and has over 65k combinations, covering an extended range of resistance – 34.7 to 385 mΩ. The values were selected by installing or removing link plates. The spreadsheet tool informed the user of the correct configuration.

Firing the fast waveform generator was simplified by using a movable spark gap. Considerable efforts were made to keep it as coaxial and short as possible to ensure it maintained a low inductance. The resulting inductance was approximately 150 nH, or 5% of the circuit inductance. The switch was pneumatically operated, ensuring electrical isolation for the control system. The mass of the moving part was made reasonably high (8 kg), so when the discharge is initiated in its small internal volume, the actuator would not be ejected by the overpressure (the whole structure was well braced also). The result was a robust and easy to use, high-voltage and high-current switch that cost approximately $1/50^{th}$ of commercial versions.

Optimisation and design of the trailing component generator was the second objective of the project. It required the synergistic design of waveform generators that could deliver the B and C waveforms and a filter that both combined their output and protected them from each other and the output of high current waveform generator.

The intermediate and trailing component generator required designing from the ground up and the purchase of all new hardware. This allowed choice of topology for the energy storage, switching and filter/pulse shaping network to deliver the waveforms.

The trailing component consists of 2 waveforms, joined together to form a composite: the B and C waveforms or the B and a truncated version of the C waveform referred to as the C* waveform.

The B waveform is described in the test standard (ED84) as double exponential, and it was found that a reasonably low voltage (14.5 kV) could be used to deliver it without compromising parameters. This was made possible by the rather slow rise time allowing this reasonably low initial voltage. Since this was the only waveform that could conceivably match exactly the test standard mathematical description, an LCR circuit was chosen to generate it.

The B waveform generator performed as expected and delivered the current within specification. However, since additional resistance was used in the filter circuit during the time of testing, it was over damped. Subsequently, this was corrected for by purchasing an additional resistor to place in parallel with the output of the protection filter.

The B waveform generator was unique in engineering implementation and its interaction with the output filter, effectively pulling current out of the C waveform generator with the output filters inductance. This ensures the C waveform starts glitch free into an arc channel and merges the 2 waveforms seamlessly.

To test the B waveform, the generator's capacitor bank was charged to 14.5 kV and triggered. It passed the waveform through a dummy test sample with a total charge transferred of 10.3 C. The test standard ED84 requires the waveform to pass 10C ±10% to be delivered within 5 ms. The charge delivered during this period was 9.25 C, which was 7.5% lower, while within specification (± 10%), this can be improved simply by increasing the charge voltage by 8% to 15.1 kV. The remaining part of the tail (after 5 ms) would merge with the C waveform, and so excess charge delivered is not of concern.

The test of the B waveform was undertaken with the higher 2 Ω filter resistor. The current profile differed from the standard waveform as expected with the high output resistance. Therefore, it is expected to more closely match the standard waveform once the filter resistance has been reduced to 1 Ω.

The C waveform is largely described as a square wave and is of much lower current than the other test waveforms. This opened up the choice different technologies.

Capacitors were chosen due to their compactness and ability to be fully drained of energy for safe access to their vicinity.

Capacitors naturally lent themselves to a CR discharge for generating a sagging waveform that would be within specification for the C waveform. The circuit was optimised for this. However, this could be improved upon by using PWM control of the current output from the capacitor bank to flatten the resulting waveform. A unique 3 phase buck converter was designed to accomplish this and implemented within the circuit also.

The C waveform generator functioned well in CR discharge mode, proving that if the capacitor bank was charged up to the full 3 kV, it could deliver up to 379 C of charge into an arc. This exceeds the 200 C requirement for the standard C waveform and ensures that it can be accomplished within the operating envelope of the waveform generator. It also allows testing this higher charge for more investigative future work beyond the scope of test standards.

While the charger failed and limited testing, the unique PWM approach was tested and levelled out the current reasonably well, extending the deliverable charge also. It was unfortunate that testing could not continue with it, as the 3 phase buck converter was a completely unique topology in lightning testing. However, once the charger was eventually fixed, the C waveform became fully operational.

In order to protect the trailing component generator from the higher voltage output of the high current generator, a filter was designed. This involved a diode protected by a damped low pass filter to prevent ringing at high voltage. Some of the inductance used to form the B waveform was placed within the filter and interspersed with capacitors resistively coupled to ground. This filtered out high frequency components but still allow the B waveform to pass unhindered.

Testing of the robustness of the diode circuit was performed by firing the high current generator at full voltage into it the filter that protects the B waveform and C waveform generators. The tests showed that the filter could successfully prevent the high current generator from damaging the B waveform and C waveform generators.

While other test facilities have been built before to generate these waveforms and have used a variety of methods to do so, there were no publications guiding the

design of lightning waveform generators and each has been built differently. The unique work in this research included the mathematical understanding of the double exponential waveform for optimizing LCR circuits. All circuits developed have unique elements and the use of PWM for flattening the C waveform is unique also.

The work in this thesis should assist future builders of high current waveform generators by presenting the decision process and analysis behind the implemented systems. While it does present the actual circuits used, it goes much further and presents how to understand them and derive one which suits a desired waveform.

The output of the theoretical work informed the design of the laboratory, which allowed academic exploration of how lightning interacts with materials; typically those used in future aircraft. Thus this work formed the basis for future development of aeronautical safety measures.

A great many engineering challenges were encountered implementing the designs, from how to keep inductance of the test rig and spark gap down, to how to design the fast waveform generator's bus bars to resist forces pushing them apart. On top of this, the project management and assembly work made this a very large project for a short period of time.

The laboratory was built on time and within budget and has been operating successfully since 2011 with the D waveform. The B and C waveforms, which were not part of the original specification but included as additions were delayed somewhat by a fault with the charger and were tested successfully in 2014. In the years following, the Ah and A waveforms were implemented as designed also.

The Morgan-Botti Lightning Laboratory is a high-quality test facility that delivers direct effects lightning testing accurately to international standards.

7. References

[1] M. A. Uman, 'The Art and Science of Lightning Protection', Cambridge University Press, Caimbridge, 2008, ISBN 978-0-521-87811-1

[2] M. A. Uman, 'The Lightning Discharge, Dover Publications, New York, 2001, ISBN 0-486-41463-9

[3] M. A. Uman, 'All About Lightning', Dover Publications, New York, 1986, ISBN-13:978-0-486-25237

[4] V. A. Rakov and M. A. Uman, 'Lightning Physcis and Effects', Cambridge University Press, Cambridge, 2003, ISBN 0-521-58327-6

[5] R. H. Golde, 'Lightning Protection', Chemical Publishing Co., New York, 2012, ISBN 978-0-8206-00264

[6] R. H. Golde, 'Lightning – Volume 1: Physics of Lightning', Academic Press Inc., London, 1977, ISBN 0-12-287801-9

[7] R. H. Golde, 'Lightning – Volume 1: Lightning Protection', Academic Press Inc., London, 1977, ISBN 0-12-287802-7

[8] V. Cooray, 'The Lightning Flash', The Institute of Electrical Engineers, London, 2003, ISBN 0 85296 780 2

[9] Sir Basil Schonland, 'Flight of the Thunderbolts', Oxford University Press, Oxford, 1950, ISBN 978-0198519058

[10] H. Cannell, 'Lightning Strikes – How Ships are Protected from Lightning', The Book Guild Ltd, Brighton, 2011, ISBN 978-1-84624-520-6

[11] H. Bluhm, 'Pulsed Power Systems', Springer, Heidelberg, 2006, ISBN 978-3-540-26137-7

[12] T. H. Martin, A. H. Guenther and M, Kristiansen, 'J. C. Martin On Pulsed Power', Springer, New York, 1996, ISBN 978-1-4899-1561-0

[13] G. A. Mesyats, 'Pulsed Power', Springer, New York, 2005, ISBN 0-306-84653-9

[14] H. M. Ryan, 'High-Voltage Engineering and Testing', The Institute of Electrical Engineers, London, 1994, ISBN 978-1-84919-263-7

[15] A. Haddad and D. Warne, 'Advances in High Voltage Engineering', The Institute of Electrical Engineers, London, 2004, ISBN 978-0-85296-158-2

[16] B. Jayant Baliga, 'Advanced High Voltage Power Device Concepts', Springer, New York, 2012, ISBN 978-1-4614-0268-8

[17] Erickson and Maksimovic, 'Fundamentals of Power Electronics', Springer, New York, 2001, ISBN 978-0-7923-7270-7

[18] J. D. Irwin and R. M. Nelms, 'Engineering Circuit Analysis', Wiley, Asia, 2011, ISBN 978-0-470-87377-9

[19] G. L. Luo and H. Ye, 'Synchronous and Resonant DC/DC Conversion Technology, Energy Factor and Mathematical Modelling', Taylor & Francis, Boca Raton, 2006, ISBN 0-8493-7237-2

[20] Grover, 'Inductance Calculations', D. Van Nostrand, New York, 1947, ISBN 978-0-486-47440-3

[21] M. A. M. Piah, P.A. Ping and Z. Buntat, 'Development of Mathematical Equation for Determining Breakdown Voltage of Electrodes Gap', 2nd IEEE International Conference on Power and Energy (PECon 08), 2008

[22] Y. Wang, Xishan Wen, Lei Lan, Yunzhu An, 'Breakdown Characteristics of Long Air Gap with Negative Polarity Switching Impulse', IEEE Transactions on Dielectrics and Electrical Insulation, Vol. 21, No. 2; 2014

[23] W. P. Winn, G. W. Schwede, C. B. Moore, 'Measurements of electric fields in thunderclouds', Journal of Geographic Research, Volume 79, Issue 12, 1974

[24] R.F. Griffiths, 'The initiation of corona discharges from charged ice particles in a strong electric field', Journal of Electrostatics, Volume 1, Issue 1, Pages 3-13, 1975

[25] G. A. Dawson, 'PRESSURE DEPENDENCE OF WATER-DROP CORONA ONSET AND ITS ATMOSPHERIC IMPORTANCE', J Geophysical Research, 1969, ASIN: B00KJ21TDG

[26] S. E. Reynolds, M. Brook, and Mary Foulks Gourley, 'THUNDERSTORM CHARGE SEPARATION', New Mexico Institute of Mining and Technology, New Mexico, 1957

[27] C. Saunders, 'Charge Separation Mechanisms in Clouds', Springer, Space Sci Rev (2008) 137: 335–353, 2008

[28] ED-84 (September 1997), 'Aircraft Lightning Environment and Related Test Waveforms Standard', EUROCAE, 1997

[29] R. Feynman, 'The Feynman Lectures on Physics, Volume II - Electricity in the Atmosphere', Addison-Wesley, Massachusetts, 1963, ISBN 0-201-02117-X

[30] Y. Hiraki, 'On polarity asymmetry of the occurrence rate of sprite discharges', 30th International Conference on Lightning Protection (ICLP), IEEE, 2010

[31] H. C. Stenbaek-Nielsen, 'Sprite halo structures and streamer onset', 2011 URSI General Assembly and Scientific Symposium, IEEE, 2011

[32] NASA, 'Global Lightning Activity', https://earthobservatory.nasa.gov/images/85600/global-lightning-activity, Accessed 12/05/2019

[33] J. Takami and S. Okabe, "Observational Results of Lightning Current on Transmission Towers," IEEE Trans. Power Deliv., Vol. 22, No. 1, pages 547–556, 2007

[34] Y. Goda, 'Arc voltage characteristics of high current fault arcs in long gaps', IEEE Transactions on Power Delivery, Volume: 15, Issue: 2, 2000

[35] R. F. Lane, "United States Navy Inservice Aircraft Lightning Strike and Damage Survey", 1981 IEEE International Symposium on Electromagnetic Compatibility, Pages 1–6. 1981

[36] FAA, 'Lightning Direct Effects Handbook', https://skybrary.aero/bookshelf/books/3352.pdf, Accessed 10/03/2017

[37] National Lightning Safety Institute, 'Aviation Losses from Lightning Strikes - National Lightning Safety Institute', http://www.lightningsafety.com/nlsi_lls/avaition_losses.html, Accessed 27/02/2017

[38] AAIB, 'Schleicher ASK 21 two seat glider', https://assets.publishing.service.gov.uk/media/542300e540f0b613420009cf/dft_avsafety_pdf_500699.pdf, Accessed 27/03/2016

[39] GOV.UK, 'Aircraft Accident Report 1/2005 - Sikorsky S-76A+, G-BJVX, 16 July 2002', https://www.gov.uk/aaib-reports/aar-1-2005-sikorsky-s-76a-g-bjvx-16-july-2002, Accessed 03/03/2017

[40] GOV.UK, 'Eurocopter AS332L2 Super Puma, G-REDM, 22 February 2008', https://www.gov.uk/aaib-reports/eurocopter-as332l2-super-puma-g-redm-22-february-2008, 03/03/2017

[41] GOV.UK, 'Embraer EMB-145EP, G-RJXG, 25 September', https://www.gov.uk/aaib-reports/embraer-emb-145ep-g-rjxg-25-september-2001, Accessed 03/03/2017

[42] GOV.UK, 'Aerospatiale AS332L Super Puma, G-TIGF, 21 January', https://www.gov.uk/aaib-reports/aerospatiale-as332l-super-puma-g-tigf-21-january-2005, Accessed 03/03/2017

[43] GOV.UK, 'Aircraft Accident Report 2/97', https://assets.publishing.service.gov.uk/media/5422fe16e5274a131400091d/2-1997_G-TIGK.pdf, Accessed 07/03/2016

[44] GOV.UK, ' Aerospatiale AS332L Super Puma, G-TIGF, 21 January 2005', https://www.gov.uk/aaib-reports/aerospatiale-as332l-super-puma-g-tigf-21-january-2005, Accessed 07/03/2016

[45] AAIB,' AAIB Bulletin No: 12/2000 - AS332L, G-TIGT', https://assets.publishing.service.gov.uk/media/5422fbd740f0b61346000909/Eurocopter_AS332L2_Super_Puma__G-CHCG_01-07.pdf, Accessed 07/03/2016

[46] AAIB, 'AAIB Bulletin No: 3/2001 Sikorsky S76A', https://assets.publishing.service.gov.uk/media/5422fc3ae5274a13170008c3/dft_avsafety_pdf_501501.pdf, Accessed 07/03/2016

[47] AAIB, 'AAIB Bulletin No: 8/99 Ref: EW/G99/02/11', https://assets.publishing.service.gov.uk/media/5422f654e5274a13140005af/dft_avsafety_pdf_500408.pdf, Accessed 07/03/2016

[48] AAIB, 'AAIB Bulletin No: 11/99 - Eurocopter AS 332L, G-BWZX', https://assets.publishing.service.gov.uk/media/54230184e5274a1317000b3d/dft_avsafety_pdf_501972.pdf, Accessed 07/03/2016

[49] STANAG 4236, 'Lightning Environmental', NATO, 2007

[50] ED-113, 'Aircraft Lightning Direct Effects Certification', EUROCAE, 2002

[51] ARP5577, 'Aircraft Lightning Direct Effects Certification', SAE, 2008

[52] ED-14G, 'Environmental conditions and test procedures for airborne equipment', EUROCAE, 2011

[53] DO-160, 'Environmental conditions and test procedures for airborne equipment', RTCA, 2010

[54] ED-105 (April 2005), 'Aircraft Lightning Test Methods', EUROCAE, 2005

[55] J. Fouladga, G. Wasselynck, D. Trichet, Shielding and Reflecting Effectiveness of Carbon Fiber Reinforced Polymer (CFRP) composite', 2013 International Symposium on Electromagnetic Theory, Pages 1–6, 2013

[56] M. Caldwell, 'The Sandia lightning simulator: recommissioning and upgrades', 2005 International Symposium on Electromagnetic Compatibility, 2005

[57] HSE, 'Using nanomaterials at work', HSG272, 2013

[58] HSE, 'An inventory of fibres to classify their potential hazard and risk', research report 503, 2006

[59] T. R. McComb, 'CALCULATING THE PARAMETERS OF FULL LIGHTNING IMPULSES USING MODEL-BASED CURVE FITTING', IEEE Transactions on Power Delivery, Vol. 6 No. 4, pages 1386-1394, 1991

[60] Wikipedia, 'Joint European Torus', https://en.wikipedia.org/wiki/Joint_European_Torus, Accessed 17/11/2018

Appendix 1 – Screenshots of Spreadsheet

Figure 79 shows the most frequently used page of the spreadsheet. It is designed to make setting up the test facility simple, but in this example is displays the circuit parameters for generating the A waveform. It performs the following functions:

- Allows save and recall of configurations (row 3)
- Suggests the most appropriate resistor configuration (row 5), and allow it to be copied into the configuration
- It calculates the required resistance based upon the capacitance, initial charge voltage and desired action integral
- The "Find" button runs a solver to adjust the charge voltage until the peak current is correct, at which point all parameters for a given waveform have been completed
- The graph displays the reference waveform (calculated from I_0, α and β), the tolerance box for the peak current and the expected waveform of the generator

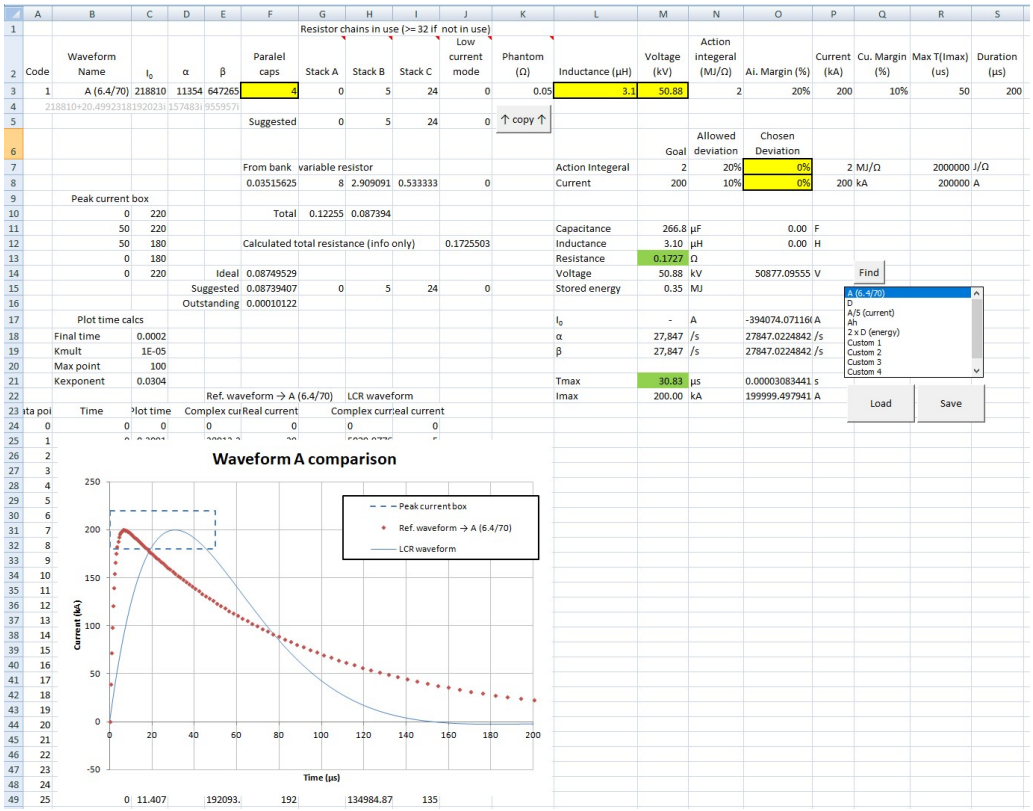

Figure 79 – Sheet 1 – Bank Setup

Figure 80 shows a calculator for I_0, α and β if given inductance, capacitance, resistance and initial charge voltage. In this example it is showing an oscillating waveform with complex number values for I_0, α and β. It performs the following functions:

- Takes values of L, C, R and initial voltage to generate values of I_0, α and β
- Additionally calculates the time to peak current, the peak current and the action integral
- Plots the waveform

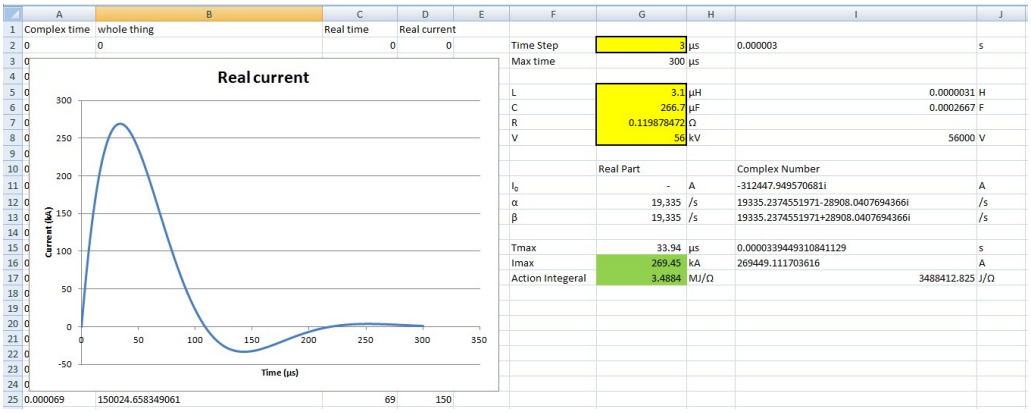

	A	B	C	D	E	F	G	H	I	J
1	Complex time	whole thing	Real time	Real current						
2	0	0	0	0		Time Step	3	µs	0.000003	s
3	0					Max time	300	µs		
4	0									
5	0					L	3.1	µH	0.0000031	H
6	0					C	266.7	µF	0.0002667	F
7	0					R	0.119878472	Ω		
8	0					V	56	kV	56000	V
9	0									
10	0						Real Part		Complex Number	
11	0					I_0	-	A	-312447.949570681i	A
12	0					α	19,335	/s	19335.2374551971-28908.0407694366i	/s
13	0					β	19,335	/s	19335.2374551971+28908.0407694366i	/s
14	0									
15	0					Tmax	33.94	µs	0.00003394493108411 29	s
16	0					Imax	269.45	kA	269449.111703616	A
17	0					Action Integeral	3.4884	MJ/Ω	3488412.825	J/Ω
18	0									
19	0									
20	0									
21	0									
22	0									
23	0									
24	0									
25	0.000069	150024.658349061	69	150						

Figure 80 – Sheet 2 – I_0, α and β calculator

Figure 81 shows spreadsheet for finding the charge voltage if capacitance, inductance, current and action integral adjusted. It also finds the values of I_0, α and β. It performs the following functions:

- Takes values of L, C, R, the action integral and peak current to calculate values of the initial charge voltage and I_0, α and β
- Plots the waveform

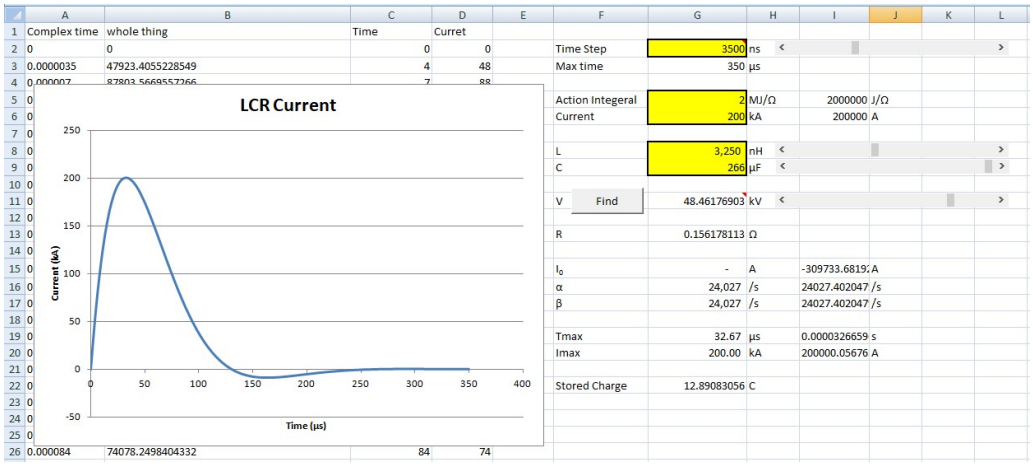

Figure 81 – Sheet 3 – Energy, Current, Capacitance and Inductance experiment

Figure 82 shows a spreadsheet for experimenting with the solution space for of peak currents, given L, C and the action integral. It performs the following functions:

- Generates I_0, α and β values, given L, C and the action integral over a range of voltages (1 kV to 100 kV)
- Has a red line across 60 kV to remind myself, that the generator cannot produce waveforms above that value
- Plots the solution space (peak current vs. charge voltage)

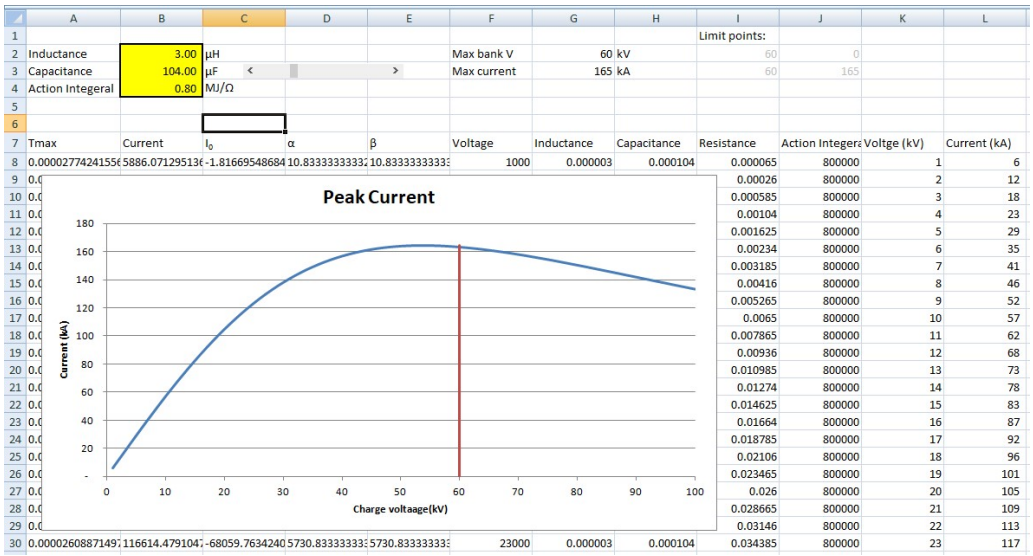

Figure 82 – Sheet 4 – Peak current as a function of L, C and action integral

Figure 83 shows a spreadsheet that calculates the remaining values of L, C, R and initial charge voltage, if one is known, to produce a waveform specified by I_0, α and β. It performs the following functions:

- Takes values for I_0, α and β values, and plots the resultant current waveform
- If L is known, solves for C, initial charge voltage, and R
- If C is known, solves for L, initial charge voltage, and R
- If initial charge voltage is known, solves for L, C, and R
- If R is known, solves for L, C and initial charge voltage

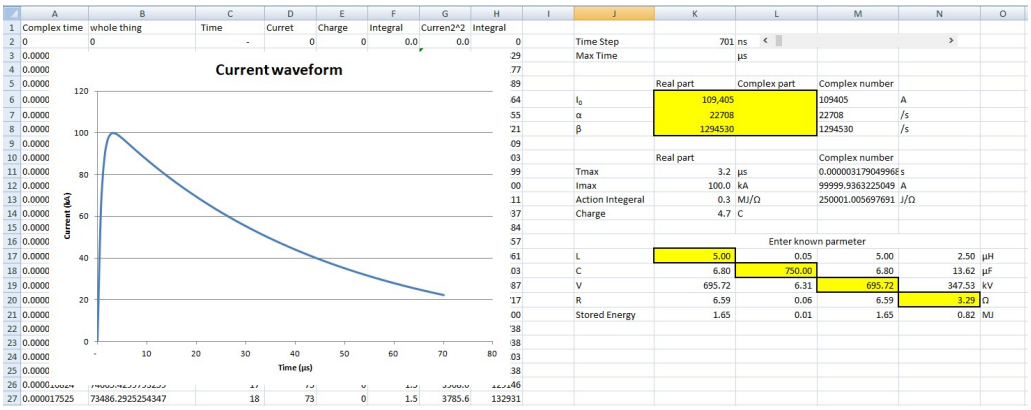

Figure 83 – Sheet 5 – Calculate circuit parameters if 1 is known

Figure 84 shows the spreadsheet that functions as the waveform database for sheet 1.

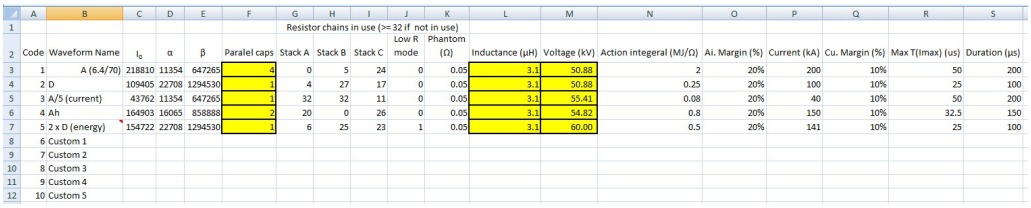

Figure 84 – Waveform database

Figure 85 shows the spreadsheet used to calculate the different values of the variable resistor. It is sorted into ascending resistance, so sheet 1 can perform a lookup for a suggested setting.

	A	B	C	D	E	F	G	H	I	J	K	L	M	N	O
1	Total resistance	A	B	C	Low R mode	A	B	C	Low R mode						
2	0.034722222	0	0	0	1	8	5.333333333	2.666667	12.8						
3	0.035187668	0	0	1	1	8	5.333333333	2.285714	12.8			A	B	C	Low R mode
4	0.035545024	0	0	2	1	8	5.333333333	2	12.8		Elements	6	4	2	8
5	0.035665761	0	1	0	1	8	4.571428571	2.666667	12.8						
6	0.035828025	0	0	3	1	8	5.333333333	1.777778	12.8		Min series	6		Series	5
7	0.036057692	0	0	4	1	8	5.333333333	1.6	12.8						
8	0.036157025	0	1	1	1	8	4.571428571	2.285714	12.8		Element value	0.125			
9	0.036157025	1	0	0	1	6.857143	5.333333333	2.666667	12.8						
10	0.036247803	0	0	5	1	8	5.333333333	1.454545	12.8		Cap series elements	4			
11	0.036407767	0	2	0	1	8	4	2.666667	12.8						

Figure 85 – Resistor settings table

Appendix 2 – Silicon switching in trailing component generators

Phil Leichauer
Cardiff University
Morgan-Botti Lightning Laboratory
Pacific Road, Cardiff, CF24 5HL
United Kingdom
pgleichauer@gmail.com

Alex Meakins
Cobham Technical Services
13/15 Nuffield Way
Abingdon, Oxfordshire, OX14 1RL
United Kingdom
Alex.Meakins@cobham.com

Abstract

The lightning trailing component waveforms deliver a relatively low current, long duration waveforms with relatively high charge transfer. Silicon switches with sufficient capability to control the waveforms are readily available. Using them within a lightning test environment where several waveforms of differing voltage, duration and current are combined poses unique challenges. This paper outlines approaches taken to limiting stress on the switches and keeping transients within their design envelope. Adding sufficient inductance and damped local capacitance has proven to limit dI/dt and suppress excessive voltages, while care had to be taken to ensure any resistance would properly handle impulse power levels. Modelling, testing and practical application have proven that silicon switches can be inexpensively, safely and robustly used to control current within a lightning trailing component generator.

1. Introduction

The lightning trailing component is usually composed of the B and C waveforms when used for aeronautical testing. As switching technology moves on, from the robust and simple spark gaps, relays and ignitrons to the controllable yet delicate SCRs and IGBTs, higher levels of protection are required. These silicon based switches can offer fast, efficient and new control methods which could potentially offer great accuracy of control.

This paper explores several options for switching the waveforms and protecting the switches.

2. Waveform characteristics

In order to best understand the requirements of the switches, the characteristics of the waveforms should be known.

Furthermore, the load to which the waveforms are delivered should be understood. An upper limit of sample resistance of 0.15Ω is used, due to experience showing it to be considerably less. Importantly, this is the maximum resistance allowable for the return stroke generator – making further increases in performance for the trailing component generator moot.

As will be seen in section 7, a resistance of 1Ω was used between the return stroke and the trailing component generators.

The arc voltage is known to be approximately 2.5 to 3V/mm (1). Though the designed spacing between the electrode and sample of 100mm would suggest a 300V drop, the arc wonders considerably during a shot and the voltage increases. This has been measured for several shots and calculated indirectly from decaying waveform shapes for others and found to be often around 600V. In order to avoid arc extinction of the C waveform, a maximum arc voltage of 1500V has been assumed, giving a generous margin.

2.1. B Component Waveform:

The B waveform (2) is described as being unidirectional and having an average current of 2kA for 5ms. The method of complying with this general specification is left open in order to allow various approaches. However, the α, β and I_0 values are given for analysis purposes. It is these parameters that shall be used for the consideration of switch types.

B waveform definition (as used within paper)		
α	700	s-1
β	2,000	s-1
I_0	11,300	A

The following parameters are calculated from the α, β and I_0 values.

B waveform calculated parameters			
Parameter	Value	Units	Equation
Charge	10.49	C	1
Charge <5ms	10.00	C	2
Time to peak	0.808	ms	3
Peak current	4.173	kA	4
Action Integral	28.55	kA^2s	5
Max di/dt	14.69	MAs^{-1}	6

These values can be calculated from the following equations:

$$Q_{total} = -I_0\left(\frac{1}{\beta}-\frac{1}{\alpha}\right) \quad (1)$$

$$Q_{<5ms} = -I_0\left(\left(\frac{1}{\beta}-\frac{1}{\alpha}\right)-\left(\frac{e^{-0.005\beta}}{\beta}-\frac{e^{-0.005\alpha}}{\alpha}\right)\right) \quad (2)$$

$$t_{peak} = \frac{ln\left(\frac{\alpha}{\beta}\right)}{\alpha-\beta} \quad (3)$$

$$I(t) = I_0\left(\mathrm{e}^{-\alpha t_{peak}} - \mathrm{e}^{-\beta t_{peak}}\right) \quad (4)$$

$$E = -{I_0}^2\left(-\frac{2}{-\beta-\alpha}-\frac{1}{2\beta}-\frac{1}{2\alpha}\right) \quad (5)$$

$$\frac{dI(t=0)}{dt} = I_0(\beta-\alpha) \quad (6)$$

Interestingly, the above shows that the action integral of the idealised B waveform is ~40% greater than if it was a 2kA square wave – which is allowed by the standard. However, the action integral is not part of the specification. In comparison to the D waveform it has 12.5% of the action integral but transfers 222% of the charge - emphasising the importance of the charge transfer.

This waveform transfers 10C of charge through the load within 5ms, the remaining 0.49C occurs after this initial period.

2.2. C Component Waveform:

The C waveform (2) is described as being unidirectional, having a current between 200A and 800A and a time duration between 0.25 and 1 second, transferring 200C (± 20%). The method of complying with this general specification is left open in order to allow various approaches. It is not expected or implied that a double exponential waveform be used to perform this test. Rather a 400A 0.5s square wave is used for analysis. This current and duration will be used for consideration of switch types.

C waveform definition (as used within paper)		
Current	400	a
Duration	500	ms
Charge	200	C
Time to peak	0.75	ms
Action integral	80	kA^2s
Max di/dt	1	MAs^{-1}

The value of 0.75ms for time to peak was chosen as this is 0.15% of the duration of the pulse, thus not overly affecting the shape while allowing a relatively large inductance to stabilise the current. With 3kV and $1MAs^{-1}$, an inductance of 3mH can be used.

The C* waveform is also specified (2) however, since it is merely a shortened C waveform, it would be less arduous on the switch and so is not considered further.

It is notable that if keeping the charge transferred to 200C and using the allowable limits of 800A and 200A, the action integral would be $160kA^2s$ and $40kA^2s$, emphasising again the importance of the charge transfer and not action integral in the trailing component specification. Furthermore, any switch used for controlling the C waveform

should be able to handle the higher action integral.

3. Energy storage – B waveform

The B waveform has relatively low energy requirements. From the action integral given above, a modest wave-shaping resistance would give a modest energy requirement; with the relatively low peak current this leads naturally towards capacitors, which in turn allow the use of an LCR circuit to produce the double exponential waveform.

The choice of component values was defined by available capacitors and the wish to use >2Ω of wave-shaping resistance. The capacitors chosen added up to 750μF and were rated to 20kV. With a maximum of 15C stored, this allows general operation below maximum voltage.

In order to store 10.49C of charge, the capacitor bank terminal voltage would be 14kV. This is generally greater than the arc voltage by a factor of 10 and therefore any variance in it would be within the ±10% allowable in the standard (2).

4. Energy storage – C waveform

The C waveform with its long duration and low current presents a very different requirement. While large amount of capacitively or inductively stored energy could be used to approximate a square wave, an active circuit can get much closer. Alternatives considered included battery banks and rotating machines. Batteries proved expensive to maintain and rather large to house safely. While rotating machines looked both expensive and difficult to develop within the scope and timeframe of the laboratory build. A transformer connection to local power distribution was quickly eliminated due to installation costs. However,it would have been favourable if sufficient power was already in place within the building.

Capacitors have advanced significantly in terms of energy density over the last half century (3) and MJ scale banks are now quite affordable. Using a capacitor bank avoids moving parts and significant maintenance costs associated with rotating machines and battery banks. The greatest benefit when compared to batter banks was the lack of permanent voltage. As the output terminals of a capacitor bank can be shorted, it can be approached and worked upon safely without having to isolate many series connections first.

Unlike the B waveform where all the stored energy is consumed, a considerable amount of the energy and charge within the capacitors for the C waveform will remain after the discharge. This is due to the minimum voltage required to drive current through the circuits and load. A minimum current here would be 200A as specified in the standard.

Passive discharge methods involve decaying sources of voltage, energy or current. These are generally exponential, linear or a combination waveform, which is acceptable by the test standard. However, it would be desirable to have a square wave and be able to choose its amplitude, duration and charge transfer by setting a dial or from the control system. If the system could be relied upon to constantly deliver the current into loads of varying voltage drop and resistance that would be useful also.

In order achieve this, the concept of using a large multiphase buck converter to act as a controlled current source was devised.

Here a current of 400A is assumed, through the 1.15Ω of resistance and 1500V arc drop. Thus a terminal voltage of 1960V is required. Since the capacitor bank can have anything between zero and infinite additional effective resistance emulated by the PWM, additional stabilising resistance is not required.

In an ideal solution, the buck converter takes a high voltage low current input and outputs a low voltage high current. The system efficiency shall be assumed, somewhat hypothetically, to be 100%.

Since the device consumes energy rather than charge, it effectively multiplies the charge within the capacitor bank by the voltage input/output ratio. So there is no charge requirement for the capacitor bank, only an energy requirement.

To deliver 400A for 0.5s (and thus 200C), across a drop of 1960V, 392kJ is required. Thus the ratio of the energy stored within a capacitor bank between the initial and final voltage (upper energy – E_U) over the energy stored below the final voltage (lower energy – E_L) should be maximised in order to minimise the total stored energy. V_i and V_f are the initial and final voltages respectively. Hence:

$$\frac{E_U}{E_L} = \frac{{V_i}^2 - {V_f}^2}{{V_f}^2} \quad (7)$$

The differential is:

$$\partial \frac{E_U}{E_L} \partial V_i = \frac{2V_i}{{V_f}^2} \quad (8)$$

Which is linear and has no root other than zero. Clearly it can't be used as an initial voltage for a capacitor bank. Thus it can be seen that to minimise the total stored energy, an infinite initial voltage is required. This is unlikely to be used as an engineering solution!

Having explored the minimum energy scenario and found it unworkable, it was best to select components and then inspect the functionality of the system.

The capacitance was chosen such that there was at least 200C above the worst case terminal voltage, thus allowing any inefficiency present to completely erode the charge multiplication effect and still deliver 200C. A buck converter cannot deliver less charge than it accepts as a diode prevents it going anywhere other than through the load. This allows the design to be built for stability rather than efficiency.

The following parameters for a capacitor bank were selected:

C waveform calculated parameters		
Capacitance	0.2	F
Initial voltage	3000	V
Initial energy	0.9	MJ
Final voltage	1960	V
Final energy	0.38	MJ
C above final V	208	C

This was based upon available switches and the desire to keep the capacitor bank terminal voltage relatively close to the output voltage. It should be noted that generally, the sample resistance and arc voltage are much less than the worst case of 1960V total drop, leading towards a stable system that is unlikely to run out of energy or charge.

The devised system has current feedback and can automatically raise and lower the output voltage to counter variations in load resistance and arc voltage. Therefore using it is a simple matter of setting a dial rather than requiring the effort of understanding the load and changing resistors and initial charge voltage to suit.

5. B waveform switch

To generate the B waveform, the switch was required only to turn on and unleash the waveform in a single shot, completely draining the energy stored. It also had to be able to be timed accurately so as to start at the appropriate time.

The devices explored included ignitrons, spark gaps and thyristors.

While ignitrons (4) are available and clearly very capable of holding off 20kV, accurately timed switching and conducting 15C and 4kA, they do contain mercury. Though this did not rule them out with proper handling, it did count against their use. Trigger circuits are relatively simple.

Spark gaps (5) are largely as capable as ignitrons, but designing them to withstand large charge transfer can be challenging (6). Without adjustment they often have a limited range over which they are triggerable (7) and require relatively complex high voltage triggers (8).

A single thyristor which could handle both the voltage and the current was not found. This presented the need to use a series chain to obtain the voltage withstand. The short pulse of the B waveform affords operation well beyond the steady state rating of the units. With series connection, triggering is complicated by the need to float all gate triggers to the local cathode potential. However, this is trivial to overcome with a multiple output isolating pulse transformer.

The choice was a thyristor string of 7 units, each with the boiler plate rating of 4500V and 800A.

The following table shows that though operating above the maximum average current, it is within specification of the surge ratings.

Parameter	Requirement	Rating
Peak voltage	2850V	4500V
Peak current	4kA < 5ms	9000A for 8.3ms
Action Integral	$59kA^2s$	$330kA^2s$
Max di/dt	$15MAs^{-1}$	$150MAs^{-1}$

If approaching the maximum rated values and requiring a large number of devices, it would be wise to experiment. However, the approach taken was to find units with around twice or preferably higher rating in all areas.

6. C waveform switch

To generate the C waveform, the switch was required to turn on and off at the beginning and end of the discharge.

The devices explored included relays, GTOs, IGCTs and IGBTs.

While devices like ignitrons and thyristors can be used, the circuitry required to turn them off is cumbersome – essentially requiring a reverse pulse to force a zero voltage commutation.

Mechanical relays have been used. With their inertia, careful timing may be required to operate them in sync with the other waveforms.

GTOs are a viable option and are extremely hardy (9). While their close cousin the IGCT is easier to trigger.

The IGBT is the fastest of the silicon switches for medium voltage, moderate current applications, and the easiest to trigger. After discovering just how fast and easy, an active control circuit was conceived.

Multiple phases with an even angular spread, running at a given frequency would produce a smoother output. The number chosen was 3, based on component cost, complexity and space required. This effectively reduces the current handling required by each device by a factor of 3.

The choice was IGBT modules capable of holding off the volts with no series connection required. The boiler plate rating was 6500V and 600A. The following table shows the required and rated parameters of the chosen switches.

Parameter	Requirement	Rating
Peak voltage	3000V	6500V
Average Voltage	2500V	6500V
Peak current	250A	1200A for 1ms
Average current	133A	600A

Keeping well below the rated voltage and current allow for relatively low switching losses. It is estimated that they will be around 1J to 2J per pulse. This necessitates a control algorithm which avoids excessive switching in order to reduce stress and excessive heating of the junctions. This is considered in a separate paper.

7. Protection methods

Protecting silicon switches from transients is important. A spark gap or ignitron can handle very large occasional discharges and survive self triggering by overvoltage, but a thyristor or IGBT usually cannot. Protecting them from excessive dI/dt, dV/dt, voltage and current is imperative.

For normal switching, dI/dt is simply controlled by local inductance. With sufficient present, this naturally prevents excessive values. The thyristor will not see any rapid increase in forward voltage as it will only be used to turn on and discharge voltage. However, the IGBT will be conducting current while it turns off. To avoid local inductances on the input side overvolting the device, it needs to be minimised. A passive snubber network can then be implemented to smooth the remaining voltage spike.

By simply placing a capacitor across the IGBT, energy present in the local inductances will flow into it as the device switches off.

For design of the protection circuit, the full device rated current will be used and the maximum charge voltage of the capacitor bank used. The datasheet states that local

inductance should be limited to 200nH or less (quite achievable using wide flat bus bars with small gaps between them). This gave 36mJ of stored energy (E_s). With a starting voltage of 3kV (V_1) and an upper limit of 6.5kV (V_2), the smallest capacitor usable for a snubber is 2.2nF, calculated using equation 9.

$$C = \frac{2 \times E_S}{V_2^{\,2} - V_1^{\,2}} \qquad (9)$$

However, it was only possible to keep the inductance below 200nH close to the IGBT. The feeds from the capacitor banks were long and narrow. Their inductance has been estimated at 2uF. Thus in addition to the local inductance around the IGBT, the snubber must also absorb energy stored within the feeds – a further 360mJ. The minimum capacitance to absorb this and keep within the voltage limits is 24nF. This is shown in the next figure.

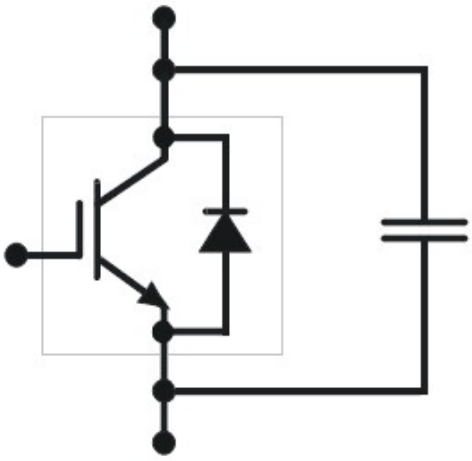

As can be envisaged, the above simple snubber circuit can effectively absorb the incoming energy. However,it presents a problem at switch on – where the IGBT shorts out this charged capacitor leading briefly to an over current of the device.

The addition of a diode and resistor can allow the inrush current to the capacitor to be high, while eliminating the over current at switch on.

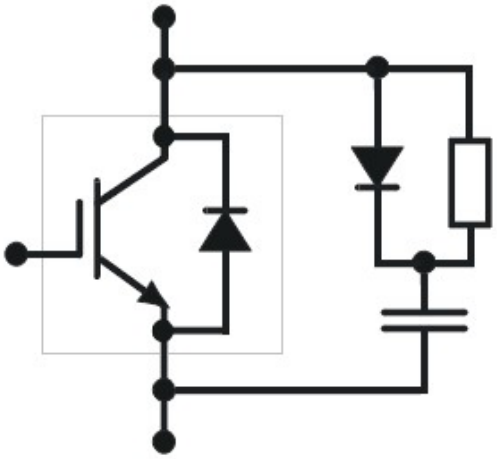

The resistor must be able to absorb all the energy delivered to the capacitor without overheating. For example, at 30kHz for ½ second and using the 396mJ, the energy delivered is 11,880J. This necessitated a resistor with a high thermal capacity to ensure it would not burn out. This snubber network was chosen for use at Cardiff University.

The similar but not identical trailing component generator at Cobham Technical Services also uses IGBTs for controlling the C waveform. Energy storage is by means of a very large fusion surplus capacitor bank of several thousand volts and a large proportion of a Farad. The exact capacitance and voltage may not be disclosed herewith, but the voltage and devices are sufficiently similar to those used at Cardiff University for confidence to be gained by measuring turnoff transients.

The following plot shows the voltage across the devices at switch off. As can be seen, there is no voltage overshoot.

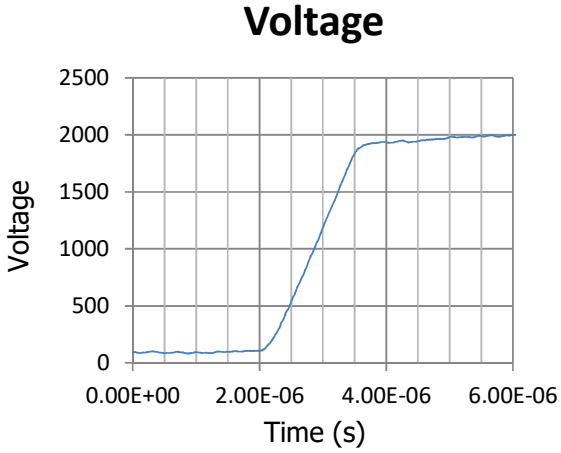

The voltage can be seen to rise from just above zero to 2kV – the final voltage for the test waveform at the time. The offset from zero was due to a small series resistance with the IGBTs in the path of measurement.

In order to protect both the thyristor and the IGBTs from excessive reverse voltage or current (the IGBTs have a reverse biased diode within), a large diode array was used. This simply prevents voltage or current from one part of the trailing component generator approaching any other part. However, these diodes need protecting from dI/dt, dV/dt and excessive current.

The first is solved, by adding sufficient inductance to limit the rate of rise of the current. An inductor carrying no current due to high impedance at one terminal can transmit very high dV/dt, limited only by local capacitance. To limit it further, large additional capacitance was added. This then presents a potential voltage source that could send too much current through the diodes. This was solved by the addition of 1Ω of resistance. The diodes, inductors, capacitors and resistance were all chosen to work in harmony with the B and C waveforms; while protecting them from the full terminal voltage of the return stroke generator.

8. Conclusion

Having outlined the waveforms to be generated, the choice of using capacitor banks for energy storage has been justified for use in Cardiff University's lightning test laboratory. This has in- turn lead to the use of silicon switches for controlling the current; the B wavefrom using a thyristor and the C waveform using IGBTs.

Keeping the components safe and within their operating limits is critical. By using sufficient local inductance and capacitive snubbers, this can be achieved.

9. References

1. Mohammad Mousavi Anzehaee1 et al., Gas Metal Arc Welding Process Control Based on Arc Length and Arc Voltage, International Conference on Control, Automation and Systems 2010, Oct. 27-30, 2010
2. EUROCAE, ED84 - AIRCRAFT LIGHTNING ENVIRONMENT AND RELATED TEST WAVEFORMS, Edition 2, 1997, Page no. 31-33
3. Weise et al., High energy density capacitors, Electromagnetic Launch Technology, 2004, page no. 255-258
4. Loree et al., Recent Advances in High-Power Ignitron Development, IEEE TRANSACTIONS ON ELECTRON DEVICES. VOL. 38. NO. 4. APRIL 1991, page no 720-725
5. Kharlov, A.V., Arc dynamics in high current rails park gaps, IEEE International Conference on Plasma Science - Abstracts, 2009. ICOPS 2009.
6. Geun-Hie Rim et al., Development of the pulse RAG switch, IEEE International on Plasma Science, 1998, page no. 228
7. McPhee, A.J. et al., An investigation of trigatron breakdown by two different mechanisms, Tenth IEEE International Pulsed Power Conference, Digest of Technical Papers, 1995, page no. 775-780
8. Ruden, EL at al., Damping resonant current in a spark-gap trigger circuit to reduce noise, IEEE PPC '09. Pulsed Power Conference, 2009, page no. 1192-1196
9. Yamamoto, M. Et al., GCT (gate commutated turn-off) thyristor and gate drive circuit, 29th Annual IEEE Power Electronics Specialists Conference, 1998, page no. 1711-1715